



CENTRO INTERNACIONAL DE ESTUDOS
DE DOUTORAMENTO E AVANZADOS
DA USC (CIEDUS)

DOCTORAL THESIS

**DEVELOPMENT OF TARGETED
THERAPEUTIC STRATEGIES FOR
METASTATIC LUNG CANCER**

Abi Judit Vázquez Ríos

INTERNATIONAL DOCTORAL SCHOOL

DOCTORAL PROGRAM IN MOLECULAR MEDICINE

SANTIAGO DE COMPOSTELA

2020



TESIS DOCTORAL

**DESARROLLO DE ESTRATEGIAS
TERAPÉUTICAS DIRIGIDAS AL
CÁNCER DE PULMÓN
METASTÁSICO**

Abi Judit Vázquez Ríos

ESCUELA DE DOCTORADO INTERNACIONAL

PROGRAMA DE DOCTORADO EN MEDICINA MOLECULAR

SANTIAGO DE COMPOSTELA

2020



AUTORIZATION OF THE THESIS SUPERVISORS

“DEVELOPMENT OF TARGETED THERAPEUTIC STRATEGIES FOR METASTATIC LUNG CANCER”

Dr. María de la Fuente Freire and Dr. Rafael López López

REPORT:

That the present thesis, corresponds to the work carried out by Ms. Abi Judit Vázquez Ríos, under our supervision, and that we authorize its presentation considering it gathers the necessary requirements of the USC Doctoral Studies regulation, and that as supervisors of this thesis, it does not incur in the abstention causes established by the Law 40/2015.

En Santiago de Compostela, 7 de septiembre de 2020

Dr. María de la Fuente

Dr. Rafael López López



AUTORIZACIÓN DE LOS DIRECTORES DE LA TESIS

**“DESARROLLO DE ESTRATEGIAS TERAPÉUTICAS DIRIGIDAS AL
CÁNCER DE PULMÓN METASTÁSICO”**

Dra. María de la Fuente Freire and Dr. Rafael López López

INFORMAN:

Que la presente tesis, corresponde con el trabajo realizado por Dña. Abi Judit Vázquez Ríos, bajo mi dirección, y autorizo su presentación, considerando que reúne los requisitos exigidos en el Reglamento de Estudios de Doctorado de la USC, y que como director de ésta no incurre en las causas de abstención establecidas en Ley 40/2015.

En Santiago de Compostela, 7 de septiembre de 2020

Dra. María de la Fuente

Dr. Rafael López López



DECLARACIÓN DE LA AUTORA DE LA TESIS

**“DEVELOPMENT OF TARGETED THERAPEUTIC STRATEGIES FOR
METASTATIC LUNG CANCER”**

Para defensas telemáticas

Dña. Abi Judit Vázquez Ríos

Presento mi tesis, siguiendo el procedimiento adecuado al Reglamento y declaro que:

- 1) La tesis abarca los resultados de la elaboración de mi trabajo.
- 2) De ser el caso, en la tesis se hace referencia a las colaboraciones que tuvo este trabajo.
- 3) La tesis es la versión definitiva presentada para su defensa y coincide con la enviada en formato electrónico.
- 4) Confirmando que la tesis no incurre en ningún tipo de plagio de otros autores ni de trabajos presentados por mí para la obtención de otros títulos.

Y me comprometo a presentar el ejemplar impreso de la tesis en el plazo de un mes desde que la EDIUS me lo requiera, así como del Compromiso Documental de Supervisión en el caso que el original no esté depositado en la Escuela.

En Santiago de Compostela, 7 de septiembre de 2020

Asdo: Abi Judit Vázquez Ríos



CONFLICT OF INTERESTS

The author of this thesis declares the ownership of two patents filed during this doctoral thesis:

- Inventors: M. de la Fuente Freire, R. López López, M. Alonso Nocelo, A.J. Vázquez Ríos.
 - Title: *Use of the TAS1R3 protein as a marker for therapeutic, diagnostic, and/or prognostic purposes for tumors that express said protein.*
 - Reference number: PCT/EP2019/050981, WO 2019/138140 A1.
 - Priority date: 15 January 2018.
-
- Inventors: M. de la Fuente Freire, R. López López, A.J. Vázquez Ríos, B. López Bouzo, M. Alonso Nocelo.
 - Title: *Nanosystems as selective vehicles.*
 - Reference number: PCT/EP2019/050979, WO2019/138139 A1.
 - Priority date: 15 January 2018.





A mi abuela



*“Porque las cosas invisibles de él, su eterno poder y deidad,
se hacen claramente visibles desde la creación del mundo,
siendo entendidas por medio de las cosas hechas.”*

N.T.





INDEX



INDEX

1	ABSTRACT	1
2	RESUMEN	3
3	RESUMEN <i>IN EXTENSO</i>	7
4	RESUMO <i>IN EXTENSO</i>	19
5	INTRODUCTION	31
5.1	LUNG CANCER	31
5.2	THE METASTATIC CASCADE	33
5.3	CURRENT THERAPEUTIC APPROACHES IN ADVANCED NSCLC	39
5.4	NOVEL AND PROMISING THERAPEUTIC STRATEGIES	49
5.5	NEW THERAPEUTIC TARGETS IN NSCLC	58
5.6	TRANSLATION OF THERAPEUTICS TO THE CLINIC	65
6	HYPOTHESIS	71
7	OBJECTIVES	73
8	MATERIALS AND METHODS	75
9	RESULTS	109
	SECTION I: STRATEGY INSPIRED BY EXOSOMES	111
9.1	DEVELOPMENT OF NOVEL MULTIFUNCTIONAL NANO-PLATFORMS	113
	SECTION II: STRATEGY INSPIRED BY CTCs	141
9.2	DISCOVERY OF A NEW TARGET FOR METASTATIC NSCLC	143
9.3	ROLE OF TAS1R3 IN NSCLC	161
10	DISCUSSION	185
11	CONCLUSIONS	219
12	REFERENCES	223
13	ABBREVIATIONS AND ACRONYMS	261

14	ETHICAL CONSIDERATIONS.....	273
15	ACKNOWLEDGEMENTS.....	277
16	ANNEXES	285



A large, light blue watermark of the USC logo is positioned diagonally across the page. The logo consists of the letters 'USC' in a large, bold, sans-serif font, with the full name 'UNIVERSITY OF SANTIAGO DE COMPOSTELA' written in a smaller font below it.

ABSTRACT / RESUMEN



1 ABSTRACT

Lung cancer is the most frequently diagnosed cancer and the leading cause of cancer death worldwide, with only 15% of patients surviving 5 years after diagnosis. Importantly, around 75% of patients are diagnosed at advanced metastatic stages, when surgery is not possible, with a dramatic drop in the 5-year survival rate to 6%. Non-small cell lung cancer (NSCLC) is the most common type and is virtually incurable to date. **The main objective of this thesis is the definition of novel bioinspired targeted therapeutic strategies for metastatic lung cancer patients.** For this purpose, a close look at the tumor biology allowed the setting of two different therapeutic strategies. One strategy comes from the tumor exosomes, and the other one, from the cells that disseminate from the primary tumor to form metastases.

Exosomes are membrane-derived natural nanovesicles (30-100 nm), secreted by most cell types, which given their ideal characteristics in cell-to-cell communication, have been postulated as ideal delivery systems. However, some concerns related to the relatively low yield of production, the cumbersome and time-consuming isolation protocols, the contamination with non-exosomal materials, the lack of standardization and validation, and most importantly, the problems according to the safety of their use in humans, make it difficult to think in their real translation to the clinic. Considering the advantages that nanotechnology brings to cancer therapy and diagnosis, this work aimed to the design of novel multifunctional nanoplatfoms inspired in exosomes for the selective delivery of bioactive therapeutic molecules (such as proteins, oligonucleotides, and drugs) to eliminate metastasis. The exosome-mimetic nanoplatfoms (EMNs) presented here, aim to maintain the most relevant characteristics as their natural counterparts and to overcome their limitations. EMNs have been engineered using simple and scalable methodologies, following a safe-by-design approach to

get biocompatible and biodegradable nanosystems. This work proves that EMNs are able to efficiently transport bioactive therapeutic RNAs to the target cells, in a comparable magnitude as tumor exosomes. Importantly, EMNs can be tunable and adapted to specific requirements and surface-decorated with macromolecules such as proteins and oligonucleotides.

Identifying new key players related to metastasis could also open new therapeutic avenues for the targeted treatment of advanced NSCLC patients. The metastatic process involves such a complex cascade of events, in which tumor cells abandon the primary tumor and migrate through the blood or lymphatic circulation, to eventually colonize distant organs and form metastasis. The presence of Circulating Tumor Cells (CTCs) can provide a valuable source of genomic and proteomic information about cancer patients of great utility for the development of novel therapeutic strategies in the era of precision oncology. In this thesis, a molecular receptor that is overexpressed in CTCs from advanced NSCLC patients was identified, the Taste receptor type 1 member 3 (TAS1R3). This research work describes its role in the progression of cancer and metastasis, endowing cancer cells with superior ability to seed and initiate metastasis at distant organs. Importantly, TAS1R3 is not only expressed in lung cancer but also other cancer types, evidencing the broad potential of a targeted therapeutic strategy to this target.

Overall, two promising strategies inspired by the tumor biology for the development of improved targeted therapeutics for NSCLC have been described. While EMNs can act as transporters for therapeutic RNAs and other biomolecules to tumor cells, TAS1R3 stands out as a promising therapeutic target that can prompt the development of new biomolecules.

2 RESUMEN

El cáncer de pulmón es el cáncer que se diagnostica con más frecuencia y la principal causa de muerte por cáncer en todo el mundo, solo el 15% de los pacientes sobreviven 5 años después del diagnóstico. Es importante destacar que alrededor del 75% de los pacientes son diagnosticados en estadios metastásicos avanzados, cuando la cirugía ya no es posible, lo que supone una caída dramática de la tasa de supervivencia a 5 años al 6%. El cáncer de pulmón de células no pequeñas (CPCNP) es el tipo más común y es prácticamente incurable hasta la fecha. **El principal objetivo de esta tesis es definir nuevas estrategias terapéuticas inspiradas en la biología para pacientes con cáncer de pulmón metastásico.** Para ello, se exploraron diferentes estrategias terapéuticas inspiradas en la biología del tumor, una de ellas proviene de los exosomas tumorales y la otra de las células que diseminan desde el tumor primario para formar las metástasis.

Los exosomas son nanovesículas naturales derivadas de membranas celulares (30-100 nm), secretadas por la mayoría de las células que, dadas sus características ideales en la comunicación de célula a célula, se han postulado como sistemas de liberación ideales. Sin embargo, existen algunas limitaciones relacionadas con el rendimiento relativamente bajo de producción, los protocolos de aislamiento engorrosos y lentos, la contaminación con materiales no exosomales, la falta de estandarización y validación y, lo más importante, problemas de seguridad para su uso en humanos, lo que dificulta una traslación real a la clínica. Teniendo en cuenta las ventajas que aporta la nanotecnología a la terapia y el diagnóstico del cáncer, este trabajo se propuso el diseño de novedosas nanoplataformas multifuncionales inspiradas en exosomas para la liberación selectiva de moléculas terapéuticas bioactivas (como

proteínas, oligonucleótidos, fármacos) para eliminar las metástasis. Las nanoplataformas miméticas de exosomas (EMN) presentadas aquí, se caracterizan por mantener las características más relevantes de los exosomas naturales, pero superar sus limitaciones. Las EMN se han diseñado utilizando metodologías simples y escalables, siguiendo un enfoque seguro por diseño para obtener nanosistemas biocompatibles y biodegradables. Este trabajo muestra que las EMNs son capaces de transportar de manera eficiente ARN terapéutico bioactivo a las células diana, en una magnitud comparable a la de los exosomas naturales. Es importante destacar que las EMNs se pueden modificar y adaptar a requisitos específicos, así como decorar la superficie con macromoléculas como proteínas y oligonucleótidos.

La identificación de nuevos actores clave relacionados con la metástasis podría abrir nuevas vías terapéuticas para el tratamiento dirigido de pacientes con CPCNP avanzado. Esto es posible utilizando técnicas como la biopsia líquida. El proceso metastásico involucra una cascada de eventos muy compleja, en la que las células tumorales abandonan el tumor primario y migran a través de la circulación sanguínea o linfática, para eventualmente colonizar órganos distantes y formar metástasis. La presencia de Células Tumorales Circulantes (CTC) puede proporcionar una fuente valiosa de información genómica y proteómica sobre los pacientes de cáncer de gran utilidad para el desarrollo de estrategias terapéuticas novedosas en la era de la oncología de precisión. En esta tesis, se identificó un receptor molecular sobreexpresado en las CTC de pacientes con CPCNP avanzado, el receptor del gusto tipo 1 miembro 3 (TAS1R3). Este trabajo de investigación describe su papel en la progresión del cáncer y la metástasis, dotando a las células cancerosas con una capacidad superior para sembrar e iniciar metástasis en órganos distantes. Es importante destacar que TAS1R3 no solo se expresa en cáncer de pulmón, sino también en otros tipos de cánceres, lo que demuestra el amplio potencial de una estrategia terapéutica dirigida a este objetivo.

Como conclusión, se han descrito dos estrategias prometedoras inspiradas en la biología tumoral para el desarrollo de terapias dirigidas mejoradas para el CPCNP. Si bien las EMN pueden actuar como transportadores de ARN terapéuticos y otras biomoléculas a las

células tumorales, TAS1R3 se postula como una diana terapéutica prometedora que puede impulsar el desarrollo de nuevas biomoléculas.





3 RESUMEN *IN EXTENSO*

Identificar nuevas dianas farmacológicas para la metástasis es una necesidad urgente para mejorar el resultado de los pacientes con cáncer de pulmón de células no pequeñas (CPCNP), dado que el 90% de las muertes por cáncer se deben a la metástasis. El cáncer de pulmón lidera las tasas de incidencia y mortalidad en todo el mundo, debido a su agresividad y elevada y rápida capacidad de crecimiento, y se espera que siga aumentando un 70% en el periodo comprendido entre 2018-2040. El 47,3% de los pacientes con CPCNP se diagnostican en estadio IV, cuando las metástasis ya son evidentes y la tasa de supervivencia a 5 años cae drásticamente a menos del 10%.

En los últimos años, el descubrimiento de nuevas dianas terapéuticas implicadas en el desarrollo de los tumores en cáncer ha llevado al desarrollo de nuevas terapias dirigidas. Esto ha supuesto una revolución en el campo de la oncología, permitiendo establecer decisiones terapéuticas de forma personalizada, es decir, en función de las características moleculares y genómicas del tumor de cada paciente y acercándonos a la medicina de precisión. Las decisiones terapéuticas para las terapias dirigidas se toman en base al estudio molecular del tumor de cada paciente, en función de la expresión de biomarcadores específicos o mutaciones de estos. Para el CPCNP avanzado, se analizan los siguientes marcadores para estratificar los pacientes con mayores posibilidades de beneficiarse de una terapia dirigida: mutaciones en EGFR, reordenamientos de ALK, translocaciones en ROS1 y mutaciones en BRAF. Este tipo de terapia dirigida presenta claras ventajas frente a la quimioterapia convencional, tales como una mayor especificidad y, por lo tanto, una mayor eficacia, y una reducida toxicidad, mejorando así, la calidad de vida del paciente. Actualmente, existen varias terapias dirigidas en la práctica clínica, indicadas para el tratamiento del CPCNP metastásico

en pacientes. La mayoría de estas terapias se basan en moléculas pequeñas, inhibidoras de la actividad de proteínas tirosina quinasa, por ejemplo, erlotinib, crizotinib o dabrafenib. También se encuentran anticuerpos monoclonales que viajan por el organismo hasta encontrar a su diana adecuada, situada en la superficie de las células tumorales, a la que se unen y atacan. Algunos ejemplos de anticuerpos monoclonales para el tratamiento de CPCNP metastásico incluyen bevacizumab, ramucirumab y necitumumab. Otra de las estrategias en clínica, es la aplicación de los anticuerpos monoclonales en la inmunoterapia, con el objetivo de unirse a las células del sistema inmune y promover un ataque contra las células cancerosas. A este tipo de anticuerpos se les llama inhibidores de punto de control inmunitario (del inglés *immune checkpoint inhibitors*) y actualmente hay cuatro aprobados para el tratamiento de cáncer de CPCNP metastásico: nivolumab, pembrolizumab, atezolizumab y durvalumab. Para seleccionar los pacientes para la inmunoterapia, se analiza la expresión de PD-1 y PD-L1. Pembrolizumab, dirigido contra PD-1, fue la primera inmunoterapia aprobada como tratamiento de primera línea en pacientes con CPCNP avanzado sin tratamiento previo.

Sin embargo, y a pesar del éxito relativo de estas terapias actualmente disponibles para el tratamiento del CPCNP, casi la mitad de los pacientes no son elegibles para una terapia dirigida, ya que se limitan a subpoblaciones de pacientes específicas. Además, menos de la mitad de los pacientes seleccionados con biomarcadores se benefician del tratamiento, y todavía se encuentran algunas respuestas en las cohortes de "biomarcadores negativos". Por lo tanto, existe una necesidad urgente en la búsqueda de nuevos biomarcadores para enriquecer las poblaciones de pacientes para respuesta y para el desarrollo de nuevas terapias dirigidas, para mejorar la supervivencia de los pacientes con CPCNP localmente avanzado o metastásico.

La aplicación de la nanotecnología en la terapia del cáncer ya es una realidad, permitiendo incrementar la administración localizada de quimioterapéuticos al tumor, lo que conduce a mejores actividades farmacológicas y minimiza significativamente los efectos secundarios. Idealmente, un sistema de liberación exitoso debería ser no tóxico, proporcionar una mejor farmacocinética y biodistribución, proteger la

carga de la degradación prematura, la opsonización y una rápida eliminación de la circulación sistémica, superar las barreras extra e intracelulares y liberar el material terapéutico en su sitio objetivo específico. En 1995, la FDA aprobó la primera nanopartícula para el tratamiento del cáncer, Doxil[®], un liposoma PEGilado cargado con el fármaco quimioterapéutico doxorubicina. Desde entonces, otros nanoterapéuticos basados en liposomas han llegado al mercado para diferentes tratamientos contra el cáncer. Hasta la fecha, Abraxane[®] es la única nanomedicina aprobada por la FDA (2012) y la EMA (2015) para el tratamiento del CPCNP avanzado.

Teniendo en cuenta estos antecedentes y la situación actual, el principal objetivo de esta tesis es **definir nuevas estrategias terapéuticas inspiradas en la biología para pacientes con cáncer de pulmón metastásico**. Para ello, nos fijamos en la biología del tumor y encontramos dos fuentes de inspiración para establecer nuevas estrategias terapéuticas con gran potencial para el tratamiento de pacientes metastásicos.

En primer lugar, observando el ambiente tumoral, se puede determinar que en nuestro organismo existe un nanosistema que reúne todas las características de un sistema de liberación ideal, los exosomas. Los exosomas son nanovesículas naturales derivadas de la membrana de los endosomas, con un tamaño de entre 30-100 nm, secretadas por la mayoría de los tipos de células que, dadas sus características ideales en la comunicación de célula a célula, se han postulado como sistemas de liberación ideales. Sin embargo, existen algunas limitaciones relacionadas con el rendimiento relativamente bajo de producción, los protocolos de aislamiento engorrosos y lentos, la contaminación con materiales no exosomales, la falta de estandarización y validación y, lo más importante, problemas de seguridad para su uso en humanos, lo que dificulta una traslación real a la clínica.

La cuestión es determinar si esos sistemas de liberación pueden diseñarse en el laboratorio de forma segura. Teniendo en cuenta las ventajas que aporta la nanotecnología, en el marco de este trabajo se propuso **el diseño de una nueva nanoplataforma multifuncionales inspiradas en exosomas para la liberación selectiva de moléculas**

antitumorales (como proteínas, oligonucleótidos, fármacos). Con fines comparativos, se aislaron y caracterizaron exosomas naturales a partir de líneas de células cancerosas y plasma. Las nanoplataformas miméticas de exosomas (EMN, del inglés “*exosome-mimetic nanoplatform*”) se han diseñado utilizando metodologías simples y escalables y permiten la modulación de sus propiedades, para obtener nanosistemas biocompatibles y biodegradables, capaces de transportar de manera eficiente macromoléculas bioactivas como proteínas y oligonucleótidos. Hemos optimizado el método de preparación para obtener EMNs nanométricas en un solo paso sin necesidad de disolventes orgánicos, calor o alto aporte energético, disminuyendo así el impacto ambiental y facilitando el proceso de escalado y su posible traslación. Las nanoplataformas desarrolladas además se pueden funcionalizar con ligandos capaces de unirse de forma selectiva y eficiente a los receptores de membrana expresados en ciertos tipos celulares como las células metastásicas.

Las EMNs destacan por tener características similares a los exosomas, con respecto a sus propiedades fisicoquímicas, composición lipídica, capacidad de carga de fármacos, baja toxicidad y capacidad para interactuar con las células diana del cáncer y entregar su carga *in vitro* e *in vivo* de manera tan eficaz como los exosomas (**Figura 1**), pero superando algunas de sus limitaciones: (i) el rendimiento de producción es mucho mayor que el de los exosomas (se obtiene 1000 veces más cantidad de partículas en tiempos mucho más cortos), un solo lote de EMN se obtiene en 10 minutos, mientras que los exosomas necesitan como mínimo 5 días, (ii) se pueden marcar fácilmente con fluoróforos unidos de manera estable (los EMN se marcaron de manera eficiente con TopFluor-SM, Cy5 y DiR al mismo tiempo), (iii) se pueden funcionalizar con proteínas de membrana para interactuar selectivamente con células y tejidos sin que haya otras moléculas desconocidas influyendo en esta interacción, y (iv) están vacíos y completamente caracterizados, lo que supone que no hay otros elementos que puedan producir efectos no deseados, para una aproximación más segura. Además, (v) los lípidos son materiales baratos y bien caracterizados, y los procesos de producción industrial

bajo condiciones GMP ya están bien establecidos para liposomas, que es muy importante desde una perspectiva de traslación.

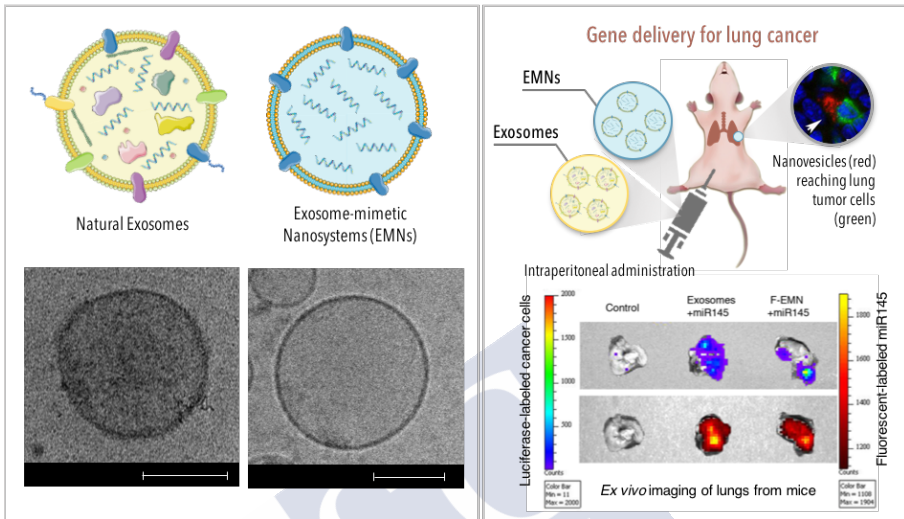


Figura 1. Estrategia inspirada en exosomas para el desarrollo de nuevas terapias dirigidas para CPCNP. Se han desarrollado EMNs morfológicamente similares a los exosomas naturales (izquierda), y probado que estas estructuras presentan una capacidad similar a los exosomas tumorales para alcanzar células tumorales y liberar oligonucleótidos terapéuticos (derecha).

Además de servir para el desarrollo de nuevas estrategias terapéuticas, la nanoplataforma aquí propuesta puede ser útil como herramienta para el estudio en profundidad de determinados lípidos y proteínas específicas que puedan proporcionar información relevante para el diseño de sistemas de liberación selectiva en el campo de la biomedicina.

Por otro lado, la identificación de nuevas dianas farmacológicas en metástasis es una estrategia prometedora para mejorar la supervivencia de los pacientes con CPCNP. Además, se necesitan con urgencia nuevos biomarcadores para aumentar el arsenal de terapias dirigidas y para seleccionar de forma eficaz el tratamiento más adecuado para cada paciente. La metástasis es un proceso ineficiente y altamente complejo en el cual las células tumorales se desprenden del tumor primario y migran a través de la circulación sanguínea o linfática, hasta finalmente colonizar órganos distales. La presencia de

Células Tumorales Circulantes (CTC) individualizadas o agrupadas, es actualmente un marcador pronóstico e indicativo de respuesta a la terapia en pacientes metastásicos. Además, las CTC también pueden proporcionar una fuente valiosa de información genómica y proteómica sobre los pacientes de gran utilidad para el desarrollo de estrategias terapéuticas novedosas en la era de la oncología de precisión. En este sentido, la biopsia líquida destaca por su papel determinante en la obtención de información valiosa para el diagnóstico, pronóstico, respuesta a regímenes de tratamiento específicos o resistencia adquirida, caracterización molecular para toma de decisiones de tratamiento y la posibilidad de descubrir nuevas dianas terapéuticas. Además, permite la evaluación repetida y no invasiva en tiempo real, evitando algunas de las limitaciones clave de las biopsias convencionales de tejido, como la disponibilidad limitada de muestra, el muestreo de tumores invasivos, la infrarrepresentación de la heterogeneidad tumoral y mala descripción de la evolución clonal. La biopsia líquida, que ahora incluye ADN tumoral circulante (ctDNA), ARN libre de células (cfRNA), CTCs, exosomas y proteínas, es una de las técnicas más prometedoras para el descubrimiento de biomarcadores, ya que pueden aislarse de diferentes fluidos corporales y revelar el panorama molecular del tumor.

Esta tesis, propone **la identificación, validación y estudio de un nuevo biomarcador de CPCNP metastásico que pueda proporcionar una nueva diana para el desarrollo de terapias dirigidas, mediante el estudio de las células responsables de las metástasis, las CTCs.** Partiendo de un enfoque basado en el paciente, se aislaron CTC de pacientes con CPCNP avanzado y se analizaron posteriormente. Realizando un perfil genético molecular se identificaron genes expresados de manera diferenciada y significativa en las CTC. A través de un análisis bioinformático los genes identificados se filtraron por su función, ubicación y vías de señalización en las que están involucrados. A continuación, los genes candidatos se analizaron y validaron. El receptor del gusto tipo 1 miembro 3 (TAS1R3) se seleccionó como el objetivo de interés y se validó en una cohorte independiente de CTC aisladas de pacientes con

CPCNP. Esta tesis, describe por primera vez la presencia de TAS1R3 en CTCs de pacientes (**Figura 2**). Posteriormente se investigó el valor pronóstico de la expresión de este biomarcador en las CTCs.

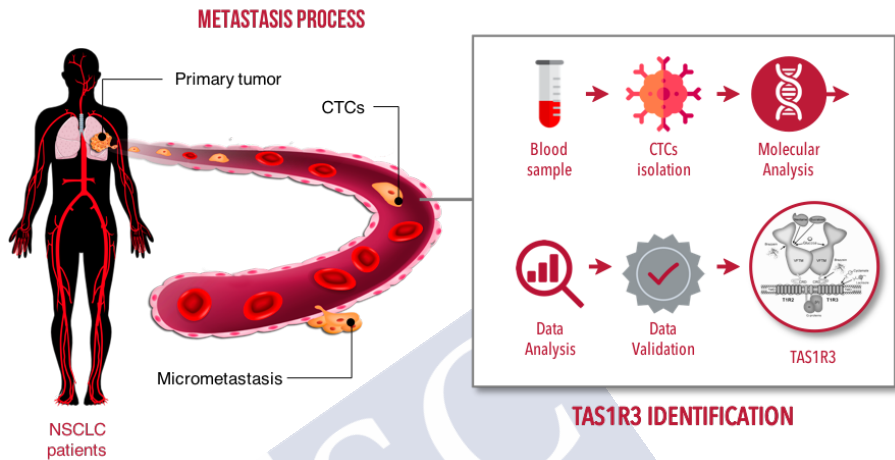


Figura 2. Estrategia inspirada en CTCs para identificar nuevas dianas terapéuticas para el CPCNP metastásico.

Con respecto a la expresión de TAS1R3 en tumores sólidos, se analizó en modelos de xenoinjerto derivado del paciente (PDX) de tumores primarios de CPCNP. Además, el análisis de una base de datos de PDXs generados a partir de tumores primarios y metástasis locales y distales, que incluye muestras de CPCNP y 16 tipos de cáncer adicionales, permitió identificar las características clínicas más relevantes de los tumores que expresan altos niveles de TAS1R3, tales como el estadio del tumor, el estado del tratamiento, la histología y el género, entre otros. Como resultado del análisis se concluye que TAS1R3 se expresa principalmente en el estado metastásico, pacientes en estadio IV, con grado tumoral pobremente diferenciado, pretratados, mayores de 40 años, caucásicos y varones.

TAS1R3 es un receptor acoplado a proteínas G (GPCR) relacionado con la percepción del gusto y el metabolismo celular, expresado principalmente en las glándulas salivales. Cada subunidad TAS1R contiene un gran dominio extracelular llamado Venus FlyTrap Module (~550 aa), vinculado a través de un dominio rico en cisteínas

(~60 aa) a un dominio de siete transmembranas (~260 aa). La proteína codificada puede formar, en combinación con los receptores TAS1R1 o TAS1R2, formas heterodiméricas que reconocen el sabor umami o dulce, respectivamente. TAS1R3 es, además, el único en la familia TAS1R que puede formar homodímeros.

La presencia de este receptor en cáncer no ha sido investigada hasta la fecha. Una mejor comprensión de su biología nos proporcionará información valiosa para el diseño racional de nuevas estrategias terapéuticas. En este sentido, y para concluir este capítulo, se estudió la expresión de TAS1R1 y TAS1R2 en la base de datos de PDXs dando como resultado que TAS1R3 se encuentra más probablemente, formando homodímeros T1R3 / T1R3 en lugar de combinaciones T1R1 / T1R3 o T1R2 / T1R3 en las células tumorales.

Todos estos resultados, en conjunto, destacan el potencial de la biopsia líquida para la identificación de nuevos biomarcadores y señalan a TAS1R3 como un biomarcador novedoso e interesante de CPCNP avanzado y otros tipos de cáncer, cuyo papel particular en el cáncer aún está por dilucidar.

En el tercer apartado de resultados de esta tesis, se realizó un estudio para profundizar en el papel que juega TAS1R3 en CPCNP y en la formación de metástasis, y para explorar su potencial como diana terapéutica. La caracterización de nuevos biomarcadores es fundamental para desarrollar terapias dirigidas eficaces. Estudiar su papel e implicación en la metástasis definitivamente nos ayudará a comprender mejor la progresión tumoral y a diseñar racionalmente la mejor estrategia para combatir la metástasis. En general, se sabe que el desarrollo de cáncer metastásico implica que las células cancerosas del tumor primario alteren varias características distintas para tener éxito en este proceso tan complejo. Algunas de estas modificaciones son i) un cambio de fenotipo epitelial a uno más mesenquimatoso, ii) la adquisición de propiedades de células madre y plasticidad fenotípica, y iii) un cambio en su metabolismo de manera que promueva la supervivencia y el crecimiento metastásico. Los tratamientos convencionales contra el cáncer se dirigen principalmente a la masa del tumor y, en la mayoría de los casos, no logran eliminar las subpoblaciones de células altamente tumorigénicas

y quimioresistentes. Las células madre tumorales (CSC, del inglés “*cancer stem cells*”) se describen como las principales causantes de recurrencia tumoral y metástasis. Desafortunadamente, no existe un marcador universal para la identificación de CSC y la terapia dirigida específicamente a CSC. A medida que aumentemos nuestros esfuerzos para identificar nuevos biomarcadores de CSC, aumentaremos nuestro conocimiento sobre su biología y su función en el cáncer, lo que nos permitirá avanzar en el desarrollo de terapias dirigidas más eficientes que brindarán oportunidades nuevas y prometedoras para tratar la metástasis.

Los primeros experimentos se llevaron a cabo para explorar si la expresión de TAS1R3 estaba relacionada con un fenotipo de célula madre. Para ello se utilizaron diferentes células de cáncer de pulmón y cultivos primarios, y se comparó la expresión de TAS1R3 en la población total con la población con más representación de células madre *in vitro* e *in vivo*. Se demostró que la expresión de TAS1R3 estaba enriquecida en las subpoblaciones CD133+ (un conocido marcador de células madre). Además, se realizó un experimento de formación de esferas, experimento usado ampliamente para la selección y enriquecimiento de células madre normales o CSC, según su capacidad de crecer en medio sin suero suplementado con mitógenos. Se observó una mayor expresión de TAS1R3 en los cultivos de esferas comparado con los controles de cultivo en monocapa y se confirmó el enriquecimiento en células madre con un aumento en la expresión de CD133. Este resultado apunta a que existe un vínculo entre TAS1R3 y CSC.

Seguidamente, para comprender mejor el papel de TAS1R3 durante la progresión de la enfermedad, se generaron dos modelos de ratón diferentes que representan etapas avanzadas de la enfermedad, los modelos CDX y DDX (del inglés *CTC-derived xenograft* y *DTC-derived xenograft*, es decir, modelos de ratón de xenoinjerto derivados de CTCs y de células tumorales diseminadas, DTCs, respectivamente). El modelo de xenoinjerto recapitula el tumor primario, mientras que los modelos CDX y DDX recapitulan mejor las etapas metastásicas. Cuando se analizaron los tumores de CDX y DDX, la expresión de TAS1R3 se vio drásticamente aumentada en

comparación con el tumor primario, sugiriendo que TAS1R3 juega un papel clave en el proceso de diseminación y metástasis (**Figura 3**).

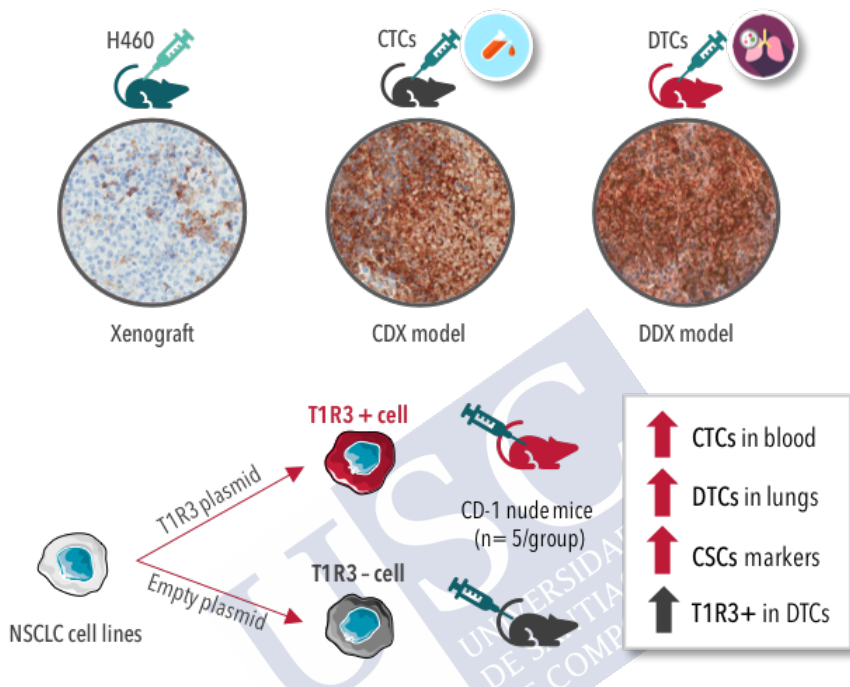


Figura 3. Patrón de expresión de TAS1R3 en el proceso de progresión tumoral en el que se puede observar un aumento de su expresión en modelos representativos de la enfermedad metastásica (CDX y DDX) (arriba). Resumen gráfico del estudio *in vivo* con células que expresan altos y bajos niveles de TAS1R3 (abajo). Las células T1R3 positivas después de la inyección subcutánea, dieron lugar a un mayor número de CTCs y DTCs, a un aumento de marcadores de células madre y TAS1R3 se vio sobreexpresado en los pulmones de los ratones con bajos niveles de TAS1R3 iniciales.

A continuación, se llevaron a cabo experimentos adicionales para comprender si la expresión de TAS1R3 podría verse influenciada por el microambiente tumoral ya que diversos estudios han reportado que está relacionado con el mantenimiento de células madre del cáncer y también con la promoción directa de diferentes procesos como angiogénesis, invasión y metástasis. Los resultados de este trabajo mostraron una ligera modulación de TAS1R3 impulsada principalmente por los macrófagos.

Después, TAS1R3 fue sobreexpresado de forma estable en células de CPCNP y se llevaron a cabo experimentos funcionales *in vitro*. Se evaluaron las capacidades de proliferación, migración e invasión de células TAS1R3 positivas y de células control transfectadas con el mismo vector pero vacío. Las células TAS1R3 positivas mostraron capacidades de proliferación comparables a las células control, una reducida capacidad de migración y una significativamente mayor capacidad de invasión. Sin embargo, teniendo en cuenta que los ensayos basados en células *in vitro* relacionados con la migración y la invasión no siempre pueden predecir de manera fiable el proceso metastásico, se pasó a realizar experimentos *in vivo*, donde el impacto total del microambiente puede influir en el proceso, para evaluar si las células TAS1R3 positivas presentaban una mayor capacidad metastásica. Para ello, se inyectaron células T1R3 positivas y T1R3 negativas en ratones *nude* y se evaluó el potencial metastásico de ambos. El grupo de células T1R3 positivas resultó ser el único en el que se identificaron CTCs en circulación y todas ellas eran TAS1R3 positivas, también se identificó un número significativamente mayor de células diseminadas con un marcado aumento en marcadores de célula madre, comparado con el grupo de ratones control. De manera sorprendente, cuando se analizaron las células diseminadas en los pulmones de los ratones a los que se les inyectaron células T1R3 negativas, se observó una elevada expresión de TAS1R3 (**Figure 3**). Este resultado evidencia que TAS1R3 confiere a las células ciertas ventajas para diseminar, sobrevivir en circulación y metastatizar y apunta nuevamente a una relación con CSCs.

A raíz de este descubrimiento, y una vez evaluada la implicación de TAS1R3 en el proceso de metástasis, este trabajo abre la puerta al desarrollo de nuevas terapias dirigidas para el tratamiento de CPCNP. Algunas de las posibles propuestas incluyen el desarrollo de un programa de descubrimiento de fármacos de molécula pequeña, que puedan inferir en el receptor directamente o en las vías en las que está involucrado, el desarrollo de un anticuerpo monoclonal que pueda sumarse al arsenal de CPCNP metastásico, para que los pacientes con expresión de TAS1R3 puedan beneficiarse de esta terapia dirigida. Finalmente, también es posible pensar en el uso de las

nanoplateformas desarrolladas en el marco de esta tesis para lograr dirigir biomoléculas terapéuticas a células que expresan TAS1R3, mediante su funcionalización con ligandos frente al receptor.

En conjunto, esta tesis propone diferentes estrategias inspiradas en la biología del tumor, para el desarrollo de nuevas terapias dirigidas que pueden suponer un gran avance en el tratamiento del CPCNP metastásico y posiblemente de otros tipos de cáncer.



4 RESUMO *IN EXTENSO*

Identificar novas dianas farmacolóxicas para a metástase é unha necesidade urxente para mellorar o resultado dos pacientes con cancro de pulmón de células non pequenas (CPCNP), dado que o 90% das mortes por cancro débense á metástase. O cancro de pulmón lidera as taxas de incidencia e mortalidade en todo o mundo, debido á súa agresividade e elevada e rápida capacidade de crecemento, e espérase que siga aumentando un 70% no período comprendido entre 2018-2040. O 47,3% dos pacientes con CPCNP diagnósticanse en estadio IV, cando as metástases xa son evidentes e a taxa de supervivencia a 5 anos cae drasticamente a menos do 10%.

Nos últimos anos, o descubrimento de novas dianas terapéuticas implicadas no desenvolvemento dos tumores en cancro levou ao desenvolvemento de novas terapias dirixidas. Isto supuxo unha revolución no campo da oncoloxía, permitindo establecer decisións terapéuticas de forma personalizada, é dicir, en función das características moleculares e xenómicas do tumor de cada paciente e achegándonos á medicina de precisión. As decisións terapéuticas para as terapias dirixidas tómanse en base ao estudo molecular do tumor de cada paciente, en función da expresión de biomarcadores específicos ou mutacións destes. Para o CPCNP avanzado, analízanse os seguintes marcadores para estratificar os pacientes con maiores posibilidades de beneficiarse dunha terapia dirixida: mutacións en EGFR, reordenamentos de ALK, translocacións en ROS1 e mutacións en BRAF. Este tipo de terapia dirixida presenta claras vantaxes fronte á quimioterapia convencional, tales como unha maior especificidade e, por tanto, unha maior eficacia, e unha reducida toxicidade, mellorando así, a calidade de vida do paciente. Actualmente, existen varias terapias dirixidas na práctica clínica, indicadas para o tratamento do CPCNP metastásico en pacientes. A maioría destas

terapias baséanse en moléculas pequenas, inhibidoras da actividade de proteínas tirosina quinasa, por exemplo, erlotinib, crizotinib ou dabrafenib. Tamén se atopan anticorpos monoclonales que viaxan polo organismo ata atopar á súa diana adecuada, situada na superficie das células tumorales, á que se unen e atacan. Algúns exemplos de anticorpos monoclonales para o tratamento de CPCNP metastásico inclúen bevacizumab, ramucirumab e necitumumab. Outra das estratexias en clínica, é a aplicación dos anticorpos monoclonales na inmunoterapia, co obxectivo de unirse ás células do sistema inmune e promover un ataque contra as células cancerosas. A este tipo de anticorpos chámasesles inhibidores de punto de control inmunitario (do inglés immune checkpoint inhibitors) e actualmente hai catro aprobados para o tratamento de cancro de CPCNP metastásico: nivolumab, pembrolizumab, atezolizumab e durvalumab. Para seleccionar os pacientes para a inmunoterapia, analízase a expresión de PD-1 e PD-L1. Pembrolizumab, dirixido contra PD-1, foi a primeira inmunoterapia aprobada como tratamento de primeira liña en pacientes con CPCNP avanzado sen tratamento previo.

Con todo, e a pesar do éxito relativo destas terapias actualmente dispoñibles para o tratamento do CPCNP, case a metade dos pacientes non son elixibles para unha terapia dirixida, xa que se limitan a subpoblacións de pacientes específicas. Ademais, menos da metade dos pacientes seleccionados con biomarcadores benefíciense do tratamento, e aínda se atopan algunhas respostas nas cohortes de "biomarcadores negativos". Por tanto, existe unha necesidade urxente na procura de novos biomarcadores para enriquecer as poboacións de pacientes para resposta e para o desenvolvemento de novas terapias dirixidas, para mellorar a supervivencia dos pacientes con CPCNP localmente avanzado ou metastásico.

A aplicación da nanotecnoloxía na terapia do cancro xa é unha realidade, permitindo incrementar a administración localizada de quimioterapéuticos ao tumor, o que conduce a mellores actividades farmacolóxicas e minimiza significativamente os efectos secundarios. Idealmente, un sistema de liberación exitoso debería ser non tóxico, proporcionar unha mellor farmacocinética e biodistribución, protexer a carga da degradación prematura, a opsonización e unha rápida

eliminación da circulación sistémica, superar as barreiras extra e intracelulares e liberar o material terapéutico no seu sitio obxectivo específico. En 1995, a FDA aprobou a primeira nanopartícula para o tratamento do cancro, Doxil[®], un liposoma PEGilado cargado co fármaco quimioterápico doxorrubicina. Desde entón, outros nanoterapéuticos baseados en liposomas chegaron ao mercado para diferentes tratamentos contra o cancro. Ata a data, Abraxane[®] é a única nanomedicina aprobada pola FDA (2012) e a EMA (2015) para o tratamento do CPCNP avanzado.

Tendo en conta estes antecedentes e a situación actual, o principal obxectivo desta tese é definir novas estratexias terapéuticas inspiradas na bioloxía para pacientes con cancro de pulmón metastásico. Para iso, fixémonos na bioloxía do tumor e atopamos dúas fontes de inspiración para establecer novas estratexias terapéuticas con gran potencial para o tratamento de pacientes metastásicos.

En primeiro lugar, observando o ambiente tumoral, pódese determinar que no noso organismo existe un nanosistema que reúne todas as características dun sistema de liberación ideal, os exosomas. Os exosomas son nanovesículas naturais derivadas da membrana dos endosomas, cun tamaño de entre 30-100 nm, segregadas pola maioría dos tipos de células que, dadas as súas características ideais na comunicación de célula a célula, postuláronse como sistemas de liberación ideais. Con todo, existen algunhas limitacións relacionadas co rendemento relativamente baixo de produción, os protocolos de illamento engorrosos e lentos, a contaminación con materiais non exosomales, a falta de estandarización e validación e, o máis importante, problemas de seguridade para o seu uso en humanos, o que dificulta unha translación real á clínica.

A cuestión é determinar se eses sistemas de liberación poden deseñarse no laboratorio de forma segura. Tendo en conta as vantaxes que achega a nanotecnoloxía, no marco deste traballo propúxose o deseño dunha nova nanoplataforma multifuncional inspirada en exosomas para a liberación selectiva de moléculas antitumorais (como proteínas, oligonucleótidos, fármacos). Con fins comparativos, illáronse e caracterizaron exosomas naturais a partir de liñas de células cancerosas e plasma. As nanoplataformas miméticas de

exosomas (EMN, do inglés “exosome-mimetic nanoplatform”) deseñáronse utilizando metodoloxías simples e escalables e permiten a modulación das súas propiedades, para obter nanosistemas biocompatibles e biodegradables, capaces de transportar de maneira eficiente macromoléculas bioactivas como proteínas e oligonucleótidos. Optimizamos o método de preparación para obter EMNs nanométricas nun só paso sen necesidade de disolventes orgánicos, calor ou alta achega enerxética, diminuíndo así o impacto ambiental e facilitando o proceso de escalado e a súa posible translación. As nanoplataformas desenvolvidas ademais pódense funcionalizar con ligandos capaces de unirse de forma selectiva e eficiente aos receptores de membrana expresados en certos tipos celulares como as células metastásicas.

As EMNs destacan por ter características similares aos exosomas, con respecto ás súas propiedades fisicoquímicas, composición lipídica, capacidade de carga de fármacos, baixa toxicidade e capacidade para interactuar coas células diana do cancro e entregar a súa carga *in vitro* e *in vivo* de maneira tan eficaz como os exosomas, pero superando algunhas das súas limitacións: (i) o rendemento de produción é moito maior que o dos exosomas (obtese 1000 veces máis cantidade de partículas en tempos moito máis curtos), un só lote de EMN obtense en 10 minutos, mentres que os exosomas necesitan como mínimo 5 días, (ii) pódense marcar facilmente con fluoróforos unidos de maneira estable (os EMN marcáronse de maneira eficiente con TopFluor- SM, Cy5 e DiR ao mesmo tempo), (iii) pódense funcionalizar con proteínas de membrana para interactuar selectivamente con células e tecidos sen que haxa outras moléculas descoñecidas influíndo nesta interacción, e (iv) están baleiros e completamente caracterizados, o que supón que non hai outros elementos que poidan producir efectos non desexados, para unha aproximación máis segura. Ademais, (v) os lípidos son materiais baratos e ben caracterizados, e os procesos de produción industrial baixo condicións GMP xa están ben establecidos para liposomas, que é moi importante desde unha perspectiva de translación.

Ademais de servir para o desenvolvemento de novas estratexias terapéuticas, a nanoplataforma aquí proposta pode ser útil como ferramenta para o estudo en profundidade de determinados lípidos e proteínas específicas que poidan proporcionar información relevante para o deseño de sistemas de liberación selectiva no campo da biomedicina.

Doutra banda, a identificación de novas dianas farmacolóxicas en metástases é unha estratexia prometedora para mellorar a supervivencia dos pacientes con CPCNP. Ademais, necesítanse con urxencia novos biomarcadores para aumentar o arsenal de terapias dirixidas e para seleccionar de forma eficaz o tratamento máis adecuado para cada paciente. A metástase é un proceso ineficiente e altamente complexo no cal as células tumorales despréndense do tumor primario e migran a través da circulación sanguínea ou linfática, ata finalmente colonizar órganos distales. A presenza de Células Tumorales Circulantes (CTC) individualizadas ou agrupadas, é actualmente un marcador prognóstico e indicativo de resposta á terapia en pacientes metastásicos. Ademais, as CTC tamén poden proporcionar unha fonte valiosa de información xenómica e proteómica sobre os pacientes de gran utilidade para o desenvolvemento de estratexias terapéuticas novas na era da oncoloxía de precisión. Neste sentido, a biopsia líquida destaca polo seu papel determinante na obtención de información valiosa para o diagnóstico, prognóstico, resposta a réximes de tratamento específicos ou resistencia adquirida, caracterización molecular para toma de decisións de tratamento e a posibilidade de descubrir novas dianas terapéuticas. Ademais, permite a avaliación repetida e non invasiva en tempo real, evitando algunhas das limitacións cruce das biopsias convencionais de tecido, como a dispoñibilidade limitada de mostra, a mostraxe de tumores invasivos, a infrarrepresentación da heteroxeneidade tumoral e mala descrición da evolución clonal. A biopsia líquida, que agora inclúe ADN tumoral circulante (ctDNA), ARN libre de células (cfRNA), CTCs, exosomas e proteínas, é unha das técnicas máis prometedoras para o descubrimento de biomarcadores, xa que poden illarse de diferentes fluídos corporais e revelar o panorama molecular do tumor.

Esta tese, propón a identificación, validación e estudo dun novo biomarcador de CPCNP metastásico que poida proporcionar unha nova diana para o desenvolvemento de terapias dirixidas, mediante o estudo das células responsables das metástases, as CTCs. Partindo dun enfoque baseado no paciente, illáronse CTC de pacientes con CPCNP avanzado e analizáronse posteriormente. Realizando un perfil xenético molecular identificáronse xenes expresados de maneira diferenciada e significativa nas CTC. A través dunha análise bioinformático os xenes identificados filtráronse pola súa función, localización e vías de sinalización nas que están involucrados. A continuación, os xenes candidatos analizáronse e validaron. O receptor do gusto tipo 1 membro 3 (TAS1R3) seleccionouse como o obxectivo de interese e validouse nunha cohorte independente de CTC illadas de pacientes con CPCNP. Esta tese, describe por primeira vez a presenza de TAS1R3 en CTCs de pacientes. Posteriormente investigouse o valor prognóstico da expresión deste biomarcador nas CTCs.

Con respecto á expresión de TAS1R3 en tumores sólidos, analizouse en modelos de xenoinxerto derivado do paciente (PDX) de tumores primarios de CPCNP. Ademais, a análise dunha base de datos de PDXs xerados a partir de tumores primarios e metástases locais e distais, que inclúe mostras de CPCNP e 16 tipos de cancro adicionais, permitiu identificar as características clínicas máis relevantes dos tumores que expresan altos niveis de TAS1R3, tales como o estadio do tumor, o estado do tratamento, a histoloxía e o xénero, entre outros. Como resultado da análise conclúese que TAS1R3 exprésase principalmente no estado metastásico, pacientes en estadio IV, con grao tumoral pobremente diferenciado, pretratados, maiores de 40 anos, caucásicos e homes.

TAS1R3 é un receptor axustado a proteínas G (GPCR) relacionado coa percepción do gusto e o metabolismo celular, expresado principalmente nas glándulas salivales. Cada subunidade TAS1R contén un gran dominio extracelular chamado Venus FlyTrap Module (~550 aa), vinculado a través dun dominio rico en cisteínas (~60 aa) a un dominio de sete transmembranas (~260 aa). A proteína codificada pode formar, en combinación cos receptores TAS1R1 ou TAS1R2, formas heterodiméricas que recoñecen o sabor umami ou

doce, respectivamente. TAS1R3 é, ademais, o único na familia TAS1R que pode formar homodímeros.

A presenza deste receptor en cancro non foi investigada ata a data. Unha mellor comprensión da súa bioloxía proporcionaranos información valiosa para o deseño racional de novas estratexias terapéuticas. Neste sentido, e para concluír este capítulo, estudouse a expresión de TAS1R1 e TAS1R2 na base de datos de PDXs dando como resultado que TAS1R3 atópase máis probablemente, formando homodímeros T1R3/T1R3 en lugar de combinacións T1R1/T1R3 ou T1R2/T1R3 nas células tumorais.

Todos estes resultados, en conxunto, destacan o potencial da biopsia líquida para a identificación de novos biomarcadores e sinalan a TAS1R3 como un biomarcador novo e interesante de CPCNP avanzado e outros tipos de cancro, cuxo papel particular no cancro aínda está por dilucidar.

No terceiro apartado de resultados desta tese, realizouse un estudo para profundar no papel que xoga TAS1R3 en CPCNP e na formación de metástase, e para explorar o seu potencial como diana terapéutica. A caracterización de novos biomarcadores é fundamental para desenvolver terapias dirixidas eficaces. Estudiar o seu papel e implicación na metástase definitivamente axudaranos a comprender mellor a progresión tumoral e a deseñar racionalmente a mellor estratexia para combater a metástase. En xeral, sábese que o desenvolvemento de cancro metastásico implica que as células cancerosas do tumor primario alteren varias características distintas para ter éxito neste proceso tan complexo. Algunhas destas modificacións son i) un cambio de fenotipo epitelial a un máis mesenquimatoso, ii) a adquisición de propiedades de células nai e plasticidade fenotípica, e iii) un cambio no seu metabolismo de maneira que promova a supervivencia e o crecemento metastásico. Os tratamentos convencionais contra o cancro diríxense principalmente á masa do tumor e, na maioría dos casos, non logran eliminar as subpoboacións de células altamente tumorixénicas e quimioresistentes. As células nai tumorais (CSC, do inglés “cancer stem cells”) describíense como as principais causantes de recorrencia tumoral e metástase. Desafortunadamente, non existe un marcador

universal para a identificación de CSC e a terapia dirixida especificamente a CSC. A medida que aumentemos os nosos esforzos para identificar novos biomarcadores de CSC, aumentaremos o noso coñecemento sobre a súa bioloxía e a súa función no cancro, o que nos permitirá avanzar no desenvolvemento de terapias dirixidas máis eficientes que brindarán oportunidades novas e prometedoras para tratar a metástase. Os primeiros experimentos levaron a cabo para explorar se a expresión de TAS1R3 estaba relacionada cun fenotipo de célula nai. Para iso utilizáronse diferentes células de cancro de pulmón e cultivos primarios, e comparouse a expresión de TAS1R3 na poboación total coa poboación con máis representación de células nai *in vitro* e *in vivo*. Demostrouse que a expresión de TAS1R3 estaba enriquecida nas subpoblacións CD133+ (un coñecido marcador de células nai). Ademais, realizouse un experimento de formación de esferas, experimento usado amplamente para a selección e enriquecemento de células nai normais ou CSC, segundo a súa capacidade de crecer no medio sen soro suplementado con mitóxenos. Observouse unha maior expresión de TAS1R3 nos cultivos de esferas comparado cos controis de cultivo en monocapa e confirmouse o enriquecemento en células nai cun aumento na expresión de CD133. Este resultado apunta a que existe un vínculo entre TAS1R3 e CSC.

Seguidamente, para comprender mellor o papel de TAS1R3 durante a progresión da enfermidade, xeráronse dous modelos de rato diferentes que representan etapas avanzadas da enfermidade, os modelos CDX e DDX (do inglés CTC- derived xenograft e DTC- derived xenograft, é dicir, modelos de rato de xenoinjerto derivados de CTCs e de células tumorais diseminadas, DTCs, respectivamente). O modelo de xenoinjerto recapitula o tumor primario, mentres que os modelos CDX e DDX recapitulan mellor as etapas metastásicas. Cando se analizaron os tumores de CDX e DDX, a expresión de TAS1R3 viuse drasticamente aumentada en comparación co tumor primario, suxerindo que TAS1R3 xoga un papel cruce no proceso de diseminación e metástase.

A continuación, levaron a cabo experimentos adicionais para comprender se a expresión de TAS1R3 podería verse influenciada polo microambiente tumoral xa que diversos estudos reportaron que

está relacionado co mantemento de células nai do cancro e tamén coa promoción directa de diferentes procesos como angiogénesis, invasión e metástase. Os resultados deste traballo mostraron unha lixeira modulación de TAS1R3 impulsada principalmente polos macrófagos.

Despois, TAS1R3 foi sobreexpresado de forma estable en células de CPCNP e levaron a cabo experimentos funcionais *in vitro*. Avaliáronse as capacidades de proliferación, migración e invasión de células TAS1R3 positivas e de células control transfectadas co mesmo vector pero baleiro. As células TAS1R3 positivas mostraron capacidades de proliferación comparables ás células control, unha reducida capacidade de migración e unha significativamente maior capacidade de invasión. Con todo, tendo en conta que os ensaios baseados en células *in vitro* relacionados coa migración e a invasión non sempre poden predicir de maneira fiable o proceso metastásico, pasouse a realizar experimentos *in vivo*, onde o impacto total do microambiente pode influír no proceso, para avaliar se as células TAS1R3 positivas presentaban unha maior capacidade metastásica. Para iso, inxectáronse células T1R3 positivas e T1R3 negativas en ratos nude e avaliouese o potencial metastásico de ambos. O grupo de células T1R3 positivas resultou ser o único no que se identificaron CTCs en circulación e todas elas eran TAS1R3 positivas, tamén se identificou un número significativamente maior de células diseminadas cun marcado aumento en marcadores de célula nai, comparado co grupo de ratos control. De maneira sorprendente, cando se analizaron as células diseminadas nos pulmóns dos ratos aos que se lles inxectaron células T1R3 negativas, observouse unha elevada expresión de TAS1R3. Este resultado evidencia que TAS1R3 confire ás células certas vantaxes para diseminar, sobrevivir en circulación e metastatizar e apunta novamente a unha relación con CSCs.

Por mor deste descubrimento, e unha vez avaliada a implicación de TAS1R3 no proceso de metástase, este traballo abre a porta ao desenvolvemento de novas terapias dirixidas para o tratamento de CPCNP. Algunhas das posibles propostas inclúen o desenvolvemento dun programa de descubrimento de fármacos de molécula pequena, que poidan inferir no receptor directamente ou nas vías nas que está involucrado, o desenvolvemento dun anticorpo monoclonal que poida

sumarse ao arsenal de CPCNP metastásico, para que os pacientes con expresión de TAS1R3 poidan beneficiarse desta terapia dirixida. Finalmente, tamén é posible pensar no uso das nanoplataformas desenvolvidas no marco desta tese para lograr dirixir biomoléculas terapéuticas a células que expresan TAS1R3, mediante a súa funcionalización con ligandos fronte ao receptor.

En conxunto, esta tese propón diferentes estratexias inspiradas na bioloxía do tumor, para o desenvolvemento de novas terapias dirixidas que poden supoñer un gran avance no tratamento do CPCNP metastásico e posiblemente doutros tipos de cancro.





INTRODUCTION



5 INTRODUCTION

5.1 LUNG CANCER

Cancer is a major public health problem worldwide and the second-leading cause of death globally (**Figure 1**). Almost ten million people die from cancer every year and this number is estimated to reach over 13 million in 2030 (Siegel, Miller and Jemal, 2017). The most common causes of cancer death are lung, liver, and stomach cancers in men, and breast, lung and colorectal cancers in women (Bray *et al.*, 2018).

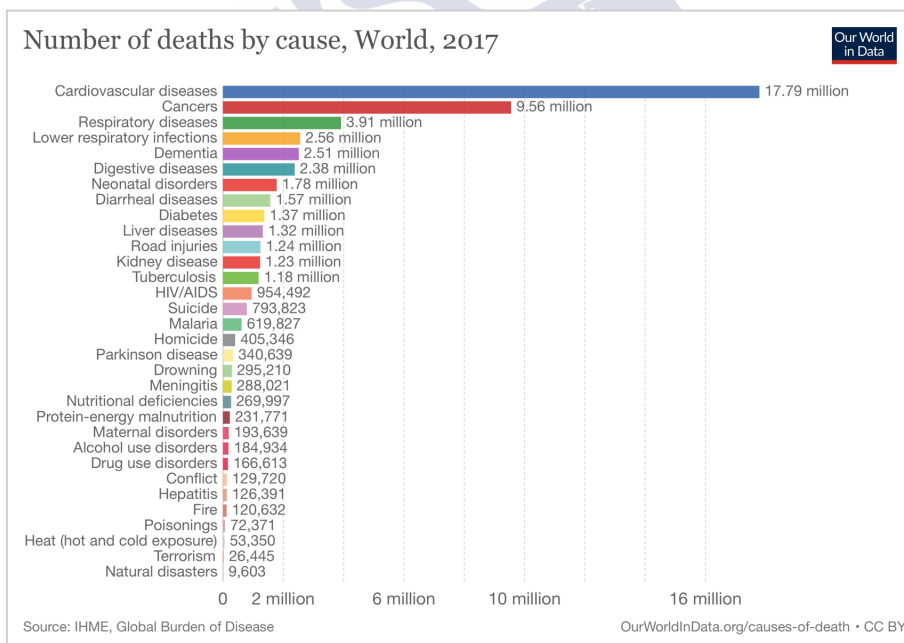


Figure 1. Number of deaths by cause in the world in 2017. Source: Our world in data.

Lung cancer is the most commonly diagnosed type of cancer and the leading cause of cancer-related deaths worldwide, with approximately 15% of patients surviving 5 years after diagnosis (Figure 2). Smoking has been definitely established as the leading cause of lung cancer. Indeed, the percentages of lung cancer estimated to be caused by tobacco smoking in males and females are 90% and 78%, respectively. Other risk factors for lung cancer include HIV infection, family history of lung cancer, exposure to secondhand smoke, radon, asbestos, arsenic, chromium, nickel, soot, tar, radiation or air pollution (National Cancer Institute, 2020).

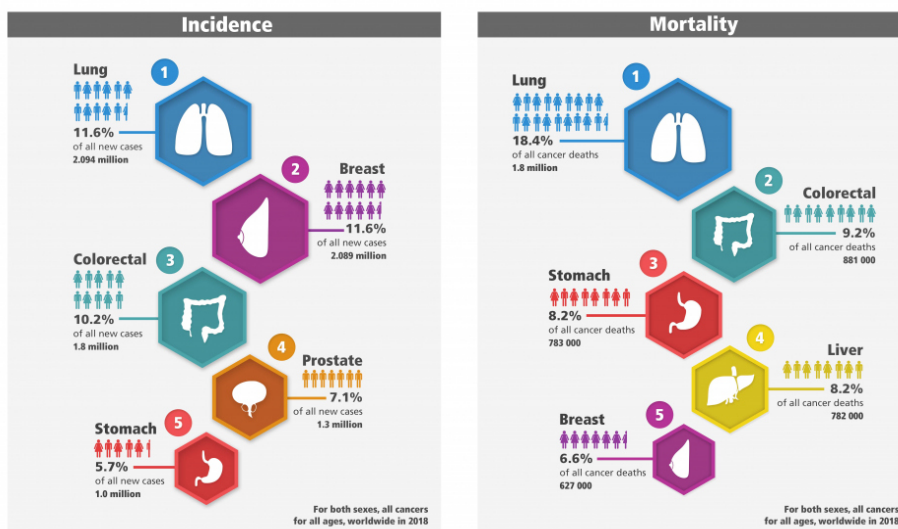


Figure 2. Percentages of new cancer cases and deaths worldwide in 2018, for both sexes and all ages. Source: Global Cancer Observatory - Globocan 2018

Lung cancer can be subdivided into two main histological groups: non-small cell lung cancer (NSCLC) and small cell lung cancer (SCLC). Each type is named for the type of cancer cells found in the tumor, and for their appearance under the microscope. NSCLC is the most common histology, representing the 85% of all diagnosed lung cancer cases, whereas SCLC only accounts for the 15%. NSCLC is generally subcategorized into adenocarcinoma (40%), squamous cell carcinoma (25%), large cell carcinoma (10%) and others of low

frequency. When biopsies and cytological species are small and poorly differentiated, the differences between adenocarcinoma and squamous cell carcinoma appear indistinguishable, therefore IHC analysis becomes essential for a precise diagnosis (Villalobos and Wistuba, 2017). However, it is not an easy task, due to the great histological and molecular heterogeneity within each of these categories (Zappa and Mousa, 2016).

Lung cancer is categorized in stages from 0 – IV based on ‘tumor, nodes and metastasis’ according to the American Joint Committee on Cancer (AJCC) TNM system (Feng and Yang, 2019). The size and extend of the main tumor (T), the spread to nearby lymph nodes (N) and the spread/metastasis to distant sites (M) are the three key pieces of information needed (Akaza, 2020). Importantly, 47.3% of patients are categorized with stage IV at the time of diagnosis when they are not suitable for tumor resection (Cancer System Performance, 2020).

In the last 20 years, great efforts have been made in order to understand the molecular abnormalities underlying lung cancer. The identification of different driver mutations has allowed further characterization of lung tumors, such as *EGFR*, *KRAS*, *ERBB2* (*HER2*), *BRAF*, *ALK*, *ROSI*, *RET*, or *MET*. This progress in the molecular characterization of lung tumors has led to the development of targeted therapies and of a new generation of immunotherapy (Testa, Castelli and Pelosi, 2018). Targeted therapeutic approaches are discussed in more detail in the section 4.3.

5.2 THE METASTATIC CASCADE

Metastases are the cause of the majority of human cancer deaths (Dillekås, Rogers and Straume, 2019). In the particular case of NSCLC, the overall 5-year survival rate is 24%, however, it falls to 6% in advanced stages of the disease when metastases occur (Howlader *et al.*, 2020).

The process of metastasis is defined by a cascade of complex events in which malignant cells detach from the primary tumor, invade through the basement membrane and then migrate into the circulation, either via the blood or lymphatic vessels, to finally spread to distant sites to form metastases (San Juan *et al.*, 2019). Despite the

fact that tumors at an early stage can many times be surgically removed, there is growing evidence that dissemination could indeed happen at a very early stage in the carcinogenesis process (Hüsemann *et al.*, 2008), a fact that could explain why, in some tumor types such as pancreatic cancer, the 5-year survival even for localized disease is so poor.

The metastatic cascade can be broadly divided into three main phases, i) pre-metastatic initiation, ii) dissemination and iii) colonization, each of these composed by different steps and participants as represented in **Figure 3**.

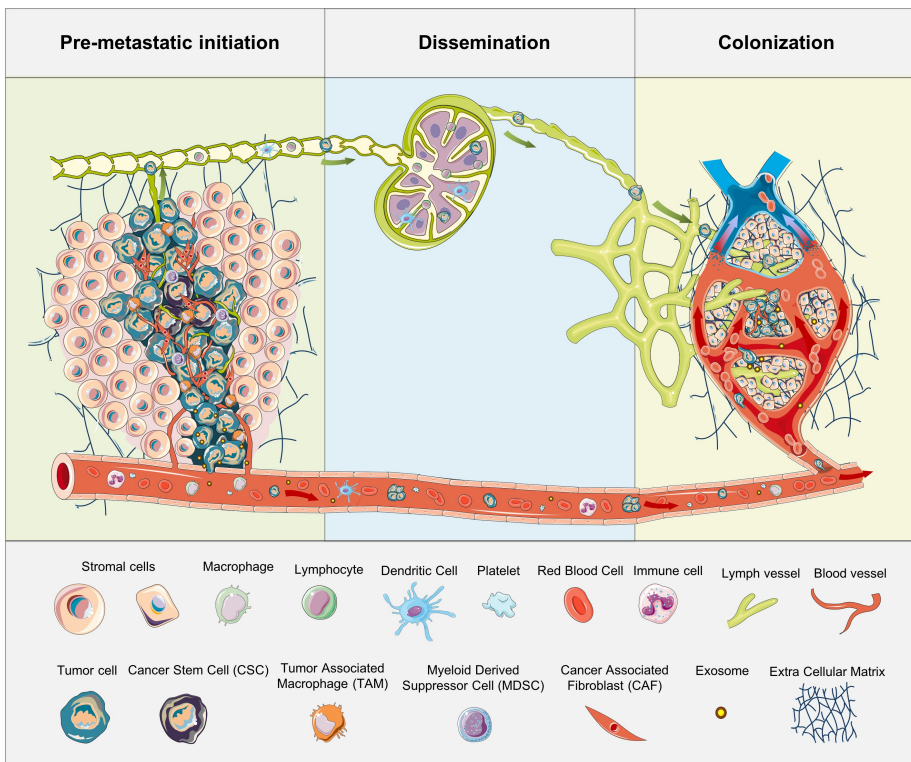


Figure 3. Process of metastatic dissemination. Different cellular types that are involved in the metastatic dissemination are represented in this image and the different stages and routes to disseminate from the primary tumor. From Vázquez-Ríos *et al.* 2018 with the permission of Elsevier, Copyright (2020).

5.2.1 Pre-metastatic initiation

Pre-metastatic initiation starts as a consequence of chromosomal instability caused by continuous errors during mitosis. It is followed by epithelial to mesenchymal transition (EMT), process that describe the acquisition of a mesenchymal phenotype by epithelial tumor cells, governed by a number of growth factors and signaling pathways, and under the influence of cancer-associated fibroblasts (CAFs) and other components, such as tumor-infiltrating leukocytes (i.e., neutrophils and macrophages) (San Juan *et al.*, 2019). It has been recently reported that tumor cells that express an intermediate epithelial to mesenchymal phenotype are more effective in circulation, colonization at the secondary site, and the development of metastasis (Andriani *et al.*, 2016; Pastushenko *et al.*, 2018; Wolf *et al.*, 2019). Local invasiveness, i.e. the entry of well-restrained cancer cells into the surrounding tumor-associated stroma requires tumor cells to reduce their adhesion to neighbor cells, increase their motility, and degrade the extracellular matrix (ECM) (Chitty *et al.*, 2018). The process of dysregulation of the ECM and their components is enabled by the functions of matrix metalloproteinases (MMPs) (Conlon and Murray, 2019).

5.2.2 Dissemination

In the next step, tumor cells intravasate into the lymphatic or blood vessels. Different molecular changes foster the ability of these cells to cross the pericyte and endothelial cell barriers (Valastyan and Weinberg, 2011). Tumor cells secrete cytokines such as vascular endothelial growth factor (VEGF), inducing the formation of leaky blood vessels, or causing endothelial cell death by releasing reactive oxygen species (ROS) (López-Otín and Matrisian, 2007). Interestingly, activated platelets at tumor vessel disruption sites can also contribute, together with cytokines and growth factors secreted by the tumor stroma, to the initial invasive phenotype of tumor cells by the release of transforming growth factor beta TGF β (San Juan *et al.*, 2019).

Once in the vasculature, tumor cells can disseminate by the hematogenous or by the lymphatic route. Lymphatic intravasation

occurs more easily than into the blood vessels, given that lymph vessels do not have as dense interendothelial junctions as blood vessels, and that lymph circulation is slower than blood circulation (Zavyalova *et al.*, 2019). When tumor cells disseminate through the lymphatic system, cells reach the lymph nodes, where they can reside in a dormant state before traveling to distant organs to form secondary metastases. For hematogenous dissemination, cells circulate into the bloodstream until they find a distant metastatic site. The direct consequence of intravasation is the appearance of circulating tumor cells (CTCs). CTCs were first identified by Thomas Ashworth in 1869 (Ashworth, 1869), however, the CTC research has been hampered by the technical difficulties to detect these rare cells (J. Zhou *et al.*, 2017). Technological advances in the last decade have facilitated the detection of CTCs within the bloodstream of carcinoma patients, as for example reported by our research group (Barbazán, Vieito, *et al.*, 2012; Muínelo-Romay *et al.*, 2014). During circulation, CTCs have to survive and overcome a range of events (e.g. anchorage-free survival and shear stress) in order to reach distant organs. Still remains controversial whether CTCs have the ability to actively target certain organs or if they are passively arrested within capillary beds, such as those in lung and liver, due to the architecture of the vasculature. CTCs can travel either as individual cells or, more often, as clusters. These clusters appear in some cases to be heterogeneous in nature, exhibiting combinations of epithelial and mesenchymal traits (Chitty *et al.*, 2018).

In addition to the invading cancer cells, clusters contain stromal cells and immune components from the original microenvironment that contribute to the heterogeneity of the cluster and enhance its survival. Association with platelets provide CTCs with both protection from shear forces and evasion from immune detection (Miles *et al.*, 2008; Joyce and Pollard, 2009; Gay and Felding-Habermann, 2011), neutrophils participate suppressing leukocyte activation, which increases the chances of CTC survival (Leach, Morton and Sansom, 2019), and tumor-associated macrophages (TAMs) (Hamilton and Rath, 2017), myeloid-derived suppressor cells (MDSCs) (Liu, Liao and Zhao, 2016; Sprouse *et al.*, 2019), and

lymphocytes (Ye *et al.*, 2017) were also found to interact with CTCs in the bloodstream (Heeke *et al.*, 2019).

5.2.3 Colonization

After intravasation, CTCs that have survived in the circulation may experience extravasation. Only a small proportion of CTCs will eventually become disseminated tumor cells (DTCs). This process includes several steps, such as cells entering into the parenchyma of distant tissues, adapting to survive in foreign microenvironments, and eventually colonizing and nesting to generate metastasis (Massagué and Obenauf, 2016). Even a smaller fraction of these DTCs are capable of progressing toward overt metastasis (Dasgupta, Lim and Ghajar, 2017; Chitty *et al.*, 2018). They create transient interactions with the endothelium, followed by stronger adhesions mediated by selectins and vascular cells adhesion molecules (VCAMs), respectively. CTCs can also be trapped into isolated small vessels into the microcirculation, becoming activated and eventually transmigrating (Gupta and Massagué, 2006; Fares *et al.*, 2020). Upon arrival the tumor cells may become dormant during months, years or even decades. Dormant tumor cells are typically seen as chemotherapy-resistant because they are not actively dividing; however, the molecular mechanisms underlying this resistance are still poorly understood (Chitty *et al.*, 2018).

Survival of micrometastases at distant organ sites involves cellular adaptation and cross-talk between tumor and the environment (Fares *et al.*, 2020). The mechanisms by which tumor cells alter this scenario, i.e. ECM remodeling and activation/modification of other stromal cellular components, still remain not fully understood. It is now well established the idea that the metastatic sites can be transformed selectively and actively prior to tumor cell arrival by the primary tumor, creating the so-called “pre-metastatic niche” (Peinado *et al.*, 2017; Guo *et al.*, 2019). In this context, extracellular vesicles, and in particular exosomes, have gained increased attention in the last years.

Exosomes are small membranous vesicles with endocytic origin, and an average size ranging from 50 to 120 nm. They are secreted by

mostly every cellular type in physiological and pathological conditions and have been found in a wide variety of biological fluids. Exosomes are really effective in cell to cell communication even at long-distances transporting different bioactive molecules, such as nucleic acids (RNAs, DNAs, mRNA, miRNA), proteins, and lipids. Exosomes provide protection of the cargo against degradation, increased stability, and the possibility to cross biological barriers such as the brain blood barrier (BBB). Tumor cell-derived exosomes are involved in several functions in cancer progression and metastasis (**Figure 4**), e.g., have been shown to accelerate tumorigenesis, by modulating the immune system and the parenchyma, and induce angiogenesis. Moreover, exosomes are also related to the formation of organ-specific metastasis and to the pre-metastatic niche modelling (Tickner *et al.*, 2014; Hoshino *et al.*, 2015; Steinbichler *et al.*, 2017).

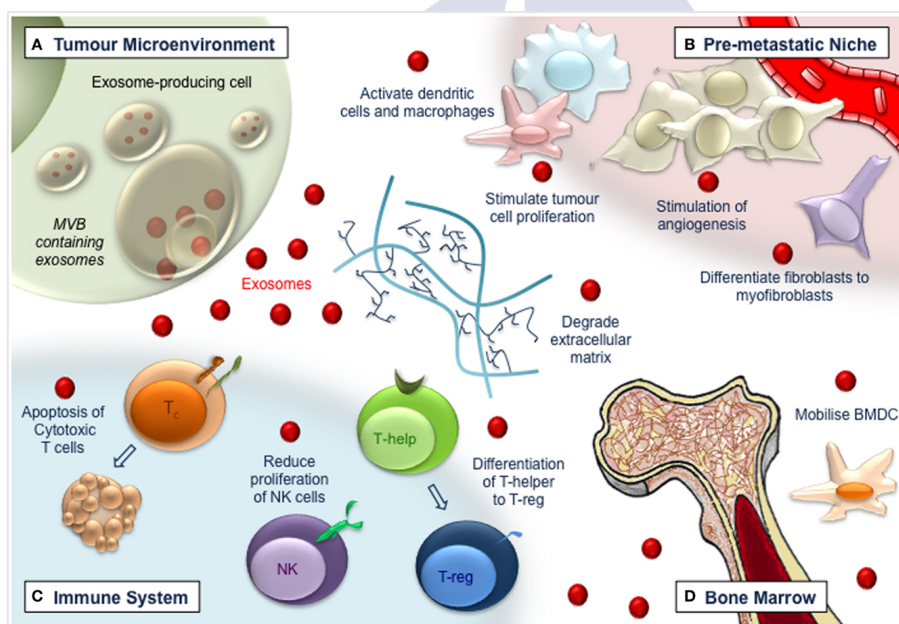


Figure 4. Exosome roles in cancer progression and metastasis. From Tickner *et al.*, 2017 .

Once the tumor cells have reached the distant pre-metastatic niche, the so-call mesenchymal to epithelial transition (MET) takes place,

reverting tumor cells to a highly proliferative phenotype to enable the formation of macrometastasis (Steinbichler *et al.*, 2017).

The metastatic process is complex and inefficient with many cancer cells initially achieving access to the circulation, but only a few of them (estimated around 0.01%), finally succeeding in proliferating as distant metastases (Massagué and Obenauf, 2016). Despite this limited efficiency, the spread of cancer cells from the primary tumor to seed secondary tumors in distant sites, continues to be one of the greatest challenges in cancer treatment today.

To summarize, metastasis is an extremely complex process, hence, the development of new approaches that target one or more steps is urgently needed, to ultimately improve the outcome of patients with metastatic cancer.

5.3 CURRENT THERAPEUTIC APPROACHES IN ADVANCED NSCLC

Lung cancer is the most commonly diagnosed type of cancer and the leading cause of cancer-related death worldwide (1.6 million deaths/year). Lung cancer also leads the economic burden worldwide with 18.8 billion euros per year cost in Europe, mainly related with the appearance of disseminated disease (Howlader *et al.*, 2020).

Curative surgery is the standard of care for early-stage patients with a good performance status, however, 35-50% of the resected patients relapse after an apparently successful surgical treatment (Herreros-Pomares *et al.*, 2019). Importantly, around 75% of patients are diagnosed at advanced stages, when surgery is not possible, and the 5-year survival rate drops to 6% for both sexes (Howlader *et al.*, 2020). For a long time, platinum-based doublets have been the standard first-line treatment option for unresectable advanced NSCLC (Schiller *et al.*, 2002). Despite the survival improvement achieved with first-line chemotherapy, about 30% of patients do not obtain a tumor response. Moreover, those patients, initially sensitive to treatment, acquire resistance and develop tumor progression after a median of about 5 months (Lazzari *et al.*, 2017). Until 2005, treatment choice was mainly based on the distinction between NSCLC and small cell lung cancer. The approval of bevacizumab in 2006 (Sandler *et al.*, 2006) and pemetrexed in 2008 (Scagliotti *et al.*, 2008) showed

that the discrimination between squamous and non-squamous histology was a crucial element for therapeutic selection, since bevacizumab and pemetrexed can be administered to patients with non-squamous tumors only, for safety and efficacy reasons (Lazzari *et al.*, 2017). The treatment strategy now considers factors such as histology, clinical stage, age, performance status, comorbidities, the patient's preferences, the molecular study and an approach to the immune situation that is becoming more and more important every time.

During the last years an increasing number of targetable major pathways have been identified, such as EGFR, PI3K/AKT/mTOR, RAS–MAPK, and NTRK/ROS1, leading to a new era of personalized medicine for NSCLC (Yuan *et al.*, 2019). Besides, immunotherapy has become the most revolutionary treatment in solid tumors patients (Pakkala and Ramalingam, 2018).

Overall, a third of the patients harbor an oncogenic driver event that is druggable, another third of the patients have an inflamed tumor micro-environment that can be targeted with an immune checkpoint inhibitor, and the remainder are treated with combination chemotherapy. Due to these novel approaches, the median overall survival (OS) for patients with metastatic cancer has moderately improved (Lazzari *et al.*, 2017). Despite this, the success of targeted therapies is still limited to a subset of patients, being therefore mandatory to focus the efforts on developing novel alternatives specifically tailored to make a breakthrough in the management of disseminated cancer. Taking a deeper look into these therapeutic options and other novel strategies that are being investigated, will provide an overview of the main therapeutic limitations, and the most promising alternatives for improvement.

5.3.1 Targeted therapy

Targeted therapy is the cornerstone of precision medicine, based on the genetic understanding of the disease to prevent, diagnose, and treat diseases. It can also be called personalized medicine, given that every patient receives the treatment that better fits their particular

genes and proteins, providing them with significant responses and lesser toxicities compared with broad spectrum cytotoxic therapy.

Targeted therapies in cancer refer to drugs (e.g., small molecules) or other substances (e.g., biologicals), that interfere with specific molecules (“molecular targets”) involved in some key aspects of cancer development, growth and spread (**Figure 5**).

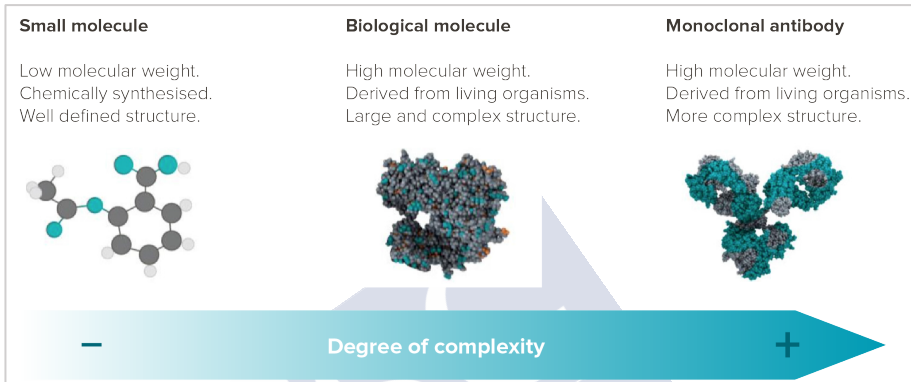


Figure 5. Different types of targeted therapeutics. Molecular weight, origin and complexity comparison. Source: mAbxience.

Small molecules are defined as compounds with relatively low molecular weight (< 900 daltons) that are able to penetrate into cells, to target specific proteins within the cells. Many known small molecule inhibitors focus on inactivating kinases and interrupting the signaling pathways that are dysregulated during carcinogenesis (e.g., crizotinib, erlotinib, and gefinitib (Lee, Tan and Oon, 2018)). On the other hand, monoclonal antibodies are of approx. 150 KDa, therefore they cannot enter cancer cells, so their targets must be extracellular (Shepard *et al.*, 2017). They have exquisite target selectivity and hence, less toxicity than small molecules. In 1985, the FDA approved the first mAb, against CD3, for the treatment of kidney transplant rejection (Norman *et al.*, 1988). From then, 76 mAb have received marketing approval, with near 30 mAb indicated for oncological treatment. The mAb field is relatively young but is growing fast, with more than 30 candidates in late-stage clinical trials for cancer therapy.

The development of targeted therapies has resulted in substantial benefits in terms of survival and quality of life for cancer patients.

Over the last twenty years, different drugs have been approved by the Food and Drug Administration (FDA) and the European Medicines Agency (EMA) for several tumor types, as for example imatinib (gastrointestinal stromal tumors and dermatofibrosarcoma protuberans) (Ri *et al.*, 2006), or cetuximab (colorectal cancer and head and neck cancer) (Bertino *et al.*, 2016), amongst others. In the particular case of NSCLC, the main breakthroughs refer to the introduction of targeted therapies against EGFR mutations, rearrangements involving the ALK or ROS1 genes, and more recently, B-RAF mutations, all known as actionable driver mutations (Planchard *et al.*, 2016, 2018). Specific treatments are disclosed in the next sections. Many of the drugs targeting these targets have shown clinical benefits and some of them have even replaced chemotherapy as the first line treatment (Yuan *et al.*, 2019). Patients with advanced NSCLC undergo routine genomic testing for clinically actionable genomic alterations. Within this scenario, detecting key driver mutations in NSCLC is currently critical for clinicians to make treatment decisions. The main driver mutations in advanced NSCLC, the currently approved targeted therapies and guidelines are represented in **Figure 6**.

5.3.1.1 ALK rearrangements

Anaplastic lymphoma kinase (*ALK*) fusion oncogene is a tyrosine kinase that can be aberrantly expressed in several tumor types by chromosomal rearrangements involving the *ALK* gene loci on chromosome 2 and 5. The resulting fusion gene leads to constitutive activation of ALK and downstream signaling pathways that drive oncogenesis. The presence of ALK in NSCLC is generally low, approximately 5% of NSCLC tumors, and occurs independently of *EGFR* or *KRAS* mutations (Golding *et al.*, 2018). Different ALK tyrosine kinase inhibitors (TKIs) have been approved by the FDA for the treatment of *ALK*-rearranged NSCLC patients. In 2011, crizotinib was approved as first-line treatment for patients with *ALK*-rearranged NSCLC. Second- ceritinib, alectinib, brigatinib and third-generation lorlatinib ALK inhibitors have also been developed to overcome acquired resistance to crizotinib (Yuan *et al.*, 2019).

5.3.1.2 BRAF mutations

BRAF is a serine/threonine kinase that is part of the canonical MAP/ERK signaling pathway. Mutations in the BRAF oncogene are found in 2-4% of all NSCLC patients. The most common activating mutation is at codon 600 position (V600E) and is associated with valine substitution for glutamate amino acid within the exon 15 of the kinase domain (Planchard *et al.*, 2016).

Recently, the EMA and FDA approved the use of the BRAF inhibitor, dabrafenib, in combination with a mitogen-activated protein kinase (MEK) inhibitor, trametinib, in patients with NSCLC and BRAF V600E mutation (Khunger, Khunger and Velcheti, 2018).

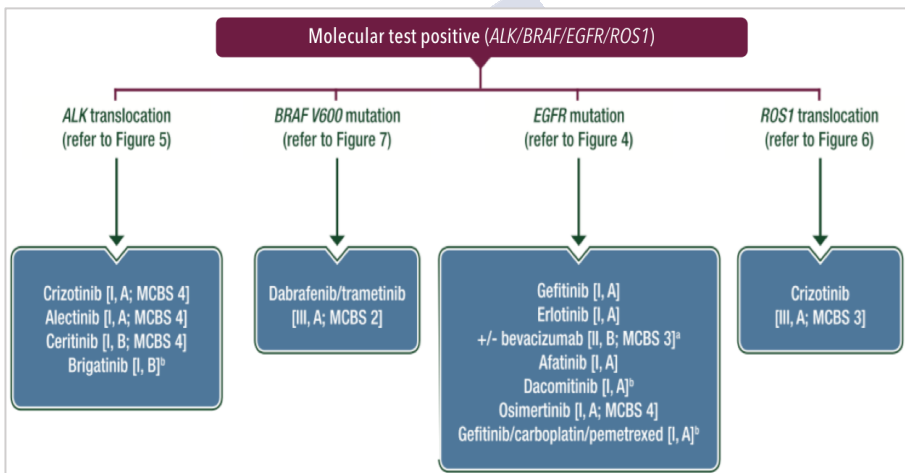


Figure 6. Clinical Practice Guidelines in Oncology for advanced NSCLC targeted therapy. Source: National Comprehensive Cancer Network (NCCN). Feb 11, 2020.

5.3.1.3 EGFR mutation

The *EGFR* gene is located in the human chromosome 7 and its protein is a member of the tyrosine kinase type I receptors family. Some of the ligands of this receptor are epidermal growth factor (EGF), transforming growth factor- α (TGF- α), amphiregulin, heparin-binding EGFR, and betacellulin, all of them binding to domains I and III of EGFR. Subsequent exposure of domain II and IV

results in receptor dimerization via disulfide bonds. When EGFR is forming dimers, the tyrosine residues of the cytoplasmic region are phosphorylated and initiate the intracellular signaling cascade and gene transcription processes. Consequences of this initiation are activation of angiogenesis, improved cell adhesion, cell motility, and proliferation, inhibition of apoptosis and formation of metastasis (Wee and Wang, 2017). Downstream signaling cascades of EGFR are triggered by the following pathways: RAS/RAF/MEK/MAPK/ERK, phosphatidylinositol 3-kinase (PI3K) and Akt, protein kinase C (PKC), Src, and JAK/STAT (Xu, Johnson and Grandis, 2017).

Some of the strategies developed to target EGFR, are monoclonal antibodies (e.g., cetuximab, nimotuzumab, panitumumab), TKIs (e.g., erlotinib, afatinib, gefitinib) or the BRAF inhibitors (Xu, Johnson and Grandis, 2017; Yuan *et al.*, 2019) defined in the previous section 4.3.1.2. EGFR mutation is the best-established oncogenic target for the management of metastatic NSCLC. Erlotinib, gefitinib and afatinib, are recommended as first-line therapy in patients with advanced NSCLC harboring activating EGFR mutations. In recent years, osimertinib has emerged as a third-generation EGFR-TKIs (Yuan *et al.*, 2019).

5.3.1.4 ROS1 translocations

ROS proto-oncogene 1 (ROS1) is a tyrosine kinase receptor that can be rearranged in NSCLC, resulting in dysregulation and inappropriate signaling through the ROS1 kinase domain. The *ROS1* locus is located on chromosome 6 and encodes for an orphan tyrosine kinase receptor, i.e., with no known ligand and biologic function in humans. The constitutive activation of the ROS1 kinase drives to cellular transformation and promotes survival and proliferation through downstream signaling via SHP-1/SHP-2, JAK/STAT, PI3K/AKT/MTOR and MAPK/ERK pathways (Sehgal *et al.*, 2018).

The ROS1 gene has homology to ALK and therefore, they are structurally similar, being this the basis for utilizing ALK TKI for ROS1 positive NSCLC patients. Crizotinib obtained FDA approval as first-line treatment for this indication in 2016 and remains to date the only approved treatment. The presence of *ROS1* translocations in

NSCLC is low, approximately 1-2% of NSCLC tumors, and is most often present in patients who have the adenocarcinoma subtype and whose tumors are negative for ALK, KRAS and EGFR mutations (Sehgal *et al.*, 2018; Patil *et al.*, 2019).

Overall, targeted therapy has already changed the landscape of advanced NSCLC treatment; however, most of the patients who benefit from targeted therapies will actually and eventually develop clinical resistance and progress, making the prognosis of advanced NSCLC patients still less than optimal. Resistance often comes from acquired mutations that render the TKIs ineffective, such as the activation of alternative cell-signaling pathways, or histologic transformation. Although some resistant mechanisms have been identified, others remain to be determined. The most known mechanisms of resistance are, in the case of EGFR, explained by the acquired *EGFR* exon 20 *T790M* mutation, and the L1196M and C1156Y mutations for ALK. The knowledge about these mechanisms of resistance have led to the development of second- and third-generation TKIs (Golding *et al.*, 2018).

Taking together all the driver mutations pursued in targeted therapies, the percentage of advanced NSCLC patients that can really benefit from them is approximately 30%. There is therefore an urgent need in identifying additional therapeutic targets to enrich patient populations likely to respond and to provide innovative approaches specifically designed to interfere with metastasis progression.

5.3.2 Immunotherapy

Avoiding immune destruction was postulated as one of the hallmarks of cancer by Hanahan and Weinberg a decade ago (Hanahan and Weinberg, 2011). Cancer cells manage to avoid immune detection and eradication by genetic and epigenetic alterations as well as by the manipulation of the tumor microenvironment. Immunotherapy has emerged as one promising approach and has revolutionized the treatment scenario for cancer patients.

Cancer immunotherapy is a treatment modality aiming to mobilize the native immune system to recognize and destroy cancer

cells by disrupting the pathways that tumors use to evade the immune system. The key players for antigen-specific cell-mediated immunity are T lymphocytes together with antigen-presenting cells (APC) such as macrophages and dendritic cells (Qin *et al.*, 2016; Brahmer *et al.*, 2018). The discovery of receptors regulating T cell activation, called immune checkpoints, has represented a major therapeutic breakthrough in the field. Immune checkpoint inhibitors (ICIs) are a group of antibodies designed to block specific targets present on tumor cells or lymphocyte surface (e.g., ipilimumab (Hodi *et al.*, 2010), the first approved anti-CTLA4 antibody, and nivolumab (Robert *et al.*, 2014; Borghaei *et al.*, 2015; Brahmer *et al.*, 2015; Motzer *et al.*, 2015) the first approved anti-PD-1 antibody), consequently boosting the immune system to attack cancer. Immune checkpoints that target the programmed cell death-1 (PD-1), programmed cell death ligand-1 (PD-L1) and cytotoxic T-lymphocyte-associated antigen-4 (CTLA-4), have received approval across a wide range of cancer types, including lung cancer, melanoma, and head and neck, among others (Yuan *et al.*, 2019).

To date, four ICIs have FDA approval for advanced NSCLC, namely nivolumab and pembrolizumab targeting PD-1, as well as atezolizumab and durvalumab targeting PD-L1 (**Figure 7**). It is now obvious that not all the patients respond in the same way to immunotherapy, mainly due to tumor heterogeneity (Rybinski and Yun, 2016) and to immuno-genetic polymorphisms (Sathyanarayanan and Neelapu, 2015). Ideally, the NCCN Clinical Practice Guidelines in Oncology (NCCN Guidelines[®]) recommends a prior patient enrichment step by an IHC analysis of PD-L1 expression before the first-line treatment in order to assess whether or not immune checkpoint inhibitors are an option. Additionally, the NCCN Panel also recommends that clinicians should obtain molecular testing for driven mutations before administering first-line ICI therapy (NCCN Guidelines[®] version 3.2020).

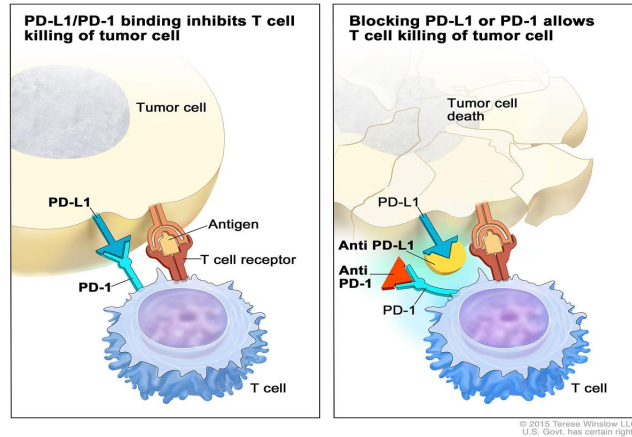


Figure 7. Immune checkpoint inhibitors for PD-1/PD-L1 pathway allow T cell killing of tumor cells. Source: National Cancer Institute.

Pembrolizumab, a fully humanized IgG4 monoclonal antibody against PD-1, was the first ICI approved as first-line treatment in patients with untreated, advanced NSCLC based on the superiority demonstrated over platinum-doublet chemotherapy in the phase III KEYNOTE-024 trial (median PFS, 10.3 versus 6 months; HR 0.50, 95% CI 0.37-0.68; ORRs, 45% versus 28%; OS, 30 versus 14.2 months with chemotherapy; HR 0.63, 95% CI 0.47-0.86) (Reck *et al.*, 2019). However, this treatment is just indicated for patients with high levels of PD-L1 expression ($\geq 50\%$), that do not have contraindications to the use of immunotherapy, and do not present *EGFR* mutation or *ALK* translocations (Majem *et al.*, 2019). For patients with low PD-L1 expression levels ($< 50\%$) or unknown PD-L1 expression, chemotherapy with platinum doublets should be considered in all stage IV PS 0–1 NSCLCs without driver mutations as shown in **Figure 8** (Majem *et al.*, 2019).

Although PD-L1 is an approved biomarker for NSCLC, is not a perfect biomarker. The discriminatory power has limitations; less than half of biomarker-selected patients benefit from treatment, and some responses may be encountered in biomarker-negative cohorts (Planchard *et al.*, 2018). More specific biomarkers are therefore needed for patient stratification and selection of the candidates that would most likely benefit from immunotherapy. One of the most

promising emerging biomarkers for immunotherapy is tumor mutational burden (TMB), commonly defined as the total number of exonic somatic mutations. TMB approximates the amount of neoantigens that potentially are recognized by the immune system (Endris *et al.*, 2019). A phase II trial of nivolumab plus ipilimumab in NSCLC (CheckMate 568 trial), identified a TMB of at least 10 mutations per megabase as an effective cut-off for selecting patients most likely to have a response, irrespective of tumor PD-L1 expression level (Hellmann *et al.*, 2018). However, the lack of consensus on how to measure TMB is hampering the adoption of TMB as a routine clinical practice biomarker.

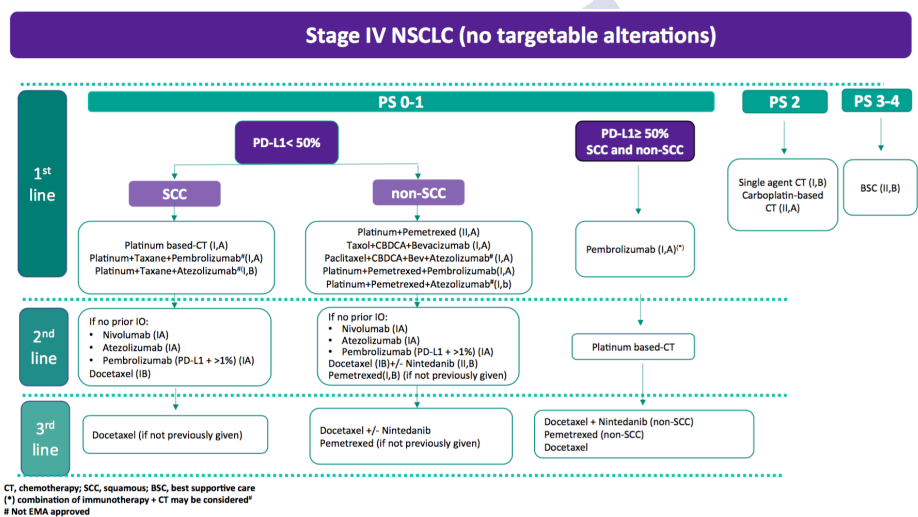


Figure 8. SEOM clinical guidelines for the treatment of non-small cell lung cancer (2018). From Majem *et al.*, 2018.

Despite the promising results of immunotherapy, the clinical benefit of ICIs has been proven limited and unsatisfactory, with the overall response rate (ORR) of monotherapy over chemotherapy about 10–20%, and only a small fraction of the patients appearing to respond to its used as monotherapy (Yuan *et al.*, 2019). To tackle this issue, as it was mentioned before, novel predictive biomarkers are under consideration. The introduction of combination treatment strategies involving different targeted therapies, immunotherapies,

chemotherapies or radiotherapies, may also help to overcome these limitations.

5.4 NOVEL AND PROMISING THERAPEUTIC STRATEGIES

Besides the above mentioned clinically available treatments for advanced NSCLC, there are many other options that have demonstrated promising results either for other indications, or in clinical trials and preclinical studies, and could become a breakthrough in the management of NSCLC in the next few years. A comprehensive description of some of the different therapeutic strategies is detailed below.

5.4.1 Antibody Drug Conjugates (ADC)

ADCs have been postulated as powerful candidates for cancer treatment as they comprise high specificity and potent cytotoxic agents. Briefly, ADC includes a target specific antibody and a small molecule (e.g., anticancer drug), linked together through a specific chemical process. The antibody acts as a targeting agent to carry the antitumor cytotoxic molecule specifically to cancer cells. With respect to the mechanisms of action, ADCs are selectively internalized by target cells via receptor-mediated endocytosis; the linker is then cleaved, and the cytotoxic drug released, leading to apoptosis and cell death (**Figure 9**) (Zhao *et al.*, 2020).

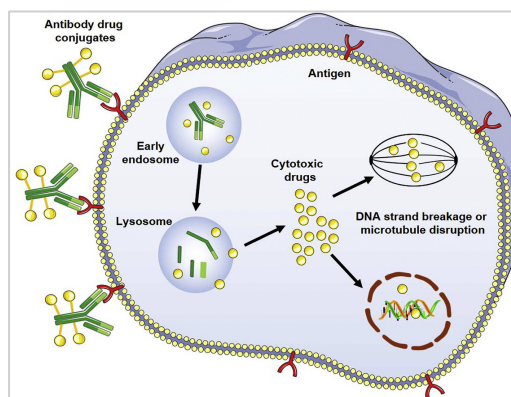


Figure 9. Illustration of the mechanism of action of ADCs. From Zhao *et al.*, 2020.

The first experimental design of an ADC was published in *Nature* more than 50 years ago (Decarvalho, Rand and Lewis, 1964). However, it was only during the last decade that they have achieved considerable success, after the introduction of the first clinically approved ADC in 2011. Brentuximab vedotin was approved by the FDA in 2011 for treating relapsed Hodgkin's lymphoma and systemic anaplastic large cell lymphoma (Katz, Janik and Younes, 2011). It was followed by ado-trastuzumab emtansine in 2013 for treating HER2-positive metastatic breast cancer (Amiri-Kordestani *et al.*, 2014), inotuzumab ozogamicin in 2017 for the treatment of adults with relapsed or refractory B-cell precursor acute lymphoblastic leukemia (ALL) (Lamb, 2017), Gemtuzumab ozogamicin, reapproved in 2017 after withdrawing in 2010 for the treatment of adults with newly diagnosed CD33-positive acute myeloid leukemia (Jen *et al.*, 2018), Polatuzumab vedotin-piiq in 2019 for relapsed or refractory diffuse large B-cell lymphoma (Deeks, 2019), and sacituzumab govitecan in April 2020 for the treatment of adult patients with metastatic triple-negative breast cancer (mTNBC) who have received at least two prior therapies for metastatic disease. These approvals have boosted the quantity of ADC in clinical trials (~200) for different indications and a mass number of research publications.

Although ADCs provide tremendous opportunities for the future of cancer treatment, some challenges still need to be overcome, such as toxicity (due to the limited dose that can be achieved, often resulting toxic before the ADC reaches its maximal efficacy), lack of specificity, and poor translation from preclinical models to humans (despite the fact that a large number of ADCs have shown therapeutic benefits in preclinical models, many of them are not as efficient in human) (Nejadmoghaddam *et al.*, 2019; Zhao *et al.*, 2020).

To date, there are no ADCs approved for the treatment of NSCLC, although some promising effects have been reported in clinical trials. Encouragingly, the FDA granted Fast Track designation for sacituzumab govitecan for the potential treatment of patients with SCLC or NSCLC, on view of the promising results in preclinical studies (Heist *et al.*, 2017) and clinical trials (NCT03964727). Furthermore, a comprehensive development programme is underway

in clinical trials for evaluation of the efficacy and safety of trastuzumab deruxtecan, a HER2-directed ADC approved for HER2 positive metastatic breast cancer on December 2020, for metastatic non-squamous NSCLC (NCT03505710). These could be the first clinically available ADCs options for advanced NSCLC patients.

5.4.2 Gene Therapy

Advances in genetics and molecular biology have led to the development of new therapies that can specifically modulate the expression of relevant genes in order to correct abnormalities and restore their original biological function. To date, the FDA has approved four gene therapy products and more than 900 Investigational New Drugs (IND) applications are ongoing clinical studies. Some of the strategies of gene therapy include (i) silencing oncogene expression, (ii) promoting tumor-suppressor genes, (iii) correcting mutations, (iv) suicide gene therapy, (v) suppressing tumor angiogenesis, and (vi) activating an immune response against tumor cells (Hardee *et al.*, 2017). For these purposes, plasmid DNA (pDNA), minicircles (supercoiled circular DNA), oligonucleotides (ASOs, decoys, aptamers), RNA interference (short-hairpin (shRNA), small interfering RNA (siRNA) and microRNA (miRNA)) are being extensively explored (Pahle and Walther, 2015). However, because naked nucleic acids are vulnerable to enzymatic degradation, rapid clearance, and non-specific biodistribution, only low gene expression efficiencies can be achieved. Hence, the primary challenge of gene therapy is to develop effective carriers able to protect the nucleic acids and facilitate their internalization into the targeted cells at the targeted site (Z. Zhou *et al.*, 2017).

Traditionally, vectors for gene therapy applications are divided into viral and non-viral carriers. Most gene vectors (~69%) currently undergoing clinical trials involve viruses (i.e., retroviruses, lentiviruses, adenoviruses, adeno-associated viruses, poxviruses, herpes simplex viruses, and vaccinia viruses). Some examples include Luxturna[®] (voretigene neparvovec-rzyl), approved in December 2017, by the FDA to treat children and adult patients with an inherited form of vision loss that may result in blindness. This disease is caused by

mutations in a single gene, the biallelic RPE65 mutation, and Luxturna delivers a normal copy of the RPE65 gene by an adeno-associated virus (Rodrigues *et al.*, 2019). Furthermore, in May 2019, Zolgensma[®] (onasemnogene abeparvovec-xioi) was approved for the treatment of pediatric patients less than 2 years of age with spinal muscular atrophy (SMA) including those who are pre-symptomatic at diagnosis. It is an adeno-associated virus vector-based gene therapy designed to provide a functional copy of the human survival motor neuron (SMN) gene to halt disease progression through sustained SMN protein expression with a single, one-time intravenous (IV) infusion. Zolgensma represents the first approved gene therapy in a proprietary platform to treat rare, monogenic diseases using gene therapy (Hoy, 2019).

Despite these advances and the examples of successful gene therapies, many concerns still remain regarding the use of viral vectors, such as their potential immunogenicity, the possibility of reversion to the virulent form or the viruses, and also their high production costs (Z. Zhou *et al.*, 2017). Moreover, viral vectors are limited to mediate only one type of gene modification, “gene addition”. New genome editing technologies can mediate gene addition, gene ablation, “gene correction,” and other highly targeted genome modifications in cells (Dunbar *et al.*, 2018). The most commonly used technologies for genome editing are (i) clustered regularly interspaced short palindromic repeats (CRISPR)-CRISPR-associated protein 9 (Cas9), (ii) transcription activator-like effector nucleases (TALENs), (iii) zinc-finger nucleases (ZFNs), and (iv) homing endonucleases or meganucleases (Gaj *et al.*, 2016).

Alternative to virus vectors, synthetic vectors, made out of natural, semi-synthetic or synthetic materials, offer a safer alternative to introduce genetic materials into the targeted cells. Numerous non-viral gene delivery systems for different types of nucleic acids (mainly pDNA, siRNA and miRNA) have been described to date (Bono *et al.*, 2020; Mohammadinejad *et al.*, 2020). Different applications for the development of novel anticancer genetic nanomedicines have similarly being explored, including suicide gene therapies, anti-angiogenic gene therapies, immunotherapies, restoration of

oncosuppressor RNAs, or gene silencing of oncogenes, or specific non-coding RNAs (antagomirs), or proteins involved in resistance to chemo- and radio-therapies, anti-apoptotic proteins, epigenetic regulation, etc., as reviewed by Bottai *et al.* (Bottai *et al.*, 2017). The design of successful synthetic nanovectors poses a big challenge since they need to overcome important biological barriers. Nanovectors need (i) to be safe and adequate for parenteral administration, (ii) efficiently protect nucleic acids from degradation, and (iii) promote their access to the target intracellular compartment in the target cell (depending on the selected gene therapeutic system, i.e., plasmid DNA, RNAi, non-coding RNA (ncRNAs), oligonucleotides, etc.), in enough amounts to mediate a therapeutic effect (depending on the potency of the molecule, specificity, and stability) (Shanker *et al.*, 2011; Pahle and Walther, 2015; Wang *et al.*, 2015; McErlean, McCrudden and McCarthy, 2016; Dowdy, 2017). All these aspects should be taken into consideration from early development to increase the chances of translation into early-phase clinical trials (de la Fuente, Seijo and Alonso, 2008; de la Fuente *et al.*, 2012; Santander-Ortega *et al.*, 2012, 2014). The development of functional assays and the selection of adequate animal models for therapeutic evaluation are also key steps that critically affect the outcome of the preclinical evaluation.

Recent advances in non-viral gene vectors regarding efficiency, specificity, safety and gene expression durability have led to an increase in the number of nanoparticle-based gene delivery vectors in clinical trials (Ramamoorth and Narvekar, 2015). Some examples in cancer are related to liposomes for siRNA, microRNA or pDNA delivery (NCT01591356, NCT01829971, NCT01489371, NCT02340156); lipid nanoparticles (NCT02314052, NCT01437007) or polymeric nanoparticles (NCT02956317). Importantly, Patisiran (ONPATTRO™) was the first FDA approved RNAi-delivering nanoparticle, and the first RNAi therapeutic in general. Patisiran is a double-stranded small interfering RNA encapsulated in a lipid nanoparticle for delivery to hepatocytes. It was approved in the USA for the treatment of the polyneuropathy of hereditary TTR-mediated amyloidosis (hATTR) in adults and subsequently approved in the EU

for the treatment of hATTR in adults with stage 1 or 2 polyneuropathy (Adams *et al.*, 2018; Hoy, 2018).

The global gene therapy market is expected to grow in the following years at a CAGR of 34,8% from 2019 to 2026. The viral vector segment was the largest contributor toward the market growth in 2018, however, the non-viral vector segment is anticipated to exhibit fastest growth during the forecast period, due to advancements in physicochemical approaches such as physical and chemical methods of non-viral vectors for gene therapies during preclinical and clinical trials, for the treatment of various diseases. The oncological disorders segment was the largest contributor in the gene therapy market in 2018 and is expected to keep growing in the forecast period. Currently, there are no gene therapies in the market for NSCLC. However, a promising phase I/II study (NCT01455389) from Genprex Inc., for metastatic NSCLC patients, has received this January 2020, the Fast Track Designation by the FDA for its Oncoprex immunogene therapy to treat lung cancer in combination. Oncoprex is basically a tumor suppressor gene called TUSC2 encapsulated in non-viral, positively charged nanovesicle made from lipid molecules (DOTAP:Chol) that have rendered impressive results in preclinical studies (Lu *et al.*, 2012).

The potential for gene therapy to provide durable benefits to human health, shown by the scientific advances and clinical successes over the past years, explains the optimism and increasing efforts toward making this therapy part of our standard armamentarium for treatment of serious human diseases (Dunbar *et al.*, 2018).

5.4.3 Nanotechnology

Nanotechnology can be defined as the science of manipulating and controlling materials and systems on a molecular scale. The merging of nanotechnology and medicine, nanomedicine, has allowed the development of several nanoparticle delivery vehicles, specifically designed for carrying and delivering their cargo to disease sites for treatment, prevention, and/or diagnosis (Farjadian *et al.*, 2019).

Nanomedicine has been widely explored during the last decades. Different nanosystems composed of a variety of materials have been

proposed for the management of several diseases, as liposomes and other lipid-based, polymer-based nanoparticles, micelles, polyplexes, dendrimers, polymersomes, and drug/protein conjugates (Vázquez-Ríos *et al.*, 2018). Nanotechnology offers many advantages in drug delivery, including (i) protection of drugs from premature degradation, (ii) increased solubility and stability in biological media, (iii) prevention of premature interactions of drugs with the biological environment, (iv) controlled pharmacokinetics and biodistribution, (v) improved delivery of therapeutics across biological barriers, and (vi) targeting of drugs to the diseased area (Peer *et al.*, 2007; Zhang *et al.*, 2018). Due to these properties and to their ability to accommodate various types of drugs and biomolecules, with different physicochemical properties and activities, nanocarriers have emerged as attractive candidates for the development of personalized medicine (Sanna, Pala and Sechi, 2014; Farjadian *et al.*, 2019).

The application of nanotechnology in cancer therapy is already a reality that increments the localized delivery of chemotherapeutics to the tumor, leading to improved pharmacological activities and significantly minimizing secondary side effects. In 1995, the FDA approved the first nanoparticle for cancer treatment, Doxil[®], a PEGylated liposome loaded with the chemotherapeutic drug doxorubicin (Barenholz, 2012). Since then, other nanotherapeutics based on liposomes have reached the market for different cancer treatments such as Pegylated liposomal doxorubicin (Doxil[®]/Caelyx[®]), liposomal cytarabine (DepoCyt[®]), daunorubicin citrate liposomes (DaunoXome[®]), liposomal doxorubicin (Myocet[®]), Liposomal mifamurtide non-PEGylated (Mepact[®]), Vincristine Sulfate Liposomes (Marqibo[®]), liposomal irinotecan (Onivyde[®]), or the combination of daunorubicin and cytarabine liposome (Vyxeos[®]). Paclitaxel polymeric nanoparticles (Opaxio[®]), pegylated L-asparaginase polymeric nanoparticles (Oncaspar[®]), leuprolide acetate polymeric micelles (Eligard[®]), oxaliplatin micelles (Eloxatin[®]), polymer–protein conjugate pegfilgrastim (Neulasta[®]), and albumin-paclitaxel (Abraxane[®]) are examples of different types of nanostructures that have led to products already in clinical use. The

impact of nanomedicine in cancer therapy can be further reviewed in the Annex 1 of this thesis.

The most translatable type of nanosystems to date, are examples of passively targeted nanoparticles, PEGylated nanomedicines that mainly rely on modifying the pharmacokinetics and biodistribution of a drug by improving its accumulation in tumors, due to the phenomenon called Enhanced Permeability and Retention (EPR) effect, first described in 1986 by Matsumura & Maeda (Matsumura and Maeda, 1986). The attachment of the polymer polyethylene glycol (PEG) is widely used in nanomedicine to increase circulation lifetimes and reduce doses. PEGylated liposomes (Doxil[®]), PEGylated L-asparaginase (Oncaspar[®]), and mPEG-PDLLA micellar paclitaxel (Genexol[®]-PM), just to name a few examples.

The other mechanism described by which nanoparticles can be accumulated in cancerous tissues is active targeting, which can be achieved by the functionalization of the surface of nanoparticles with bioactive molecules able to recognize cancer-specific targets overexpressed in malignant cells, such as transferrin, engineered antibodies or fragments, peptides, enzymes, and folic acid, among others (Bregoli *et al.*, 2016). Although active targeted nanomedicines are advanced at the preclinical stage, to date only antibody- and protein-based nanomedicines (Adcetris[™], Kadcyla[®] and Ontak[®]) have been FDA approved. Several ongoing clinical trials with nanotherapeutics are on their way, suggesting that we are prone to see a growth in the number of FDA-approved therapeutic nanoparticles over the foreseeable future.

Few years ago, the failure in phase II clinical trials of a promising targeted polymeric nanocarrier containing the chemotherapeutic drug docetaxel, BIND-014, developed by the pharmaceutical company Bind Therapeutics, ended up filing for bankruptcy (Bobo *et al.*, 2016; Ledford, 2016). It opened several questions regarding the inter- and intra- individual factors affecting the EPR effect which was initially presumed to be homogeneous and omnipresent in all tumor types (Dasgupta *et al.*, 2020). Similarly, several other promising cancer nanomedicine platforms based on polymeric nanoparticles (CRLX101) and polymeric micelles (NK105) have also reported

disappointing clinical outcomes (Dasgupta *et al.*, 2020). Moreover, according to a work published in 2016, the average tumor uptake of nanoparticles is only about 0.7% of the injected dose (Wilhelm *et al.*, 2016). This fact supports the idea that models fail to predict accumulation of systemic delivered nanoparticles into the tumor, being over simplified and overlooking multiple biological steps in the process. In order to overcome this hurdle, many efforts are being made to modulate the tumor vasculature and microenvironment for improved EPR-mediated delivery of drugs and drug delivery systems, by means of pharmacological interventions, to enhance vascular disruption/permeabilization, or by physical modalities, such as hyperthermia and photodynamic therapy (Al-Ahmady and Kostarelos, 2016; Ojha *et al.*, 2017; Dasgupta *et al.*, 2020). Another strategy is the use of companion diagnostics and theranostics to image EPR-mediated drug delivery and classify patients by high EPR effect to determine if they are suitable candidates for nanotherapies (Dasgupta *et al.*, 2020). Understanding individual predisposition to accumulate nanoparticles in tumor sites is essential for selecting the correct nanotherapy. The contribution of nanotheranostics to overcome this challenge was reviewed in the Annex 1 of this thesis.

To date, Abraxane[®] is the only nanomedicine approved by the FDA (2012) and EMA (2015) for the treatment of advanced NSCLC (Green *et al.*, 2006). Promising clinical trials are ongoing such as: NBTXR3 (a 50 nm crystalline hafnium oxide nanoparticle with negatively charged phosphate coating) activated by radiotherapy in combination with an anti-PD-1 (Phase I: NCT03589339), and Oncoprex, TUSC2-lipid nanoparticles (DOTAP:Chol) in combination with Erlotinib (NCT01455389), already described in the section 4.4.2 of gene therapy (Anselmo and Mitragotri, 2019).

Nanotechnology-based therapeutics are paving the way in the diagnosis, imaging, screening, and treatment of primary and metastatic tumors; however, translating such advances from the bench to the bedside has been severely hampered by challenges encountered in the areas of pharmacology, toxicology, immunology, large-scale manufacturing, and regulatory issues.

5.4.4 Others

The current scenario for cancer research is wide and offers many possibilities for the constant improvement of therapies. In recent years, research into cancer medicine has taken remarkable steps towards more effective, precise and less invasive cancer treatments. There is a plethora of newly proposed therapeutic options for cancer that are currently under investigation at different levels of maturity of the research stage and some of them in clinical trials. Examples of innovative therapies, recently reviewed by Pucci *et al.* (Pucci, Martinelli and Ciofani, 2019), including cellular therapies, oncolytic viruses, immune check-point antagonists, therapeutic cancer vaccines, natural antioxidants, hormone replacement therapy, exosome delivery platforms, aptamers, thermal ablation and magnetic hyperthermia, and radiomics/phantomics (Rafei, Mehta and Rezvani, 2019). These strategies aim to provide the best personalized therapies for cancer patients and highlight the importance of combining multiple disciplines to get innovative approaches for the best outcome.

5.5 NEW THERAPEUTIC TARGETS IN NSCLC

Developing innovative treatments for this practically incurable disease constitutes a priority. The strategy to develop satisfactory antitumor agents capable of treating tumor cells, therefore, involves the design of agents that selectively kill tumor cells, while exerting relatively few, if any, adverse effects against normal tissues. This objective has been difficult to achieve because there are few qualitative differences between neoplastic and normal tissues. In recent years, many efforts have been devoted to the identification of tumor-specific biomarkers for diagnostic and prognostic purposes, as well as for the development of more specific and more efficient targeted therapies. As mentioned in section 4.3.1, these efforts are in line with the potentiation of personalized medicine, with the premise that each tumor is unique, and undergoes dynamic changes over time, making it important to determine the best therapeutic approach at all stages of development.

5.5.1 Emerging biomarkers

The therapeutic landscape of advanced NSCLC is evolving towards the identification and validation of additional biomarkers beyond EGFR, ALK, ROS1, and BRAF, allowing more patients the possibility to benefit from a personalized treatment. The emerging list of biomarkers for metastatic NSCLC includes ERBB2 mutations (also known as HER2), RET gene fusions, neurotrophin tyrosine receptor kinase (NTRK) gene fusions, high-level MET amplifications or MET exon 14 skipping mutations (METex14), and KRAS mutations. Some of them have already been included in panels of predictive or prognostic biomarkers, or are analyzed as complementary biomarkers when the reference biomarkers (i.e., EGFR, ALK, ROS1, and BRAF) are negative (Lindeman *et al.*, 2018). Treatments for these targets are currently being developed in clinical trials, offering great promise in the future.

5.5.1.1 HER2 biomarker

HER2 (Erb-b2 receptor tyrosine kinase 2) is a member of the ErbB family of tyrosine kinases, which also includes EGFR (ErbB1), ErbB3, and ErbB4. Genetic alterations of HER2 in cancer result in constitutive dimerization with other family members and activation of a variety of signaling pathways including MAPK, PI3K/AKT, PKC and STAT that promotes cell growth, survival and tumor progression. HER2 has also been recognized as an oncogenic driver in other types of cancers such as breast and gastro-esophageal cancer (Baumgart and Pandya, 2016).

In NSCLC adenocarcinoma, HER2 mutations are estimated in 1-2% of patients and most of the HER2 mutations observed correspond to exon 20 insertions, a recurrent 12 base-pair insertion causing duplication of amino acids YVMA at codon 75, the Y772_A775dup insertion (Jebbink *et al.*, 2020). HER2 mutations have also been described as a mechanism of acquired resistance during EGFR TKI treatment (Kosaka *et al.*, 2017). There are no effective or approved targeted therapies against HER2 mutations for advanced NSCLC. However, given the clinical experience of targeting HER2 mutations in breast cancer, similar approaches are being explored for lung

cancer, including anti-ErbB2 agents such as afatinib, dacomitinib, neratinib, trastuzumab, and the antibody-drug conjugate trastuzumab emtansine (Robichaux *et al.*, 2018; Lai *et al.*, 2019). Encouragingly, the pan-ErbB TKI poziotinib is currently being investigated in a phase II clinical trial of patients with advanced NSCLC, including those with insertion mutations in exon 20 of ERBB2 (NCT03318939).

5.5.1.2 RET biomarker

The *RET* (Proto-oncogene tyrosine-protein kinase receptor Ret) gene encodes for a cell surface tyrosine kinase receptor which is activated when the glial cell line-derived neurotrophic factor family ligands (GFL) binds to the RET coreceptor, the glycosylphosphatidylinositol-anchored coreceptor (GFR- α). This binding leads to cellular proliferation and migration by the activation of RAS/RAF/MAPK, PI3K/AKT/mTOR and PLC- γ pathways (El Osta and Ramalingam 2020). Mutations of the RET gene are most commonly associated with medullary thyroid cancer; however chromosomal rearrangements involving the RET gene occur in approximately 1–2% of patients with NSCLC (Chu 2020). Despite there is no RET-specific inhibitor currently approved, multitarget kinase inhibitors (e.g., cabozantinib, vandetanib, lenvatinib, sitravatinib, alectinib and ponatinib) and some specific RET inhibitors (e.g., RXDX-105, BLU-667, LOXO-292, BOS172738), are undergoing clinical development. To date, BLU-667 and LOXO-292 have demonstrated robust clinical results with favorable toxicity profiles (Bronte *et al.*, 2019). The potential approval of these two highly specific RET inhibitors would represent a major breakthrough as the first effective targeted therapy for RET fusion-positive NSCLC patients.

The potential approval of these two highly specific RET inhibitors would represent a major breakthrough as the first effective targeted therapy for RET fusion-positive NSCLC patients.

5.5.1.3 NTRK biomarker

NTRK (neurotrophin tyrosine receptor kinase) gene fusions encode tropomyosin receptor kinase (TRK) family proteins (including

TRKA, TRKB, TRKC as members) that act as oncogenic drivers for solid tumors including lung, salivary gland, thyroid, and sarcoma. TRKs play a role in neuronal development and differentiation when activated, through the MAPK, PI3K and PLC- γ downstream pathways. The oncogenic activation can be driven by different mechanisms, although gene fusions involving NTRK1, NTRK2 or NTRK3 are the most commonly observed in solid tumors (Russo *et al.*, 2020). It is estimated that NTRK fusions occur in <1% of patients with NSCLC and do not typically overlap with other oncogenic drivers such as EGFR, ALK, or ROS1. Several TKIs against TRKA, TRKB and/or TRKC have been developed and two of them (larotrectinib and entrectinib) have been recently approved by the FDA. Larotrectinib and entrectinib are oral TKIs that inhibit TRK across a diverse range of solid tumors in younger and older patients with NTRK gene– fusion positive disease.284,292 Ongoing clinical trials with TRK inhibitors in NTRK fusion-positive solid tumors, including NSCLC can be consulted in ref. (Russo *et al.*, 2020).

5.5.1.4 MET biomarker

MET (mesenchymal-to-epithelial transition factor) is a heterodimer tyrosine-kinase receptor with an exclusive ligand, the hepatocyte growth factor (HGF) ligand. The ligand binding leads to homodimerization and activation of the receptor by the phosphorylation of the tyrosine residues, stimulating downstream signaling pathways such as RAS/ERK/MAPK, PI3K/PKB, and JAK/STAT pathways, and triggering in cell proliferation, migration, motility angiogenesis, survival and the epithelial-to-mesenchymal transition (Bylicki *et al.*, 2020; Liang and Wang, 2020). Aberrant MET signaling in oncology can be manifested in several ways: genetic mutation, amplification, rearrangement or overexpression of proteins. A plethora of MET-targeted agents (TKIs and antibodies against MET or HGF) have been investigated for several years, but their results failed to demonstrate meaningful efficacy (Scagliotti *et al.*, 2015). These disappointing results have led to pessimism about MET as targetable driver in NSCLC. However, recent developments about MET exon 14 (METex14) splicing, have put MET back on the

list of promising targetable mutations that may lead to the approval of specific MET inhibitors in NSCLC (Awad *et al.*, 2016; Reungwetwattana *et al.*, 2017). Mutations in METex14 (resulting in exon 14 skipping) are found in approximately 3–4% of lung adenocarcinomas and may predict response to MET-targeted therapy (Paik *et al.*, 2015). MET is also one of the mutations that causes acquired resistance in patients with a different driver mutation treated with a TKI, as an example, MET amplification is the most common resistance mechanism after first-line treatment with osimertinib (Engelman *et al.*, 2007). Dedicated clinical trials with MET TKIs in METex14-positive NSCLC patients are underway, which are likely to lead to the eventual approvals of MET TKIs in the near future (Wolf *et al.*, 2019). Indeed, on 6th May 2020, the FDA granted accelerated approval to capmatinib (Tabrecta[®]) for adult patients with metastatic non-small cell lung cancer (NSCLC) whose tumors have a mutation that leads to mesenchymal-epithelial transition (MET) exon 14 skipping as detected by an FDA-approved test.

5.5.1.5 KRAS biomarker

KRAS (Kirsten rat sarcoma viral oncogene homolog) mutations are the most frequent oncogene driver mutation in patients with NSCLC. It is estimated to be found in approximately 20-25% of lung adenocarcinomas in western countries and is typically associated with smoker patients, only 5-10% corresponds to never or light smokers (Ferrer *et al.*, 2018). *KRAS* is a G-protein with GTPase activity that is part of the MAP/ERK pathway. *KRAS* mutations occurs most commonly at codon 12 and do not generally overlap with *EGFR*, *ROS1*, *BRAF*, and *ALK* genetic variants. Therefore, *KRAS* testing may identify patients who may not benefit from further molecular testing. *KRAS* mutation is also predictive of lack of therapeutic efficacy with EGFR TKIs and a prognostic biomarker of poorer overall survival than *KRAS* wild-type (Wood *et al.*, 2016). Unfortunately, despite the high prevalence, targeted therapy is not currently available for patients with *KRAS* mutations. Current clinical trials are evaluating inhibiting downstream effector pathways for

improved efficacy as well as ICIs and MEK inhibitors that appear to be effective (Blumenschein *et al.*, 2015; Torralvo *et al.*, 2019).

5.5.1.6 Experimental biomarkers

The field of biomarker discovery is constantly growing. Numerous potential therapeutic targets can be easily found in the literature in early stages of development for every type of cancer. Research papers show promising results *in vitro* and/or *in vivo* of the functional relevance and therapeutic potential of novel biomarkers. Recently, Li *et al.* described the role of the epididymal protein 3A (EDDM3A) in non-small cell lung cancer (NSCLC). EDDM3A expression levels were found to be significantly overexpressed in NSCLC tissue compared to adjacent healthy tissue (n=30). When EDDM3A was downregulated in NSCLC cell lines, the proliferation of the tumor cells was inhibited as well as the colony formation ability, and cell apoptosis was promoted (Li *et al.*, 2020). In 2017, Adams *et al.* identified the cell division cycle associated 3 protein (CDCA3) overexpressed in NSCLC tissue (n=74 ADC and n=84 SCC) and showed its prognostic value in NSCLC. Depletion of CDCA3 resulted in inhibition of tumor growth and promotion of tumor senescence *in vitro* (Adams *et al.*, 2017). Another recent finding is the research done by Yang *et al.*, that used four gene expression datasets of lung adenocarcinoma from the GEO database, including GSE7670, GSE10072, GSE68465, and GSE43458, and identified genes differentially expressed in lung cancer. Among those genes, they found the matrix metalloproteinase 11 (MMP11) to be increased in tumor tissue and sera from NSCLC patients and to play a critical role in cell proliferation, migration and invasion. Interestingly, by adding a monoclonal antibody against MMP11, tumor growth in both *in vitro* experiments and *in vivo* xenografts was inhibited, demonstrating its potential as a therapeutic target (Yang *et al.*, 2019).

Importantly, searching in the patent database Espacenet (www.espacenet.com), a large number of therapeutic targets whose results may not be published in a research paper yet, showed up. Some examples are: “Application of ILK gene as biomarker and therapeutic target for lung squamous cell carcinoma” (CN109385477A),

“Application of IL-12 to diagnosis and treatment of non-small cell lung cancer (NSCLC) distant metastasis” (CN105572380A), “Novel biomarker as therapeutic target in lung cancer” (ES2339524A1), and “Application of FOXP1 gene and inhibitor of FOXP1 gene in preparing medicine for inhibiting lung cancer metastasis” (CN109939234A).

It is noteworthy highlighting the trajectory of the fatty acid receptor CD36 as a novel metastatic stem cells therapeutic target. It was described for the first time by Pascual *et al.* in the journal *Nature*. In their paper, they demonstrated that CD36+ cells are highly predisposed to promote metastasis and predominantly defined by a lipid metabolism signature, and its expression is amplified in most type of tumors. By adding to xenografted mice a neutralizing antibody against CD36, the metastasis formation was completely inhibited and more strikingly, in mice that had already developed metastasis, a reduction of 80-90% of metastasis was observed and a complete remission of metastasis in 15% of mice was observed (Pascual *et al.*, 2017). This receptor was previously patented in 2015 by a research group of the *Fundacio institut de recerca biomedica IRB Barcelona* (WO2017055411A1). In 2018, a new biotech spin-off company was incorporated, Ona Therapeutics, to develop a novel therapy against metastasis by targeting CD36+ cells and in June 2020, Ona Therapeutics raised €30M in Series A financing.

The field of biomarker discovery in advanced NSCLC is not fully covered yet, taking together the therapeutic targets that are being used in clinics (*EGFR*, *ALK*, *ROS1*, *BRAF*) and the emerging biomarkers that are on the way in clinical trials (*KRAS*, *RET*, *MET*, *NTRF1*, *HER2*), there are still 36% of NSCLC patient with no actionable mutations (**Figure 10**), therefore, not suitable for a targeted therapy. In summary, further research is needed in order to comprehensively understand the mechanisms underlying metastasis dissemination and to identify more reliable biomarkers able to predict patients that will benefit from a specific treatment and to be able to provide, hopefully, a precision and personalized medicine for every patient.

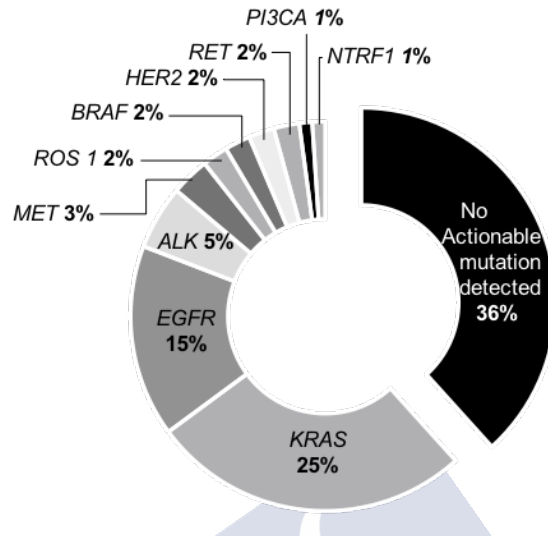


Figure 10. Specific genomic alterations identified in lung adenocarcinoma. (Adapted from Pakkal *et al.*, 2018).

5.6 TRANSLATION OF THERAPEUTICS TO THE CLINIC

There are many different definitions of what translational medicine/science/research is. It can be defined by the transformation of scientific discoveries arising from laboratory, clinical or population studies into new clinical tools and applications to address a health need (e.g., reducing disease incidence, morbidity and mortality) (Wang, 2012; Wagner and Kroetz, 2016). The translation of therapeutics to the market has a very high technical risk, with a slow entry into the market and patents are the way to protect the intellectual property. A patent is a right granted to an inventor by a federal government that gives its owner the right to exclude others for making, using, or selling the invention for a limited period of time. An invention must meet the criteria of novelty, useful (sufficiently described) and non-obvious for an expert in the field.

As it was mentioned before, NSCLC accounts for 80%-85% of the total cases of lung cancer globally, and this significant share has driven the majority of key market leaders to focus on constant innovation of advanced therapeutics, as well as in increasing the

efficacy of the existing therapeutics. This is also due to the status of lung cancer as one of the most commonly occurring cancers in the world and its contribution to a significant number of deaths worldwide.

The Global Non-Small Cell Lung Cancer (NSCLC) Therapeutics Market is expected to grow at a CAGR of 13.4% during the forecast period (2019-2026). The market size was valued at USD 16 Billion in 2018 and is projected to reach USD 44 Billion by the end of 2026. Targeted therapy segment is estimated to have the largest market share among therapy types (immunotherapy, chemotherapy, radiotherapy, etc.). The targeted therapy segment accounted for a market share of 51.1% in 2018 and is expected to rise. The market growth is driven by several factors such as the rising incidence and mortality expected of NSCLC patients in the following years and growing investments by the companies in R&D activities (**Figure 11**). The inclusion of NSCLC therapeutics in pipelines of major market players are also boosting the market growth globally. Greater adoption and increasing demand for targeted therapies, which is considered to be the foundation of precision medicine due to the increasing R&D initiatives and also due to its sophistication in targeting cancerous cells, is one of the most prominent leading factors that are responsible for the growth of the global NSCLC market in 2018 (www.gco.iarc.fr/, www.fortunebusinessinsights.com).

Targeting metastatic NSCLC is also an attractive sector due to the high costs that healthcare systems invest in the management of the disease considering also the societal impact. However, the market is negatively affected by the high costs involved in the development of these advanced techniques and regulatory issues faced by the countries for the rolling out of these products. Based on the distribution channel, the global market segments include public healthcare systems and private hospitals. Based on cancer type, the global NSCLC therapeutics market segments include adenocarcinoma, squamous cell carcinoma, and large cell carcinoma. Geographically, the market is segmented into North America, South America, Europe, Asia-Pacific, and RoW. North America dominates the global NSCLC therapeutics market due to the well-established

healthcare infrastructures, and increased spending by the government. Europe is estimated to be the second most dominant market after North America, driven by the adoption and R&D initiatives of advanced therapeutics.

As long as the cost of health care continues to increase, more pressure will be to find more reliable biomarkers able to predict which patients are more likely to respond to a certain treatment and to reduce the use of ineffective therapies and off-target effects. Biomarkers will become more and more relevant in making treatment decisions, and molecular testing will necessarily be expanded and accessible in the hospitals. As additional targeted therapies reach the market, there will be an increased need to better understand drug resistance mechanisms. However, the validation process of a novel biomarker is arduous and often requires large numbers of patients and takes a lot of time and money making that precision oncology is still far from being a reality for every patient.

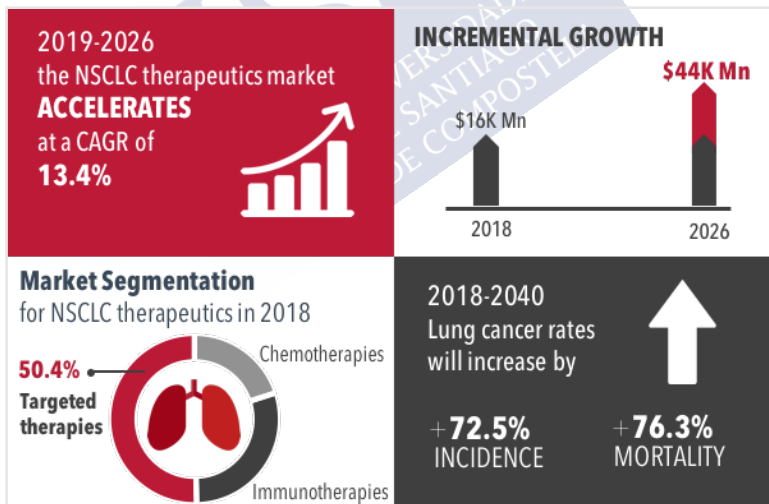


Figure 11. NSCLC therapeutics market globally. Market size, share, growth and key market drivers in the forecast period.



A large, light blue watermark of the USC logo is centered on the page. The logo consists of the letters 'USC' in a large, bold, sans-serif font, with the text 'UNIVERSITY OF SANTIAGO DE COMPOSTELA' written in a smaller font below it, all contained within a tilted rectangular border.

HYPOTHESIS AND OBJECTIVES



6 HYPOTHESIS

On the basis of general knowledge in clinical use, biomedical and pharmaceutical science, the main hypothesis is “**it is possible to define novel therapeutic strategies for metastatic lung cancer inspired by the tumor biology**”.

SECTION I: STRATEGY INSPIRED BY EXOSOMES

The hypothesis of this section is that “it is possible to rationally design nanoplatfoms mimicking natural exosomes for the targeted delivery of therapeutic biomolecules to the tumor cells”, following these partial hypotheses (H):

- H1.** Nanoplatfoms mimicking natural exosomes and maintaining the physicochemical properties of natural exosomes can be prepared by making use of the nanotechnology.
- H2.** This type of nanoplatfoms could be used for the encapsulation of different drugs and biomolecules and could be decorated with proteins, thereby leading to the formation of functionalized delivery systems.
- H3.** By properly defining the composition, it is possible to develop nanoplatfoms that could perform as effectively as tumor-derived exosomes to reach the targeted cancer cells and to deliver therapeutic biomolecules, while overcoming significant limitations of their natural counterparts.

SECTION II: STRATEGY INSPIRED BY CTCs

The hypothesis of this section is that “it is possible to identify novel biomarkers related to metastasis by analyzing CTCs, which can have the potential for the development of new targeted therapeutics”, following these partial hypotheses:

- H4.** The liquid biopsy is a useful tool for the isolation of CTCs from advanced NSCLC patients and for the analysis of differentially expressed genes that might lead to the identification of new targets with prognostic, diagnostic, and therapeutic value.
- H5.** Newly identified biomarkers might be differentially expressed during different stages of the metastatic cascade in NSCLC (i.e., primary tumor, CTCs, and metastasis) and might have significance in other tumor types.
- H6.** Newly identified biomarkers might be correlated with a cancer stem cell phenotype, and might provide cells with superior capabilities to metastasize, therefore holding potential for the development of novel targeted therapeutic strategies.

7 OBJECTIVES

Considering the established hypothesis, the main goal of this thesis is “**the definition of novel bioinspired targeted therapeutic strategies for metastatic lung cancer patients**”.

SECTION I: STRATEGY INSPIRED BY EXOSOMES

The objective of this section is “the rational design of a multifunctional nanoplatform inspired by natural exosomes for the selective delivery of anticancer therapies”. This goal has been pursued after setting up specific objectives (O):

- O1.** To develop a nanoplatform that resembles exosomes for their composition and physicochemical properties, Exosome-mimetic Nanoplatform (EMN), following simple, reproducible, and cost-efficient methodologies.
- O2.** To functionalize EMNs with active proteins with organotropic properties, and to load them with therapeutic RNA.
- O3.** To determine EMNs biological behavior and therapeutic potential, and compare these properties with those of tumor-derived exosomes *in vitro* and orthotopic mice models.

SECTION II: STRATEGY INSPIRED BY CTCs

The objective of this section is “the identification, validation and study of a novel biomarker for metastatic NSCLC with the potential for the development of targeted therapies”. This goal has been pursued following the next specific objectives:

DISCOVERY OF A NEW TARGET FOR METASTATIC NSCLC

- 04.** To isolate and characterize CTCs from NSCLC patients in order to identify novel biomarkers that can be of interest for diagnostic and therapeutic purposes.
- 05.** To validate the results and determine the prognostic value of the expression of this biomarker.
- 06.** To study the expression of the identified biomarker in primary tumors from NSCLC, as well as in other types of tumors.

ROLE OF TAS1R3 IN NSCLC

- 07.** To generate representative animal models of the primary tumor and metastatic stages of NSCLC, in order to study the biomarker distribution.
- 08.** To generate a stable NSCLC cell line that overexpresses TAS1R3 in order to study the produced phenotypic changes *in vitro* and *in vivo*.
- 09.** To study the role and correlation of TAS1R3 with CSC, metastasis initiation and progression, to understand its potential as a therapeutic target.

8 MATERIALS AND METHODS



SECTION I: STRATEGY INSPIRED BY EXOSOMES

8.1.1 Materials

Phosphatidylcholine (Lipoid E PC) and sphingomyelin (Lipoid E SM) were obtained from Lipoid GmbH. Cholesterol (CH) was purchased from Sigma-Aldrich. C16 Ceramide (Cer), NDB-6 Cholesterol, and C11 TopFluor Sphingomyelin, were all purchased in Avanti Polar Lipids. MilliQ® water (Simplicity 185, Millipore,) was used throughout the study. Ethanol of analytical grade was purchased from VWR. Tetramethylindotricarbocyanine iodide (DiR) and tetramethylindotricarbocyanine perchlorate (DiD) were acquired from Thermo Fisher Scientific. miRNA-145 (miR145; sense strand 5'-GUCCAGUUUCCCCAG GAAUCCCU-3', antisense strand 5'-GGAUUCCUGGAAAUACUGUUCU-3'), miRNA-145-Cy5 (miR145-Cy5), miRNA-scramble (miRscr) and a model small interfering RNA (siRNA) were synthesized by Eurofins Genomics. DNA-CH was kindly provided by Ramon Eritja (Nucleic Acids Chemistry Group, Institute for Advanced Chemistry of Catalonia, Barcelona, Spain).

8.1.2 Cell culture

SW480 (ATCC® CCL-228), PC-3 (ATCC® CRL-1435) and A549 (ATCC® CCL-185) cells were grown in Dulbecco's modified Eagle's medium (DMEM) high glucose (Gibco, Thermo Fisher Scientific), supplemented with 10% fetal bovine serum (FBS, Thermo Scientific), and 1% penicillin/streptomycin (Thermo Scientific). Cells were maintained at 37 °C in a 5% CO₂ humidified atmosphere. Trypsin and Phosphate Buffered Saline (PBS) were purchased from Sigma-Aldrich. All cell lines were tested routinely and confirmed to be mycoplasma-free. The A549 cells were authenticated by Short Tandem Repeat (STR)-profiling according to American Type Culture Collection (ATCC) guidelines.

8.1.3 Exosome isolation and characterization

8.1.3.1 Exosome isolation protocol

When cells reached a confluence of 80%, cells were washed with PBS 1X and cultured in serum-free DMEM, called conditioned

medium (CM), for 16 hours. Exosomes secreted in the CM were isolated as previously described with minor modifications (Théry *et al.*, 2006). Briefly, the CM was first centrifuged to remove cells and debris at 300 xg for 10 min and 16,500 xg for 20 min at 4°C. Then, the supernatant was collected, filtered by a 0,22 µm syringe filter (Pall PharmAssure) and centrifuged at 120,000 xg for 90 min at 4 °C using a SW 32 Ti Rotor (Optima TL Ultracentrifuge; Beckman Coulter). The exosome pellet was then washed with abundant PBS 1X at 120,000 xg for 70 min at 4°C. Exosomes from plasma were isolated following the same protocol with a slight modification due to plasma viscosity and protein and lipid abundance compared with the cell supernatant. Briefly, venous blood samples were collected in lavender-top tubes of 10 mL with Ethylenediaminetetraacetic acid (EDTA, BD Vacutainer™ K2E) and were centrifuged at 2,000 xg for 15 min at 4°C, then, plasma was collected and centrifuged at 500 xg for 30 min at 4°C to remove cells and at 12,000 xg for 45 min at 4°C to sediment cell debris and macrovesicles. Next, supernatant was filtered through a 0.22 µm syringe filter to remove particles larger than 200 nm and diluted in PBS 1X (1:6). After that, the sample was ultracentrifuged at 120,000 xg for 90 min at 4°C. The exosome pellet was washed in a large volume of PBS 1X (36 mL), ultracentrifuged at 120,000 xg for 70 min at 4°C. This step was repeated one more time (wash and centrifuge). Exosome pellets from cells and plasma were finally resuspended in 50 µL of the appropriated buffer (PBS 1X for dynamic light scattering (DLS) measurements and transmission electron microscopy (TEM) or in radioimmunoprecipitation assay buffer (RIPA buffer 1X) for protein quantification and western blotting) and immediately used for experiments or stored at -80 °C for later analysis.

8.1.3.2 Western Blot analysis of exosomes

The protein level of the isolated exosomes was determined using the micro bicinchoninic Acid (microBCA) protein assay kit according to the manufacturer's instructions (Thermo Scientific). WB analyses were performed using standard techniques. Total exosomal protein (16 µg per lane) was run on 10% sodium dodecyl sulfate–

polyacrylamide gel electrophoresis (SDS-PAGE) and transferred to polyvinylidene fluoride (PVDF) membranes. After blocking and washing, the membranes were incubated with antibodies against Alix (3A9, NOVUS, 1:200) and CD9 (C-4, Santa Cruz Biotechnology, 1:200) in Tween 20-Tris-buffered saline (TTBS) 5% milk overnight at 4 °C. After that, membranes were incubated with the secondary antibody Peroxidase AffiniPure Goat Anti-Mouse IgG (H+L) (114094, Jackson ImmunoResearch®) and proteins were detected using the enhanced chemiluminescence (ECL) kit according to the manufacturer's protocol (Thermo Scientific).

8.1.3.3 Protein identification of exosomes by LC-MS/MS

Proteomic analysis was performed in the Proteomic Service of Instituto de Investigación Sanitaria de Santiago de Compostela (IDIS), Santiago de Compostela, Spain. Exosomes from A549 cells were loaded on a 10% SDS-PAGE gel. The run was stopped as soon as the front had penetrated 3 mm into the resolving gel (Bonzon-Kulichenko *et al.*, 2011; Perez-Hernandez *et al.*, 2013). The protein band was detected by Sypro-Ruby fluorescent staining (Lonza), excised, and processed for in-gel, manual tryptic digestion as described elsewhere (Shevchenko *et al.*, 1996). Peptides were extracted by carrying out three 20-min incubations in 40 µL of 60% acetonitrile dissolved in 0.5% HCOOH. The resulting peptide extracts were pooled, concentrated in a SpeedVac, and stored at -20 °C.

8.1.3.4 Mass spectrometric analysis

Digested peptides were separated using Reverse Phase Chromatography. Gradient was created using a micro liquid chromatography system (Eksigent Technologies nanoLC 400, SCIEX) coupled to high speed Triple TOF 6600 mass spectrometer (SCIEX) with a micro flow source. The chosen analytical column was a silica-based reversed phase column YMC-TRIART C18 150 × 0.30 mm, 3 mm particle size and 120 Å pore size (YMC Technologies, Teknokroma). The trap column was a YMC-TRIART C18 (YMC Technologies, Teknokroma with a 3 mm particle size and 120 Å pore size, switched on-line with the analytical column. The loading pump

delivered a solution of 0.1% formic acid in water at 10 $\mu\text{l}/\text{min}$. The micro-pump generated a flow-rate of 5 $\mu\text{l}/\text{min}$ and was operated under gradient elution conditions, using 0.1% formic acid in water as mobile phase A, and 0.1% formic acid in acetonitrile as mobile phase B. Peptides were separated using a 90 minutes gradient ranging from 2% to 90% mobile phase B (mobile phase A: 2% acetonitrile, 0.1% formic acid; mobile phase B: 100% acetonitrile, 0.1% formic acid). Injection volume was 4 μl .

Data acquisition was performed in a TripleTOF 6600 System (SCIEX) using a Data dependent workflow. Source and interface conditions were the following: ion spray voltage floating 5500 V, curtain gas 25, collision energy 10 and ion source gas 1 25. Instrument was operated with Analyst TF 1.7.1 software (SCIEX). Switching criteria was set to ions greater than mass to charge ratio (m/z) 350 and smaller than m/z 1400 with charge state of 2–5, mass tolerance 250ppm and an abundance threshold of more than 200 counts (cps). Former target ions were excluded for 15 s. The instrument was automatically calibrated every 4 hours using external calibrant tryptic peptides from PepCalMix.

8.1.3.5 Data Analysis

After MS/MS analysis, data files were processed using ProteinPilot™ 5.0.1 software from Sciex which uses the algorithm Paragon™ for database search and Progroup™ for data grouping. Data were searched using a Human specific Uniprot database. False discovery rate (FDR) was performed using a non-linear fitting method displaying only those results that reported a 1% Global false discovery rate or better (Shilov *et al.*, 2007). Functional analysis was performed by FunRich open access software (Functional Enrichment analysis tool) for functional enrichment and interaction network analysis (<http://funrich.org/index.html>). For statistics, FunRich uses hypergeometric tests, BH and Bonferroni (Pathan *et al.*, 2015, 2017).

8.1.3.6 Transmission Electron Microscopy (TEM)

Morphology and structure of the nanovesicles were observed by TEM (JEOL JEM-2010) in the service of Electronic microscopy of

the University of Santiago de Compostela. 10 μL of the sample was loaded on the grid, incubated for 3 min at room temperature (RT) and stained in 10 μL of 2% phosphotungstic acid solution for 1 min. The excess of phosphotungstic solution was removed with filter paper and the grid was washed seven times in a water droplet for 2-3 sec and then air-dried overnight prior to visualization by TEM.

8.1.4 EMNs preparation and characterization

8.1.4.1 Preparation of EMNs

EMNs with a well-defined composition (CH:PC:SM:Cer) were prepared following the ethanol injection methodology. In brief, lipids were dissolved in ethanol, at defined ratios (0,9:1:0,4:0,03 w/w), and a total lipid concentration of 0,92 mg/ml. 200 μL of the ethanol solution was injected with an insulin syringe (0.5 ml, 0.33x12mm ICO.C.1) into 2 mL of milliQ water, under magnetic stirring. EMNs were spontaneously formed.

8.1.4.2 Dynamic Light Scattering and Laser Doppler Anemometry

The hydrodynamic diameter, polydispersity index and superficial charge of the exosomes and EMNs were measured using a Zetasizer Nano ZS (Malvern Instruments). Measurements were performed in PBS 1X (exosomes) and MilliQ water (EMNs) at room temperature (RT). For the zeta potential measurements, samples were diluted in 1 mM potassium chloride (KCl).

8.1.4.3 Nanoparticle Tracking Analysis (NTA)

Particle size and concentration distribution of the EMNs and exosomes were also measured using NTA (v2.3; Malvern Instruments) according to manufacturer's instructions. Briefly, EMNs samples were vortexed and diluted to a final dilution of 1:1000 in milliQ H₂O and exosomes 1:100. Blank-filtered H₂O was run as a negative control. Each sample analysis was conducted for 60 s and measured five times using Nanosight automatic analysis settings. The detection threshold was set to level 11 and camera level to 15.

8.1.4.4 Colloidal stability

A stability study was performed in human plasma and cell culture media (DMEM supplemented with 1% FBS) incubated at 37 °C. The colloidal properties of EMNs were determined using the Zetasizer Nano ZS each hour up to 5h for human plasma and 20h for DMEM. Stability of the formulation under storage conditions was also tested in PBS 1X at 4°C up to 3 months. All measurements were performed in sextuples.

8.1.4.5 Cellular uptake

Uptake was investigated by using fluorescent-labeled EMNs (TopFluor-SM) by means of a Confocal Laser-Scanning Microscope (CSLM; Leica TCS SP5). Cancer cell lines (SW480, A549 and PC3) were grown on coverslips in a P24 plate at a density of 10^5 cells/well for 24 hours at 37°C. Fluorescent-labeled EMNs were added in fresh medium without supplements to cultured cells and incubated for 4 hours in the dark. After incubation, cells were rinsed with PBS 1X (pH 7.4) three times and then were treated with paraformaldehyde (PFA; 4% v/v in PBS) in the dark at RT for 15 minutes. Cells were washed again with PBS at least three times, and then the nuclei were counterstained with Diamino Phenyl Indol (DAPI; Cell Search, Sigma-Aldrich) or Hoechst (Thermo Scientific) for 3 minutes in the dark at RT. Finally, cells were washed again, and coverslips were mounted on clean slides with 8 μ L of Mowiol (Calbiochem®), dried at RT, and conserved in the dark at -20°C to be analyzed later on by CSLM. The three-dimensional (3D) structure of the cells treated with EMNs-NBD+miR145-Cy5 was reconstructed from corresponding confocal images using Leica Application Suite X (LAS X) software.

8.1.4.6 Cytotoxicity assay

The cytotoxicity of EMNs were assessed by the 3-(4,5-dimethylthiazol-2-yl)-2,5-diphenyltetrazolium bromide (MTT, Thermo Fisher Scientific) assay. Briefly, cells were seeded at a density of 10^4 cells/well in a 96-well plate containing 100 μ L of fresh culture medium and incubated overnight to allow cell attachment for subsequent study. Then, cells were cultured in the presence of

different concentrations of EMNs for 48h at 37°C. After the incubation, MTT (5 mg/mL) was added to medium and further incubated for 4 h, then 100 μ L DMSO was added to dissolve the formazan crystals formed in the live cells for 10 min at 37°C. The absorbance at 570 nm was recorded using a spectrometer.

8.1.4.7 Nuclear magnetic resonance spectroscopy (NMR)

NMR spectroscopy experiments relying on ^1H and ^{31}P detection were measured on a Varian Inova 17.6 T spectrometer (750 MHz proton resonance) equipped with a triple resonance HCP probe and z- gradient in the service of Nuclear Magnetic Resonance of the University of Santiago de Compostela. The ^{13}C NMR spectra were measured on a Varian Mercury 7.04 T (75.4 MHz, ^{13}C resonance) equipped with a double resonance ATB probe with z-gradient. The spectra were processed and analyzed with MestreNova software v11.0 (Mestrelab. inc.).

8.1.5 Loading of therapeutic molecules

8.1.5.1 Loading of exosomes

Exosomes were loaded with different molecules. The hydrophobic drug Curcumin (Acros Organics™, Thermo-Fisher Scientific) was loaded into exosomes (0,5% loading w/w) by incubation for 10 min in the dark. Curcumin–exosomes were then isolated by ultracentrifugation at 120,000 xg for 1 hour at 15°C in an SW32Ti rotor (Optima TL Ultracentrifuge, Beckman Coulter) and resuspended in MilliQ water. Exosomes were also loaded with nucleic acids (random siRNA, DNA-CH or miRNA145) by electroporation as previously described (Kooijmans *et al.*, 2013). Briefly, exosome pellet was resuspended in PBS 0.1X and gently mixed with the appropriated μ L of siRNA, DNA-CH or miRNA (same loading than for EMNs) in a final volume of 400 μ L into 0.4 cm electroporation cuvettes. Exosomes were then electroporated using a Gene Pulser II Electroporator (Bio-Rad), at 300V and 25 μ F of capacitance. Lastly, exosomes were incubated in ice for 30 min to allow the exosome membrane to be fully restored. To get rid of free nucleic acids, exosomes were diluted with cold PBS and isolated again by

ultracentrifugation at 120,000 xg for 90 min at 15°C in 70.1 Ti rotor (Optima TL Ultracentrifuge).

8.1.5.2 Loading of EMNs

Loading with curcumin was accomplished by adding the drug (0,5% loading w/w) to the ethanolic lipidic phase prior injection into the aqueous phase. The suspension was then kept under stirring for 10 min in the dark at RT and ultracentrifuged at 35,000 rpm for 1 h at 15 °C. To associate siRNA and double stranded DNA (dsDNA) to EMNs, the required amount of each nucleic acid was dried up (to eliminate the water content) using miVac DUP with Quattro pump (Genevac) and the organic phase was added, vortexed at 12 rpm for 1 min and injected in the aqueous phase together with the lipids. MiR145 and miR-scramble (8µg) was associated with EMNs by adding directly 4 µL (8 µg/µL) of miRNA into the organic phase and injecting it in the aqueous phase. The formulation was kept 10 min under magnetic stirring.

8.1.5.3 Encapsulation efficiencies (%EE)

%EE of the drug and nucleic acids in the nanovesicles were determined indirectly by the difference between the total amount of the theoretical amount added in the sample and the free amount found in the supernatant after isolation by ultracentrifugation. The free drug was detected by measuring the emission of the fluorescence curcumin ($\lambda_{Ex} = 420 \text{ nm}$, $\lambda_{Em} = 535 \text{ nm}$). Free nucleic acids were detected by using the SYBR[®] Gold solution ($\lambda_{Ex} = 500 \text{ nm}$, $\lambda_{Em} = 550 \text{ nm}$) and the %EE was calculated following the next equation: $\%EE = (W_{\text{theoretic}} - W_{\text{free}}) / W_{\text{theoretic}} \times 100$.

Semi-quantification of miR145 encapsulated in EMNs was performed by agarose gel retention assay. Briefly, EMNs+miR145 were concentrated 10 times by a rotavapor and loaded onto a 2% agarose gel in TAE 1X buffer. Electrophoresis was performed at 100V for 40 min. MiR145 was visualized by SYBR[®] Gold Nucleic Acid Gel Stain (Invitrogen) by UV transillumination and gel photography. Free miR145 was used as a control.

8.1.6 EMNs functionalization with proteins

EMNs were functionalized with different proteins, recombinant human integrin alpha 6 beta 4 (ITG α 6 β 4) protein (Vitro), Bovine Serum Albumin (BSA, VWR) and Lysozyme (LYS, Sigma-Aldrich) by incubation. Briefly, EMNs were prepared as described above, and proteins were added to the formulation at a ratio 1:100 w/w (protein:lipids) on an orbital shaker for 20 min at RT. To assess the protein association of ITG α 6 β 4, functionalized-EMNs (F-EMNs) were ultracentrifuged at 60,000 rpm 1h 15°C in a Beckman 70.1 Ti rotor (Optima TL Ultracentrifuge) to isolate F-EMNs from free protein, and both fractions were loaded on 10% acrylamide gel and detected by fluorescent WB using the primary monoclonal antibody ITG β 4 (G-7, Santa Cruz Biotechnology). Physicochemical properties of functionalized EMNs were also measured by DLS and LDA. EMNs+miRNA145 were functionalized with ITG β 4 following the same procedure.

8.1.6.1 Association efficiency of BSA and LYS to EMNs

BSA and LYS association to EMNs was measured by using Amicon Ultra – 0,5 mL centrifugal filters (100 K) (Merk Millipore) at 2700 xg for 20 min to separate the free protein from the liposomes. The association efficiency of the proteins to EMNs was calculated by measuring the concentration of free protein using Quick Start Bradford 1X Dye Reagent (BioRad), reading the absorbance at 595 nm in a spectrophotometer (Tecan Infinite M1000), and following the next equation: %AE = $(C_{\text{theoretic protein}} - C_{\text{free protein}}) / C_{\text{theoretic protein}} \times 100\%$ where C is concentration in mg/mL.

8.1.7 Binding assay for the evaluation of specific interaction integrin-laminin

Coverslips were coated with 1 mL (10 μ g/mL) of Laminin-V (Cultrex[®], Vitro) and incubated at 37°C o/n. Coverslips were then washed twice with PBS 1X and 100 μ L of EMNs with/without integrin functionalization (EMNs and F-EMNs) were added and incubated for 24h at 37°C. Then, the coverslips were washed again 3x5min with PBS 1X and mounted on slides with 8 μ L of Mowiol 4-

88 Reagent (Merck, Spain), dried at RT and conserved in the dark at -20°C to be analyzed later on by fluorescence microscopy.

8.1.8 Immunofluorescence protocol for laminin

A549 cells were seeded onto coverslips in a 24-well plate and incubated overnight at 37°C. The following day, cells were washed with PBS twice and fixed with PFA 4% for 15 min at RT. After two more washing steps, cells were permeabilized with 0.2% triton x-100 for 10 min at RT, washed again, and subsequently incubated with PBS + 3% BSA for 1h at RT. Next, cells were incubated with the primary monoclonal antibody Laminin-5 (1:50, Dako) in BSA 2% for 1h at RT, washed with PBS 1X 3x5 min and for visualization, DyLight™ 680 conjugated secondary antibody (#35518, Thermo Fisher Scientific) was used. Coverslips were washed again with PBS 1X and treated with DAPI for cell nuclei staining. Lastly, coverslips were mounted on slides with 8 µL of Mowiol, dried at RT and conserved in the dark at -20°C to be analyzed later on by confocal microscopy.

8.1.9 Perfusion of EMNs in a 3D model of tumor cells

The 3D model was performed as previously reported (Marta Alonso-Nocelo *et al.*, 2016). Briefly, 1×10^6 cells were added in a 50 µL drop on the surface of the 3D polystyrene scaffolds (Alvetex®) and incubated for 5h at 37°C. After that, 10 mL of fresh culture medium was added to the P6 well plate. Then, the scaffold was placed inside a bioreactor and coupled to an automatic syringe pump (New Era Pump Systems, Inc.). EMNs were diluted in fresh culture medium and perfused under dynamic conditions (250 µL/h for 2h) and then, the Scaffold was washed with cold PBS (500 µl/h for 1 h). Finally, the scaffold was removed from the bioreactor and fixed with PFA 4% for 15 min and washed 3x5 min with PBS 1X prior the immunofluorescence protocol. Scaffolds were then incubated with the primary antibody against Laminin-5 (M7262, Dako) for 1h at RT, washed with PBS 1X 3x5 min and for visualization, DyLight™ 680 conjugated secondary antibody (#35518, Thermo Fisher Scientific) was used. Scaffolds were washed again with PBS 1X and then treated

with DAPI for cell nuclei staining. Scaffolds were analyzed by CLSM at 630x magnification.

8.1.10 miR145 delivery and transfection

The loading and encapsulation efficiency of miRNA145 to EMNs and exosomes have been already described in the section 7.1.5 of *Loading of therapeutic molecules*.

8.1.10.1 Confocal microscopy analysis

A549 cells were seeded on coverslips in a 24-well plate at a density of 8×10^4 cells/well in complete medium. The following day, the same quantity of EMNs or F-EMNs labeled with NBD-CH and loaded with miR145-Cy5 were incubated with the cells in medium without supplement for 4 hours in the dark. After incubation, the medium was removed, cells were washed with PBS three times and then, fixed with PFA 4% (v/v in PBS) in the dark at RT for 15 minutes prior to countersaining the nuclei with DAPI for 10 min. Lastly, coverslips were mounted on clean slides with 8 μ L of Mowiol, dried at RT, and conserved in the dark at -20°C to be analyzed later on by CSLM. Cells were also transfected with miR145-Cy5-loaded exosomes and F-EMNs, adding the same amount of miR145-Cy5 (8 μ g) to the cells and following the just mentioned protocol.

8.1.10.2 Flow cytometry analysis

MiR145-Cy5-loaded EMNs, F-EMNs, and exosomes were incubated with the cells as described above. After incubation, the medium was removed, cells were washed with PBS three times and trypsinized. A549 cells incubated with PBS instead of nanovesicles were also included as a control. Collected cells were fixed at 0,4 % PFA and kept at 4 $^\circ\text{C}$ until FACS analysis. The percent of Cy5 positive cells was determined by a FACScan flow cytometer (BD Biosciences). A minimum of 10,000 events per condition was measured. The analysis of the results was performed using FlowJo Software (TreeStar Inc.).

8.1.10.3 Cell transfection

24 hours before transfection, A549 cells were seeded on a 6-well plate at a low density of 25×10^4 cells/well in complete DMEM. The next day, the complete medium was removed, cells were washed with PBS 1X and a new medium without supplement was added. 8 μ g of miR145 associated with EMNs and F-EMNs, as well as miR145 free in solution (as a control) were added to each well and incubated at 37°C and 5% CO₂ atmosphere for 4h. After incubation, the culture medium was removed, cells were washed with PBS and fresh complete medium was added and further incubated for 96h prior to being collected for analyses by RT-qPCR and functional assays (colony forming assay (CFA) and WB).

8.1.10.4 RT-PCR analysis

Total microRNA was extracted from transfected A549 cells using the microRNA Purification Kit (Norgen Biotek Corp.) following the manufacturer's protocol. After nanodrop RNA quantification, the RNA was retrotranscribed into cDNA using the qScript™ microRNA cDNA Synthesis Kit (Quanta Bioscience™) according to manufacturer's instructions. Quantitative Real Time-PCR was performed using PerfeCta SYBR® Green SuperMix (Quanta Bioscience™) in an AriaMx Real-time PCR System (Agilent Genomics). The relative quantities of miR145 were normalized using the housekeeping RNU-6 and using the comparative CT method. For miRNA quantitation, specific forward, reverse and universal primers were acquired from Eurofins (Fisher Scientific): hsa-miR145-5p (5'-CGCGCGTTCCAGTTTTCCCAGG-3') and universal reverse PCR primer (5'-GTGCAGGGTCCGAGGT-3'), and the housekeeping small RNA control primer RNU6 (5'-CTCGCTTCGGCAGCAC-3', 5'-AACGCTTCACGAATTTGCGT-3'). The PCR conditions consisted of 2 min of initial denaturation at 95 °C, 40 cycles of denaturation at 95 °C for 5 sec and annealing at 60 °C for 30 sec, and lastly, 1 min of activation at 95 °C, annealing at 55 °C for 15 sec and elongation at 95 °C for 30 sec. Each experiment was performed at least in triplicates.

8.1.10.5 Colony forming assay

After 4 hours of transfection with EMNs, transfected A549 cells were seeded at 400, 600 and 800 cells per well in a 12 well plate. Cell colonies were allowed to grow for 6 days in complete DMEM medium. Colonies were then stained with MTT solution (5 mg/ml) for 3 hours, washed with PBS 1X and air dried. The number of colonies per well was determined by imaging and analyzed with Image J software. All experiments were carried out in triplicate.

8.1.10.6 Chloroquine treatment

After transfection, 600 cells were seeded in a 12-well plate in complete DMEM medium and treated with 40 μ M chloroquine (Sigma-Aldrich) overnight. The next day, cells were washed with PBS 1X and fresh culture medium was added.

8.1.10.7 N-Cadherin downregulation by WB

Protein levels of transfected cells and controls were determined by DCTM protein assay (Bio-Rad Laboratories). Equivalent levels of proteins were separated by SDS-PAGE and transferred to a PVDF membrane and incubated with primary monoclonal antibodies against N-Cadherin (1:500, 3B9, #33-3900, Life Technologies) and β -actin (1:2000, T6199, Sigma-Aldrich). The ECL method (Thermo Scientific) was used to visualize the expression of proteins.

8.1.11 Fluorescent labelling of exosomes and EMNs

Exosomes were labeled with the lipophilic fluorescent DiD, according to Tian *et al.* protocol (Tian *et al.*, 2010), with some modifications. Briefly, exosome pellet was resuspended in PBS 1X mixed with DiD (0,5% loading w/w) and incubated for 10 min in the dark. Labeled exosomes were then ultracentrifuged at 200,000 xg for 1 hour at 15°C in a SW32Ti rotor (Optima TL Ultracentrifuge, Beckman Coulter) to remove free DiD and resuspended in PBS 1X. EMNs were labelled with different fluorophores (DiD, NBD, TopFluor, DiR, Nile Red and Cy5) separately or in combination, by adding them to the organic phase together with the lipids and injecting

them into the stirred aqueous phase. The suspension was kept under stirring for 10 min in the dark at RT. EMNs were then ultracentrifuged at 30.000 rpm for 1 h at 15°C in a Beckman 70.1 Ti rotor (Optima TL Ultracentrifuge). %AE was determined, in all cases, indirectly by the difference between the total amounts of the theoretical fluorophore added in the sample and the free fluorophore found in the supernatant after isolation. Free fluorophore intensity was detected by EnVision multilabel plate reader (Perkin Elmer, Waltham, MA, USA), DiD ($\lambda_{Ex} = 644$ nm, $\lambda_{Em} = 665$ nm), NBD ($\lambda_{Ex} = 466$ nm, $\lambda_{Em} = 535$ nm), TopFluor ($\lambda_{Ex} = 495$ nm, $\lambda_{Em} = 503$ nm), DiR ($\lambda_{Ex} = 750$ nm, $\lambda_{Em} = 780$ nm), Nile Red ($\lambda_{Ex} = 553$ nm, $\lambda_{Em} = 610$ nm), Cy5 ($\lambda_{Ex} = 647$ nm, $\lambda_{Em} = 665$ nm), and the %AE was calculated following the next equation: $\%AE = (W_{theoretic} - W_{free}) / W_{theoretic} \times 100$.

8.1.12 Cryogenic transmission electron microscopy

Samples were initially vitrified according to Dubochet protocol (Dubochet *et al.*, 1988). Briefly, an aliquot of 3,5 μ L of each sample was applied to glow-discharged holey grids for 1 min, blotted, and rapidly plunged into liquid ethane at -180 °C and kept at this temperature until visualization. Images were obtained at 0°-tilt under minimum dose conditions using a field emission gun Tecnai 20 G2 Microscope (FEI, Eindhoven) equipped with a Gatan cold stage operated at 200 keV. Low-dose images were collected at a nominal magnification of $\sim 50,000\times$ by using a FEI Eagle CCD camera with a step size of 15 μ m. The original pixel size of the acquired images was 2.74Å.

8.1.13 *In vivo* assays

The animal handling and the experimental procedures were performed in collaboration and approved by the internal ethical research and animal welfare committee (IIB, UAM), and by the Local Authorities (Comunidad de Madrid, PROEX 424/15) which complied with the European Union (Directive 2010/63/UE) and Spanish Government guidelines (Real Decreto 53/20133).

8.1.13.1 Development of orthotopic NSCLC mouse model

1×10^6 A549 lung cancer Luc cells, kindly provided by Dr. Anxo Vidal (Santiago de Compostela, Spain), were injected in 0.1 mL of PBS into the tail vein of 7-week-old female nu/nu mice (Charles River). The tumor growth was follow-up by *in vivo* bioluminescence imaging using the Xenogen IVIS (IVIS Lumina II). Mice were anesthetized and injected retro-orbitally with 1.5 mg of d-luciferin (15 mg/mL in PBS), images were taken during 5 min with a Xenogen IVIS system coupled to Living Image acquisition and analysis software (Xenogen Corporation). For bioluminescence intensity (BLI) plots, photon flux was calculated as previously described (Hergueta-Redondo *et al.*, 2014). Measurements were performed once a week starting 1 week after tail vein injection and up to 15 weeks.

8.1.13.2 Comparative biodistribution of different administration routes

Once the tumors were visible by bioluminescence, mice were treated with EMNs + miR145-Cy5 injected by retro-orbital inoculation (n=3) or by intraperitoneal route (n=3). 8 hours later, mice were sacrificed and biodistribution of miR145-Cy5 quantified by *ex vivo* fluorescence of different organs, lung + tumor, heart, spleen, kidney and liver, using Xenogen IVIS (IVIS Lumina II). In each experiment, mice treated with EMNs without miR145-Cy5 were used as control in order to reduce the background tissue.

8.1.13.3 miRNA145 biodistribution with EMNs and exosomes

Mice were randomly divided into two groups and treated with miR145-Cy5-loaded F-EMNs (n=5) or miR145-Cy5-loaded exosomes (n=5). Each mouse was injected with a dose of 2,5 μ g of miR145-Cy5. After 8h, mice were sacrificed, and the biodistribution of miR145-Cy5 was quantified by *ex vivo* fluorescence of different organs, lung + tumor, heart, spleen, kidney, and liver, using Xenogen IVIS. In each experiment, mice treated with F-EMNs without miR145-Cy5 were used as a control in order to reduce the background tissue.

8.1.13.4 Confocal analysis in tissue samples

At the end of the experiment, once the mice were sacrificed and the fluorescence quantified, lung tumors were extracted and frozen in optimal cutting temperature (OCT) compound (Tissue-Tek, Sakura). The xenografted tumors were stained with DAPI and Ki67 (Rabbit Anti-Human Ki-67 Monoclonal Antibody (Clone SP6, #MAD-020310Q, Master Diagnostica) for the identification of metastatic cells. Images were captured in Cy5 emission on an LSM710 Confocal microscope (Zeiss), analyzed and quantified using Fiji software.

8.1.13.5 Statistics

Statistical analyses were performed with a GraphPad Prism[®] software (version 6.0c). All data are expressed as mean \pm standard deviation (SD). Significant differences between two groups were determined by a Student's t-test and multiple comparisons among conditions were done using one-way analysis of variance (ANOVA) followed by Bonferroni post hoc test. All experiments were performed at least in triplicate. * $p < 0,05$, ** $p < 0,001$, *** $p < 0,0001$.

SECTION II: A STRATEGY INSPIRED BY CTCs

8.1.14 Patient selection

The study included patients who fit the eligibility criteria: unresected, non-pretreated stage III to IV (according to the International Association for the Study of Lung Cancer (IASLC)/ American Thoracic Society (ATS)/ European Respiratory Society (ERS) classification criteria), with a histological diagnosis of NSCLC (see Supplementary material Mariscal *et al.* 2016). Blood samples were collected before the initiation of chemotherapy, in accordance to the guidelines and protocols approved by the Institutional Ethical Committee (*Galician Clinical Research Ethics Committee*, SERGAS; code 2008/277), and signed informed consent was obtained from all participants. CTCs evaluation cohort included 42 NSCLC patients, 36 of them diagnosed with distant metastasis by computed tomography (CT) scan.

Microarray gene-expression analysis was conducted in an independent set of 10 patients following the same criteria (advanced NSCLC, stage IIIB-IV) and healthy age-matched donors. Distant metastasis was present in 8 out of 10 patients at the moment of recruitment (see Supplementary material Mariscal *et al.* 2016).

Validation of the target was performed in an independent cohort of 41 patients, stage III to IV (according to the AJCC staging manual), with a histological diagnosis of NSCLC, from the *Consortio Hospital General Universitario de Valencia*. The study was conducted in accordance with the Declaration of Helsinki, and the institutional ethical review board approved the protocol.

8.1.15 Immunoisolation, molecular profiling and Significance Analysis Microarray

Analysis of CTCs in advanced NSCLC was performed by Dr. Marta Alonso-Nocelo as previously described by Mariscal *et al.* Briefly, CTC isolation was performed from 7.5 ml of peripheral blood from advanced NSCLC patients (n=10) or healthy donors (n=4) using the EpCAM-based CELlection™ Epithelial Enrich Dynabeads® kit (Invitrogen) according to manufacturers' instructions. Total RNA

from CTC was then extracted with the QIAmp viral RNA mini kit (Qiagen), specifically designed for very low cellularity samples. Then, it was subjected to Complete Whole Transcriptome Amplification PCR for 20 cycles using the maximum amount of RNA; Cy3 labeled and hybridized onto Agilent 4 x 44 k gene expression arrays. Upon hybridization, signal was captured and submitted to Significance Analysis for Microarray to identify differentially expressed genes as described in Mariscal *et al.* supplementary material and methods (Mariscal *et al.*, 2016).

8.1.16 Significance Analysis for Microarrays (SAM)

Upon microarray hybridization, the signal was captured and processed using an Agilent scanner (G2565B, Agilent Technologies). The scanner images were segmented by the Agilent Feature Extraction Software (v9.5) with the protocol GE1-v5_95. Extended dynamic range implemented in the Agilent software was applied to avoid saturation in the highest intensity range. The processed signal (gProcessed-Signal) value was chosen for the statistical analysis instead of the signal with subtracted background (gBGSubSignal) since it produces lower average coefficient of variation (CV) in Spike-In and gene replicates ((Klebanov and Yakovlev, 2007) Spatial Detrend correction was applied using the Agilent Feature Extraction algorithm. *Biol Direct* 2:9; (Zahurak *et al.*, 2007) *BMC Bioinformatics* 8:142).

The following features and/or genes which did not conform to the established quality criteria were filtered: (a) non-uniform pixel distributed outliers and population replicate outliers according to the default Agilent feature extraction criteria; (b) spots not differentiated from background signal (as estimated for each spot); (c) spots in the range of negative controls.

Normalization among all microarray data was performed by the quantile method implemented in the limma package of the Bioconductor statistical software. In addition, probes with no signal in more than one patient were not included in the analysis. Finally, two class unpaired SAM algorithm implemented in the R package samr4 was used to identify differentially expressed genes.

8.1.17 Ingenuity Pathway Analysis (IPA) and Gene Ontology analysis

Gene set characterizing the CTC population was analyzed with IPA software for representative biological pathways and functions in our data set; 349 probes were identified as annotated genes (65.97%). Fisher's exact test was applied to calculate p value of biological related functions.

8.1.18 Real-Time Quantitative PCR Validation of CTCs

CTC were isolated as described and RNA was purified. cDNA was synthesized using SuperScriptIII chemistry (Invitrogen) following manufacturer's instructions. To further enhance the sensibility of detection, we performed a pre-amplification step by using the TaqMan® PreAmp Master Mix kit (Applied Biosystems) with 14 reaction cycles. Preamplified products were subjected to TaqMan® RT-PCR amplification for 15 candidate genes (**Table 1** details probes information). Expression values for each gene were normalized to CD45 as a marker of non-specific isolation. The same extraction protocol was applied to healthy volunteer's blood to evaluate the levels of unspecifically hematopoietic isolated cells. Validation of TAS1R3 in the cohort of 41 independent NSCLC patients was performed following the same protocol.

Table 1. TaqMan RT-qPCR probes characteristics for the validation of the 15 candidate genes.

Gene	Reference	RefSeq	Amplicon length (bp*)
GAPDH	Hs99999905_m1	NM_002046.4	122
CD45	Hs00894734_m1	NM_002829.3	70
CX3CL1	Hs00171086_m1	NM_002996.4	72
EBF2	Hs00224081_m1	NM_022659.3	124
ICOS	Hs00359999_m1	NM_012092.3	103
KLK6	Hs00160519_m1	NM_001012964.2	119
TAS1R3	Hs01026531_g1	NM_152228.2	56
TGFA	Hs00608187_m1	NM_001099691.2	70
AQP1	Hs00166067_m1	NM_198098.2	86
DAB1	Hs00221518_m1	NM_021080.3	140

GDF15	Hs00171132_m1	NM_0048655.2	78
NOTCH1	Hs01062014_m1	NM_017617.4	80
SEMA3F	Hs00188273_m1	NM_004186.4	108
SNCG	Hs00268306_m1	NM_003087.2	111
PTPRS	Hs00370080_m1	NM_002850.3	72
TNR	Hs00990097_m1	NM_003285.2	79
SNAI2	Hs00161904_m1	NM_003068.4	79

*bp: base pairs

8.1.19 Establishment of patient derived xenografts

Patient derived xenografts were established at the *Fondazione IRCCS, Istituto Nazionale dei Tumori* (Milan, Italy), as described in ref. (Moro *et al.*, 2012). The experimental protocol was approved by the C.E.S.A. (Ethical Committee for Animal Experimentation, of the National Cancer Institute Foundation), and animal experimentation was performed following guidelines drawn-up by C.E.S.A. according to ref. (Workman *et al.*, 2010).

8.1.20 Immunohistochemistry analysis

Immunohistochemistry was performed on formalin fixed and paraffin embedded PDX tumor samples with a commercially available detection kit (EnVision™ FLEX+, Dako) in an automated immunostainer (Dako Autostainer System, Dako). Briefly, sections (1,5 µm-thick) were cut from paraffin blocks, deparaffinized and rehydrated. Then, antigen retrieval was performed in Dako PT-link (EnVision FLEX Target Retrieval Solution, high pH, 30 min, 98°C). After peroxidase inhibition with Dako peroxidase block for 5 min, slides were incubated with the primary antibody for 60 min (TAS1R3 ab150525, 1:250 with EnVision FLEX Antibody Diluent). The primary antibody detection was performed using a Dako EnVision FLEX rabbit linker for 15 min, followed by incubation with Dako EnVision FLEX HRP polymer and DAB substrate chromogen (Dako DAB + Chromogen and DAB+substrate buffer) and lastly, counterstain with haematoxylin. This analysis was performed at *Fondazione IRCCS, Istituto Nazionale dei Tumori* (Milan, Italy).

8.1.21 Statistical validation and clinical database contrast

The data are displayed as the means \pm SD and categorical data are presented as frequencies and proportions. The significance of differences was examined by Student's t-test for continuous variables as well as Mann-Whitney U-test as indicated.

To analyze the prognostic potential of TAS1R3, patients were grouped based on TAS1R3 expression according to the 50th percentile into low (TAS1R3 < 50%), and high (TAS1R3 > 50%). OS and PFS were determined by the Kaplan-Meier method and compared with using the log-rank test. Multivariable analysis of the independent factors associated with disease-free survival was performed using the Cox proportional hazard model. The statistical analysis of the data was performed using IBM SPSS Statistics 22 (IBM Co.). $P < 0.05$ was considered statistically significant.

Clinical data from the Champions TumorGraft[®] database (Champions Oncology), were analyzed setting the cut-off for high levels of TAS1R3 in >2-fold expression, $\text{Log}_2(\text{RPKM}+1) > 0,7$. The fold expression compares the RPKM (Reads Per Kilobase Million) value of the model to the mean RPKM value across the entire bank.

8.1.22 Cell lines culture

Six human NSCLC cell lines were purchase from the American Type Culture Collection (ATCC, LGC Standards): A549, NCI-H23 (H23), NCI-H460 (H460), PC9, NCI-H1993 (H1993), SW900, and NCI-H1299 (H1299). Cell lines were maintained in the media suggested by the manufacturers, supplemented with 10% fetal bovine serum (FBS) and 1× penicillin/streptomycin at 37°C, 5% CO₂ in a humidified incubator (**table 2**). All cell lines were routinely tested for mycoplasma contamination.

Table 2. Clinicopathological characteristics of the cell lines included in the study and culture conditions

Cell lines	Gender	Culture media	Resource	Histology	Mutational status
A549	Male	DMEM 10%FBS	ATCC	Lung ADC	KRAS 12 Ser
H23	Male	RPMI 1640 10%FBS	ATCC	Lung ADC	KRAS 12 Cys
H460	Male	RPMI 1640 10%FBS	ATCC	Lung LCC	KRAS 61 His; PI3K p.E545K
PC9	Male	RPMI 1640 10%FBS	ECACC	Lung ADC	EGFR exon 19 Del
H1993	Female	RPMI 1640 10%FBS	ATCC	Lung ADC	c-MET amplification
SW900	Male	RPMI 1640 10%FBS	ATCC	Lung SCC	KRAS 12 Val
H1299	Male	RPMI 1640 10%FBS	ATCC	Lung ADC	P53 partial Del

ADC, adenocarcinoma; LCC, large-cell carcinoma; SCC, squamous cell carcinoma.

8.1.23 Establishment of primary cell cultures

Six additional primary human NSCLC cell lines were established in the laboratory at the *Istituto Nazionale dei Tumori* (LT215) and the *Fundación Investigación Hospital General Universitario de Valencia* (LT301, LT302, LT303, LT315, LT320), from surgical specimens of patients with lung adenocarcinoma as described in ref. (Andriani *et al.*, 2016; Herreros-Pomares *et al.*, 2019).

8.1.24 Flow Cytometry Analysis (FACS)

Single cell suspensions were washed and incubated in a staining solution containing 1% bovine serum albumin (BSA) and 2 mM ethylenediaminetetraacetic acid (EDTA) with the specific antibodies

at appropriate dilutions. Antibodies used were TAS1R3 (abcam, ab150525) and the secondary antibody anti-rabbit Alexa-647, phycoerythrin (PE)-conjugated anti-CD133/1 (AC133 clone; Miltenyi Biotec), and mouse H2K (H-2Kd/H-2Dd) monoclonal antibody (34-1-2S) peridinin-chlorophyll-protein (PerCP)-eFluor 710 (eBioscience™). H2K was used for the *in vivo* experiments to discard mouse cells. For CD133 staining, cells were incubated with 10 μ L of CD133/1-PE antibody diluted in 80 μ L of staining solution and 20 μ L of FcR blocking reagent (MiltenyiBiotec) for 10 min at 4 °C. 7-aminoactinomycin D (7-AAD) Viability Staining Solution (BD Pharmingen™) was added to the cells to exclude dead cells. Lung DTCs were identified using a negative gating strategy to exclude 7-AAD+ dead cells and mouse H2K+ cells. Samples were acquired and analyzed by using a FACSCalibur and FlowJo software.

8.1.25 Sphere formation assay

Sphere-forming assays were used for CSCs enrichment and 3D culture and analyzed by RT-qPCR and FACS. RT-qPCR was performed in collaboration with the *Fundación Investigación Hospital General Universitario de Valencia*, where cells were grown in serum-free medium supplemented as previously described in ref. (Herrerospomares *et al.*, 2019). Cells were plated at low density in ultra-low attachment (ULA) plates (Corning) with serum-free DMEM-F12 medium supplemented with 0.4% BSA, 50 μ g/mL epidermal growth factor (EGF), 20 μ g/mL basic fibroblast growth factor (bFGF), 5 μ g/mL insulin-transferrin-selenium (ITS) PREMIX, 2% B-27, 200 μ g/mL penicillin/streptomycin, and 2mM L-glutamine. Cultures were expanded by mechanical dissociation of spheres until RT-qPCR analysis. Medium was replaced twice a week and was maintained at 37°C in 5% CO₂ atmosphere. FACS analysis was performed in collaboration with the *Istituto Nazionale dei Tumori*, Milan. Briefly, cells were plated in ULA flasks in Stem Cell Medium (SCM): DMEM F-12 medium containing EGF (Peprotech, 20 ng/mL), bFGF (Peprotech, 20 ng/mL), B27 supplement minus vitamin A (Gibco, Life Technologies, 1X) and heparin sodium (Hospira, 0.6 IU/ml). For

FACS analysis, spheroids were disaggregated by incubation with Accumax (Sigma-Aldrich) at 37 °C for 5 min.

8.1.26 Anoikis assay

Selected cell lines (A549 and H460) were seeded at low density in 6-well plates of either ultra-low attachment grade, or normal tissue culture grade for control. Cells were incubated for 48 hours in complete medium prior to flow cytometer analysis for TAS1R3 expression.

8.1.27 Conditioned medium supplement

For preparation of conditioned media (CM), RAW264.7 macrophages, mouse endothelial cells, and mouse fibroblast were cultured in 6-well plates with 1 mL of serum-free medium for 24 hours. CM were then centrifuged (5000 xg, 10 min), mixed in a 2:1 ratio with fresh medium RPMI-1640 with 10% FBS, and used to culture A549 and H460 cells with 1,5 mL of CM:RPMI (2:1) in 6-well plates for 48 hours. CM from A549 and H460 was used as control. After 48 hours, cells were harvested and analyzed for TAS1R3 expression by flow cytometry.

8.1.28 Co-culture experiment

For the coculture experiment, a total of 1×10^5 of A549 or H460 tumor cells were seeded in a 6-well plate together with either RAW264.7 macrophages or mouse endothelial cells, in a ratio 1:3 (tumor:stroma cells) with RPMI-1640, 10% FBS. After 48 hours, cells were harvested and analyzed for TAS1R3 expression by flow cytometry.

8.1.29 Plasmids

Vectors was purchased from Tebu-bio, open reading frame (ORF) expression clone for TAS1R3 (NM_152228.2) and Enhanced Green Fluorescent Protein (eGFP) in 3rd generation HIV lentiviral pReceiver-Lv205 vector with cytomegalovirus (CMV) promoter, and Internal Ribosome Entry Site (IRES) IRES2-eGFP-IRES-puromycin in

bacterial stock (217EX-H0151-Lv205-B). An empty vector (217EX-NEG-Lv205) of the same characteristics was purchased as control.

8.1.30 Generation of lentiviral vectors encoding TAS1R3-IRES-GFP

HEK293T cells were thawed from liquid nitrogen and cultured in DMEM containing 10% FBS. 5 million cells were seeded in a 100 mm plate the day before transfection. When cells are 70-80% confluent the transfection mix was prepared as follows: 1.25 μg packaging plasmids (PpLp1 + pLp2 + pLVSVG) were co-transfected with 1.25 μg of the target plasmid by polyethylenimine (PEI, #23966-1, Polysciences Europe GmbH; ratio 1:6, DNA:PEI). Packaging plasmids were kindly provided by Dr. M Collado (IDIS, Santiago de Compostela, Spain). DNA/PEI mixtures were incubated at room temperature for 10 min and then added to the plate drop by drop. 8 hours later, cells were washed with PBS and a new fresh culture medium was added. 24 hours later, transfection efficiency was verified by the intensity of the GFP signal in an inverted fluorescence microscope (Zeiss). Then, the medium was harvested, filtered through a 0.45- μm pore size filter (#FPV-403-030, Biofilm) and completed up to 10 ml with fresh medium. Fresh medium was added to the cells and the process was repeated two more times every 8 hours.

8.1.31 Viral infection of A549 cells

The day of transfection 1.2×10^6 A549 cells were seeded into a 100 mm plate. 8 hour later, Polybrene 2000 (#TR-1003, Sigma Aldrich) was added to the vector-containing medium at a final concentration of 8 $\mu\text{g}/\text{ml}$ and incubated with the cell line. This step was repeated three times every 8 hours. Once the three rounds were completed, cells were washed with PBS and fresh medium was added. Cells were incubated at standard conditions until GFP signal was observed by fluorescent microscopy and then, puromycin (#P8833, Sigma Aldrich) was added at the concentration determined previously through a kill curve (1.2 $\mu\text{g}/\text{ml}$). TAS1R3 overexpression was determined and verified by RT-qPCR, Western blotting, immunofluorescence and proteomics.

8.1.32 Western blot analysis

Western blot was performed to confirm the overexpression of TAS1R3 in the transfected cells. A549 T1R3⁺ and non-targeting control (NTC) T1R3⁻ cells were harvested for protein extraction by radioimmunoprecipitation assay buffer (RIPA). Protein lysates were quantified by detergent compatible (DC) protein assay kit according to the manufacturer's instructions (Thermo Scientific) and afterwards, separated by 10% SDS-PAGE and transferred to PVDF membrane. After blocking, membranes were incubated with primary antibodies against TAS1R3 (ab150525, abcam, 1:1000) and the housekeeping anti- β -actin (#A228, Sigma Aldrich, 1:2000) in Tween 20-Tris-buffered saline (TTBS)-5% milk overnight at 4 °C and then, with secondary antibodies (Goat Anti-Rabbit IgG (H+L), #111-035-003) and Goat Anti-Mouse IgG (H+L, #115-035-003); from Jackson ImmunoResearch®) for 1h at RT. Proteins were detected using the ECL kit according to the manufacturer's protocol (Thermo Scientific) and analyzed by Image Lab software.

8.1.33 Immunofluorescence

Cells were fixed in 4% PFA, permeabilized with 0.1% Triton X-100, and blocked in PBS containing 3% BSA. Cells were stained with first rabbit polyclonal antibody against TAS1R3 (#150525, abcam, 1:100 dilution), 1h at RT. After being washed with PBS, cells were incubated with goat anti-rabbit Alexa Fluor 555 secondary antibody for 30 min at RT in the dark. Nuclei were counterstained with 4',6-diamidino-2-phenylindole (DAPI). Cells were mounted on glass slides in an antifade mounting medium. Fluorescence microscopy was performed using the JuLI™ Stage (NanoEntek) or using a confocal laser scanning microscope Leica TCS SP8 X.

8.1.34 Gene expression Analysis

RNA from cell pellets and frozen tissue samples was extracted using RNA purification kits according to the manufacturer's instructions. Reverse transcription reactions were performed from 1.0 μ g of total RNA using random hexanucleotides and a High-Capacity

cDNA Reverse Transcription Kit (Applied Biosystems, USA) following the manufacturer's instructions. RT-qPCR was performed with assays based on hydrolysis probes using 1 μ L of cDNA, TaqMan Gene Expression Master Mix, and a TaqMan Gene Expression Assay (see **table 3**). Different housekeeping genes such as *ACTB*, *GUSB*, *GAPDH*, *HPRT*, *B2M* and *CDKN1B* were selected as endogenous controls for the normalization of different samples and for the relative quantification of gene expression. Relative gene expression levels were expressed as the ratio of target gene expression to the geometric mean of the endogenous gene expressions according to the Pfaffl formula (Pfaffl, 2001) and normalized using the comparative cycle threshold (C_t) method ($\Delta\Delta C_t$).

Table 3. TaqMan RT-qPCR probes characteristics

Gene	Reference	RefSeq	Amplicon length (bp*)
GAPDH	Hs99999905_m1	NM_002046.4	122
GUSB	Hs00171086_m1	NM_002996.4	72
HPRT	Hs00224081_m1	NM_022659.3	124
NANOG	Hs02387400_g1	NM_024865.3	109
TAS1R3	Hs01026531_g1	NM_152228.2	56
SNAI2	Hs00161904_m1	NM_003068.4	79
CADH1	Hs00170423_m1	NM_001317184.1	117
SOX2	Hs01053049_s1	NM_003106.3	91
OCT4	Hs01895061_u1	NR_036440.1	130
B2M	Hs99999907_m1	NM_004048.2	75
CDKN1B	Hs00153277_m1	NM_004064.4	71

8.1.35 Proliferation assay

The proliferation assay was performed in transfected A549 cells (T1R3+/-) using the Click-iT™ Plus EdU Alexa Fluor™ 647 Flow Cytometry Assay Kit (ThermoFisher) following manufacturer's instructions. Fluorescence signal of proliferative cells was measured by flow cytometry analysis. For confocal images, 8×10^4 cells were seeded on cover slips in a 24-well plate, and the following cell, medium containing 20 μ M 5-Ethynyl-2'-deoxyuridine (EdU) in DMEM (1:1000) was added. 24 hours later, cells were washed with

PBS 1X, fixed with 4% PFA, permeabilized with 0,1% Triton X-100, and incubated with the label mix (1M Tris pH 8.5, 100 mM Cu(II)SO₄, 10 mM sulfo-Cy3-azide, 0,5 M Sodium-Ascorbate) for 30 mins in the dark. Then, cells were washed, incubated with 2 µg/ml of DAPI and mounted with mounting media (prolong) onto glass slides. EdU incorporation by the proliferating cells was visualized using confocal microscopy (Leica TCS SP8).

8.1.36 Wound healing assay

For *in vitro* migration assay, cancer cells were seeded at high density (1×10^5 cells) in 24-well plates. When cells were confluent, an artificial wound was created using a 10-µL micropipette tip. Medium was replaced with fresh medium and images were taken at 0, 24, and 48 hours. Assays were performed at least in triplicate. Migration rate into the wound was also monitored at real-time with JuLI™ Stage software.

8.1.37 Matrigel invasion assay

For *in vitro* invasion assay, 5×10^4 cancer cells were resuspended in the upper half of a polyester (PET) membrane transwell insert chamber (BD Bioscience) coated with Matrigel (1 mg/mL; BD Biosciences) on a 24-well plate. The lower chamber was filled with medium supplemented with 10% FBS as chemoattractant. After incubation at 37°C for 72 hours, cells on the top of the insert membrane were removed by gently scraping with a sterile cotton swab and cancer cells that passed through the insert were fixed in methanol for 10 min, washed in sterile water, briefly air-dried and mounted on slides using the VECTASHIELD Mounting Medium, containing DAPI. For each insert, cells in 5 random fields were counted by fluorescence microscope visualization at 20X magnification and the values were averaged. Each experiment was performed in triplicate.

8.1.38 Animal studies

The animal handling and the experimental procedures were approved by the Ethics Committee for Animal Experimentation of the

Fondazione IRCCS Istituto Nazionale dei Tumori, Milan, according to institutional guidelines.

For the development of CTC-derived xenograft (CDXs) and DTC-derived xenograft (DDXs) models from primary xenografts, human CTC and DTCs were enriched from pooled blood and dissociated lung tissues of $n=3$ PDX-bearing mice, respectively, by murine cells immune-depletion using Mouse Cell-Depletion kit and AutoMACS™ Pro Separator (Miltenyi). CTC and DTC enriched samples were then suspended in complete medium (RPMI 10%FBS) and Matrigel (BD Biosciences) at a ratio of 1:1 and injected on both flanks of severe combined immunodeficiency (SCID) female mice (Charles River Laboratories).

In vivo tumorigenic and metastatic experiments were carried out using CD-1 nude female mice, 7-10 weeks old (Charles River Laboratories). Mice were randomly divided into two groups of 5 mice each (A549 T1R3+ and T1R3-). For establishment of xenograft models, 1×10^5 cells of A549 T1R3+/- were suspended in Matrigel (BD Biosciences) at a ratio of 1:1, and 200 μ L of suspension was injected subcutaneously (sc) in both flanks of nude mice. Tumor volume measurements were performed once a week starting in week 2 after s.c. injection and up to week 7 with a Vernier caliper following the next formula $(L*W^2)/2$, where L is the length and W the width. At the end of the observation period, tumors and lungs were removed and dissociated for further analysis and blood was extracted from the heart.

For the experimental metastasis assay, 7.5×10^5 cells of A549 T1R3+ or T1R3- were injected intravenously (i.v.) in 150 μ L of PBS in the tail vein of 5 mice each group. Two months later (64 days), mice were sacrificed by cervical dislocation under light anesthesia, and lungs resected for FACS analysis.

8.1.39 Immune infiltration analysis

For analysis of immune cells in murine lung tissue, dissociated single cells suspension was washed in staining buffer (PBS1X+ 0.5% BSA+ 2mM EDTA) and incubated with the following antibodies at the proper dilution: anti-mouse CD11c-FITC (N418 clone), anti-

mouse Ly6C APC (1G7.G10 clone), anti-mouse CD49b PeVio770 (DX5 clone), anti-mouse Ly6G PercpVio700 (1A8 clone), anti-mouse CD192 (CCR2)-APC-Vio770 (REA538 clone), anti-mouse CD45 VioGreen (REA737 clone), all from Miltenyi Biotec; anti-mouse CD11b-PE (M1/70 clone), from BD Biosciences, and F480 Alexa 700 (MB8 clone) from eBioscience.

Cells were pre-labeled with LIVE/DEAD Violet Viability/Vitality Kit (ThermoFisher), for exclusion of dead cells. Gating strategy for immune cells analysis: immune cells subset was analyzed within CD45+ live cells gate after exclusion of doublets. Natural killer cells (NKs) are defined based on low SSC and the expression of the DX5 (pan-NK cells) marker. Neutrophils are next gated as CD11b+ LY6G+ cells. Within the gate of NKs/neutrophils negative cells, macrophages are identified as Ly6G-Ly6C-F480 high cells and classified as CD11b+ monocyte derived macrophages and CD11c+ alveolar macrophages. After exclusion of macrophages (gate DX5-CD11b+Ly6C+LY6G-F480-/low), conventional dendritic cells (DC) are defined as CD11b+CD11c+ cells and monocytes as CD11b+CD11c- cells and discriminated according to the expression of Ly6C marker, as Ly6CHigh inflammatory and Ly6Cdim resident monocytes. Reported percentages refer to the absolute number of immune cells in the tissue, relative to ancestor gate on vital cells.

8.1.40 Tissue dissociation of primary tumors and lungs

Solid tissues were finely minced by razorblade, suspended in tissue disruption medium (collagenase IV (5mg/mL) and DNase (100U/mL) (Sigma-Aldrich) in DMEM/F12) and incubated for 1h at 37°C in a gentleMACS™ Octo Dissociator with Heaters (MiltenyiBiotec). Single-cell suspension was obtained by filtering digested tissue through a 100 µm cell strainer (BD Falcon), and red blood cells were removed by Lysing Buffer 1X (BD Bioscience). Then, samples were analyzed by flow cytometry and RT-qPCR.

8.1.41 Detection of TAS1R3 expression in CTCs

CTCs were first pre-enriched by depletion of immunomagnetic labelled hematopoietic murine cells (Mouse Cell Depletion Kit) using

the AutoMACS™ Pro Separator (Miltenyi). Unbound cells enriched in CTCs were immunostained with TAS1R3 antibody (ab150525, abcam, 1:100) in blocking buffer solution. Single cells were visualized using DEPArray™ according to morphology and expression markers. TAS1R3-PE and GFP signals were used to identify T1R3+ CTCs and H2K to discard murine cells.

8.1.42 Statistical analysis

Statistical analyses were performed with a GraphPad Prism® software (version 6.0c). All data are expressed as mean \pm standard deviation (SD) or standard error of the mean (SEM), as indicated in each graph. Significant differences between two groups were determined by t-test, and in case of non-normal distribution, pairwise two-tailed Mann-Whitney U-test and multiple comparisons among conditions were done using one-way analysis of variance (ANOVA) followed by Bonferroni post hoc test. All experiments were performed at least in triplicate. * $p < 0,05$, ** $p < 0,001$, *** $p < 0,0001$.





9 RESULTS





**SECTION I:
STRATEGY INSPIRED BY EXOSOMES**



9.1 DEVELOPMENT OF NOVEL MULTIFUNCTIONAL NANO-PLATFORMS

Some of the results presented in this section have been already published (annex 3).

This work has been done in collaboration with the "Alberto Sols" Biomedical Research Institute CSIC-UAM.

SUMMARY

Nanotechnology has shown a good promise for improving delivery of drugs to the tumor, mainly when these drugs are labile biomolecules, such as RNAs. Commercialized nanomedicines in oncology are typically liposomes. Additionally, the first RNA nanomedicine, patisiran (Onpattro®), based on a lipid nanoparticle formulation of short interfering RNA, has already been approved for the treatment of a rare condition, polyneuropathies induced by hereditary transthyretin amyloidosis, in 2018. Design of innovative nanomedicines should aim for simple and translatable nanosystems, which are safe and can be adapted to specific conditions. In cancer, one of the main limitations is to mediate an accumulation in the cancerous cells. Different targeted approaches, based in surface decoration with antibodies, aptamers and/or other ligands, have been proposed to improve access to cancer cells. Looking at the tumor biology, exosomes, with tumor-homing properties, seem to be a promising approach for the development of efficient delivery systems in oncology.

Exosomes have been suggested as ideal drug delivery systems with application in a broad range of pathologies including cancer. Given their role in intercellular communication, exosomes fulfill the requirements of an ideal drug delivery system. They can i) transport molecules, ii) cross biological membranes, iii) overcome peripheral macrophages, and iv) reach specific cell types to release their content. Exosomes loaded with anticancer drugs have already shown promise as a new therapeutic approach in animal models. Tumor-derived exosomes, having tumor-homing properties, can efficiently reach cancer cells and therefore behave as carriers for improved drug

delivery to the primary tumor and metastases. However, due to their complex composition, and still undefined biological functions, safety concerns arise, hampering their translation into the clinic. Making use of the well-known liposome technology, Exosome-mimetic Nanoplatforms (EMNs) have been engineered. They can be tailored with specific proteins and nucleic acids, showing great similarities to natural exosomes with respect to their physicochemical properties, drug loading capacity, and ability to interact with the cancer target cells *in vitro* and *in vivo*, while offering competitive advantages in terms of safety, production and characterization processes. EMNs are highly versatile systems that can be tailored for a broader range of applications.



9.1.1 Isolation and characterization of exosomes

The purpose of this work was to design a nanoplatform that resembles exosomes for their composition and physicochemical properties, of utility for the selective delivery of anticancer therapies with a performance similar to natural exosomes while overcoming their limitations. For reference, extracellular vesicles derived from human plasma and different cancer cell lines were isolated and characterized them in terms of protein composition, morphology and physicochemical properties. Exosomes with the characteristic cup-shape morphology and a homogeneous distribution were observed by transmission electron microscopy (TEM) (**Figure 12**).

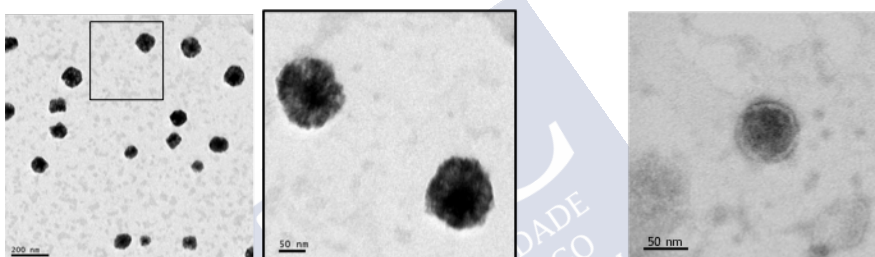


Figure 12. Exosome morphology. Representative TEM images of exosomes from SW480 cell line (left) and PC-3 (right). Scale bars represent 200 nm (left) and 50 nm (center and right).

WB analysis allowed confirming the effectiveness of the isolation protocol showing conventional exosome protein markers (e.g., Alix and CD9) in all samples (**Figure 13a**). Moreover, extensive proteomic analysis (LC-MS/MS) led to the identification of other 90 exosomal protein markers described in the top 100 proteins of the ExoCarta and EV Vesiclepedia databases (**Figure 13b**). Nearly 80% of the identified proteins were also classified as part of the “exosome component” in the Gene Ontology Cellular Component section of the FunRich tool (**Figure 13c**). Their yield of production from cancer cell lines was determined (**Table 4**) and their physicochemical properties measured by DLS and LDA (**Table 5**), showing a nanometric size (91 ± 11 nm) with a narrow distribution ($PdI = 0,3$), and a negative superficial charge ($ZP = -23 \pm 2$). These results indicate that natural

exosomes have been isolated with certainty, and conveniently characterized for their physicochemical properties and morphology.

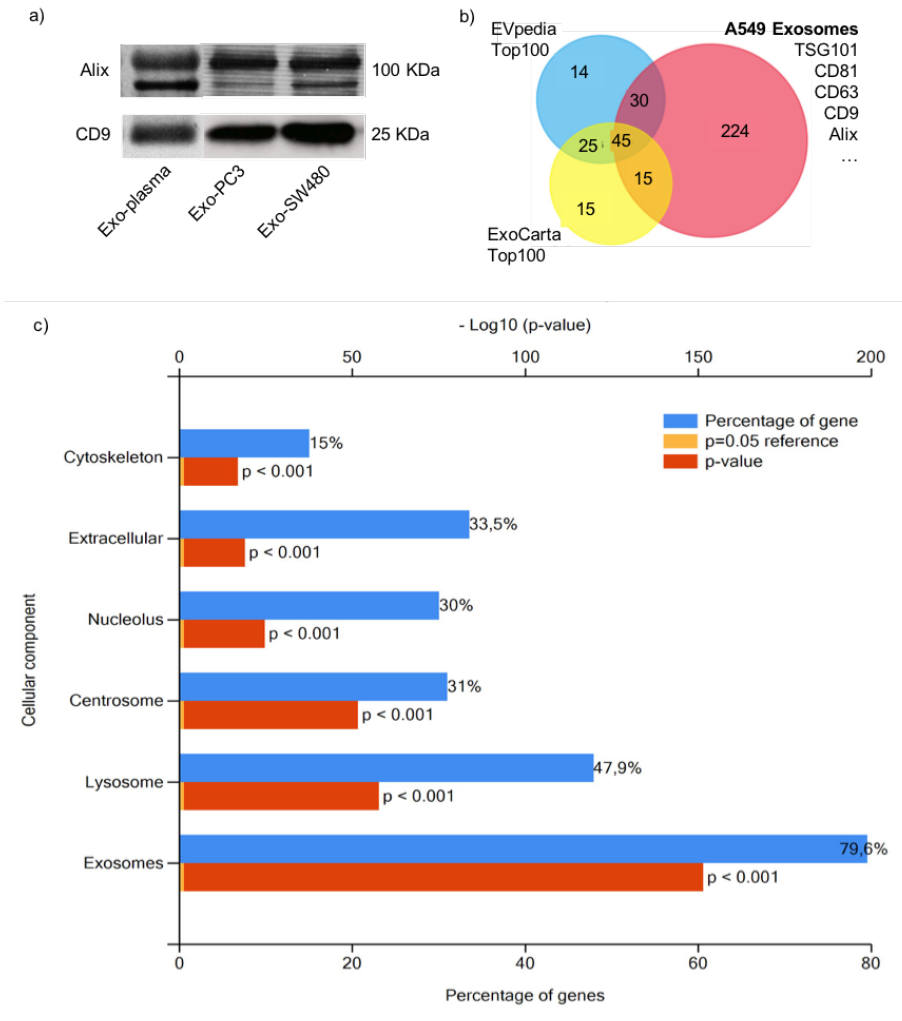


Figure 13. Exosome characterization. (a) Western Blot analysis for exosome markers (Alix and CD9) of exosomes from different sources (human plasma and cancer cell lines). (b) Venn diagram illustrating common proteins identified in A549-exosomes (1% FDR) with EV vesiclepedia database and Exocarta database top 100 proteins. (c) The Gene Ontology analysis of the proteins identified by cellular component was performed using FunRich tool.

Table 4. Yield of production of A549 cell-derived exosomes.

N° of P150 plates	Secretion time (h)	Final n° of cells	Final n° of particles	µg protein
12	16	$3 \times 10^8 \pm 2 \times 10^7$	$2 \times 10^9 \pm 8 \times 10^7$	19.86

Table 5. Physicochemical properties of exosomes.

	Size (nm)*	Pdl	ZP (mV)
Exosomes from human plasma	98 ± 12	0.4	- 16 ± 1
Exosomes from cancer cell lines	91 ± 11	0.3	- 23 ± 2

Note: Data presented as mean ± standard deviation; n = 3. *Size corresponds to number measurement in DLS.

9.1.2 Development and characterization of EMNs

Next, the preparation of the exosome-mimetic nanoplateforms (EMNs) was attempted. Previously published lipidomics works describing the most common lipid species enriched in tumor exosomes compared to parent cells, were taken into consideration to define the EMNs composition (Llorente *et al.*, 2013; Record *et al.*, 2014; Lydic *et al.*, 2015). Exosomes were mainly enriched in phospholipids (PL, 37,5%), cholesterol (CH, 43,5%), sphingomyelin (SM, 16,3%), ceramide (Cer, 1,2%) and other minority lipids, such as glycosphingolipids (1,6%) (**Figure 14a**). The preparation methodology was optimized based on previous knowledge using the ethanol injection method (the influence of several parameters, such as lipid concentration, volumes, and the ratio of each component was evaluated, with respect to their influence in the physicochemical properties of the resulting EMNs), in order to obtain nanoplateforms structurally similar to exosomes in a single step (**Figure 14b**).

EMNs composition can be modulated in order to obtain nanovesicles of different sizes, properties and combinations (**Table 6**). For this work, we opted for the PC:CH:SM: Cer composition (with a final formulation lipid ratio of 0,9:1:0,4:0,03 (w/w), schematically represented in **Figure 14c**), given that it mimics the most important physicochemical features of natural exosomes, related to lipid composition (all these lipid species are described as majoritarian in exosomes), and size (100nm, see **Table 6**).

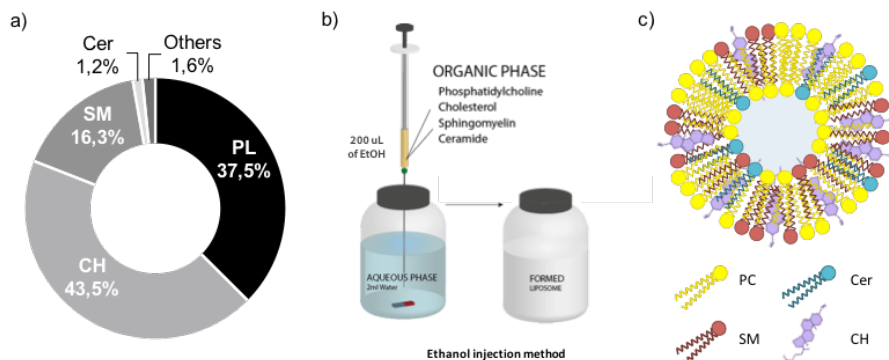


Figure 14. EMN composition and preparation. (a) Lipidomic assay showing a comprehensive and quantitative profiling of lipid species in PC-3 exosomes that was followed for the engineering of EMNs. (b) Schematic illustration of the ethanol injection method for the EMNs preparation. (c) Illustration of exosome-mimetic EMNs and its final lipid composition.

Table 6. Different possible compositions of EMNs and physical properties.

Composition	Ratio (w/w)	Mass (mg)	Size (nm)	Pdl
PC:CH	2:1	4.5	84 ± 8	0.1
PC:CH	1.5:1	2.5	89 ± 2	0.1
PC:CH:SM	0.9:1:0.4	1	87 ± 2	0.1
PC:CH:SM	0.9:1:0.4	2	134 ± 1	0.1
PC:CH:SM: Cer	0.9:1:0.4:0.03	2.02	100 ± 8	0.2
PC:CH:SM:PE: Cer	0.4:1:0.4:0.2:0.03	0.6	98 ± 2	0.2
PC:CH:SM:PE: Cer	0.4:1:0.4:0.2:0.03	0.9	109 ± 1	0.1
PC:CH:SM:PE: Cer	0.4:1:0.4:0.2:0.03	1.6	126 ± 3	0.1
PC:CH:SM:PE: Cer	0.4:1:0.4:0.2:0.03	2	147 ± 2	0.1
PC:CH:SM: Cer:DC-CH	0.4:1:0.4:0.2:0.03:0.04	2.07	102 ± 3	0.2
PC:CH:SM: Cer:DC-CH	0.4:1:0.4:0.2:0.03:0.07	2.09	147 ± 5	0.2
PC:CH:SM: Cer:ST	0.4:1:0.4:0.2:0.03:0.002	2.03	74 ± 1	0.3
PC:CH:SM: Cer:CTAB	0.4:1:0.4:0.2:0.03:0.005	2.033	91 ± 3	0.3
PC:CH:SM: Cer:DOTAP	0.4:1:0.4:0.2:0.03:0.01	2.038	67 ± 4	0.4

Abbreviations: PC, phosphatidylcholine; CH, cholesterol; SM, sphingomyelin; Cer, ceramide; PE, phosphatidylethanolamine; DC-CH, 3beta-(N(N',N'-dimethylaminoethane)-carbamoyl) cholesterol; ST, sterilamine; CTAB, cetyltrimethylammonium bromide; DOTAP, 1,2-dioleoyl-3-trimethylammonium-propane. Size corresponds to number measurement in DLS and is presented as mean ± standard deviation of three independent formulations.

This specific formulation was further characterized, showing a similar morphology to exosomes, and a great colloidal stability in culture media and human plasma (t=1h-20h), and under storage conditions (for up to 4 months) (**Figure 15a,b**). Assessment of stability in biological media is extremely important prior *in vitro* and *in vivo* experiments. Moreover, size characterization of 19 independent batches of EMNs prepared on different days, demonstrated an excellent reproducibility of the preparation method (**Figure 15c**).

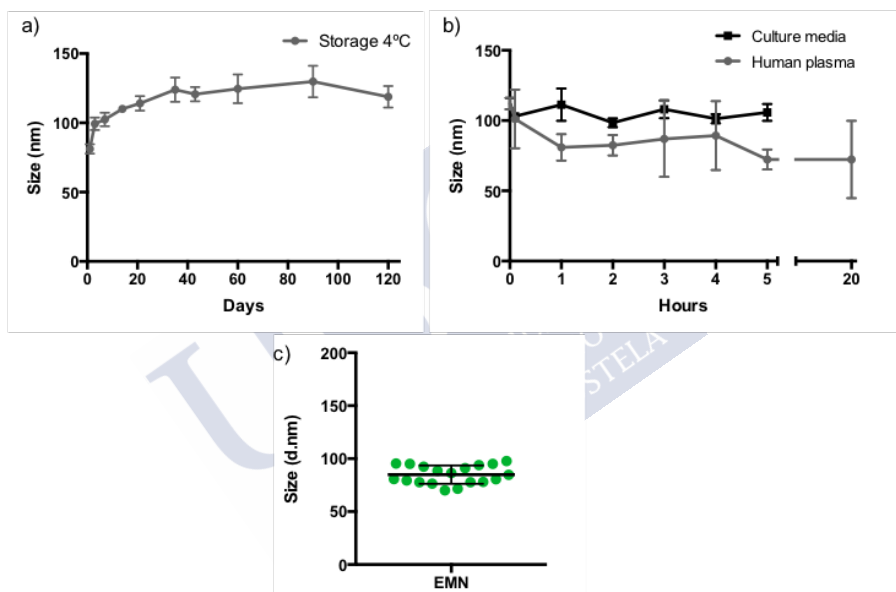
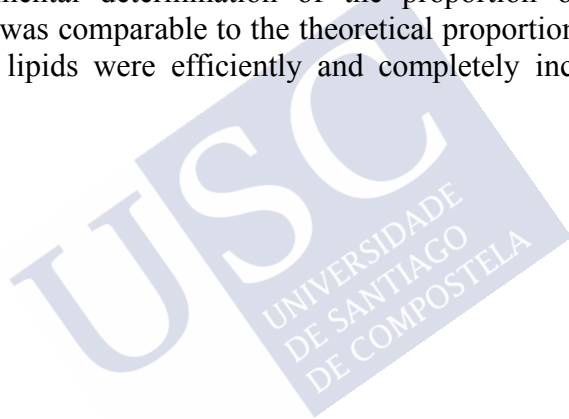
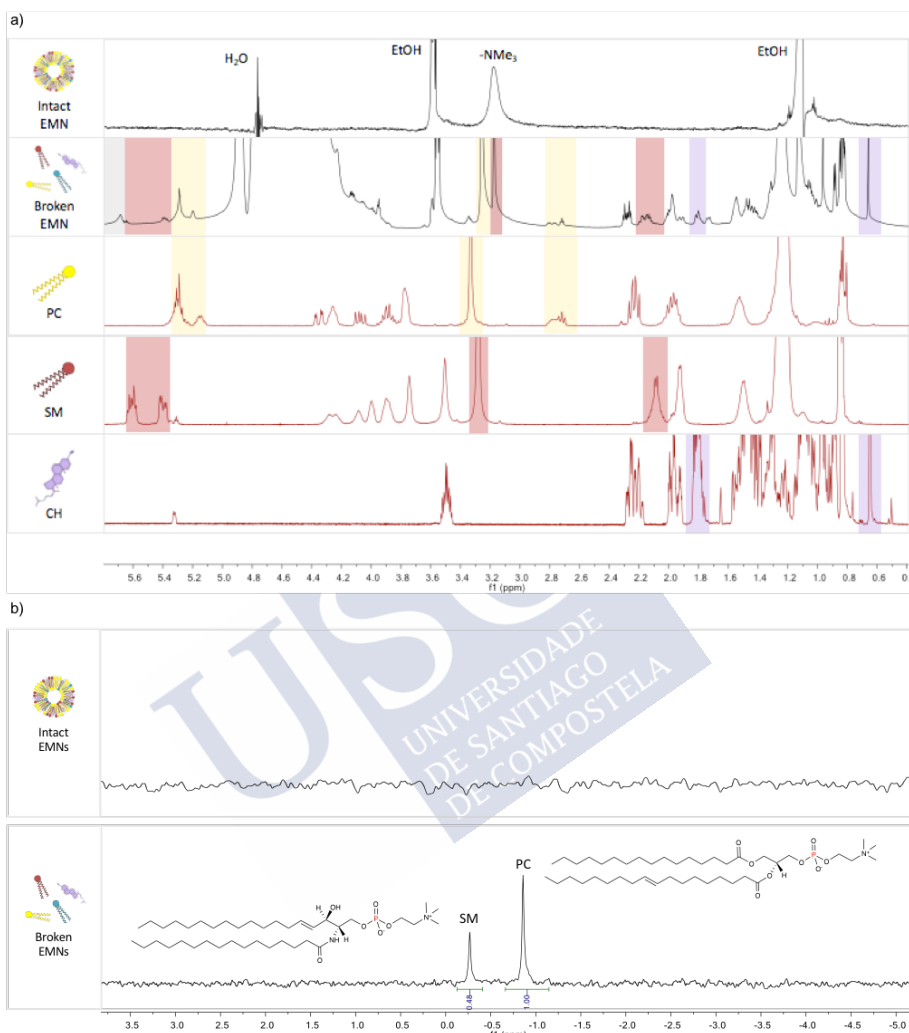


Figure 15. Exosome-mimetic nanoplateforms characterization. (a) Hydrodynamic size (Z-average) of EMNs measured by dynamic light scattering (DLS) under storage conditions (4°C) and (b) in culture media and human plasma, over the time (from t=0 to 120 days, 5 hours and 20 hours, respectively; n=6). (c) Hydrodynamic size measured by DLS of 19 independent batches of EMNs (green dots); horizontal bar represents mean \pm SD.

NMR analysis confirmed the effective incorporation of each lipid into EMNs (**Figure 16**). The presence of the incorporated lipid species was studied by ^1H and ^{31}P NMR. While the spectrum corresponding to broken EMNs displayed relevant peaks due to the free lipid

molecules (according to the spectra of the pure components PC, SM, and CH, colored rectangles), the sample of intact EMNs (treated with deuterium oxide (D₂O) instead of deuterated methanol (CD₃OD), did not display practically any peak (only a terminal methyl group), meaning that free unreacted lipids were not present in the suspension, and therefore, it was possible to prove that all lipids were successfully incorporated in the formulation (**Figure 16a**). The ³¹P NMR spectrum was also acquired for a double-checking, allowing the observation of two peaks (broken EMNs) corresponding to the phosphorylated species of SM and PC; these peaks were completely absent in the same spectrum of the intact EMNs (**Figure 16b**). The analysis allowed experimental determination of the proportion of SM:PC (0.48:1), which was comparable to the theoretical proportion (0.44:1), suggesting that lipids were efficiently and completely incorporated into EMNs.





9.1.3 EMNs have similar physicochemical properties to exosomes

A methodology for preparation of EMNs structurally similar to exosomes has been provided. NTA and DLS analysis confirmed the similar size and the mono-disperse size distribution of exosomes and EMNs (**Figure 17a,b**).

Besides, a single batch of EMNs (2'2 ml), can be produced in 10 min, while the exosome isolation time from the conditioned medium by serial ultracentrifugation (protocol detailed in methods) takes several days (**Figure 17c**). Other exosome-mimetic nanosystems in the literature have been attempted by serial extrusion of cells (Cell-derived NV) (Jang *et al.*, 2013; Lunavat *et al.*, 2016), however, the production process also takes several days (**Figure 17c**). Moreover, the production yield, measured by the number of obtained particles, is 1000-fold higher for EMNs than for exosomes (**Figure 17d**). Additional comparative experiments among EMNs and natural exosomes were carried out. Loading studies showed that EMNs have a similar drug loading capacity than exosomes in the case of RNA and DNA, while showing superior efficiencies with hydrophobic compounds such as curcumin (**Figure 17e**).

9.1.4 EMNs can efficiently interact with cancer cells

EMNs were then subjected to different experiments with cancer cells from different origins (PC-3 prostate cancer cells, SW480 colon cancer cells, and A549 lung cancer cells). Confocal images revealed that EMNs (green signal) could be efficiently internalized by different cancer cells, and subsequently, deliver their payload intracellularly (**Figure 18a**). They do not present any problem of toxicity at any of the concentrations tested (**Figure 18b**), and interestingly, EMNs could be simultaneously labeled with three different fluorophores (TopFluor-SM, Cy5 and DiR) for broader applications *in vitro* and *in vivo* (**Figure 18c**). These results demonstrated that EMNs can efficiently interact with cancer cells without compromising cell viability.

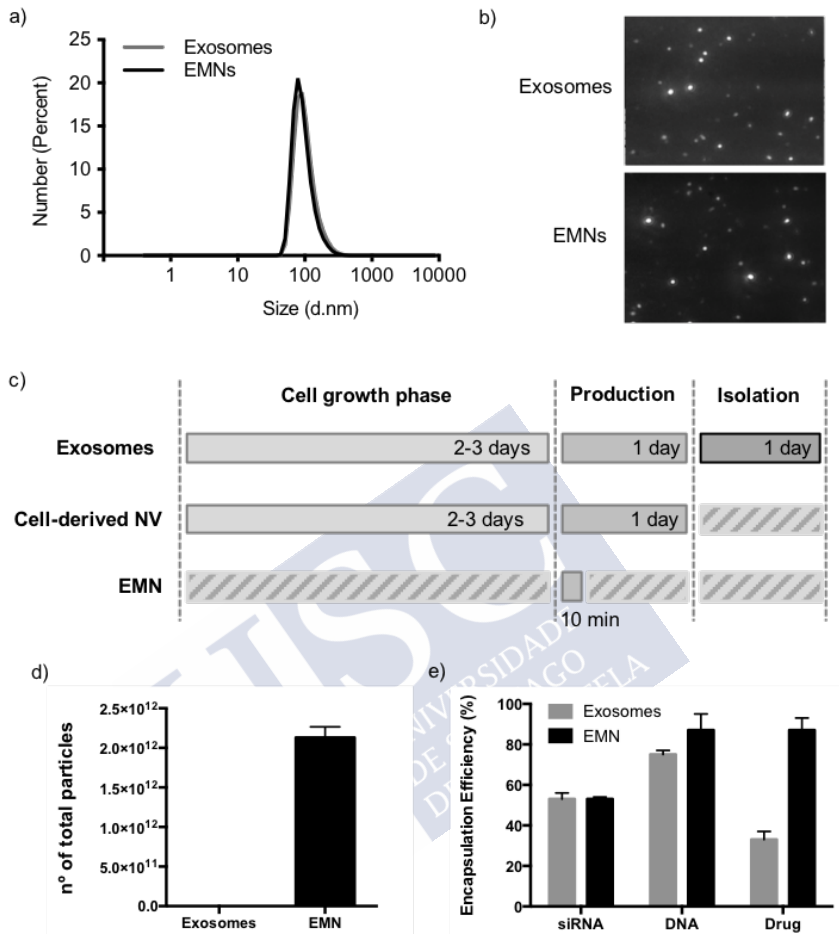


Figure 17. Comparison between exosomes and EMNs. (a) Size distribution graph of exosomes and EMNs measured from dynamic light scattering (DLS) and (b) video frame of the nanoparticles by nanoparticle tracking analysis (NTA). (c) Time-consuming comparison for obtaining natural exosomes from cell lines and isolation by serial ultracentrifugation, cell-derived nanovesicles (NV) and EMNs. (d) The number of particles obtained in 216 ml of conditioned medium (16 h) of A549 exosomes and of one batch of EMNs (2'2 ml) measured by NTA. (e) Encapsulation efficiencies of therapeutic model molecules comparing the loading capacity of natural exosomes and EMNs. Bar charts represent mean \pm standard deviation, $n=3$. Data without statistical significance were not indicated.

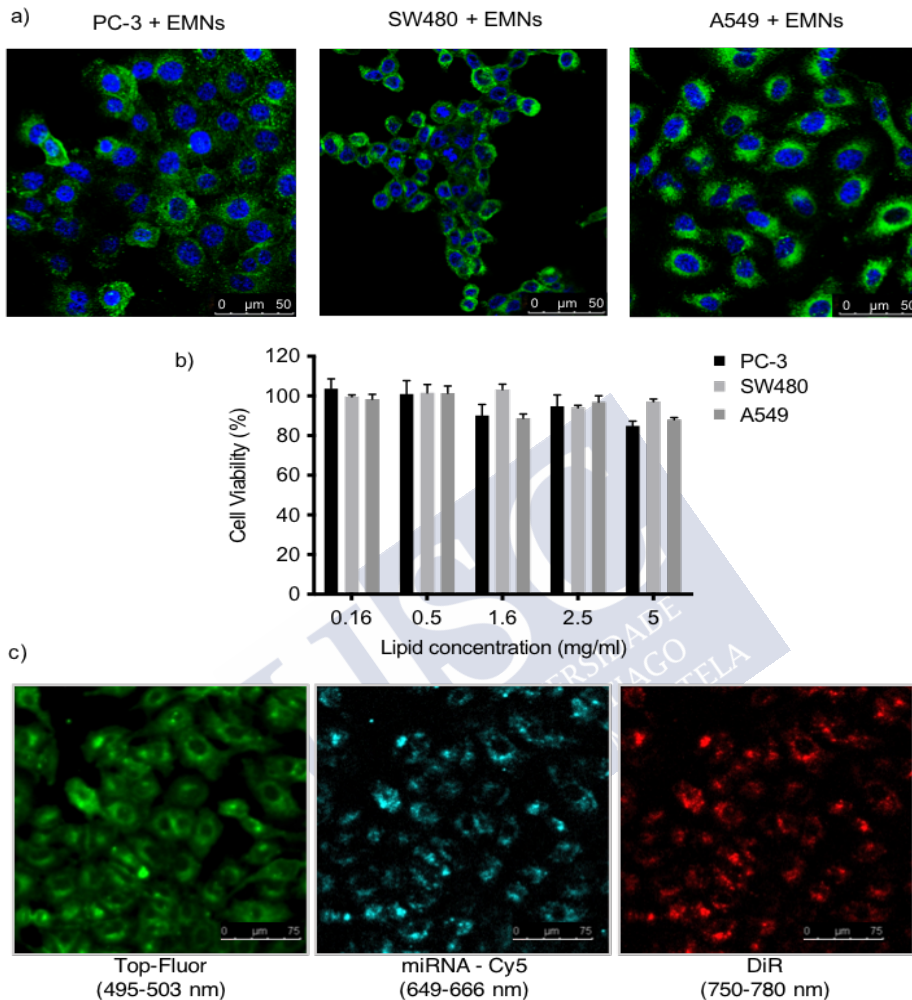


Figure 18. EMNs efficiently interact with cancer cells. (a) Confocal images showing the effective interaction and internalization of EMNs (green signal) by different cancer cell lines (PC-3, SW480 and A549). Blue channel: nuclei (Hoechst); green channel: EMNs (TopFluor). Scale bars represent 50 μm . (b) Effect of EMNs on the viability of PC-3, SW480 and A549 cells. Cytotoxicity was determined by MTT assay and calculated as percentage of inhibition of cell proliferation. Data without statistical significance were not indicated. (c) Confocal images of triple labelled EMNs internalized by A549 cells. Green channel: EMNs (TopFluor); blue channel: miRNA145 (Cy5); red channel: EMNs (DiR). Scale bars represent 75 μm .

9.1.5 Functionalization of EMNs for a selective transport

Next, the complexity of the formulation was increased to include bioactive macromolecules, RNAs and proteins. The purpose was to provide EMNs with functionalities characteristic from exosomes, i.e. proteins that can foster tumor-homing properties.

First, the capacity of EMNs to associate proteins was tested. As appreciated in **Table 7**, EMNs showed a good capacity to associate different types of proteins, irrespective of their MW and pI. Significant changes in the physicochemical properties of ENMs (nanoparticle size, distribution, and surface charge) were not observed upon incubation with the proteins, providing evidence that EMNs can be functionalized with different proteins for conferring specific properties. This is particularly important, allowing envisioning a versatile nanosystem that can be tailored with active proteins providing organotropic functionalities, as for example integrins.

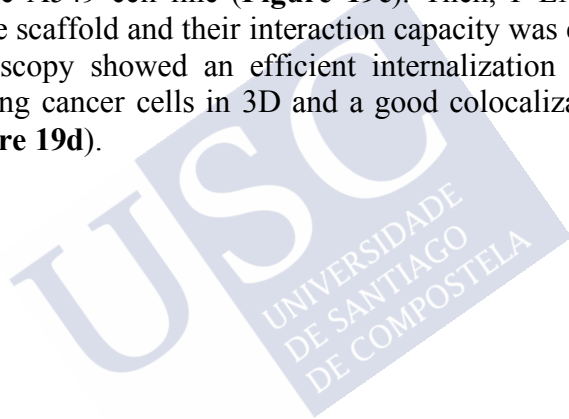
Table 7. Physicochemical properties of EMNs after association of proteins.

Protein name	MW (KDa)	pI	Size (nm)	PdI	ZP (mV)
BSA	66	5.6	112 ± 1	0.2	-1 ± 1
Lysozyme	16.5	9.4	118 ± 8	0.2	-4 ± 1
Integrin $\alpha 6 \beta 4$	188.8	5.3	110 ± 2	0.3	-6 ± 1

BSA, bovine serum albumin; MW, molecular weight; pI, isoelectric point; PdI, Polydispersity index; ZP, Zeta potential.

Integrin alpha6 beta4 (ITG $\alpha 6 \beta 4$), which has been associated with lung organotropism (Hoshino *et al.* 2015), was bound to EMNs to increase their targeting capabilities to the lung and enhance their adhesive properties to recipient cells. The effective association of ITG $\alpha 6 \beta 4$ (ITG) to EMNs, providing functionalized EMNs (F-EMNs), was verified by fluorescent WB. **Figure 19a** showed a red signal in the fraction of EMNs isolated by ultracentrifugation and no signal was observed in the supernatant where the unbound protein was supposed to be. To evaluate whether the integrin maintained its activity and correct conformation after association to EMNs, a binding assay with its ligand, laminin-5, was performed. Laminin-5 coated plates were incubated with fluorescently labelled EMNs and F-EMNs. To guarantee that the signal observed from the EMNs was not an artefact

of the labeling approach, we formulated the EMNs with a fluorescent labeled cholesterol (NBD-CH) and purified the sample by ultracentrifugation (to get rid of any free NBD-CH molecule). NBD-labelled plain EMNs (without ITG) were used as control. Confocal images revealed that F-EMNs had the capacity to mediate specific and effective interactions with laminin-5 and confirmed that the bound protein was biologically active (**Figure 19b**). Additionally, F-EMNs were perfused through a 3D culture model, previously developed by our group (M Alonso-Nocelo *et al.*, 2016), in order to evaluate their interaction with A549 cells under dynamic conditions that better mimic the *in vivo* situation. The expression of laminin-5 was first confirmed in the A549 cell line (**Figure 19c**). Then, F-EMNs were perfused into the scaffold and their interaction capacity was evaluated. Confocal microscopy showed an efficient internalization of the F-EMNs in the lung cancer cells in 3D and a good colocalization with laminin-5 (**Figure 19d**).



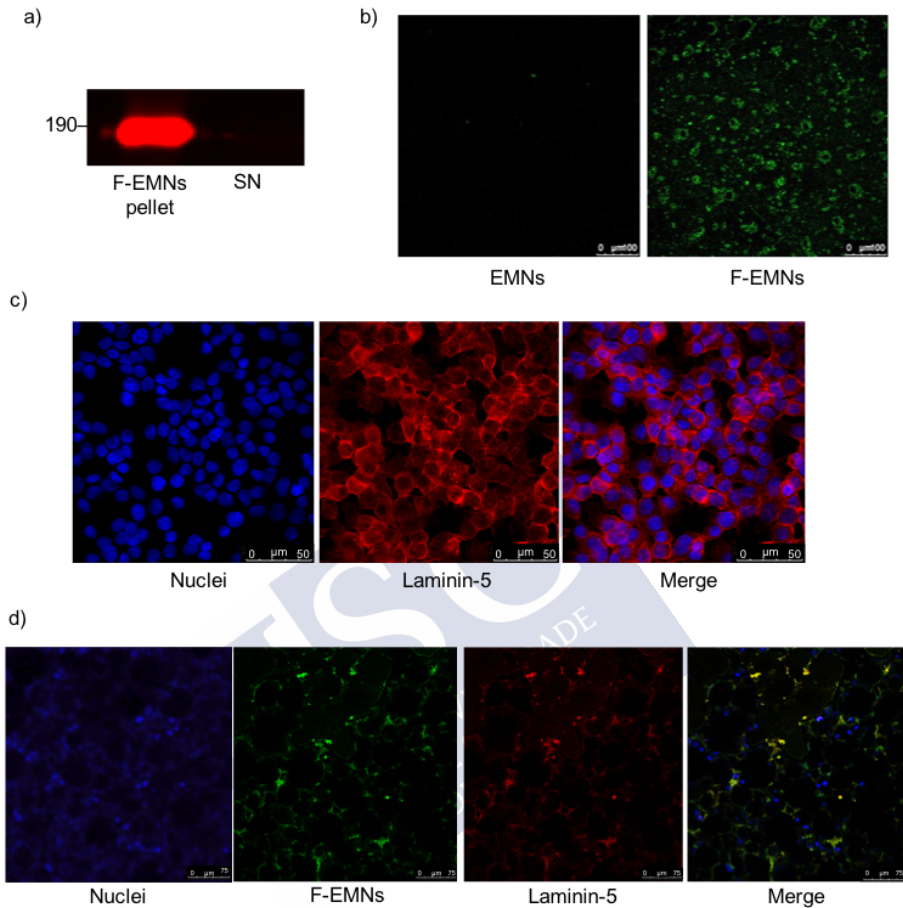


Figure 19. Functionalization of EMNs with a biologically active integrin. (a) Fluorescent Western blot showing the effective association of ITG α 6 β 4 with EMNs (F-EMNs) by ultracentrifugation at 120,000 xg (pellet) compared to the supernatant (SN). (b) Specific interaction of F-EMNs to coverslips coated with laminin-5. EMNs and F-EMNs were labeled with the fluorophore NBD-CH (green). Scale bars represent 100 μ m. (c) Confocal images showing Laminin-5 expression (red) in A549 cells (nuclei, blue). Scale bars represent 50 μ m. (d) Confocal images showing F-EMNs (green) interaction with A549 cells (blue) expressing Laminin-5 (red) seeded in a 3D scaffold. Colocalization of F-EMNs and laminin-5 can be observed in the merge image in color yellow. Scale bars represent 75 μ m.

9.1.6 EMNs as vectors for gene therapy

Subsequent experiments were conducted to explore the potential of EMNs to transport RNAs to cancer cells. Although cationic lipids are not present in the composition, we proved that EMNs efficiently associate therapeutic oncosuppressor miR145 by performing an agarose gel retention assay (**Figure 20**).

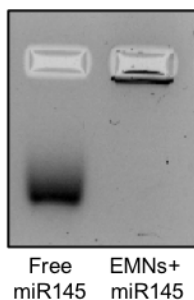


Figure 20. Gel retention assay showing the free microRNA145 compared to the miR145 encapsulated in EMNs that remains stacked in the well of the gel

Hence, we eventually engineered EMNs that simultaneously incorporated lipids, proteins, and RNAs, and resembled simplified exosomes with respect to their composition, physicochemical properties, and functionalities (**Table 8**).

Table 8. Physicochemical properties of exosomes and EMNs.

	Size (nm)*	Pdl	ZP (mV)
Exosomes from human plasma	98 ± 12	0.4	- 16 ± 1
Exosomes from cancer cell lines	91 ± 11	0.3	- 23 ± 2
EMNs	100 ± 8	0.2	- 7 ± 2
F-EMNs	110 ± 2	0.3	- 6 ± 1
EMNs + miR145	104 ± 2	0.3	- 16 ± 2
F-EMNs + miR145	113 ± 1	0.3	- 5 ± 2

Abbreviations: Pdl, Polydispersity index; ZP, Zeta Potential; EMNs, Exosome-mimetic Nanosystems; F-EMNs, functionalized EMNs with a specific integrin; miR145, microRNA-145; EMNs+miR145, EMNs loaded with miR145; F-EMNs+miR145, F-EMNs loaded with miR145.

Note: Data presented as mean ± standard deviation; n = 3. *Size corresponds to number measurement in DLS.

Confocal images proved that EMNs mediated an efficient delivery of miR145-Cy5 to A549 cells and supported our notion that integrin functionalization indeed increases the adhesive properties in the case of F-EMNs (**Figure 21a**). Moreover, looking at the 3D reconstruction of the confocal images (**Figure 21b**) and xz and yz-slices (**Figure 21c**), a clear colocalization of NBD-labeled F-EMNs and miR145-Cy5 can be observed, proving that the payload and the carrier were traveling together). Comparable results were obtained by flow cytometry, as miRNA-145 was effectively detected into the cells upon association to EMNs, and the efficiency of the delivery was significantly improved with F-EMNs (**Figure 22**).



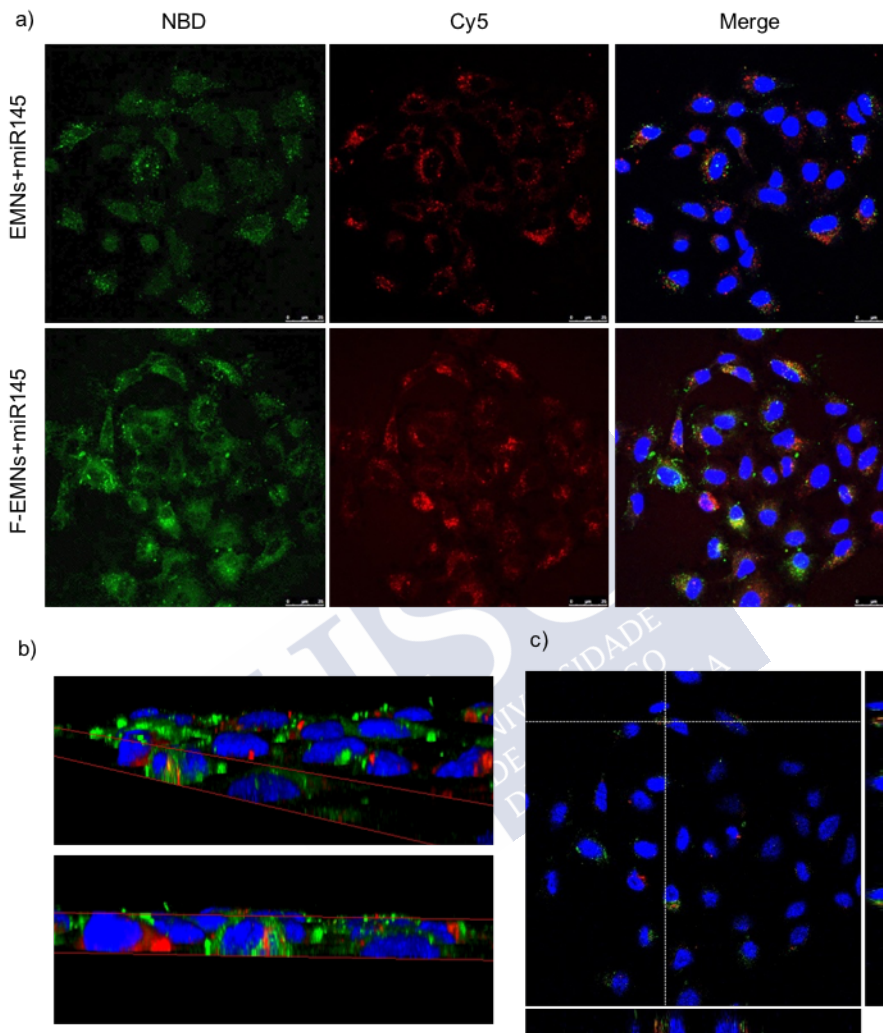


Figure 21. Targeted delivery of miR145 to cancer cells. (a) Confocal microscopy images after 4h transfection of A549 cells with EMNs+miR145 and F-EMNs+miR145. Blue channel: nuclei (DAPI); green channel: EMNs and F-EMNs (NBD-CH); red channel: miR145 (Cy5). Scale bars represent 25 μm . (b) 3D reconstruction of confocal analysis of F-EMNs+miR145 internalization in cancer cells. Images show the colocalization of the nanosystems (green) with the miRNA (red) in the cells and (c) z-stack projection with orthogonal cross. Blue channel, nuclei (DAPI); green channel, F-EMNs (NBD); red channel, miR145 (Cy5).

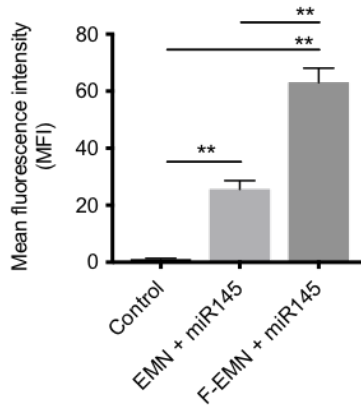


Figure 22. FACS quantitative analysis showing the mean fluorescence intensity of the transfection efficiency of F-EMNs+miR145-Cy5 compared to EMNs+miR145-Cy5, and to the control cells. Data represent mean \pm SD of three independent experiments and were analyzed by two tailed t-Student tests (** $p < 0.01$).

RT-qPCR assays also confirmed the superior behavior of F-EMNs for delivery of therapeutic RNAs to cancer cells, which rendered a 5-fold increase in the expression of miR145 with respect to the control formulation without ITG α 6 β 4 (EMNs+miR145) (**Figure 23a**). As expected, control cells transfected with miR145 in solution (miR145 free) or with EMNs loaded with a scrambled sequence (EMNs + miRscr) did not show differences in the expression of miR145 compared to untreated cells. This increase in the intracellular levels of miR145 produced by F-EMNs was translated into a significant reduction of the clonogenic capacity of the transfected cells (**Figure 23b**). Additionally, to evaluate whether F-EMNs could be trapped in the endolysosomal degradation pathway (Lönn *et al.*, 2016), a lysosomotropic agent that induces lysosomal membrane perturbation, called chloroquine (Stremersch *et al.*, 2016; Pelt *et al.*, 2018), was added to the previously transfected cells. Results of a colony formation assay showed that no significant differences were observed when chloroquine was added, proving that F-EMNs could efficiently escape the endolysosomal system (**Figure 23c**). Moreover, at the protein level, F-EMNs loaded with miR145 significantly reduced the expression of N-cadherin in the transfected cells, a protein that promotes tumor cell survival, migration, and invasion, and one of the

targets of miR145 in lung adenocarcinoma (Mo *et al.*, 2017) (**Figure 23d**). Therefore, F-EMNs were able to deliver functional miR145 to cancer cells, overcoming the main barriers in gene delivery.

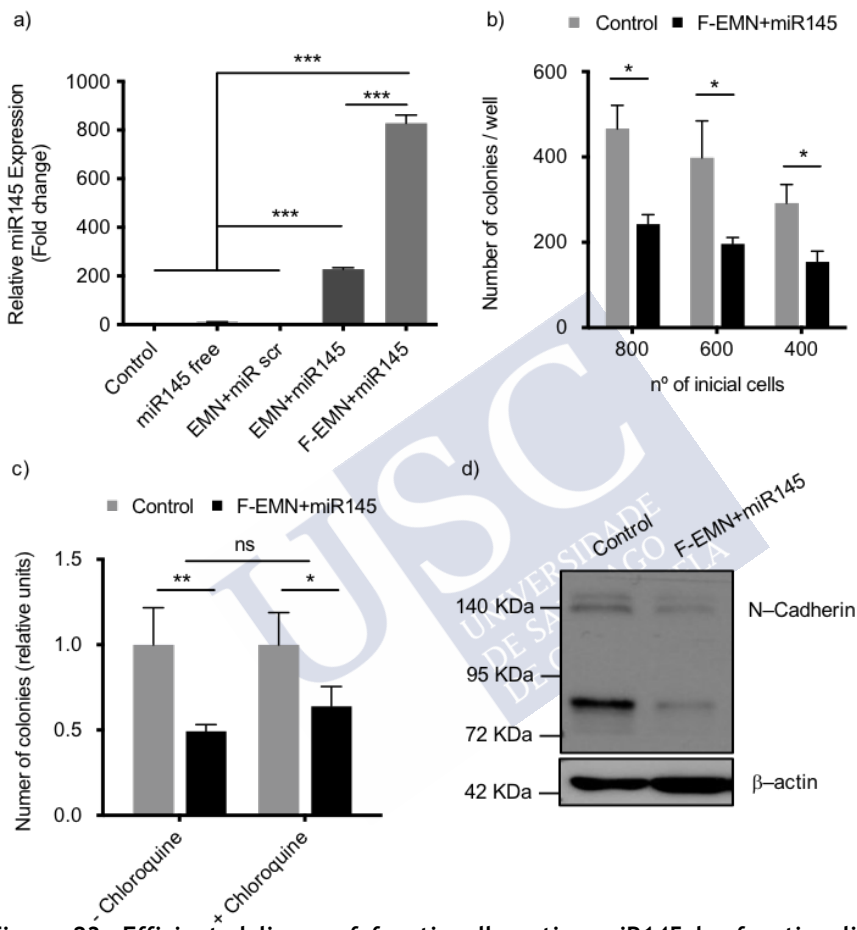


Figure 23. Efficient delivery of functionally active miR145 by functionalized EMNs. (a) Real time-qPCR of miR145 levels in A549 cells after 4h transfection with miR145 free, a scramble sequence, EMNs+miR145 and F-EMNs + miR145. Data are representative of three independent experiments. (b) Colony forming assay of A549 cells transfected with F-EMNs+miR145 compared to A549 control starting from 400, 600 or 800 initial cells. (c) Colony forming assay with and without the lysosomal disruption agent (chloroquine). (d) Western blot result showing down regulation of A549 when transfected with EMNs compared to control (untreated cells). Data represent mean \pm SD of three independent experiments and were analyzed by two tailed t-Student tests (** $p < 0.01$). (* p value $< 0,001$).

9.1.7 F-EMNs have a similar capacity than exosomes to transport RNAs

Final experiments were established to compare tumor-derived exosomes with engineered F-EMNs loaded with miR145. Cryo-TEM images revealed similarities with respect to the vesicle size, spherical shape, and membrane thickness (**Figure 24**).

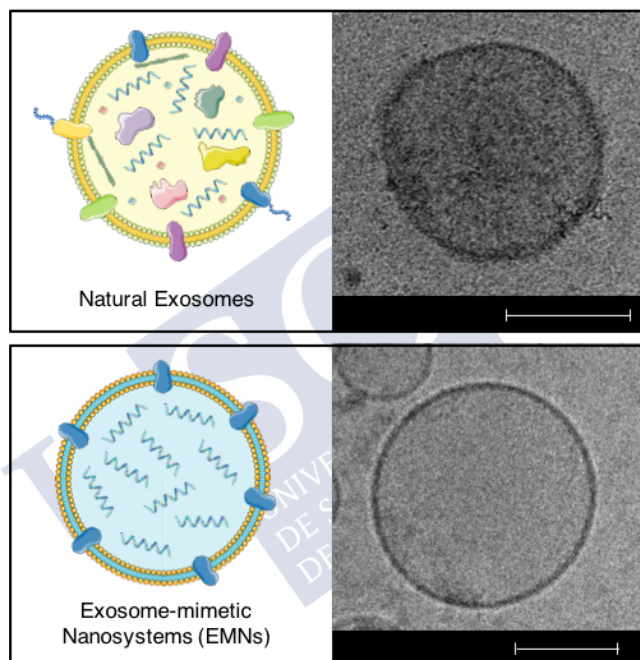


Figure 24. Morphological comparison of natural exosomes and F-EMN+miR145. Schematic representation of the composition and morphology of natural exosomes (upper) and functionalized miR145-loaded EMNs (lower). Cryo-TEM images of natural exosomes loaded with miR145 (upper) and F-EMNs+miR145 (lower). Scale bar represents 100 nm.

Transfection experiments *in vitro* proved that F-EMNs were able to transport genetic material (miR145) to tumor A549 cells in a comparable fashion to exosomes isolated from the same cell culture, as it can be seen by confocal microscopy pictures and FACS analysis (**Figure 25**).

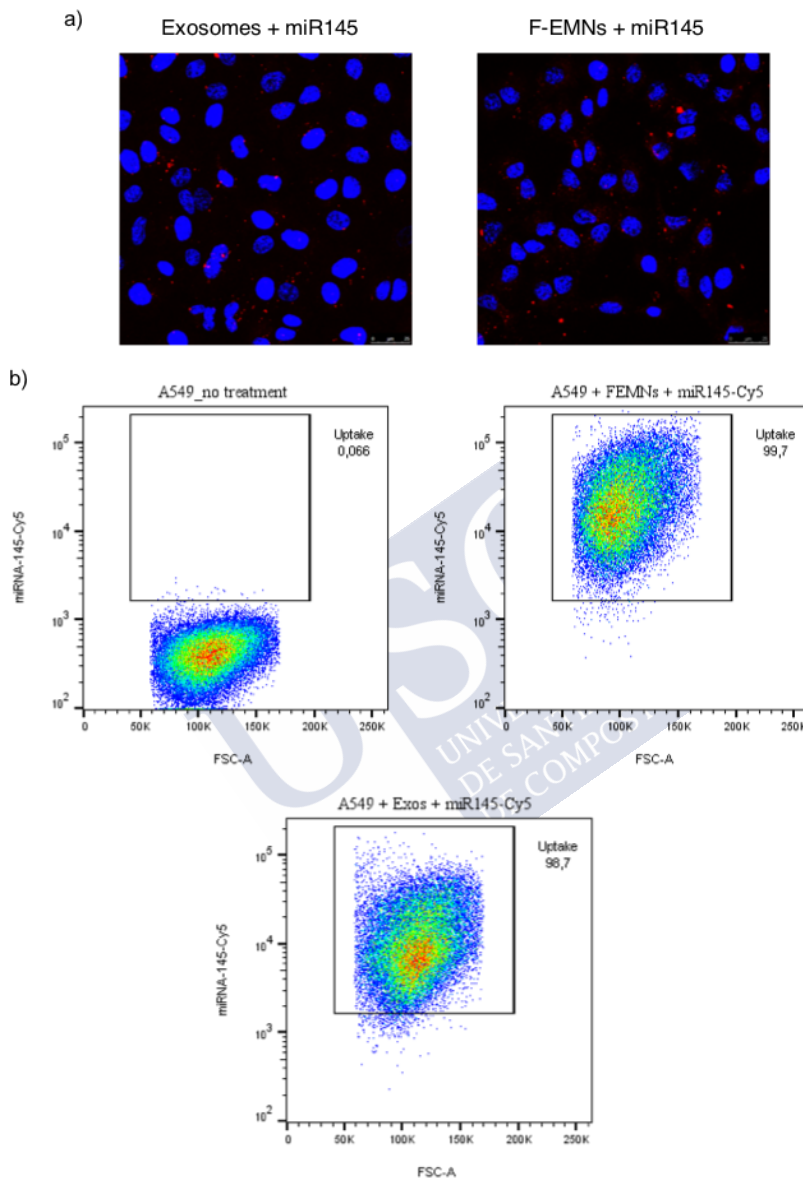


Figure 25. Cellular uptake of miRNA-145-Cy5 encapsulated F-EMNs and exosomes into A549 cells after 4h incubation. Comparison of the uptake efficiency of F-EMNs and exosomes by (a) confocal microscopy. Blue channel: nuclei (Hoechst); red channel: microRNA145 (Cy5). Scale bars represent 25 μ m. (b) FACS analysis showing the Cy5 signal of the miR145 loaded in F-EMNs (99,7%) and exosomes (98,7%) incubated with A549 cells for four hours. PBS was used as no treatment control.

Finally, *in vivo* biodistribution experiments in mice bearing lung cancer (inoculation of luciferase-expressing A549 lung carcinoma cells into the tail vein of nude mice leading to tumor formation) showed a comparable behavior of F-EMNs and tumor-derived exosomes, both loaded with miR145-Cy5. Preliminary experiments were conducted to determine the most suitable administration route. miR145-Cy5-loaded F-EMNs were administered either intraperitoneally (IP) or retro-orbitally (RO), since by these routes, lungs are not reached directly after injection. Results prove that F-EMNs+miR145-Cy5 could efficiently reach the tumors irrespective of the administration route (**Figure 26a,b**), but a higher fluorescent signal in the liver, kidney, and spleen, was observed after RO in comparison to IP injection, indicative of a higher accumulation in these organs following the first administration route (**Figure 26c,d**). Importantly, we did not observe any signal in the heart, supporting the idea that F-EMNs treatment would avoid cardiotoxicity, one of the main concerns related to the development of cancer therapeutics (Zamorano *et al.*, 2016).

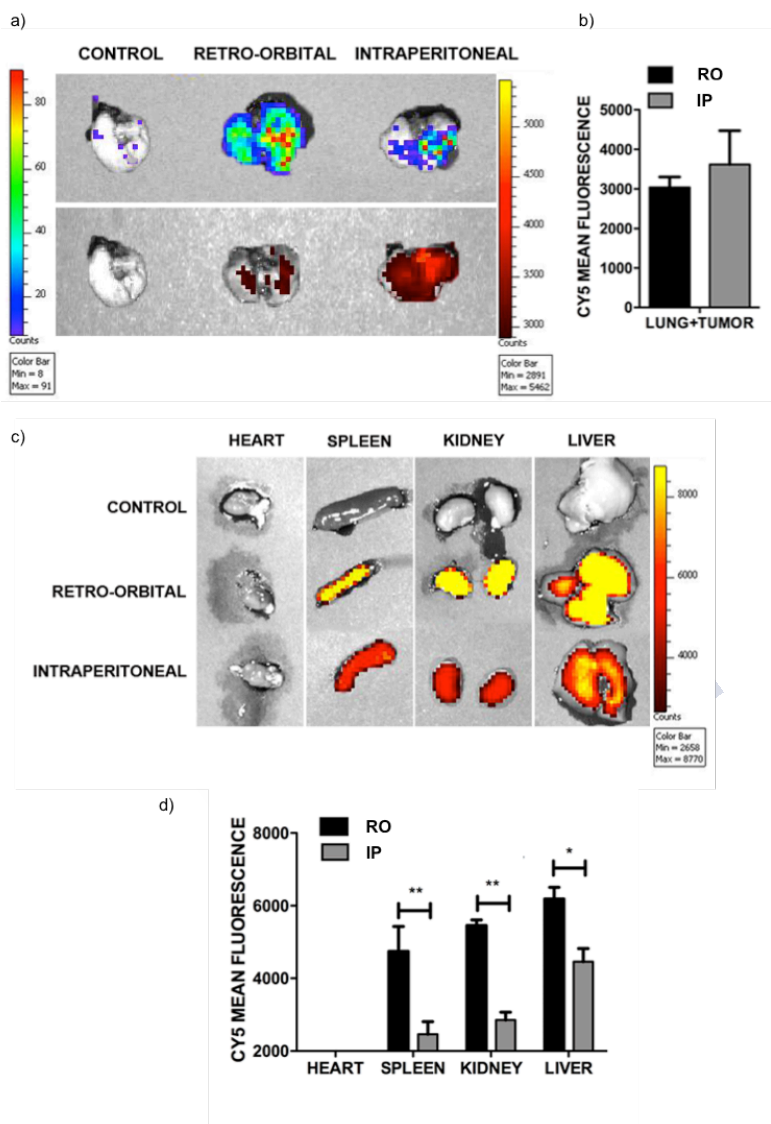


Figure 26. Comparative *in vivo* biodistribution of two different administration routes. Analysis of the retro-orbital and intraperitoneal inoculation methods of EMNs+miR145-Cy5. A representative image *ex vivo* (a,c) and quantification of the Cy5 fluorescence (b,d) of the (a,b) lung (tumor) and (c,d) indicated organs *ex vivo*. The scale bars (a,c) represent the luciferase intensity (left) and Cy5-fluorescence (right, arbitrary units). The data in graphs denote the mean values \pm SEM from n=3 mice per condition and Cy5 fluorescence signal was normalized to the background obtained from tumors of mice control. *p<0.05; **p<0.01; ***p<0.001. Data without statistical significance were not indicated.

According to these results, we decided to pursue the IP modality, which also proved to be adequate for the administration of other types of nanocarriers loaded with biomolecules (Cirstoiu-Hapca *et al.*, 2010). We injected miR145-Cy5-loaded F-EMNs and tumor-derived exosomes and confirmed that both treatments could mediate the accumulation of miRNA in the lung and the tumor with similar efficiency (**Figure 27**).

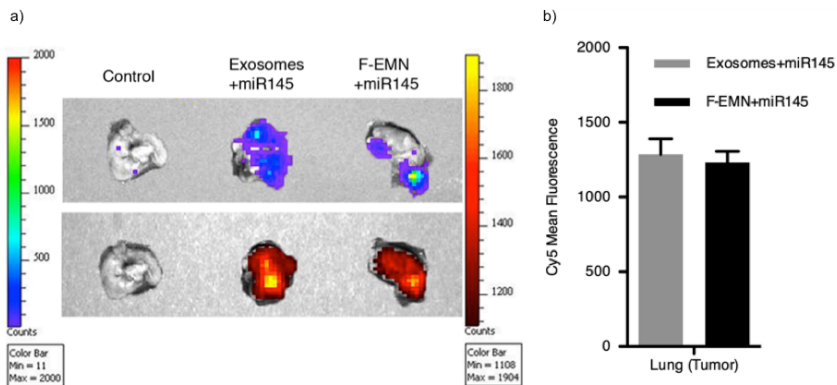


Figure 27. *In vivo* biodistribution of natural exosomes and F-EMNs loaded with miR145-Cy5. (a) Representative image *ex vivo* and (b) quantification of the Cy5 emission (right) of the lung (tumor) after treatment with natural exosomes or F-EMNs. The luminescence signal of tumor cells (left) and Cy5 fluorescence (right) of the same tumor are shown. Data without statistical significance were not indicated.

Immunofluorescence studies with the excised tissue revealed localization of miR145-Cy5 in the neighborhood of Ki67 positive proliferative tumor cells (**Figure 28**). In addition, there was a significant reduction in the fluorescence signal observed in the kidney and the liver for mice receiving F-EMNs+miR145-Cy5 with respect to mice receiving exosomes+miR145-Cy5, suggesting that F-EMNs could reach the tumor efficiently (**Figure 29**).

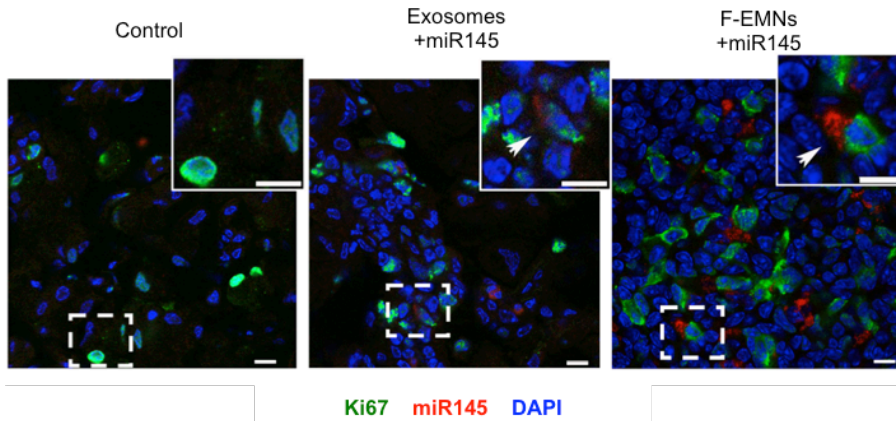


Figure 28. Representative confocal microscopy images of lung tumor cryosections stained with DAPI (blue) and ki67 (green) for analyzing the miR145-Cy5 intracellular uptake *in vivo* (red) in the metastatic cells after internalization of exosomes+miR145 and F-EMN+miR145. The arrows label the areas of miR145-Cy5 accumulation and the scale bar represents 10 μ m.



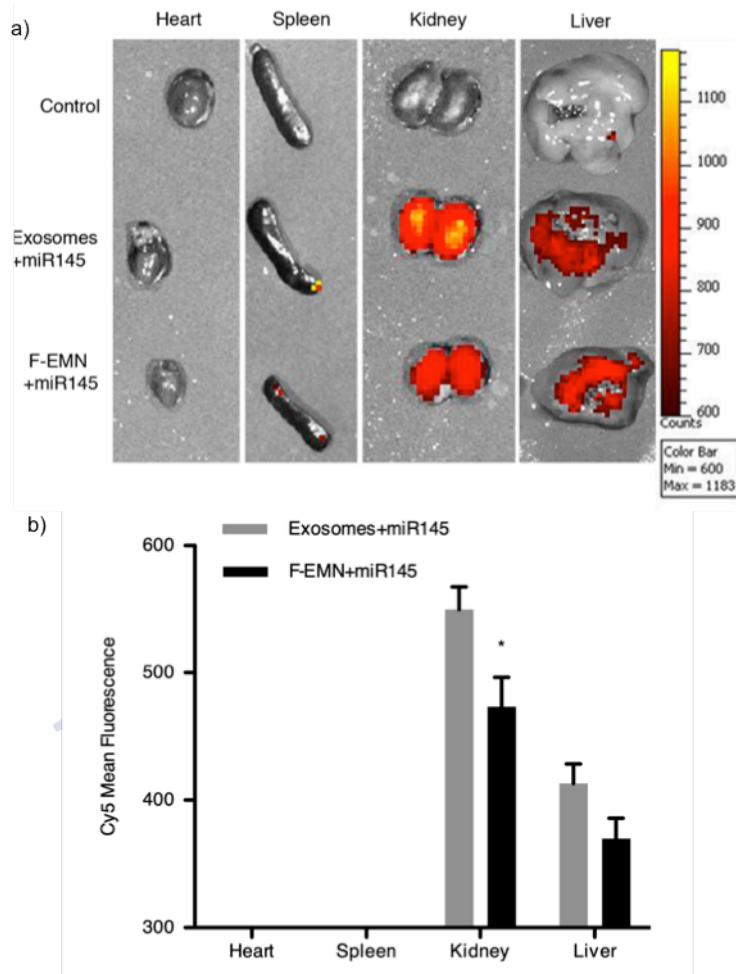
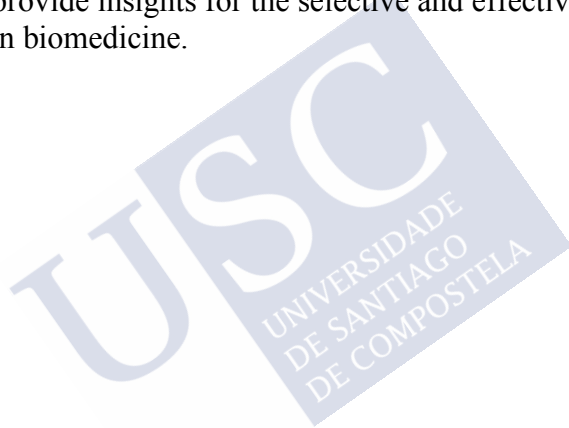


Figure 29. miRNA145 loaded exosomes and EMNs biodistribution. (a) Representative image *ex vivo* and (b) quantification of the Cy5 emission of the indicated organs. The scale bars represent the Cy5-fluorescence (right, arbitrary units). The data in the graph denote the mean values \pm SEM from $n=5$ mice per condition and Cy5 fluorescence signal was normalized to the background obtained from tumors of mice control. * $p<0.05$. Data without statistical significance were not indicated.

9.1.9 Conclusion

Overall, we have developed a multifunctional vector, the exosome-mimetic nanoplatform, which can be manufactured by a fast, simple, mild, reproducible, and easily scalable methodology with a controlled and fully characterized composition for a safer biomedical approach for its use in preclinical or clinical settings. EMNs have demonstrated to efficiently transport bioactive macromolecules, such as proteins and RNAs, and can be successfully functionalized with membrane proteins with organotropic properties for exploitation for therapeutic purposes. Moreover, the nanoplatform proposed here can be a powerful tool for the in-depth study of the role of specific lipids and proteins to provide insights for the selective and effective delivery of therapeutics in biomedicine.





**SECTION II:
STRATEGY INSPIRED BY CTCs**



9.2 DISCOVERY OF A NEW TARGET FOR METASTATIC NSCLC

This work has been done in collaboration with the *Fondazione IRCCS Istituto Nazionale dei Tumori*, the *Fundación Investigación Hospital General Universitario de Valencia*, and the Liquid Biopsy Analysis Unit (ONCOMET) at the *Instituto de Investigación Sanitaria de Santiago de Compostela (IDIS)*.

SUMMARY

Metastases are still the major cause of morbidity and mortality in cancer patients with solid tumors. Identifying new targets related to tumor progression and metastases formation could open new therapeutic avenues for the treatment of NSCLC patients. Circulating Tumor Cells (CTCs), originated from solid tumors, are involved in the process of metastatic spread and represent a valuable source of information to improve understanding, to identify novel biomarkers and to develop more efficient diagnosis and treatment procedures for metastatic patients. Indeed, in the field of personalized medicine, liquid biopsy stands out for its determining role. To date, the study of CTCs through liquid biopsy has led to the identification of numerous biomarkers of interest for patient stratification and diagnosis, as well as for monitoring therapeutic efficiency. Analysis of CTCs has also been explored as a strategy for the identification of novel targets that might lead to the development of innovative targeted cancer therapeutics.

The identification and validation of a novel biomarker in NSCLC, which might also be relevant for more types of tumors, is described in this section. Starting from a patient-based approach, CTCs were isolated from advanced NSCLC patients and subsequently analyzed. A molecular-genetic profile allowed identification of differentially significantly expressed genes in CTCs. A bioinformatic analysis allowed filtering the identified genes for their function, location, and signaling pathways in which they are involved. Candidate genes were then analyzed by RT-qPCR.

Taste Receptor Type 1 Member 3 (TAS1R3) was selected as the target of interest and further validated in an independent cohort of

CTCs isolated from NSCLC patients. The prognostic value of the expression of this biomarker in CTCs was also investigated. With respect to the expression of TAS1R3 in solid tumors, it was analyzed in Patient-derived Xenograft (PDXs) models from NSCLC primary tumors. Additionally, analysis of a larger PDX database that includes NSCLC samples and 16 additional cancer types, allowed characterization of relevant clinical features of tumors expressing high levels of TAS1R3 such as tumor stage, treatment status, histology, and gender, among others. To conclude, this section describes the identification, for the first time, of TAS1R3 as a target of interest in oncology.



9.2.1 Isolation and characterization of CTCs from advanced NSCLC patients

Immunoisolation and molecular profiling of CTCs in advanced NSCLC were performed as previously described by Mariscal *et al.* (Mariscal *et al.*, 2016). Briefly, blood samples from 42 advanced NSCLC patients and 16 healthy donors from the *Hospital Clínico Universitario de Santiago de Compostela* (same cohort as described in Mariscal's work) were subjected to EpCAM-based immunoisolation of CTCs and subsequent RT-qPCR analysis. *GAPDH* was used as a marker of global cellularity and normalized to *CD45*, a marker of non-specific isolation (Barbazán, Alonso-Alconada, *et al.*, 2012). After the presence of CTCs in patients' blood was confirmed, 10 samples of patients and 4 samples of controls were selected for molecular characterization. Total RNA was amplified, and complementary DNA hybridized onto Agilent gene expression microarray. Genes characterizing the CTC population were identified by using the MeV v4.7 (Multiexperiment Viewer) software (TM4 Microarray Software Suite (Saeed *et al.*, 2003, 2006). Two class Significance Analysis for Microarrays (SAM) algorithm was applied for the selection of the candidate genes with stringent criteria to obtain significance within a slide, and among all slides. A list of 2461 genes were obtained, being considered only the 529 probes with \log_2 ratio greater than 1.5, specifically characterizing the CTC population from advanced NSCLC patients (**Figure 30a**). Hierarchical clustering (HCL) was performed with these significantly expressed genes using MeV. Pearson correlation as distance metric, absolute distance and complete linkage clustering parameters in MeV options (**Figure 30b**).

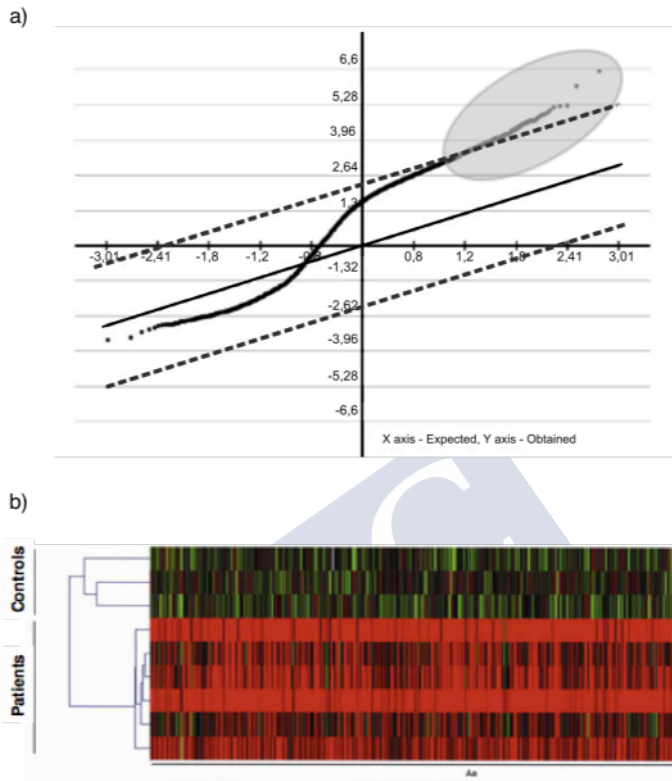


Figure 30. CTCs identification process and gene expression profile. (a) SAM analysis output graph showing gene expression differences between the group of patients and controls. Highlighted dots correspond to genes with statistically significant increased levels of expression in the group of patients compared to the control background, being considered to characterize the CTC population from metastatic lung cancer. (b) Hierarchical clustering of differentially expressed genes between patients (n=6) and controls (n=4) (CTC specific genes).

9.2.2 TAS1R3 is identified in CTCs from advanced NSCLC

Experimental workflow for gene filtration is depicted in **Figure 31**. 349 (out of the 529 significant genes) were annotated genes and thus identified using the Ingenuity Pathway Software (IPA). Genes were classified within Top networks. Top canonical pathways characterizing CTCs from metastatic lung cancer patients are shown

in **Table 9** and **Figure 32**. The main molecular and cellular functions represented by the

set of CTC-specific genes were related to lipid metabolism, molecular transport, small molecule biochemistry, cell death, cell-to-cell signaling, and interaction, and were mainly orchestrated by G-Protein coupled receptor (GPCR) signaling and complement system pathways.

Table 9. Top networks, molecular and cellular functions and top canonical

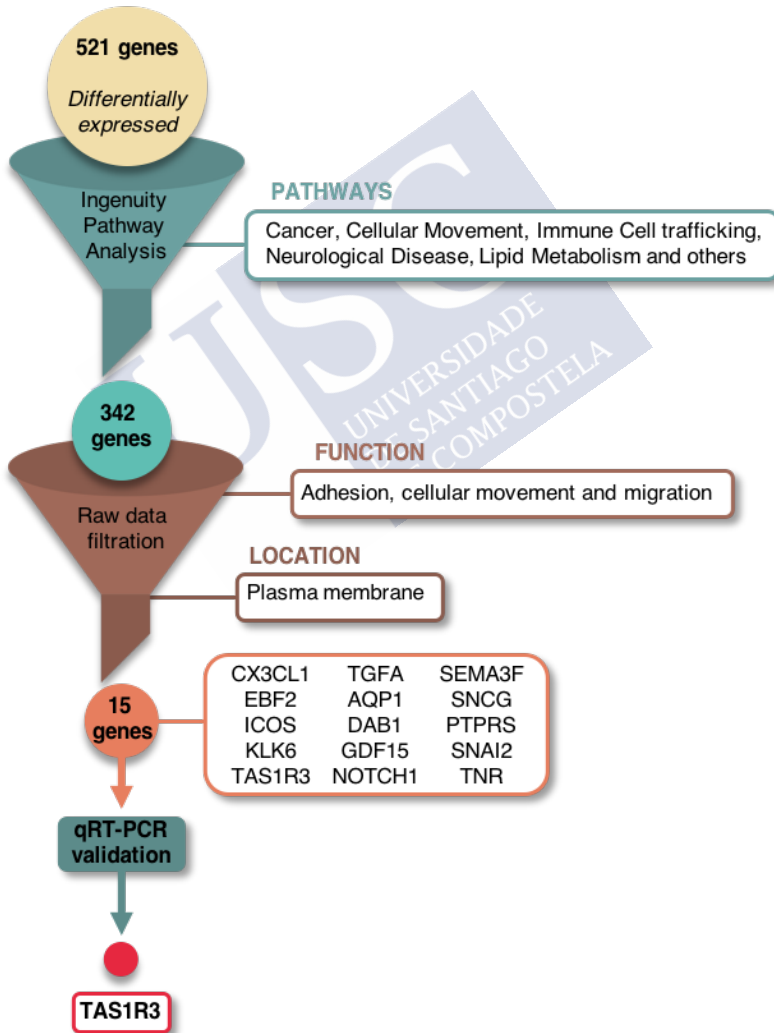


Figure 31. Schematic workflow for gene filtration analysis.

pathways by IPA analysis

Top Networks	Molecular and Cellular Functions	Top Canonical Pathways	p-value
Cancer, Cardiovascular System Development and Function, Cell Cycle	Lipid metabolism	Complement System	9,99 E-04
Cellular Movement, Hematological System Development and Function, Immune Cell Trafficking	Molecular Transport	Tyrosine Metabolism	2,97 E-03
Lipid Metabolism, Small Molecule Biochemistry, Organismal Functions	Small Molecule Biochemistry	G-Protein Couple Receptor Signaling	2,31 E-02
Carbohydrate Metabolism, Behavior, Neurological Diseases	Cell Death	Methionine Metabolism	5,88 E-02
Molecular Transport, Organ Morphology, Endocrine System Disorders	Cell-to-Cell Signaling and Interaction	Selenoamino Acid Metabolism	6,24 E-02

Genes were further filtered based on 1) function related to adhesion, cellular movement and migration and then 2) location on the cell surface (**Figure 31**). It generated a final list of 15 candidate genes: *CXC3CL1*, *KLK6*, *TNR*, *SNAI2*, *PTPRS* and *TGFA* (cellular movement); *GDF15*, *NOTCH1*, *ICOS*, and *SEMA3F* (cellular growth, proliferation and signaling); *EBF2* (apoptosis); *AQP1*, *DAB1* (cellular migration), *SNCG* (hypoxia and metastasis); and *TASIR3* (taste sensing and metabolism).

The next step involved RT-qPCR validation of these 15 genes in an independent series of NSCLC patients and controls. Only 6 out of the 15 candidate genes rendered a CT value (*AQP1*, *NOTCH1*, *PTPRS*, *SNCG*, *TASIR3*, and *TGFA*), and just 4 of them, significant overexpression over controls (*AQP1*, *NOTCH1*, *SNCG*, *TASIR3*). The specific expression of these genes was evaluated by comparing the CTC populations from the group of NSCLC patients (n=10) with the background from healthy controls (n=10), once they had been normalized to CD45 as a marker of non-specificity during CTC isolation (**Figure 33**).

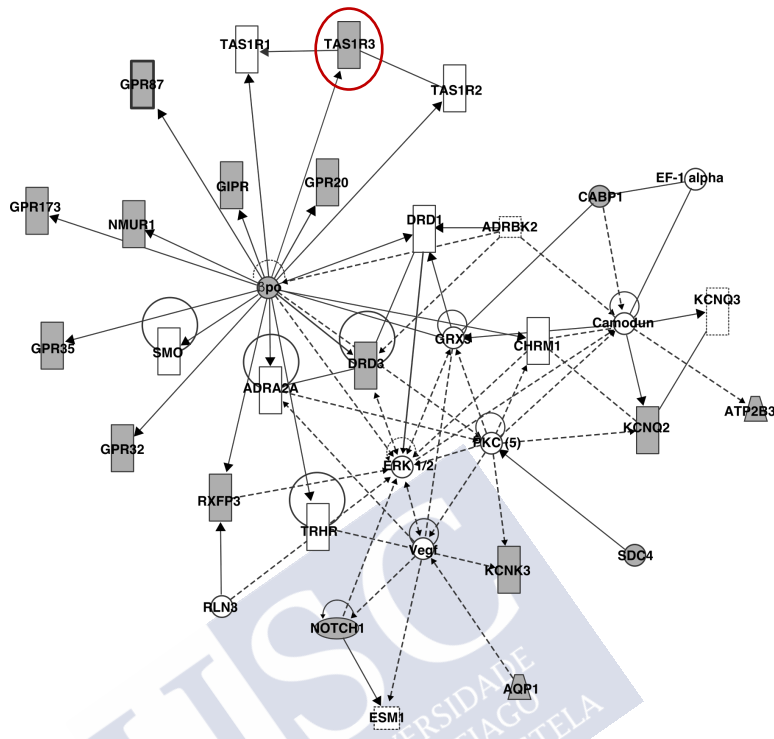


Figure 32. Gene expression bioinformatic analysis and validation. Ingenuity Pathway Software (IPA) analysis showing top networks and top canonical pathways characterizing CTCs from metastatic lung cancer patients.

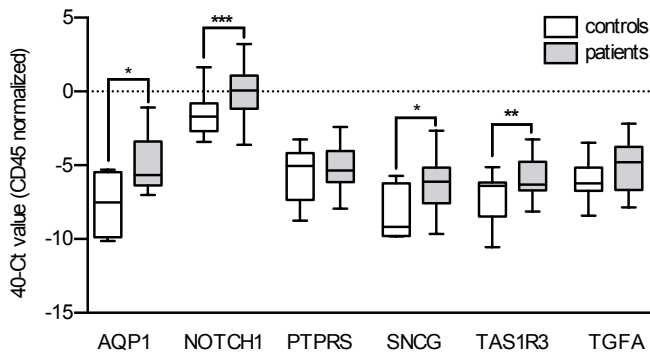


Figure 33. RT-qPCR result of validation of candidate genes. Tukey box and whiskers plot shows 40-Ct value of genes normalized to CD45. The line between boxes indicates the median value, while the outer boxes represent the 25th and the 75th percentiles and whiskers show the non-outlier range. Data was analyzed by two tailed t-Student tests (*p < 0,05, **p < 0,01, *** p < 0.001). Data without statistical significance were not indicated.

After searching in literature, the differential expression of *TAS1R3* in patient samples, compared to controls revealed as a promising discovery, given that this is a taste receptor, related to cell metabolism, which had not been described in cancer to date (Cui *et al.*, 2006; Dotson *et al.*, 2008; Treesukosol, Smith and Spector, 2011; Glendinning *et al.*, 2012; Dalesio *et al.*, 2018; Di Pizio, Behrens and Krautwurst, 2019; Schier *et al.*, 2019). For validation, *TAS1R3* expression was additionally determined in CTCs isolated from an independent cohort of advanced NSCLC patients (stages III-IV, treated with platinum-based doublet therapy, n=41, **Table 10**) provided by the *Hospital General Universitario de Valencia*, and compared to healthy donors (n=31). Consistently, RT-qPCR showed a significant increase in *TAS1R3* expression in patients at the baseline when normalized to the recovery of CD45 and, interestingly, this higher expression was maintained during the different cycles of chemotherapy (**Figure 34**).

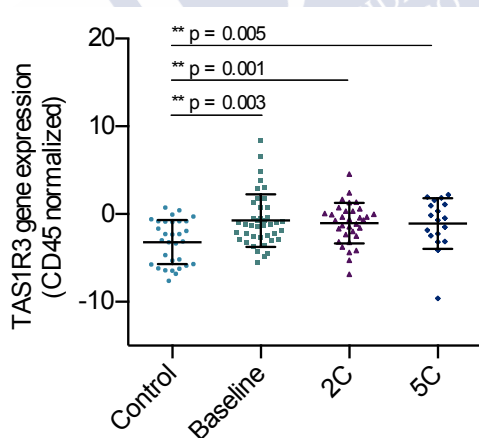


Figure 34. *TAS1R3* validation in an independent cohort of patients. At the baseline (n=41, stage IIIb-IV) compared to controls (n=31), and monitorization during second cycle (2C, n=37) and fifth cycle (5C, n=21) of treatment with cisplatin. Data represent mean \pm SD and significance was examined by two-tailed Mann-Whitney U-test. **p < 0,001.

Table 10. Clinicopathological parameters of the cohort of NSCLC patients for TAS1R3 validation in CTCs.

Parameters		Number	%
Sex	Male	28	92
	Female	13	8
Smoking habits	Smoker (current & former)	34	83
	Non-smoker	3	7,3
	Unknown	4	9,7
Histology	Adenocarcinoma	28	68,2
	Squamous cell carcinoma	8	28,6
	Other	5	12,2
Tumor stage	IIIA	3	7,3
	IIIB	5	12,2
	IV	33	80,5
Tumor size (T)	T1	2	4,9
	T2	8	19,5
	T3	4	9,7
	T4	20	48,8
	Unknown	7	17,1
Node affectation (N)	N0	1	2,4
	N1	8	19,5
	N2	11	26,8
	N3	14	34,2
	Unknown	7	17,1
No. of focus of metastasis	None	8	19,5
	Low (< 2)	10	24,4
	High (\geq 2)	23	56,1
Metastasis location	Brain	5	12,2
	Bone	15	36,6
	Liver	8	19,5
	Supra-adrenal	7	17,1
Therapy	Platinum-Pemetrexed	21	51,2
	Platinum-Vinorelvina	12	29,3
	Others	8	19,5

9.2.3 Prognostic value of TAS1R3 in CTCs from NSCLC

The prognostic significance of TAS1R3 was evaluated in the same cohort of CTCs, used for TAS1R3 validation (n=41; **Table 10**). Univariate Cox regression and Kaplan-Meier analysis were applied in order to assess the association between the Overall Survival (OS) and Progression-Free Survival (PFS) with TAS1R3 expression levels. Samples were stratified according to *TAS1R3* gene expression levels representing the 50th percentile (TAS1R3-low n=21 and TAS1R3-high n=20).

The graphs in **Figure 35** revealed that TAS1R3 expression in CTCs (isolated by EpCAM-based immunoisolation), was not statistically significantly associated with worse OS or PFS ($p > 0.05$, log-rank test). Similar results were obtained with 25th and 75th percentiles (data not shown).

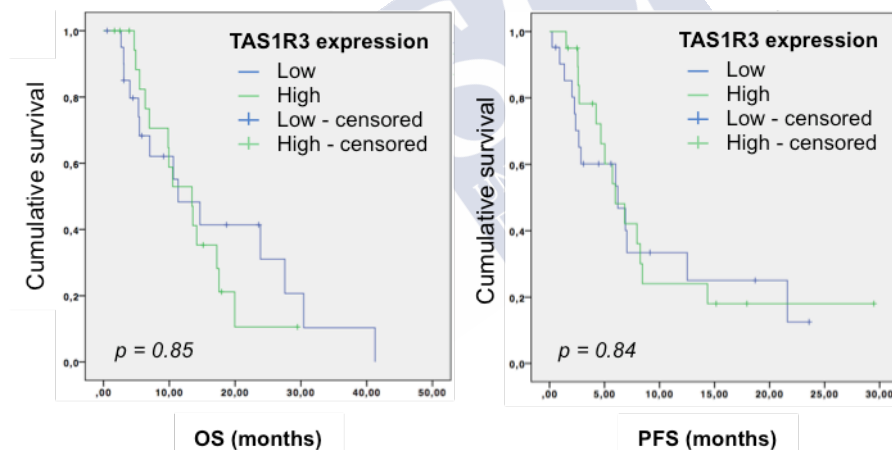


Figure 35. Prognostic value of TAS1R3 from CTCs. Kaplan-Meier plots for Overall Survival (OS) and Progression Free Survival (PFS) of patients with high (>50th percentile) or low (< 50th percentile) transcriptional levels of TAS1R3 measured in CTCs from peripheral blood. Log-rank test P-value = 0.58 and 0,84, respectively.

9.2.4 TAS1R3 expression in primary tissue from PDXs

In order to get additional data, PDX models were established in nude mice at the *Istituto Nazionale dei Tumori*, Milan, from freshly resected primary tumors of patients with advanced NSCLC adenocarcinoma (IIIb-IV stages, n=9, **table 11**). Stably histopathological characteristics of NSLC patients' tumors and their corresponding PDXs were previously evaluated in order to confirm the accuracy of these *in vivo* models (Moro *et al.* 2017). IHC staining on paraffin-embedded tumor sections showed a non-homogeneous positive signal for TAS1R3 that is more evident in some cells or small clusters and within areas of pseudoglandular organization. TAS1R3 presents a membranous pattern of expression (LT66) or membranous and cytoplasmic staining (LT302). Looking carefully at the positive cells, a morphology of undifferentiated cells was well-appreciated, resembling a previously observed CD133 staining of CSC clusters (Bertolini *et al.*, 2009) (**Figure 36**).

Table 11. Clinicopathological parameters of the NSCLC patients for PDX establishment.

LT	Sex	Histology	Grade	Stage	TNM	Smoking habits	Pre-treatment
66	Female	ADC	G3	IIIA	T1aN2M0	former	NO
111	Female	ADC	G3	IIB	T2bN1M0	non-smoker	NO
128	Male	ADC	G3	IIIA	T2bN2M0	smoker	Platinum+ Pemetrexed
138	Male	ADC	G3	IA	T1aN0M0	former	NO
187	Male	SCC	G3	IIIA	T3N2M0	smoker	NO
302	Female	ADC	G3	IIIA	T3N1M0	non-smoker	NO
297	Male	SCC	G3	IIIA	T1bN2M0	na	NO
258	Male	SCC	na	IIIB	T2bN2M0	smoker	NO
732	Male	ADC	na	IIIA	T1N2bM0	non-smoker	Platinum+ Pemetrexed

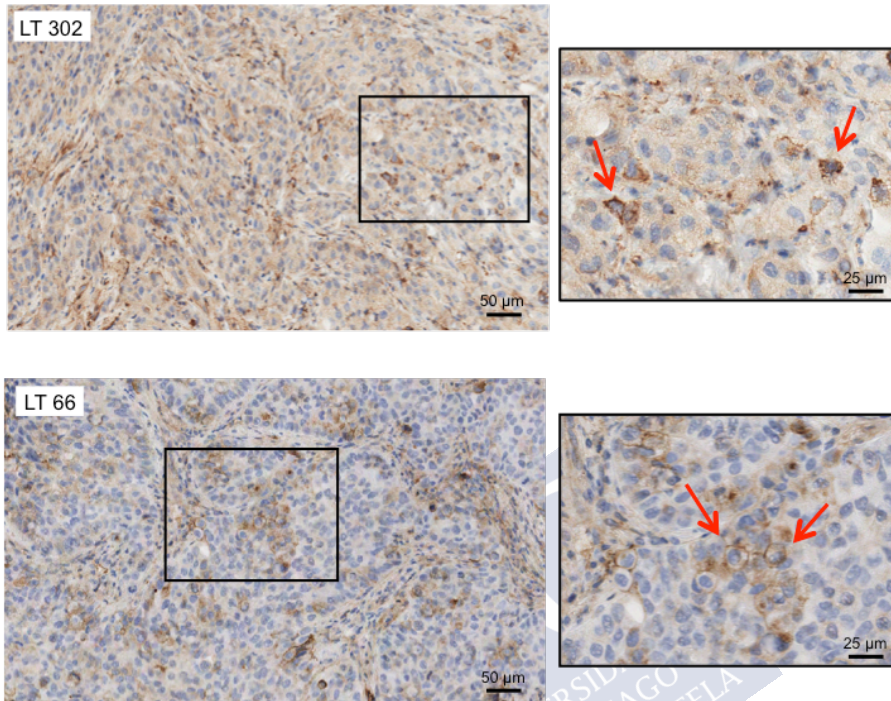


Figure 36. Representative images of IHC analysis of TAS1R3 in PDXs models from NSCLC patients (stage IIIb-IV). Scale bars represent 50 µm (left) and 25 µm (right).

Next, TAS1R3 expression was evaluated in the Champions TumorGraft[®] database from Champions Oncology, a leading global oncology pharmacology Contract Research Organization (CRO) (<https://www.championsoncology.com/software-solutions/champions-tumorgraft-database>). Their online searchable database contains key data on a compendium of PDX models with demonstrated correlations to patient outcomes (Izumchenko *et al.*, 2017). Out of the 141 PDXs in the database for NSCLC, 17% expressed high levels of TAS1R3 (>2-fold expression, $\text{Log}_2(\text{RPKM}+1) > 0,7$). The fold expression compares the RPKM (Reads Per Kilobase Million) value of the model to the mean RPKM value across the entire bank (**Figure 37**).

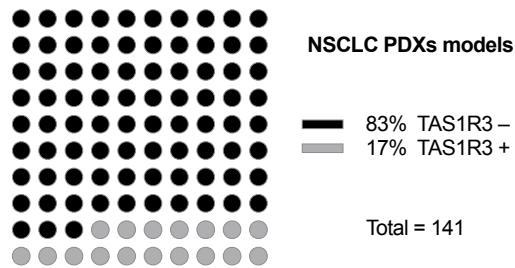


Figure 37. Champions TumorGraft® database for NSCLC. Percentage of TAS1R3 positive (17%) and TAS1R3 negative (83%) PDXs for NSCLC.

The analysis of the clinical data (from patients) collected in the database, and represented in **Figure 38**, showed that TAS1R3 positive PDXs correlate more with adenocarcinoma (70,4%) than with a squamous histology (29,6%), and with patients in end-stage of disease (19% stage I, 11,3% stage II, 12,5% stage III, 57,1% stage IV). A higher expression of TAS1R3 is also more associated with metastatic sites (75%), either local (43%) or distal metastasis (32%), than with primary tumor (25%). Local metastases were harvested from the lung, and the thoracic and chest wall, equally, whereas distal metastases were found mainly in the lymph nodes (42%), followed by the liver (31%) and the brain (27%). Remarkably, 65,5% of the TAS1R3 positive tumors presented an undifferentiated tumor grade, 25% poorly-differentiated, 9,6% moderately-differentiated, and none well-differentiated. Lastly, the treatment status (52% pretreated vs. 48% naïve), smoking history (48% smoker vs. 52% non-smoker), and gender (49% male vs. 51% female), seemed to be independent of TAS1R3 expression for NSCLC.

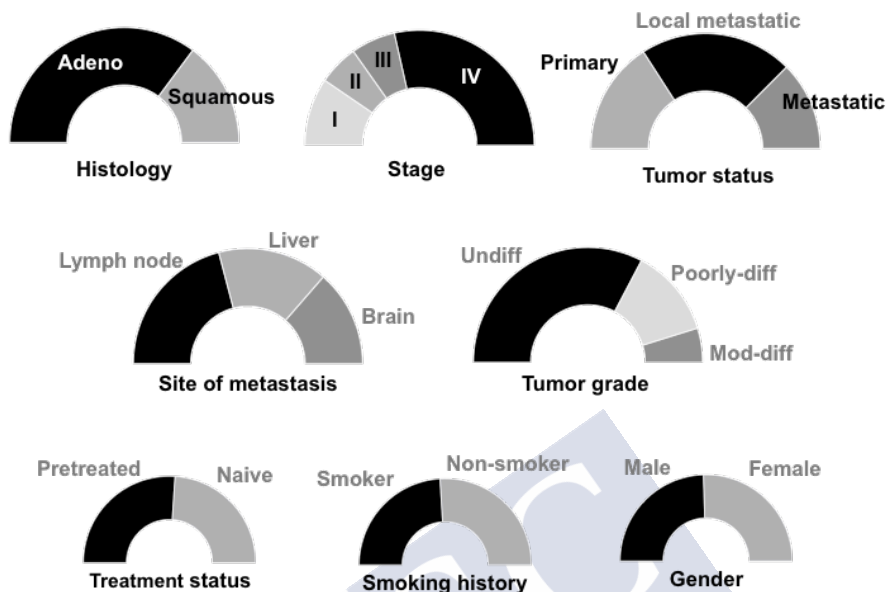


Figure 38. TAS1R3 positive NSCLC PDX models classified by relevant clinical data.

9.2.5 TAS1R3 expression in other cancer types

Making use of the Champions TumorGraft® database, TAS1R3 expression was also evaluated in other cancer types, including bladder, breast, colorectal, cholangiocarcinoma, endometrial, esophageal, gastric, head and neck, lymphoma, melanoma, NSCLC, SCLC, ovarian, pancreatic, prostate, sarcoma, uterine and glioblastoma (GBM), making a total of 749 available PDXs. Out of them, TAS1R3 was highly expressed in 116 PDXs (15,8%) across all tumor types (>2 -fold expression, $\text{Log}_2(\text{RPKM}+1) > 0,7$). Specific details regarding each cancer type are shown in **Table 12**. Percentages of TAS1R3 positive PDXs, considering only the cancer types with more than 40 PDX models, are represented in **Figure 39**. Taking together all cancer types (also including NSCLC) and the clinical data of the TAS1R3+ patients, this analysis leads to relevant conclusions. TAS1R3 is highly expressed mostly in the metastatic state (52,4%), stage IV patients (78%), with poorly differentiated tumor grade

(58%), pretreated (67,5%), older than 40-year-old, Caucasian (71,4%) and males (56,5%) (**Figure 39**). These results are consistent with the analysis presented for NSCLC, except for the treatment status and the gender, since TAS1R3, in the overall analysis, seems to be more related to pretreated patients and males.

Table 12. PDX models of different cancer types in the Champions TumorGraft® database. Number of PDXs models, number of PDXs expressing high levels of TAS1R3 and percentage of TAS1R3+ PDXs for each cancer type.

Cancer type	PDXs	TAS1R3+ PDXs	TAS1R3+ PDXs (%)
Bladder	11	2	18,2
Breast	115	17	14,8
Cholangiocarcinoma	15	3	20
Colorectal	116	29	25
Endometrial	8	1	12,5
Esophageal	13	4	30,8
Gastric	26	3	11,5
GBM	11	0	0
Head & neck	42	8	19,05
Lymphoma	4	1	25
Melanoma	28	0	0
NSCLC	141	24	17,0
Ovarian	45	2	4,4
Pancreatic	71	15	21,1
Prostate	10	1	10
Sarcoma	64	4	6,25
	732	116	15,8

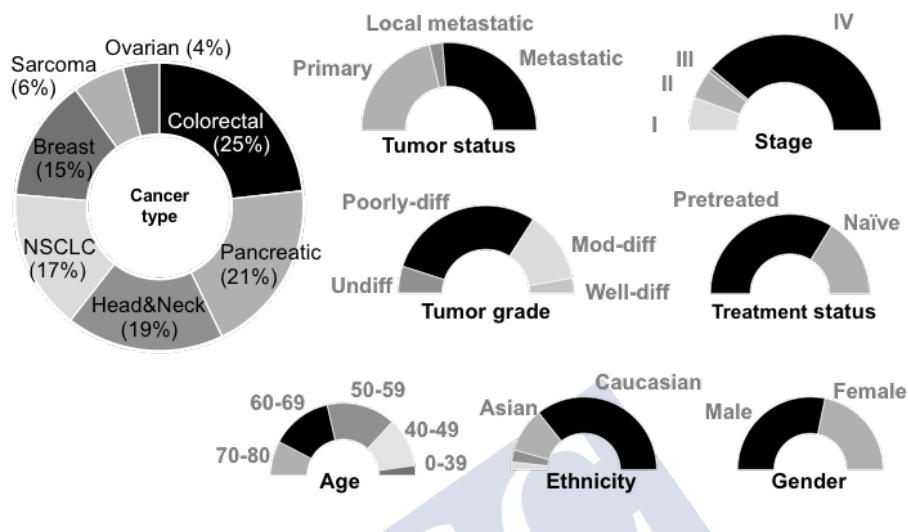


Figure 39. TAS1R3 expression in PDX models by cancer type and analysis of different clinical data in combination.

Lastly, in order to elucidate whether TAS1R3 is forming heterodimers with TAS1R1 or TAS1R2, as described for umami and sweet perception, or homodimers, when it is expressed in cancer cells, a correlation study was additionally performed making use of the TumorGraf[®] Database. TAS1R2 was not identified in the entire database. TAS1R1 was found highly expressed in 52 PDXs (out of the 749 PDXs) for all the cancer types, with a percentage of positivity shown in **Figure 40a**. TAS1R1 correlated with TAS1R3 in only 14 PDXs (5 NSCLC, 3 head and neck, 2 sarcoma, 2 ovarian, 1 bladder, 1 breast cancer; **Figure 40b**). **Figure 40c** shows the different levels of expression and the correlation between TAS1R1/TAS1R3 for all the PDX models in the database.

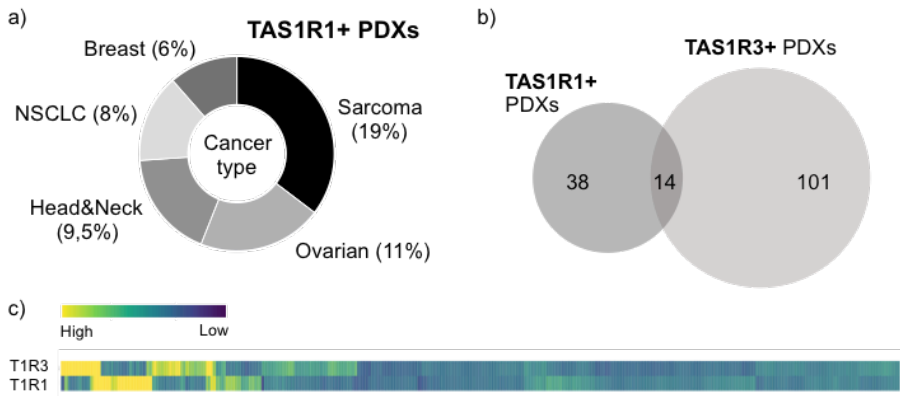


Figure 40. TAS1R1 expression in the TumorGraft® Database. (a) Percentage of TAS1R1 positive PDXs for each cancer type. **(b)** Correlation between TAS1R1 and TAS1R3 across all cancer types in the database. **(c)** Heat map showing the different expression levels.

9.2.6 Conclusions

All together, these results highlight the potential of liquid biopsy for the identification of novel biomarkers, and point out that TAS1R3 is an interesting novel biomarker, which particular role in cancer should be further elucidated.



9.3 ROLE OF TAS1R3 IN NSCLC

This work has been done during my stay (9 months) in the *Istituto Nazionale dei Tumori*, Milan, Italy, and in collaboration with the *Fundación Investigación Hospital General Universitario de Valencia*.

SUMMARY

The characterization of new biomarkers is essential to develop effective targeted therapies. Studying its role and implication in metastasis will definitely help us to better understand tumor progression and to rationally design the best strategy to combat metastasis in NSCLC. According to the results shown in the section 8.2 of this thesis, TAS1R3 appears to be an interesting target in NSCLC as well as in other cancer types. A deeper study was then required to shed light on the possible role of TAS1R3 in cancer. First experiments were conducted to explore if TAS1R3 expression could be related to a stem-like phenotype. For this, different cells lines as well as cells derived from patients were used. Additional experiments were carried out to understand if the expression of TAS1R3 could be influenced by the tumor microenvironment. Next, TAS1R3 was stably overexpressed in NSCLC cells and functional experiments were carried out. Proliferation, migration, and invasion capabilities of transfected TAS1R3 positive and control cells were evaluated *in vitro*. Their capability to disseminate from the primary tumor, to reach the lungs and metastasize, was additionally assessed *in vivo*. On the one hand, blood was taken from the heart and CTCs were subsequently isolated and characterized. Complementary, an experimental metastasis assay was performed to further evaluate the ability of TAS1R3 positive cells to colonize and grow in distal organs. Importantly, our results suggest that TAS1R3 enhances the metastatic capabilities of cells. All these results confirmed the relevance of TAS1R3 in NSCLC metastasis dissemination and propose TAS1R3 as a key player in the development and progression of human NSCLC metastasis. Correlation with stem markers suggests that TAS1R3 could be a novel diagnostic biomarker for Cancer Stem Cells and may

serve as a suitable target for the further development of novel therapeutics to impair metastatic dissemination in NSCLC.



9.3.1 TAS1R3 is co-expressed with CSC markers and possesses functional traits

In view of the results shown in section 8.2 that evidence expression of TAS1R3 in PDX in a similar pattern as described for CD133, and considering that CTCs with a more stem-like phenotype are described to be responsible for successful cancer metastasis (Cristofanilli *et al.*, 2004; Oskarsson, Batlle and Massagué, 2014; Gkoutela and Aceto, 2016; Cho *et al.*, 2018), the relation of TAS1R3 expression with the acquisition a stem-like phenotype was investigated.

First experiments were conducted to compare the TAS1R3 expression in the bulk tumor population and in a specific cell subpopulation positive for CD133, a cancer stem cell biomarker (Eramo *et al.*, 2008; Curley *et al.*, 2009; Liou, 2019), using for that purpose different NSCLC cell lines (H1299, H460 and A549) and a primary culture (LT215). Cells were analyzed by flow cytometry, following the gating strategy represented in **Figure 41**. Briefly, live cells were first selected based on size and complexity parameters, to identify the cells of interest and to exclude cell debris and aggregates. Then, IgG controls (IgG-Alexa 647 and IgG-PE) were analyzed to set the negative population for each marker. TAS1R3 expression was measured in the bulk population and in the CD133 positive subpopulation. Importantly, it was confirmed that the expression of TAS1R3 significantly increases in the cell subpopulation enriched for CD133, in relation to the bulk (**Figure 42**).

To verify these results, we additionally pursued a similar approach, but *in vivo*, using xenografted mice subcutaneously injected with H460 and A549 cells. Following this methodology the full impact of the microenvironment and the 3D conformation can influence the expression of TAS1R3 and CD133 (Luca *et al.*, 2013; Oczko-Wojciechowska *et al.*, 2020). FACS analysis of the dissected recovered tumors further confirmed a significant increase in TAS1R3 expression in the CD133+ subpopulation (**Figure 43a**). Remarkably, H460 rendered a 9,29% of TAS1R3 positive cells in the tumor bulk, whereas this percentage dramatically rose to 72% in the CD133 positive subpopulation (**Figure 43b**).

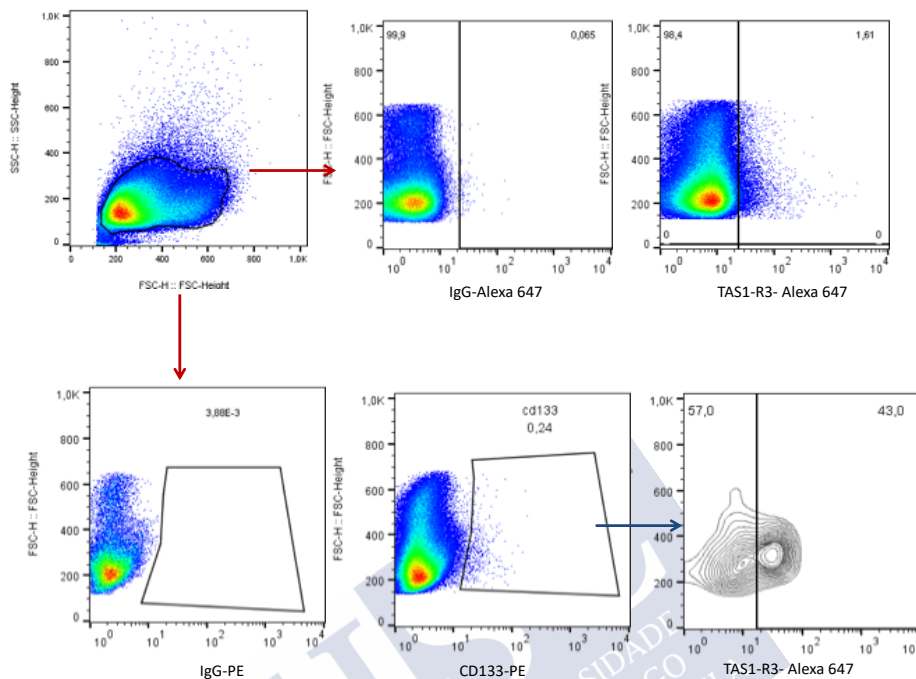


Figure 41. Gating strategy for TAS1R3 expression in the bulk population and in the CD133+ subpopulation.

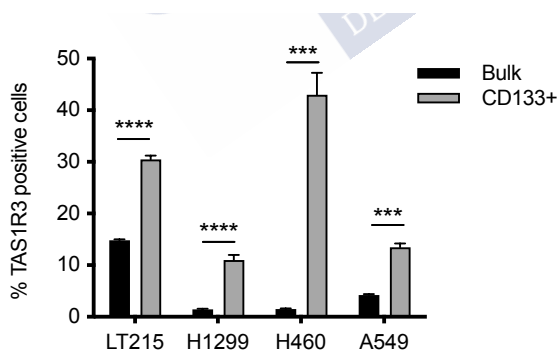


Figure 42. FACS analysis results showing that TAS1R3 expression is strongly enriched in the CD133+ subpopulation for primary lung cancer cells (LT215) and NSCLC cell lines (H1299, H460 and A549). Bars represent mean \pm SD of three independent experiments. Data was analyzed using a two-tailed t-Student test (** $p < 0,001$; **** $p < 0,0001$).

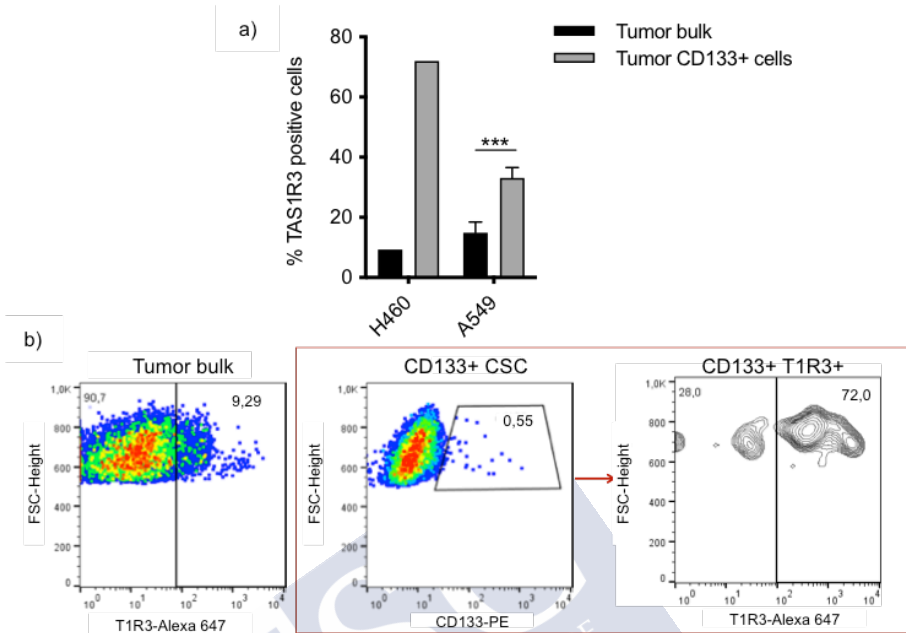


Figure 43. TAS1R3 correlation with CD133+ cell *in vivo*. **(a)** TAS1R3+ cells in the tumor bulk and the CD133+ subpopulation after s.c injection of H460 or A549 cells into the flanks of nude mice (n=1 for H460 and n=4 for A549). The A549 bars represent four independent experiments and replicates are expressed as mean \pm SD. Data was analyzed using a two-tailed t-Student test (***) $p < 0,001$. **(b)** Representative gating strategy for FACS analysis of TAS1R3+ and CD133+ H460 cells from tumors.

A sphere formation assay was subsequently performed in H460 and A549 cells to provide additional evidence that TAS1R3 expression could be related to a stem-like phenotype. It has already been described that a more physiological 3D conformation fosters cancer cells with a CSC phenotype (Bertolini *et al.*, 2015; Herreros-Pomares *et al.*, 2019). FACS analysis confirmed that cells growing in spheres (3D) compared to adherence (2D) rendered an increased expression of TAS1R3 (4-fold and 5-fold for H460 and A549, respectively), as well as of the CD133 stem marker (17-fold and 12-fold for H460 and A549, respectively) (**Figure 44a,b**). A similar tendency was obtained by RT-qPCR analysis at *TAS1R3* gene expression, providing a 3,4-fold and 2,5-fold increase for H460 and A549, respectively (**Figure 44c**). Moreover, this result was further validated in a wider battery of

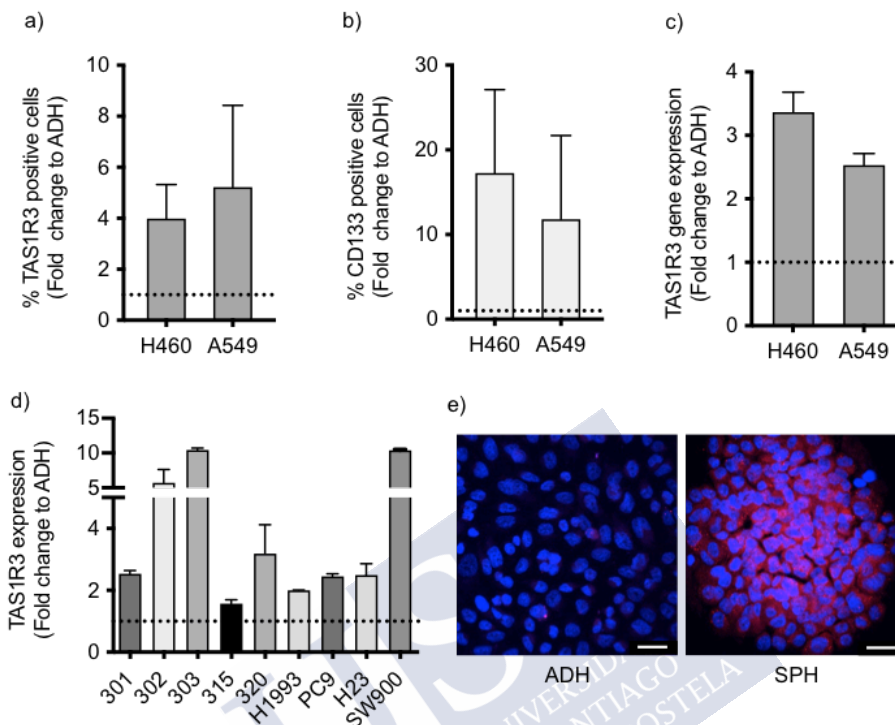


Figure 44. TAS1R3 increased expression in spheroids. (a) Fold change of TAS1R3+ cells and (b) CD133+ cells after spheres are formed and compared to adherent cells by FACS. (c) Fold change of TAS1R3 gene expression by RT-qPCR of spheroids to adherent cells of H460 and A549, as well as (d) a broader battery of NSCLC cell lines and primary cultures. (e) Representative pictures of immunofluorescence showing the overexpression of T1R3 (red) in spheres (SPH, 3D culture) compared to ADH (adherence, 2D culture) in the SW900 cell line. Nuclei are stained with Hoechst (blue). Scale bars represent 25 μm. The data represent three independent experiments and replicates are expressed as mean ± SEM. Data without statistical significance were not indicated.

NSCLC cell lines (H1993, PC9, H23 and SW900) and primary cultures (301, 302, 303, 315, 320) from NSCLC patients. In all cases, an increase in the fold change for *TAS1R3* expression was observed (**Figure 44d**). This result was also validated by immunostaining of SW900 spheroids vs adherent cells (**Figure 44e**).

However, when we cultured the cells in ultra-low attachment plates (ULA) with complete medium to perform the anoikis experiment, no differences were observed, confirming that it is not driven by growing in anchoring-independent conditions but an enrichment of cancer stem-like properties (**Figure 45**).

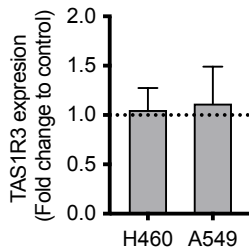


Figure 45. FACS analysis of Anoikis experiment incubating H460 and A549 cell lines in normal plates or ultra-low attachment plates (ULA). The data represent three independent experiments and replicated are expressed as mean \pm SD. Data without statistical significance were not indicated.

As such, these results indicate that TAS1R3 expression is correlated with the stem marker CD133 and with the functional trait of cancer stem cells of growing in 3D spheres.

9.3.2 TAS1R3 is increased in representative advanced models of the disease

To try to understand the pattern of TAS1R3 expression during disease progression, two different mouse models representing advanced stages of the disease, CDX and DDX (meaning CTC- and DTC-derived xenograft mouse models, respectively), obtained from H460 xenograft mice, were generated (**Figure 46**). CDX models were formed after subcutaneous implantation of the CTCs isolated from blood circulation of mice with H460 primary tumor xenografts, and DDXs models were formed by subcutaneous injection of disseminated tumor cells (DTCs) isolated from the lungs of the xenografted mice. The H460 xenograft model recapitulates the primary tumor whereas the CDX and DDX models better recapitulate the metastatic stages (Tellez-Gabriel *et al.*, 2019). Once the tumors from CTCs and DTCs had grown, mice were sacrificed, and tumors analyzed by IHC, flow cytometry and RT-qPCR (**Figure 47**). As it can clearly be observed in the IHC images, there is a dramatic increase in TAS1R3 expression in both models of advanced disease (CDX and DDX), with respect to the

primary tumor (**Figure 47a**). In the primary tumor a diffuse TAS1R3 staining of single cells or small clusters is observed as in the PDXs of section 8.2.4. This result was also validated by FACS (**Figure 47b**), with a moderate increase in CDXs and a significant rise in the percentage of TAS1R3 positive cells in the DDXs. RT-qPCR analysis resulted in similar readouts (**Figure 47c**).

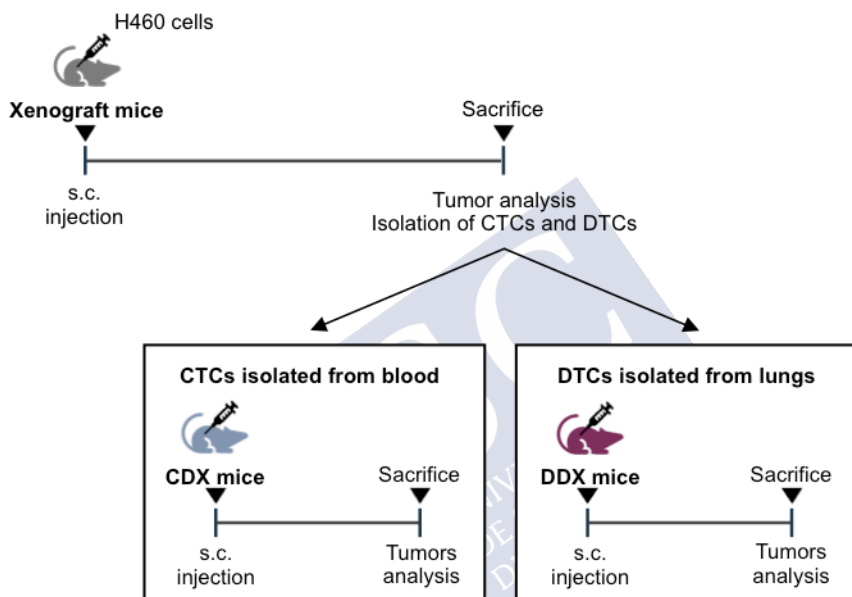


Figure 46. Schematic representation of the generation of CDX and DDX mice models. CDX and DDXs are generated by the subcutaneous injection of H460 cells in the flank of nude mice, followed by the isolation of CTCs from the blood and DTCs from the lungs of to reinject them in in the flanks of new mice subcutaneously.

Next, the number of TAS1R3+ cells for cells growing in cell culturing and in mice were compared. As observed, the number of TAS1R3+ cells were augmented *in vivo* compared to *in vitro* culture for both cell lines (**Figure 48**). This modulation of the TAS1R3 expression could be influenced by the tumor microenvironment.

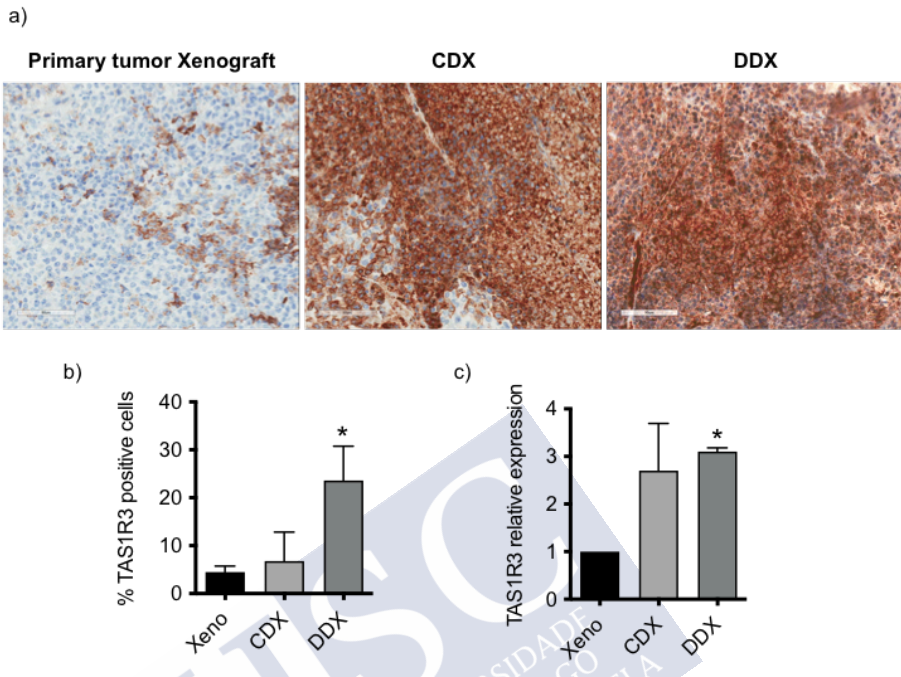


Figure 47. Evaluation of TAS1R3 expression during disease progression. (a) Immunohistochemistry analysis of TAS1R3 in CDXs and DDXs mice. Scale bars represent 90 μ m. (b) Flow cytometry and (d) RT-qPCR analysis. Bars represent mean \pm SEM of two independent experiments. Data was analyzed using a two-tailed t-Student test (* $p < 0.05$). Data without statistical significance were not indicated.

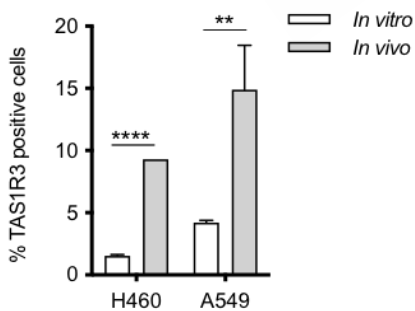


Figure 48. TAS1R3 expression in H460 and A549 cells is significantly increased when cultured *in vivo* compared to *in vitro*. Data represents mean \pm SD and was analyzed using a two-tailed t-Student test (** $p < 0,01$; **** $p < 0,0001$).

In order to study the effect of the microenvironment, H460 and A549 cells were incubated with conditioned medium (CM) from murine stromal cells (macrophages, endothelial cells and fibroblasts) for 48 hours, and TAS1R3 expression was analyzed by FACS. A slight increase in the culture with the CM from macrophages and endothelial cells was observed for H460 (**Figure 49a**) and only with macrophages for A549 (**Figure 49b**). In order to get a stronger effect in TAS1R3 modulation, tumor cells were directly coculture with the stromal cells for 48 hours. Despite the effect was not as strong as expected, a slight modulation of the expression of TAS1R3 could be observed for macrophages (**Figure 49c**). Further experiments should be carried out to better understand the effect of the microenvironment and to validate these results.

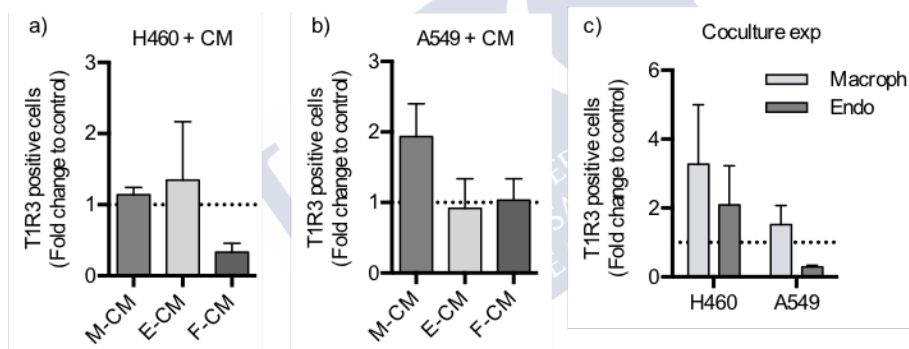


Figure 49. Tumor microenvironment influence in TAS1R3 expression. (a) FACS analysis of H460 and (b) A549 cells incubated during 48h with conditioned medium (CM) from RAW 264.7 macrophages (M), mouse endothelial cells (E) and mouse fibroblast (F). (c) FACS analysis of H460 and A549 in coculture with RAW 264.7 macrophages and mouse endothelial cells in a proportion 1:3 (tumor:stroma cells). The data represent three independent experiments and replicates are expressed as mean \pm SD. Data without statistical significance were not indicated.

9.3.3 TAS1R3 alters the migration and invasion

To investigate the role of TAS1R3 in tumor progression and metastasis, a stable cell line overexpressing TAS1R3 was generated from A549 cells, using a plasmid that co-expresses TAS1R3 and the reporter gene enhanced green fluorescent protein (eGFP) (**Figure 50a**). A non-target control (NTC) plasmid was used for TAS1R3 negative and eGFP positive (T1R3⁻ GFP⁺) control cells. Plasmids were first co-transfected with packaging plasmids into HEK293T cells to generate lentiviral vectors, and the eGFP signal was confirmed by fluorescent microscopy (**Figure 50b**).

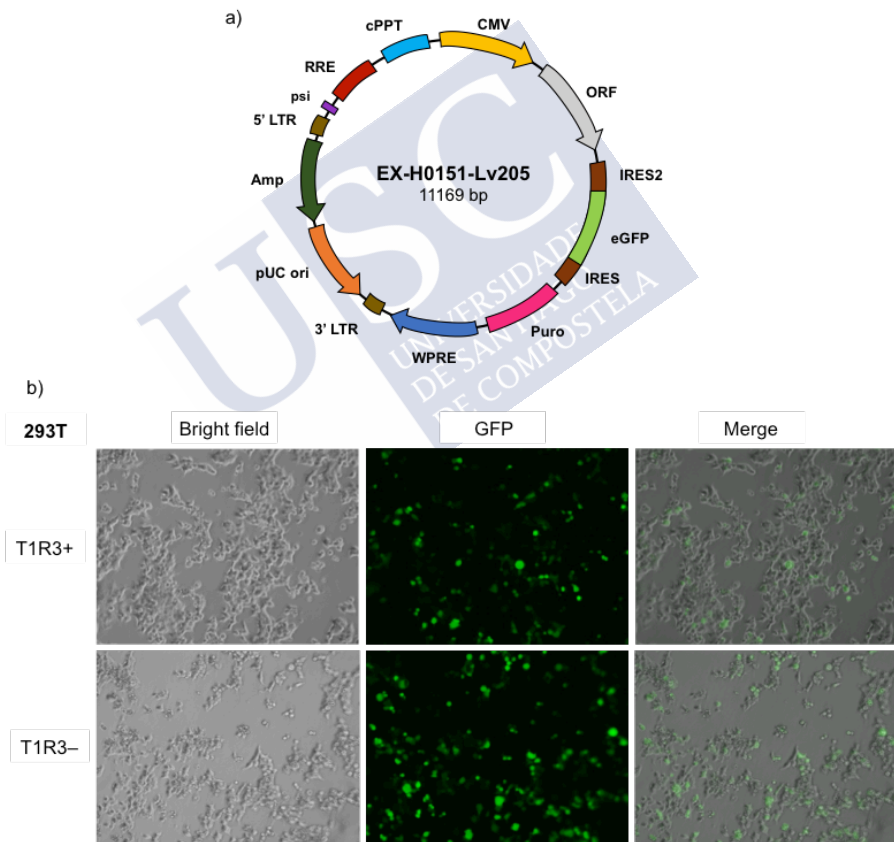


Figure 50. TAS1R3 overexpression in NSCLC cell lines. (a) The vector with CMV promoter, encoding IRES2-eGFP-IRES-puromycin was used for T1R3 overexpression in NSCLC cells with a previous step of (b) lentiviral production by HEK 293T cells. Green signal corresponds to eGFP production by the cells. Pictures were taken 24 hours post-transfection with a 10x objective.

Generated lentiviral vectors were used to transduce A549 cells. After selection of the transduced cells with puromycin, the transduction efficiency was evaluated by different methods including immunofluorescence, western blot and RT-qPCR. Confocal microscopy images revealed a clear overexpression of TAS1R3 compared to the control, whereas both transformed cells expressed eGFP in green as control, indicative of a successful transfection (**Figure 51a**). Western blot analysis further confirmed the expression of TAS1R3 in the whole lysate of transduced cells (**Figure 51b**) and RT-qPCR showed a dramatic increase by over 400 times at RNA level (**Figure 51c**).

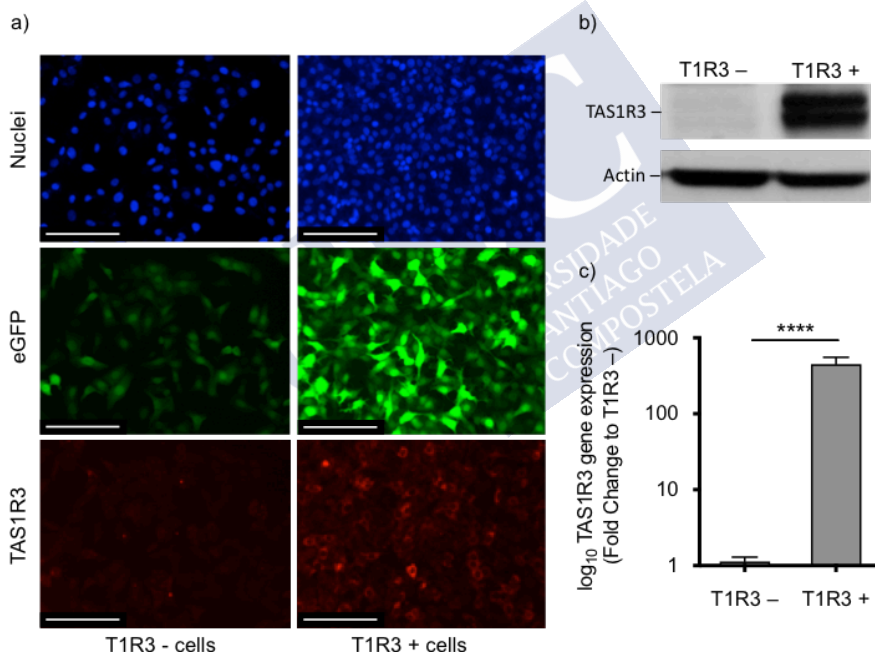


Figure 51. Evaluation of the transduction efficiency. (a) Immunofluorescence images of transfected cells with T1R3 plasmid (T1R3+) and with the empty vector (T1R3-). Blue signal: Hoechst, green signal: eGFP, red signal: TAS1R3-Alexa Fluor 647. Scale bars represent 125 μm. (b) Western blot showing the T1R3 overexpression in total protein lysate of T1R3+ and T1R3- cells. (c) Relative gene expression of TAS1R3 by RT-qPCR showing the fold change of T1R3+ to T1R3-. Bars represent mean \pm SD of three independent experiments. Data was analyzed using a two-tailed t-Student test (**** $p < 0.0001$).

Then, a number of studies were addressed to evaluate the effect that TAS1R3 produces in the cells *in vitro*. We carried out the EdU proliferation assay, and proliferating cells were analyzed by FACS and confocal microscopy. Results showed no differences between T1R3+ and T1R3- cells in proliferation (**Figure 52**).

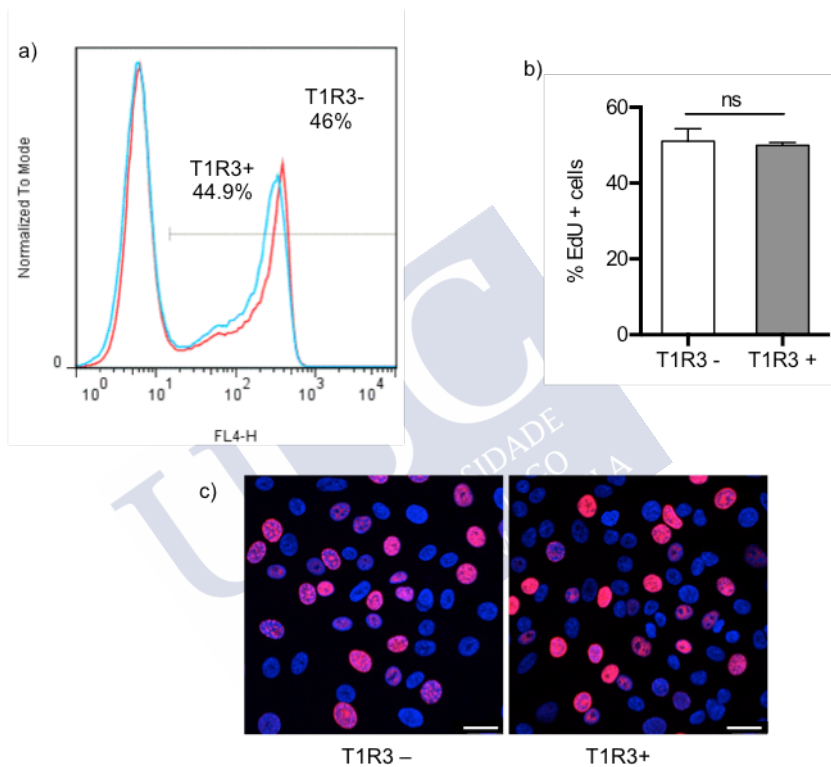


Figure 52. *In vitro* proliferation comparison of T1R3 +/- cell behavior. (a) Proliferation assay evaluated by FACS showing the fluorescence intensity and (b) the percentage of proliferative T1R3+ and T1R3- cells. (c) Confocal microscopy images showing proliferating cells in pink (EdU+ staining). Scale bars represent 25 μm.

Next, a wound healing assay was performed to analyze the ability of cells to migrate. We observed a significant reduction in the migration capability of cells overexpressing TAS1R3 (**Figure 53a,b**). To examine the role of TAS1R3 expression in regulating the ability of

NSCLC cell invasion, an *in vitro* Matrigel invasion assay was performed. Results showed that the number of cells invading Matrigel was significantly higher in T1R3+ cells than in control T1R3- cells ($1.17 \pm 0,15$ vs. $1,54 \pm 0,35$ respectively, $p < 0.0001$) (Figure 53c).

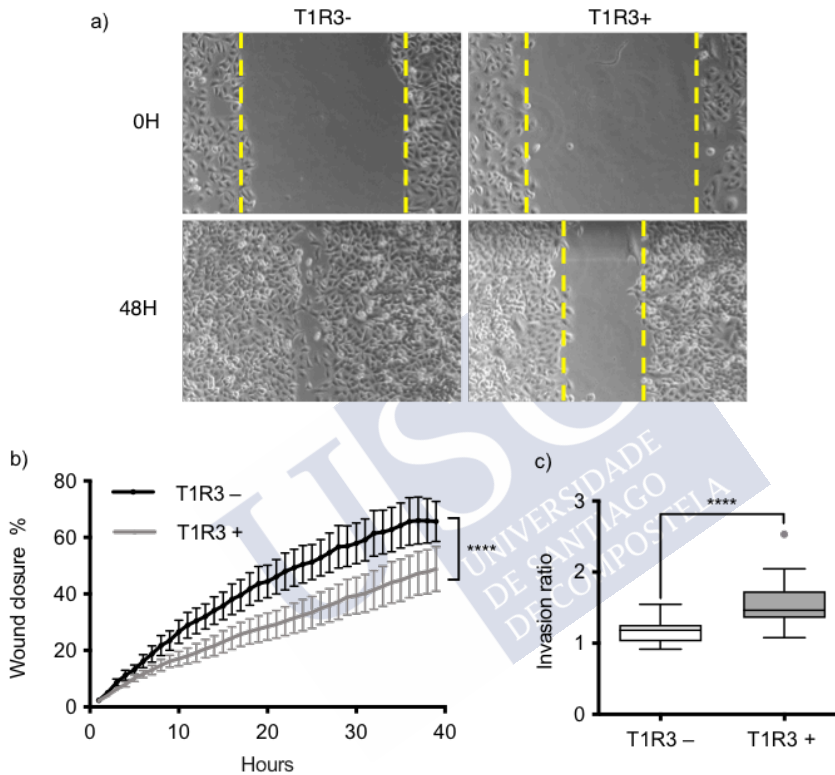


Figure 53. *In vitro* migration and invasion comparison of T1R3 +/- cells. (a) Representative images of wound healing experiment at starting point and after 48 hours. Brightfield images were taken with a 10x objective. (b) Migration rate into the wound was monitored at real time by JuLI™ Stage software. (c) Tukey box and whiskers plot shows the cell invasion analysis through Matrigel coated transwells with an FBS gradient. The line between boxes indicates the median value, while the outer boxes represent the 25th and the 75th percentiles and whiskers show the non-outlier range. Data was analyzed by two tailed t-Student tests (n.s.= not significant, **** $p < 0.0001$).

9.3.4 TAS1R3 plays a role in tumor progression and dissemination *in vivo*.

To determine whether TAS1R3 affects the capacity of cancer cells to disseminate from the primary tumor and form distal metastases in the lungs, T1R3⁺ and T1R3⁻ cells were subcutaneously injected into the flanks of CD-1 nude mice, and at the end of the experiment, the tumors, the blood and the lungs were analyzed (**Figure 54a**). Body weight and tumor volume were monitored periodically during the experiment showing no differences among the groups (**Figure 54b**). T1R3⁺ cells seemed to be significantly less tumorigenic, according to the recorded tumor growth (**Fig. 54c**).

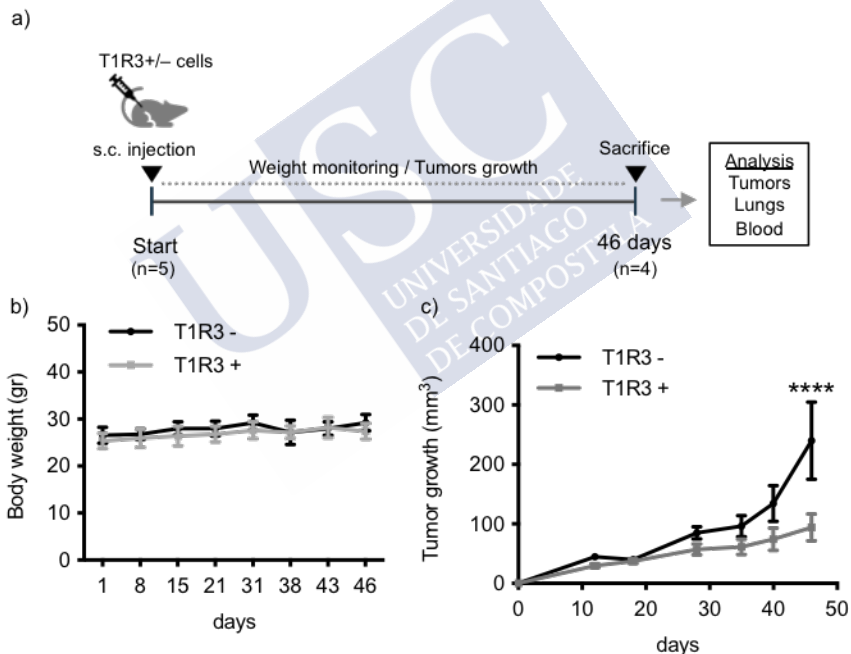


Figure 54. TAS1R3 effect in primary tumor. (a) Schematic representation of the experimental design, starting from the s.c. injection of T1R3^{+/-} cells in two groups of mice (n=5). (b) Mean body weight of mice after subcutaneous injection of T1R3^{+/-} A549 cells. Data are presented for the duration of tumor growth (46 days). Not differences were observed between groups (n=5). (c) Tumorigenicity of T1R3⁺ cells in nude mice compared to T1R3⁻ cells (n=10 tumors in each group, 2 tumors per mouse). Data was analyzed by Two-way ANOVA (****p<0,0001).

However, cells in the tumor formed from T1R3+ cells, presented a significant increase in CD133 at the end of the experiment as shown by FACS analysis, but not in TAS1R3 (**Fig. 55a**). To better understand the phenotypic changes that cells were experiencing within the tumor bulk, and correlate this with results obtained *in vitro*, we evaluated the expression of epithelial–mesenchymal transition (EMT) and stem markers (**Figure 55b**). RT-PCR results showed a modest tendency in the T1R3+ group towards a more intermediate phenotype (a slight downregulation of ECAD and upregulation of SNAI2 was observed), together with an increase in stem markers (such as SOX2, OCT4 and NANOG) that could be an indicative of a moderately progressive acquisition of enhanced aggressiveness.

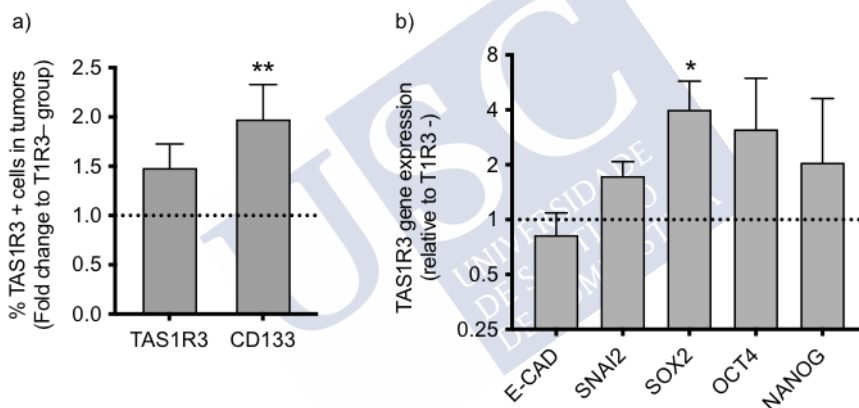


Figure 55. Characterization of primary tumors at the end of the experiment. (a) FACS analysis showing the fold change of the percentage of TAS1R3+ and CD133+ cells in the tumors of T1R3+ group relative to T1R3- group, at the end-point of the experiment. **(b)** RT-qPCR analysis of EMT and STEM genes showing the fold change of the T1R3+ group compared to T1R3-. Data is presented as mean \pm SD and analyzed by a two-tailed t-Student test ($n=4$ per group, $*p<0,05$, $**p<0,01$). Data without statistical significance were not indicated.

Blood samples were also taken from the heart of mice, pooled together and subjected to a pre-enrichment step and immunomagnetic labelling of hematopoietic murine cells and T1R3+ cells. Then, CTCs were isolated and visualized according to morphology and fluorescent labelled markers in the DEPArrayTM. The number of CTCs was

counted for T1R3+/- mice and the percentage of TAS1R3 positive CTCs was evaluated. A total of 5 CTCs/mL were found in T1R3+ group while none was detected in the T1R3- group (**Figure 56a**). Moreover, all CTCs found in the T1R3+ were actually positive for TAS1R3 staining and GFP+ signal. The H2K marker was used to differentiate human cells from murine cells (**Figure 56b**).

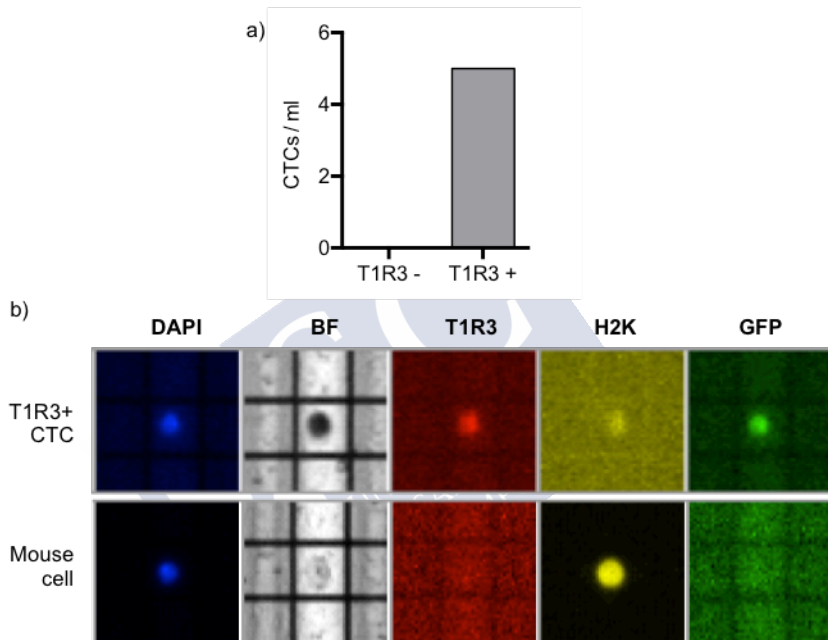


Figure 56. Analysis of CTCs from xenograft T1R3+/- mice. (a) Number of CTCs detected per mL of blood by DEPararray analysis (poll of blood from 4 mice in each group). (b) Representative DEPararray pictures showing the positivity of TAS1R3 (red signal) and GFP (green signal) from the CTCs found in the TAS1R3 + cells group. (DAPI: nuclei; BF: bright field; PE: TAS1R3; H2K: mouse marker; GFP: green fluorescent protein).

To evaluate the metastatic potential of T1R3+ cells, the presence of cancer cells in a distal site was analyzed. A significant increase in the number of DTCs was observed in the T1R3+ group, suggesting that TAS1R3 enhances the capability of the cells to disseminate and colonize murine lungs (**Figure 57a**). Next, the expression of TAS1R3

and CD133 in the DTCs that reached the lungs was analyzed by FACS analysis. In T1R3⁺ mice, the expression of TAS1R3 in DTCs was 30-fold higher, compared to the primary tumor cells ($p = 0,002$). Additionally, an increase in CD133 expression of 14-fold ($p = 0,03$) was observed (**Figure 57b**). Strikingly, the T1R3⁻ control group also reported a significant upregulation of TAS1R3 (19-fold change, $p = 0,007$) and CD133 (10-fold, $p = 0,01$) in DTCs compared to the primary tumor cells (**Figure 57c**). This result highlights the fact that TAS1R3 provides cells with additional advantages to metastasize and colonize distant organs, given the fact that, even the cells that do not express high levels of TAS1R3 *in vitro* and *in vivo* in the primary tumor, can endogenously upregulate it to successfully metastasize.

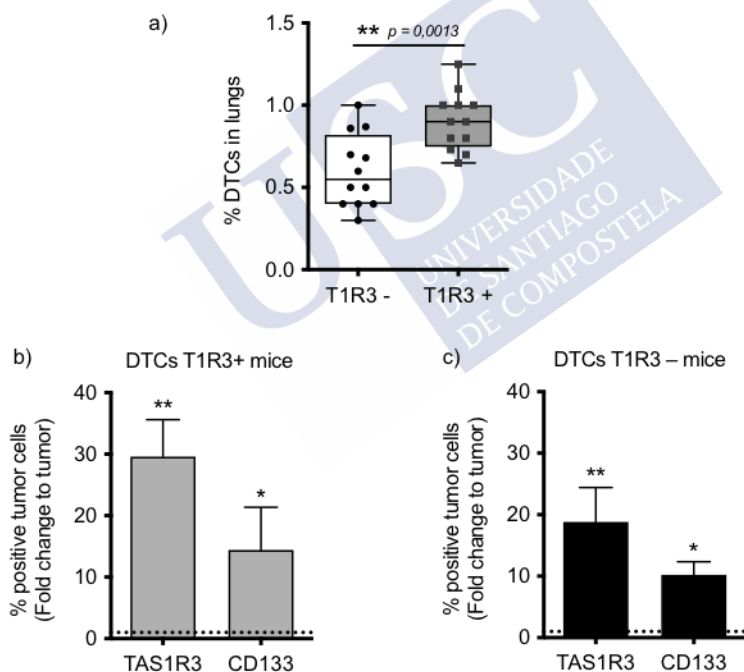


Figure 57. TAS1R3⁺ cells have enhanced metastatic potential. (a) Percentage of Disseminated Tumor Cells (DTCs) in the lungs from the primary tumor (n=4 mice per group). (b) Fold change of TAS1R3 and CD133 positive DTCs in the lungs compared to the cells in primary tumors for the T1R3⁺ group and (c) the T1R3⁻ group of mice (n=4 mice per group). Data was analyzed using a two-tailed t-Student test (* $p > 0,05$; ** $p < 0,01$; *** $p < 0,001$).

9.3.5 TAS1R3 promotes colonization of lung cancer cells

In order to further evaluate the metastatic potential of T1R3+ cells *in vivo*, an experimental metastasis assay was established using immunodeficient mice through the injection of the same number of T1R3+ or T1R3- cells in the tail vein of nude mice, in the absence of a primary tumor, so that the number of cells found in the lungs could be correlated with the metastatic ability of the injected cells. Mice were sacrificed two months later, and the extent of lung metastases and the immune infiltration were determined (Figure 58a). Body weights were monitored during the experiment, showing no differences among the two groups (Figure 58b).

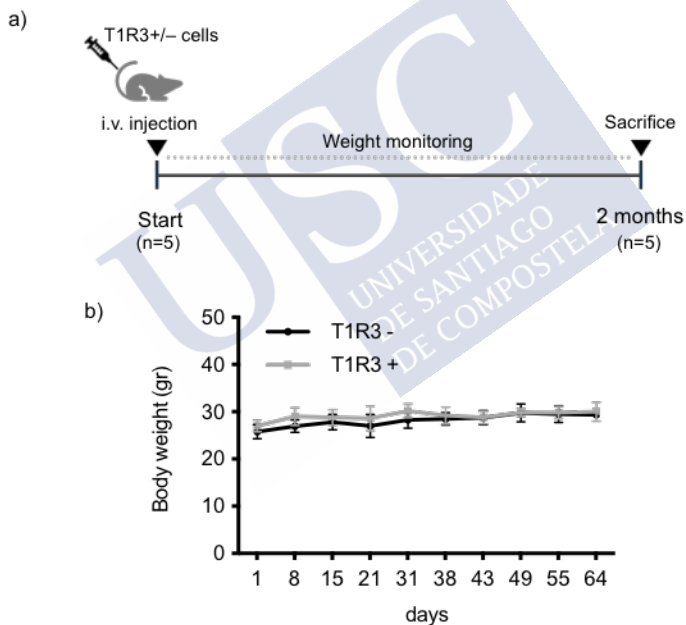


Figure 58. Experimental metastasis assay *in vivo*. (a) Schematic representation of the experiment design, starting with the intravenous injection of T1R3 +/- A549 cells in the tail vein of nude mice, followed by the sacrifice of 2 mice per group the next day and of 5 mice per group at the end of the experiment (64 days). (b) Bodyweight of mice after intravenous injection of T1R3 +/- cells and during the time of the assay. Not significant differences at any time point were observed between groups.

FACS analysis revealed a significant increase in the number of DTCs in the lungs for the TAS1R3+ group (**Figure 59a**), and notably, FACS analysis confirmed that metastatic cells from this group have a higher expression of TAS1R3 and CD133, compared to the T1R3- control group (**Figure 59b**).

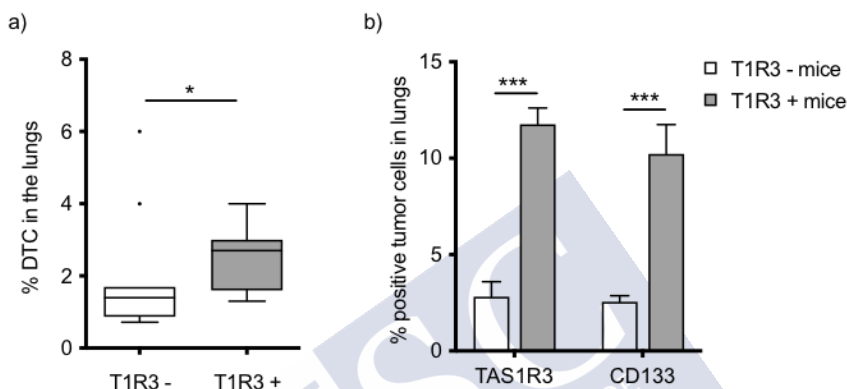


Figure 59. Dissemminated tumor cells evaluated by the experimental metastasis assay. (a) FACS analysis of DTCs found in the lungs after 1-day post i.v. administration (n=2) of T1R3 +/- cells and at the end-point (64 days, n=5). No significant differences were observed in the short-term analysis, whereas at the end-point, T1R3+ cells metastasized significantly higher than T1R3- cells. Data was analysis by non-parametric Mann-Whitney t-test considering *p-value<0,05. (b) FACS results showing the expression of T1R3 and the stem marker CD133 of the DTCs from the lungs at the end of the experiment. Data are represented as mean \pm SD and analyzed using a two-tailed t-Student test (**p<0,001).

A significant decrease in the number of neutrophils infiltrating the lungs of mice injected with TAS1R3+ cells was observed when compared to TAS1R3- cells (**Figure 60**), which might be indicative of a differential ability of TAS1R3+ cells to chemoattract neutrophils and to escape their cancer immune control that counteracts metastasis establishment.

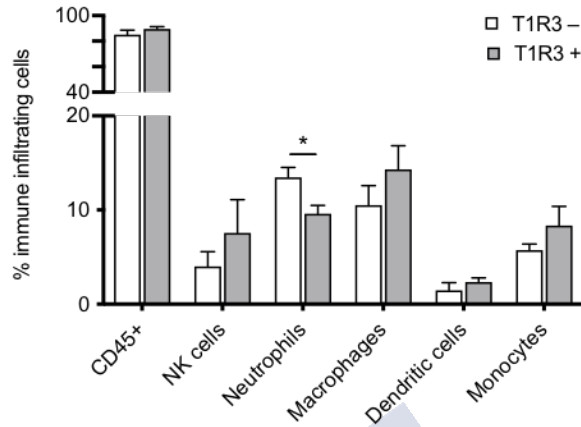


Figure 60. Immune infiltration in the lungs. Representative analysis by Flow cytometry of the different immune infiltrating populations in the lungs post iv administration of T1R3+/- cells at the end of the experiment. Data are represented as mean \pm SD and analyzed using a two-tailed t-Student test (* $p < 0,05$). Data without statistical significance were not indicated.

9.3.6 Conclusion

To conclude, these results position TAS1R3 as a potential target for the development of therapeutics aimed to interrupt metastasis progression in NSCLC. Although more in-depth studies are still needed, these results demonstrate that TAS1R3 endows cells with certain advantages to disseminate and initiate metastasis. Further understanding of the biology of this receptor may allow us to more accurately design novel therapeutic strategies to impair metastasis.





DISCUSSION



10 DISCUSSION

STRATEGY INSPIRED BY EXOSOMES

Nanotechnology has been postulated as a promising alternative to overcome delivery drawbacks associated to gene therapies and other types of labile biomolecules since the oncological therapeutic can be encapsulated into a nanocarrier that would protect it from premature degradation and thus, keep it longer in the bloodstream with a higher chance to reach the diseased tissue and cells (Roma-Rodrigues *et al.*, 2020). Nanocarriers also facilitate intracellular delivery and therefore access to intracellular targets (Sun and Duan, 2020).

More than 20 years ago, the FDA approved the first nanoparticle drug called Doxil[®] (Barenholz, 2012), a long-circulating liposome loaded with the chemotherapeutic doxorubicin and from then, some other nanotherapeutics have reached the market based mainly in PEGylated liposomes (Vázquez-Ríos *et al.*, 2018). While a number of nanocarrier-based platforms have been approved for the treatment of various diseases (including tumors), many others are in different phases of clinical trials. Nanotechnology also provides effective carriers for application in gene therapy, since non-viral vectors have become a realistic alternative to viral vectors for achieving better efficacies and safer treatments (Xu, Li and Si, 2014). Despite the plethora of gene modulation approaches, e.g., gene silencing, antisense therapy, RNA interference, gene and genome editing, given that naked nucleic acids are vulnerable to enzymatic degradation, rapid clearance, and non-specific biodistribution, only low gene expression efficiencies can be achieved. Hence, the primary challenge of gene therapy is to develop effective carriers able to protect the nucleic acids and facilitate their internalization into the targeted cells at the targeted site (Z. Zhou *et al.*, 2017). In 2018, the first RNA nanomedicine, patisiran (Onpattro[®]), was approved by the FDA for hereditary transthyretin-mediated amyloidosis and opened up new

horizons for researchers to pursue efficient delivery systems enabling the nucleic acids to be used as therapeutic agents (Adams *et al.*, 2018; Akinc *et al.*, 2019; Mohammadinejad *et al.*, 2020). Patisiran has been formulated as lipid nanoparticles of 100 nm to deliver short interfering RNA (siRNA) against factor VII (FVII) for intravenous administration (Mohammadinejad *et al.*, 2020). Moreover, a promising phase I/II study (NCT01455389) for non-viral positively charged lipid nanovesicles encapsulating a tumor suppressor gene called TUSC2, has received this January 2020 the Fast Track Designation by the FDA to treat metastatic lung cancer in combination.

However, and besides the successful cases exemplified above, the overall success of nanotechnologies translated to the clinic is still quite limited. Wilhelm *et al.* revealed one of the main problems of nanotechnology so far. They analyzed the delivery efficiency of nanoparticles in preclinical studies over the last decade and found out that the median delivery efficiency of the injected dose in the tumor is only 0.7%, regardless their size, superficial charge, shape, tumor model, cancer type, and targeting strategy (active or passive) (Wilhelm *et al.*, 2016). This study highlights the strong need for developing novel and more rational alternatives to overcome the delivery problem.

A successful delivery system would ideally be nontoxic, provide improved pharmacokinetic and biodistribution, protect the cargo from premature degradation, avoid opsonization and a rapid clearance from systemic circulation, overcome extra- and intracellular barriers, and deliver the therapeutic material to its specific target site (McErlean, McCrudden and McCarthy, 2016). The question is to determine if such delivery systems can indeed be engineered.

Nature offers a wide range of sources of inspiration to synthesize novel delivery systems. Looking at the tumor biology, it can be observed that in fact, in our organism, it already exists a nanosystem that meets all the mentioned characteristics, called exosomes. Nearly 40 years ago, membrane-derived natural nanovesicles (30-100 nm), secreted by most cell types, were discovered and termed as exosomes (Harding and Stahl, 1983; Harding, Heuser and Stahl, 2013). At first,

they were thought to be “garbage bags” of the cells, useful to get rid of the unnecessary material; however, we know now that exosomes are extremely efficient in cell-to-cell communication, carrying selectively nucleic acids, lipids, proteins, and other components. They are also able to successfully overcome all the biological barriers, such as the blood-brain barrier, and to maintain its integrity in each fluid type (e.g., breast milk, urine, blood, vitreous) (Wang, 2017; Diaz *et al.*, 2018; Z. Liu *et al.*, 2018; Zhao *et al.*, 2018). For all this, exosomes have been postulated as the ideal delivery system, and great efforts have been made worldwide to explore their potential as vectors in different applications over the last years (Alvarez-Erviti *et al.*, 2011; El-Andaloussi *et al.*, 2012; Hall *et al.*, 2016; Das *et al.*, 2019). As a matter of fact, in the last decade, there have been numerous research works exploring the potential of exosomes in drug delivery. **Figure 61** shows the increasing number of publications published per year, in PubMed, containing the term “exosomes” and “drug delivery”.

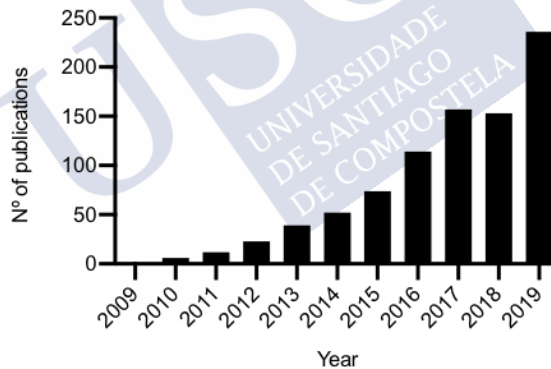


Figure 61. The number of publications per year containing the term “exosomes” and “drug delivery” in PubMed. Accessed on 27th August 2020.

Some of the strategies investigated for the use of exosomes as drug delivery systems have already been extensively reviewed (Li *et al.*, 2018; Patil, Sawant and Kunda, 2020; Peng *et al.*, 2020), and include naive exosomes with their endogenous content, exosomes secreted by cells prior modifications (e.g., cell transfection, drug loading), and exosomes loaded directly afterwards with an exogenous cargo (by electroporation, sonication, or lipofection). Although some

encouraging results were obtained *in vivo*, there are still some concerns with this novel approach of exosomes as delivery vehicles. They are mainly related to the low yield of production, the cumbersome and time-consuming isolation protocols that are not standardized and validated, the low purity levels (due to potential contamination with non-exosomal materials), the high production costs, and their limited loading capacity. Importantly, safety concerns also arise regarding their use in humans since endogenous and potentially dangerous material is typically delivered together with the therapeutic cargo. Indeed, exosomes are known to play a crucial role in several pathological processes, such as neurodegeneration, tumor metastasis, and infections, while their mechanisms of targeting, uptake, and action, remain poorly understood (Jan *et al.*, 2019; Li *et al.*, 2019; Liu and Wang, 2019; Adem, Vieira and Melo, 2020).

Researchers have tried to overcome some of these challenges by pursuing different strategies, as for example, by generating nanovesicles by serial cell extrusion of different cell types, or by coating of polymeric nanoparticles with cell membranes, rendering what they called exosome-mimics or synthetic exosomes, as they resemble exosomes in some way (Jang *et al.*, 2013; Molinaro *et al.*, 2016; Sato *et al.*, 2016; Parodi *et al.*, 2017; Li *et al.*, 2019; Van Deun *et al.*, 2020). Additionally, different bioinspired nanosystems have been proposed to date, mimicking other biological entities such as platelets, leukocytes, or red and white blood cells (Ben-Akiva *et al.*, 2020; Molinaro *et al.*, 2020). Although these methods have shown favorable results in preclinical testing, they face problems of reproducibility, their composition is not fully-characterized, and most of them require sophisticated and high-energy methodologies (e.g., extrusion, sonication, homogenizers), hampering its translation into clinics.

In an attempt to overcome technical limitations and regulatory issues related to the clinical use of exosomes in cancer drug delivery, and to engineer a multifunctional nanoplatform for the delivery of anticancer therapies, we have pursued a rational design of exosome-mimetic nanoplatforms (EMNs), based on the well-known liposome technology. Liposomes are one of the most widely studied types of

nanosystems in drug delivery and the most used in clinics. For comparative purposes, natural exosomes were successfully isolated and characterized from cancer cell lines and plasma.

Given the determinant role of lipids for the structural and biological functions of exosomes (Skotland *et al.*, 2020), we have carefully selected and optimized the lipid composition of our nanoplatform. For this, published information related to lipidomic analysis of exosomes has been considered (Llorente *et al.*, 2013; Record *et al.*, 2014; Lydic *et al.*, 2015). The lipid composition of parent cells and exosomes vary considerably, being the exosome membranes enriched in certain species, e.g. SM and CH (Llorente *et al.*, 2013). Sphingolipids, and especially the main sphingolipid SM, are certainly important for the structure of exosomes (Skotland *et al.*, 2020). Cholesterol plays a fundamental role in increasing the cohesiveness of the bilayer, reducing leakage, and also creating cholesterol-enriched regions called lipid rafts, which also congregate a lot of specific proteins (de Oliveira Andrade, 2016; Yang *et al.*, 2016). Little amounts of specialized lipids such as ceramides may have crucial functions, such as the formation and release of exosomes. In the last years, the interest in the research community regarding the lipid composition of exosomes and their function is increasing, however, the general knowledge at the moment is quite limited (Skotland, Sandvig and Llorente, 2017; Skotland *et al.*, 2020).

In this work, we have developed a nanoplatform which lipid composition can be easily tailored maintaining optimal physicochemical properties. This indicates that these nanoplatform might also allow the incorporation of additional species that could be described in future for having relevant roles in trafficking, cell communication, or cell-to-cell interaction processes, accompanying advances in the lipidomic field (Record *et al.*, 2014; Skotland, Sandvig and Llorente, 2017). They can also be tailored based on the superficial charge preferences, being possible to obtain anionic-, neutral-, or cationic-EMNs. By using the ethanol injection methodology, we were able to produce small nanoplatforms in few minutes, without needing additional steps for adapting the size and lamellarity (e.g. extrusion or sonication) and keeping the amount of

ethanol in the formulation below 10%, meaning that it does not need to be removed prior to *in vivo* administration (Sermons, Verbruggen and Bormans, 2008). This preparation method resulted in a substantially increased production yield and reduced preparation time with respect to isolated tumor-derived exosomes. After several optimization steps, the selected formulation was composed by the following combination of lipids, PC:CH:SM:Cer, with a constant ratio of 0,9:1:0,4:0,03 (w/w). Importantly, this composition rendered liposomes that mimic the most important physicochemical features of natural exosomes, related to lipid composition, size, surface charge and morphology. The effective incorporation of each component in the formulation was confirmed by NMR analysis, as reported for other liposomal formulations given that NMR is a useful tool for the quantitative and absolute quantification of lipids (Hein, Uzundal and Hennig, 2016; Khoury *et al.*, 2018). Noteworthy, we were able to get all these properties in our EMNs without using any unusual, artificial, or sterically stabilized lipids (e.g., GM1), and avoiding extreme conditions (e.g., pH changes or high temperatures). The selected production method is fast, simple, mild, reproducible, and easily scalable for its use in preclinical or clinical settings, features that would facilitate their use for a variety of disorders and increase the probability of translation.

Moreover, the developed nanoplatform showed a higher internalization efficiency and a versatile payload capacity of molecules with different nature and rendering similar encapsulation efficiencies than natural exosomes.

Compared to the liposome field, EMNs engineered from a purely biological approach and simplified methodologies, can offer a series of advantages. Despite the extensive research in the last 50 years, and their overall success, the clinical translation of liposomes has not progressed as quickly as the impressive preclinical results would have suggested (Moro *et al.*, 2019). The major reasons for their bottleneck have been attributed to issues surrounding the pharmaceutical manufacturing and government regulations (Sercombe *et al.*, 2015). Limitations in pharmaceutical development are related to manufacturing processes (scalability, reproducibility, reliability, and

chemical instability), and costs. As an example, a recent paper published in the *Journal of Controlled Release* shows amazing results in reducing the tumor growth of lung cancer PDXs using coated cationic liposomes entrapping miR-660 (Moro *et al.*, 2019). However, looking carefully to the preparation methodology, organic solvents (chloroform and methanol) were used to resuspend the components and the miRNA, and different steps such as centrifugation, rotary evaporation, sonication, and sequential extrusion through 400, 200, and 100 nm polycarbonate filters were needed in order to obtain nanometric liposomes (Di Paolo *et al.*, 2011; Moro *et al.*, 2019). On the contrary, we have optimized our preparation method to obtain nanometric EMNs with a single step without the need of organic solvents, heat or high energy input, decreasing the environmental impact and making it easier to scale up and translate. Another advantage is that EMNs are composed of natural lipids already approved for human use and parenteral administration, rather than synthetic components or cationic surfactants, reducing the associated toxicity and providing great biocompatibility and biodegradability.

Exosomes are also known to express several proteins on their membrane, such proteins can actively participate in exosome adhesion, binding, and fusion with recipient cells, and in the last years, it has been demonstrated that some of them are also involved in organotropic mechanisms (Peinado *et al.*, 2017; Steinbichler *et al.*, 2017; Guo *et al.*, 2019; Nie *et al.*, 2020). Hoshino *et al.* have reported that exosomal integrins are responsible for preparing the premetastatic niche and can determine the organ specificity of the metastasis. Particularly, exosomes from breast cancer cells, expressing integrin $\alpha 6\beta 4$, move to the lung, and prepare the niche for homing metastatic cells in orthotopic nude mouse models (Hoshino *et al.*, 2015). Interestingly, Nie *et al.* have recently proven the organotropic feature given by overexpressed integrin $\beta 4$ on the exosome surface to selectively deliver miRNAs to the lungs, generating a potent anti-metastasis effect for breast cancer *in vivo* (Nie *et al.*, 2020). These results suggest that functionalizing nanosystems with exposed key proteins onto their surface could efficiently determine the fate of the delivery system and provide, therefore, a springboard for a novel class

of bioinspired targeted nanocarriers. In our hands, we have proven the association of diverse proteins, with different molecular weights and isoelectric points, to the developed nanosystems. Importantly, the membrane protein integrin $\alpha 6\beta 4$, was successfully associated to EMNs, and it was proved that its presence improves their adhesion properties and ability to deliver the associated therapeutics to cancer cells. Similarly, other nanosystems have been successfully functionalized with proteins rendering enhanced permeability and cellular uptake (Cox *et al.*, 2019).

As we mentioned before, natural exosomes have a natural ability to transport functional biomolecules, including oligonucleotides (miRNA, mRNA, DNA), which are delivered to recipient cells producing functional changes (Jan *et al.*, 2019). Therefore, their use for exogenous delivery of oligonucleotides, i.e. for gene therapy, can be envisioned. This has already been reported with different types of therapeutic RNAs and DNAs showing promising results *in vitro* and *in vivo* for different applications (Alvarez-Erviti *et al.*, 2011; El-Andaloussi *et al.*, 2012; Shtam *et al.*, 2013; Lamichhane, Raiker and Jay, 2015; Naseri *et al.*, 2018; O'Brien *et al.*, 2020). Here, we demonstrate that EMNs can also associate miRNAs with comparable efficiency to exosomes loaded by electroporation following well-established protocols (El-Andaloussi *et al.*, 2012; Tian *et al.*, 2014), besides they are neutrally charged. Typically, nanocarriers for gene delivery incorporate cationic compounds bearing intrinsic toxicity (Lv *et al.*, 2006), but neutral ones have been claimed as a much safer alternative avoiding off-target effects (Ozpolat, Sood and Lopez-Berestein, 2014). MiRNA-145 (miR145) is a potent tumor-suppressor downregulated in lung cancer and known to inhibit right open reading frame kinase 2 (RIOK2) and NIN1 binding protein (NOB1) (K. Liu *et al.*, 2018). Transfection studies show that EMNs decorated with integrins, i.e. F-EMNs, can mediate an increase in the intracellular levels of miR145 of over 800-fold higher than the free miR145, and 5-fold higher than the control formulation (EMNs). However, it is known in the nanotechnology field that the endosomal entrapment is the predominant barrier that limits functional delivery of macromolecular biologic therapeutics intracellularly (Lönn *et al.*,

2016). In an attempt to evaluate whether EMNs were trapped in the endolysosomal degradation pathway, a lysosomotropic agent that induces lysosomal membrane perturbation, chloroquine, was added to the cells previously treated with miR145 loaded in F-EMNs. Colony formation assay results showed that no significant differences were observed when chloroquine was added compared to the control, supporting the idea that EMNs are efficiently escaping from the endolysosomal system. Additionally, the increased expression of miR145 in the transfected cells led to relevant changes in the cancer cell phenotype, such as, a significant reduction of the clonogenic capacity of the transfected cells and the downregulation of the protein N-cadherin. N-cadherin has been reported as a target of miRNA-145 in lung adenocarcinoma (Mo *et al.*, 2017). This protein promotes tumor cell survival, migration and invasion, and high expression levels is frequently associated with poor prognosis (Cao, Wang and Leng, 2019). Together these results suggest that EMNs can be functionalized with bioactive targeting molecules and are capable of effectively transport functionally active therapeutic RNAs into tumor cells. Therefore, the nanoplatform presented here, holds great potential for the development of non-viral nanoscale delivery platforms in the cancer field, however, the high versatility of this approach suggests that EMNs might be an efficient delivery vehicle for the treatment of a broad range of disorders with low therapeutic alternatives.

In vivo experiments carried out in a lung cancer mice model allowed us confirming that F-EMNs show a similar capacity to transport their therapeutic cargo (miR145) to the target as compared to tumor-derived exosomes. Importantly, F-EMNs do not apparently provide cardiotoxicity (on view of the low accumulation shown in this organ), and a lower accumulation by the liver and kidney than their natural counterparts.

Taking together all the results, EMNs show great similarities to natural exosomes with respect to their physicochemical properties, drug loading capacity, low toxicity, and ability to interact with the cancer target cells and deliver their cargo *in vitro* and *in vivo*, while EMNs can overcome important limitations of exosome: (i) a single

batch of EMNs (2'2 ml), can be produced in 10 min, offering a time-saving efficiency of at least 5 days for each production run; this production process is also faster than other current alternatives to exosomes, such as cell-derived nanovesicles by serial extrusion, which also requires time for cell growing and production (Goh *et al.*, 2017), (ii) the production yield, measured by the number of particles obtained, is 1000-fold higher for EMNs than for exosomes, (iii) EMNs also provide great opportunities for tracking them by adding different fluorophores (EMNs were efficiently labeled with TopFluor-SM, Cy5 and DiR), (iv) EMNs can be functionalized with membrane proteins to selectively interact with cells and tissues, (v) lipids are cheap and well-characterized materials, and finally and very importantly from a translational perspective, (vi) industrial production processes under GMP conditions are already well established for liposomes (Bulbake *et al.*, 2017).

EMNs provide additional opportunities of being further amenable to surface functionalization, lipid composition, as well as loading of therapeutic cargo for a broader application in other fields. From our perspective, rather than just for competitive purposes, our nanoplatform could also serve as a tool for a deeper understanding of the still not answer questions of exosomes, allowing the study of the role of specific lipid species in protein-lipid and lipid-lipid interactions with the targeted tumor cells, and also the study of the organotropic effect of different proteins separately. This would allow us to select a combination of proteins of interest in a unique nanometric delivery system. This application would benefit both fields for reaching sooner a novel clinically relevant drug delivery system. Moreover, considering that liposomes are typically used as controls for preclinical evaluation of exosomes as drug delivery carriers, rational-designed EMNs can also have an application in this regard. Indeed, a recent review by Johnsen *et al.*, highlights the crucial need for an adequate choice of liposomal controls in preclinical exosome-based drug delivery studies before postulate any potential superiority of exosomes over their liposomal counterparts (Johnsen *et al.*, 2018). Authors often choose over-simplified liposomes for their comparisons and rarely would choose a clinically

relevant liposomal formulation. Gold standard liposome controls are urgently needed for a much fairer comparison.

Overall, EMNs provide a multifunctional nanoplatform with multiple opportunities for different purposes and indications, in a safe, efficient and cost-effective alternative to exosomes.

DISCOVERY OF A NEW TARGET FOR NSCLC

Metastases are still the major cause of morbidity and mortality in cancer patients with solid tumors, but little is known about specific determinants of successful dissemination from primary tumors and metastasis initiation. Identifying new key players related to this multistage process could open new therapeutic avenues for the treatment of NSCLC patients. Moreover, novel biomarkers are urgently needed to effectively select the most appropriate treatment for each cancer patient and to increase the targeted therapeutics arsenal.

Liquid biopsy stands out for its determining role to obtain valuable information amenable to repeated and real-time noninvasive assessment, while avoiding some key limitations of conventional tissue biopsies such as limited availability of samples, invasive tumor sampling, under-representation of tumor heterogeneity, and poor description of clonal evolution (Finotti *et al.*, 2018). Liquid biopsy is one of the more promising contenders for biomarker discovery, which now includes circulating tumor DNA (ctDNA), cell-free RNA (cfRNA), CTCs, exosomes, and proteins that can be isolated from different body fluids to reveal the molecular landscape of the tumor (Z. Wu *et al.*, 2019). CTCs are originated by shedding from solid tumors, followed by intravasation into the circulation system, and dissemination to distal organs for nesting and metastasis formation (Gribko *et al.*, 2019).

Applications of the study and analysis of CTCs are that they allow the molecular analysis of the intra-tumor heterogeneity, provide valuable information for the diagnosis, prognosis, response to specific treatment regimens or acquired resistance, molecular characterization for treatment decisions, and the possibility to discover novel therapeutic targets (Calabuig-Fariñas *et al.*, 2016; Habli *et al.*, 2020).

Compared to ctDNA, cfRNA, or exosomes, CTCs have the advantage of being the ultimately responsible entities of metastasis formation, therefore, they hold invaluable information not only about the molecular and genetic features of tumors but also about the intrinsic biology of the tumors and their dominant clones (Kidess-Sigal *et al.*, 2016). Main disadvantages refer to the extreme rarity and heterogeneity of CTCs, the disparity of techniques used for CTC isolation, the limited amount of available sample for analysis, and the need of analytic methods with very high sensitivity and specificity to avoid false positives and false negative errors (Calabuig-Fariñas *et al.*, 2016; Saxena, Subbalakshmi and Jolly, 2019; Habli *et al.*, 2020; Zavridou *et al.*, 2020).

Analysis of CTCs has been widely claimed as prognostic and predictive tools for clinical outcome in cancer patients (Amantini *et al.*, 2019), and as a tool to uncover key drivers of metastatic spread (Lianidou, 2014; Mwesige, Yeo and Yoo, 2019). Most of the reports to date refer to enumeration of CTCs, optimization and validation of different isolation techniques, or to the identification of known actionable mutations in CTCs (e.g. EGFR T790M or ALK-, ROS-, RET- rearrangements) to guide treatment decisions (Tan *et al.*, 2016; Yanagita *et al.*, 2016; Catelain *et al.*, 2017; Mwesige, Yeo and Yoo, 2019; Habli *et al.*, 2020). However, to our knowledge, very few reports have been addressed to the evaluation of gene expression profiles of CTCs for the discovery of novel biomarkers. One of them is the work by Mariscal *et al.* who have identified Notch1 as a principal regulator in metastasis dissemination and as a potential therapeutic target to impair metastasis dissemination, from peripheral blood of NSCLC patients following a gene expression analysis of EpCAM-positive CTCs. In addition, Notch1 demonstrated high prognostic value for PFS (Mariscal *et al.*, 2016). More recently, Dimitrov-Markov *et al.* isolated CTCs from metastatic pancreatic ductal adenocarcinoma PDXs (n=7) and by single-cell RNA sequencing identified survivin (BIRC5) upregulated in CTCs as compared to primary tumor. Pharmacological inhibition of survivin *in vivo* resulted in reduced metastatic development and improved survival (Dimitrov-Markov *et al.*, 2020). Another recent work by

Franses et al. refers to RNA-sequencing of CTCs purified from the blood of patients with treatment-naïve pancreatic cancer. CTCs were isolated by negative selection using a leucocyte depletion microfluidic CTC-iChip. LIN28B was identified as a metastasis driver and a druggable target. CRISPR mediated LIN28B knockout revealed a functional decrease in invasive and metastatic features *in vitro* and *in vivo*, and a small molecule proved that LIN28B can be therapeutically targeted (Franses *et al.*, 2020). These works exemplify the huge potential of translating CTC expression signatures to the identification of novel biomarkers for metastasis and to select specific patients that may benefit from novel targeted therapeutics.

In this work, CTCs from the peripheral blood of advanced NSCLC patients have been isolated by EpCAM-based immunoisolation. CTCs were then molecularly analyzed by gene expression microarray in order to identify the genes characterizing the CTC population of metastatic NSCLC patients. Statistical and bioinformatic analysis of the resulting genes led us to the identification of a set of genes mainly related to lipid metabolism, cell-to-cell signaling, cell death, and molecular transport. Then, genes involved in (i) adhesion, cellular movement, and migration, and (ii) located on the cell surface were selected for further validation by RT-qPCR, since they are potential characteristics of a metastatic therapeutic target. Being located in the cell membrane offers a great advantage for the development of targeted therapeutics (e.g. monoclonal antibodies), avoiding the challenge of intracellular delivery. Among the potential biomarkers that were identified, Taste receptor type 1 member 3 (TAS1R3) resulted of high interest, considering that there was no previous knowledge related to its role in cancer and metastasis formation. Indeed, this study reveals, for the first time, the expression of TAS1R3 in NSCLC CTCs.

TAS1R3 is a G-protein couple receptor (GPCR) related to taste-sensing and cell metabolism, mainly expressed in salivary glands (Treesukosol, Smith and Spector, 2011). The encoded protein can form, in combination with either TAS1R1 or TAS1R2, heterodimeric taste receptors that will recognize umami or sweet taste stimuli, respectively, being TAS1R3 the only one in the TAS1R family that

can form homodimers (Li *et al.*, 2002; Assadi-Porter, Maillet, *et al.*, 2010; Dalesio *et al.*, 2018) (**Figure 62**). Each TAS1R subunit contains a large extracellular domain called the Venus FlyTrap Module (VFTM, ~550 aa), linked via a Cysteine-Rich Domain (CRD, ~60 aa) to a seven-Transmembrane Domain (TMD, ~260 aa). Different molecules can bind to the VFTM domain, such as sugars (e.g., glucose, fructose, sucrose) or amino acids (e.g., glycine, alanine, threonine). Human-specific sweet proteins, such as brazzein, thaumatin and monellin, interact with surfaces that include the CRD region of TAS1R3 (Jiang *et al.*, 2004). The TMD of T1R3 has been shown to have overlapping binding sites for artificial sweeteners such as cyclamate (activating) and lactisole (inactivating), located within the intrahelical space of the TM barrel near its extracellular side (Assadi-Porter *et al.*, 2008; Assadi-Porter, Tonelli, *et al.*, 2010; Kojima *et al.*, 2014).

To date, the role of TAS1R3 in cancer has not been disclosed, and it is not clear whether TAS1R3 is present in cancer cells forming hetero- or homo-dimers. The heterodimer T1R2/T1R3 has been described in type II taste cells in the taste buds, but also in the extragustatory system, including the gastrointestinal tract, pancreatic β -cells, and glucose-responsive neurons in the brain (Kojima and Nakagawa, 2011), and is activated with various sweet compounds such as sugars, artificial sweeteners, sweet amino acids, sweet proteins and stevioside (Masubuchi *et al.*, 2017). The heterodimer T1R1/T1R3 responds to the umami taste, and is reported to be expressed apart from the taste buds, in the pancreatic β -cells, in the duodenal cells, and in the liver, and it is activated mainly by amino acids (Toyono *et al.*, 2007; Wauson, Zaganjor and Cobb, 2013; Wauson *et al.*, 2015). The homodimer T1R3/T1R3 has only been reported in preadipocytes as well as in primary adipose tissue, and in pancreatic beta cells (Kojima *et al.*, 2014; Masubuchi *et al.*, 2017). Most of the research work found in the literature regarding TAS1R3 are related to perception and intake of sweet substances, responsiveness to sweeteners, meals and diet, diabetes, or obesity (Treesukosol, Smith and Spector, 2011; Glendinning *et al.*, 2012; Kojima *et al.*, 2014; Robino *et al.*, 2019). Therefore, many of the

functions of this receptor are still unknown, and this also refers to its role in cancer. TAS1R3 has been related to the activation of different metabolic pathways, the PI3K-AKT-mTOR pathway, the secretion of insulin, the regulation of autophagy, and intestinal immunity, which could definitely have implications in cancer (Dotson *et al.*, 2008; Wauson, Zaganjor and Cobb, 2013; Zhou *et al.*, 2018; Howitt *et al.*, 2020). These studies have shown that cells use TAS1R3 to manipulate nutrients uptake, reducing or increasing its expression to produce the energy and macromolecules necessary to continue growing and proliferating. Interestingly, Fleischmann *et al.* found in 2014 that after MLL-AF9 gene knockdown in infant acute myeloid leukemia THP1 cells, TAS1R3 was identified as an indirect target downstream of MLL-AF9 and as a potential therapeutic target of leukemia (Fleischmann *et al.*, 2014). However, its role in leukemia was not investigated.

This work was built upon the evidence that TAS1R3 is statistically differentially expressed in CTCs from a cohort of advanced NSCLC patients (stage IIIb-IV, n=41). This higher expression was maintained during different cycles (second and fifth cycle were analyzed) of chemotherapy with cisplatin. This result may suggest that TAS1R3 is not involved in cisplatin response. With respect to the application of TAS1R3 as a prognostic biomarker of advanced NSCLC, providing information about the patients' overall cancer outcome (OS) and/or progression-free survival (PFS) regardless of therapy, analysis of data from this cohort (univariate Cox regression and Kaplan-Meier analysis of TAS1R3 highly expressing CTCs vs. low expressing CTC, 50th, 25th, and 75th percentile), showed no differences in OS and PFS. Nevertheless, this may not be a concluding result given the fact that the CTCs used for the analysis were isolated based on EpCAM positive expression (EpCAM-based CELLection™ Epithelial Enrich Dynabeads kit). Isolation methodologies can have serious implications in cases where CTCs are characterized by a phenotypic plasticity that mainly reflects an epithelial to mesenchymal transition state (EMT) (Alix-Panabières, Mader and Pantel, 2017). EMT describes a transformation from well-differentiated epithelial cells into a more mesenchymal-like

phenotype, alongside the acquisition of chemoresistance, immune escape and stemness properties, which provides cancer cells with higher capabilities to disseminate and metastasize (Santamaría, Moreno-Bueno and Cano, 2019). EMT results in down-regulation of epithelial markers like EpCAM and simultaneous up-regulation of mesenchymal markers (Kyung-A Hyun *et al.*, 2016). Indeed, it is now largely accepted that EMT is no longer a binary phenotype as it was considered. Recent studies have demonstrated that a hybrid epithelial/mesenchymal (E/M) phenotype is endowed with the highest plasticity, higher tumor-initiation and metastatic potential as compared to canonical mesenchymal or epithelial cells (Andriani *et al.*, 2016; Jolly *et al.*, 2019; Saxena, Subbalakshmi and Jolly, 2019). The prevalence of hybrid E/M CTCs has been already reported in aggressive tumors such as advanced prostate, breast, and NSCLC cancer (Armstrong *et al.*, 2011; Lecharpentier *et al.*, 2011). For a more accurate evaluation of the prognostic value of TAS1R3, CTCs should be isolated avoiding the bias introduced by marker selection, such as based on physical properties or negative CTC enrichment, instead of immunoaffinity. Microfluidics, microfiltration, dielectrophoresis or density gradient are among the isolation techniques based on physical properties. The most extended technologies based on physical characteristics are the DEPArray™ System and the Parsortix Cell Separation System. However, the CellSearch® system, based on a positive selection targeting EpCAM-positive cells, is still the only approach approved by the FDA for CTC detection and enumeration so far (Zavridou *et al.*, 2020). Zavridou *et al.* have recently compared the performance of a label-independent size-based microfluidic device versus an EpCAM-based CTC enrichment system using identical blood draws from 50 Head Neck Squamous Cell Carcinoma (HNSCC) patients, followed by downstream molecular characterization (Zavridou *et al.*, 2020). Results showed a much higher number of positive events and higher purity of CTCs by the size dependent isolation (Zavridou *et al.*, 2020). For future experiments, a different isolation technique will be used to elucidate the real value of TAS1R3 as a biomarker for metastatic NSCLC patients.

For a better understanding of the role of TAS1R3 in cancer progression and metastasis, 10 patient-derived xenograft (PDX) models were established in nude mice from primary lung cancer from advanced NSCLC patients. on paraffinPDX models have emerged as a powerful tool for understanding tumor characteristics since they closely resemble the original features of patient tumors (Moro *et al.*, 2017). PDX models have also been useful for identifying and validating potential biomarkers (Bertotti *et al.*, 2011; Huang *et al.*, 2017; Chen *et al.*, 2018; Inoue *et al.*, 2019). PDXs were subjected to IHC analysis for TAS1R3 expression-embedded tumor sections. Pictures showed a non-homogeneous positive signal for TAS1R3 that is more evident in some single cells or small clusters and within areas of pseudoglandular organization. This pattern of expression, evidenced as membranous staining or membranous and cytoplasm staining, resembles the CD133 staining published in previous works by Bertolini *et al.* (Bertolini *et al.*, 2009, 2015). The fact that CD133+ cells, isolated from primary lung tumors, showed higher tumorigenic and metastatic potential with stem-like properties (Bertolini *et al.*, 2009), led us to investigate the correlation of TAS1R3 with cancer stemness as discussed in section 8.3.

The analysis of the expression levels of TAS1R3 in the Champions TumorGraft® database from Champions Oncology, a leading global oncology pharmacology CRO, allowed us calculating the prevalence of TAS1R3 positive tumors in 141 PDXs from NSCLC. 17% of NSCLC PDXs presented high levels of TAS1R3 expression (>2-fold expression, $\text{Log}_2(\text{RPKM}+1) > 0,7$). This percentage is encouraging considering the prevalence of the biomarkers currently used in clinics for targeted therapies in advanced NSCLC (5% *ALK*, 1-2% *ROS1*, 2-4% *BRAF*), as reviewed in section 4.3.1 TAS1R3 showed no association with any particular mutation.

Moreover, the analysis indicated other clinical parameters of NSCLC patients with high levels of TAS1R3, which can be of relevance for the future development of targeted therapeutics, such as a more prevalent adenocarcinoma histology and undifferentiated tumor grade. Importantly, tumor grade is the description of a tumor that considers how abnormal the tumor cells are and the overall

appearance of the tumor tissue under a microscope, and it is a good indicator of how quickly a tumor is likely to grow and spread. If the cells and tissue are organized and similar to normal cells, the tumor is called “well-differentiated”. On the contrary, if the cells have abnormal-looking cells, lacking normal tissue structures, it is called “undifferentiated” (Tumor Grade Fact Sheet – National Cancer Institute, accessed on 29th July 2020). The less differentiated a tumor is, the worse the prognosis (Yasukawa *et al.*, 2018).

In addition, 75% of the TAS1R3 positive tumor samples account for local or distant metastatic sites (mainly lymph nodes, liver, and brain. The predominant stage is stage IV, accounting for 57% of the cases. All this clinical data nicely correlates TAS1R3 with advanced disease and a metastasis setting, and suggests that TAS1R3 could be an interesting target for the development of innovative treatments for advanced NSCLC.

Although it is not the focus of this work, centered on NSCLC, TAS1R3 was further evaluated across the entire TumorGraft[®] Database for different tumor types. Interestingly, the prevalence of TAS1R3 is even higher in tumor types such as head and neck (19%), pancreatic (21%), and colorectal (25%) cancer. A stronger correlation with stage IV patients (78%) was confirmed, mainly in distal metastasis (52,4%) of poorly-differentiated cells (52,4%). These promising results obtained with the PDX database should be validated in paired primary and metastatic tumor samples of patients for the assessment of the real clinical relevance, however, they already provide important evidence that TAS1R3 could be a determinant player in the progression and development of metastasis across different cancer indications. The development of therapies specifically designed to target TAS1R3 could represent a breakthrough in metastatic cancer management.

A better understanding of the biology and pathways related to this novel receptor will provide valuable information for the rational design of new therapeutic strategies. In this regard, we also evaluated the expression of TAS1R1 and TAS1R2 in the PDX database. TAS1R2 was not identified in any tumor type, whereas TAS1R1 was present in 7% of all PDXs and 8% of the NSCLC PDXs. Furthermore,

TAS1R1 only correlated with TASR3 in 14 out of 115 PDXs. This evidence suggests that TAS1R3 is more likely to be found in cancer cells forming homodimers T1R3/T1R3 rather than T1R1/T1R3 or T1R2/T1R3 combinations. To date, homodimers of TAS1R3 are only described in pancreatic beta cells and adipocytes, where it plays a role in adipogenesis and glucose metabolism (Kojima *et al.*, 2014; Nakagawa *et al.*, 2014; Masubuchi *et al.*, 2017). TAS1R3 positive cells may have certain ability to modify their metabolism when needed in order to successfully metastasize, however, further experiment should confirm this hypothesis.

ROLE OF TAS1R3 IN NSCLC

It is generally accepted that the development of metastatic cancer implies cancer cells from the primary tumor to alter several distinct features in order to succeed in this very complex process. Some of these modifications are i) a change from epithelial to a more mesenchymal phenotype, ii) the acquisition of stem-cell properties and phenotypic plasticity, and iii) a change in their metabolism in a way that promotes survival and metastatic outgrowth (Tinhofer *et al.*, 2014; Mason *et al.*, 2017; De Francesco, Sotgia and Lisanti, 2018; Santamaria, Moreno-Bueno and Cano, 2019). Conventional anticancer treatments mainly target the bulk tumor, and most often fail to eliminate the highly tumorigenic and chemo-resistant cell subpopulations. CSCs are described to be the prime sources of tumor recurrence and metastasis that should be specifically targeted, but unfortunately, there is no universal marker for CSC identification (Alcalá *et al.*, 2019). As we increase our efforts to identify novel CSC biomarkers, we will increase our knowledge on their biology and role in cancer, allowing us moving forward in the development of more efficient targeted therapies that will provide new and promising opportunities to treat metastasis.

In section 8.2, a similar pattern of expression for TAS1R3 in PDXs was described for CD133 (Bertolini *et al.*, 2015), and considering the results in section 8.2.4, we wanted to investigate whether TAS1R3 expression is related to the acquisition of a stem-like phenotype. Scientists have reported that only a small subset of

CTCs, with a more stem-like phenotype, are described to be responsible for successful cancer metastasis (Cristofanilli *et al.*, 2004; Oskarsson, Batlle and Massagué, 2014; Gkountela and Aceto, 2016; Cho *et al.*, 2018). In section 8.3, the correlation of TAS1R3 with the CD133 CSC biomarker and a common stem-like feature is described. The enrichment of TAS1R3+ cells in the CD133+ subpopulations of different lung cancer cells and primary cultures, compared to the bulk population *in vitro* and *in vivo* was proved (reaching percentages of over 70% of TAS1R3+ CD133+ cells compared to 10% in the bulk). CD133+ CSCs have been widely identified in brain (Ahmed *et al.*, 2018), lung (Bertolini *et al.*, 2009; Herreros-Pomares *et al.*, 2019), colon (Kazama *et al.*, 2018), ovarian (Curley *et al.*, 2009), prostate (Sohn *et al.*, 2019), gastric (Xia *et al.*, 2015; W. T. Liu *et al.*, 2019), breast (Brugnoli *et al.*, 2017), and pancreatic cancers (Hermann *et al.*, 2007; Miranda-Lorenzo *et al.*, 2014); expression of CD133 protein has been shown to increase the tumorigenic potential and treatment resistance of tumor cells in these cancers (Glumac and LeBeau, 2018; Varillas *et al.*, 2019). However, CD133 is not the perfect cancer stem cell biomarker, since CD133 negative cells have also demonstrated the ability for self-renewal and enhanced tumor initiation capacity when transplanted into mice (Meng *et al.*, 2009). Moreover, the accuracy of CD133 as a cancer stem cell biomarker has been highly controversial, and contradictory data can be found in the literature (Glumac and LeBeau, 2018). For example, Eramo *et al* identified rare undifferentiated lung cancer stem cells from tumor samples expressing CD133 (Eramo *et al.*, 2008). Meng *et al* reported that both CD133+ and CD133- subpopulations of A549 and H446 cells contained CSCs (Meng *et al.*, 2009). Qiu *et al* found no statistical difference between the ability of CD133- and CD133+ cell populations to form pneumospheres (Qiu *et al.*, 2012). In addition to CD133, other CSC biomarkers include CD44, CD34, ALDH1A, and others (Nguyen *et al.*, 2012; Kim and Ryu, 2017), but unfortunately, there is no universal CSC biomarker across all cancer types. Hence, there is a need to define more specific biomarkers of CSCs. The fact that TAS1R3 was expressed only in a fraction of the CD133+ population is not surprising, since it is already known that there are

hierarchies within the CSC population, as for example reported with other stem cells biomarkers such as CXCR4 (Miranda-Lorenzo *et al.*, 2014; Alcalá *et al.*, 2019). In a paper by Bertolini *et al.*, it was reported that the CD133+CXCR4+ population directly isolated from PDXs of NSCLC was endowed with superior ability to seed and initiate metastasis at distant organs rather than the CD133+ alone (Bertolini *et al.*, 2015). Whether TAS1R3+CD133+ cells also present a superior ability than TAS1R3+ or CD133+ alone to disseminate and metastasize, should be further investigated.

The sphere formation assay is widely used in selection and enrichment of normal stem cells or CSCs, based on their ability to grow in serum-free medium supplemented with mitogens such as epidermal growth factor (EGF) and basic fibroblast growth factor (bFGF) for clonal proliferation (Zhao, Setrerrahmane and Xu, 2015). It has been successfully applied for the generation and maintenance of CSCs with higher tumorigenicity in various human cancers including carcinomas of breast (Wang *et al.*, 2014), colon-rectum (Li *et al.*, 2012), lung (Eramo *et al.*, 2008; Zhao, Setrerrahmane and Xu, 2015), pancreas (Miranda-Lorenzo *et al.*, 2014), head and neck (Shrivastava *et al.*, 2015), and bone (Wang, Park and Lin, 2009). In the present study, lung tumor spheres were generated from lung cancer cell lines and primary cultures in order to enrich the CSC population; TAS1R3 expression was then evaluated. We observed increased expression of TAS1R3 in CSC-enriched sphere cultures versus adherent monolayer controls. This increase was evident at protein and mRNA levels and correlated with higher expression of CD133 for H460 and A549 cell lines. Interestingly, when cells were cultured in anchorage independent condition only (ULA plates with complete medium), no increase in TAS1R3 surface expression was observed, suggesting that TAS1R3 is more related to the acquisition of a stem-like phenotype rather than the culture in anchorage-independent conditions. This data strongly suggests a link between TAS1R3 and CSCs. Future experiments will be carried out to fully understand the CSC features of TAS1R3+ spheres, including self-renewal, differentiation, proliferation, tumorigenicity, metastatic capacity, and multidrug resistance (Eramo *et al.*, 2008).

To better understand the pattern of TAS1R3 expression during disease progression, two different mouse models representing advanced stages of the disease, CDX and DDX models (meaning CTC- and DTC-derived xenograft mouse models, respectively), were generated. The xenograft model recapitulates the primary tumor whereas the CDX and DDX models better recapitulate the metastatic stages (Tellez-Gabriel *et al.*, 2019). These models offer great opportunities to provide insight into the complex biology of the metastatic process and to uncover new therapeutic targets (Lallo *et al.*, 2017; Tayoun *et al.*, 2019). Interestingly, when tumors from CDXs and DDXs were analyzed, the expression of TAS1R3 dramatically increased in the CDXs and DDXs compared to the primary tumor, as revealed by immunohistochemistry. Complementary, FACS and RT-qPCR analysis showed a moderate increase in TAS1R3 protein and RNA expression in the CDX while a statistically significant rise in the DDXs. These results point to TAS1R3 as a key player in the process of dissemination and metastasis.

We observed that when cells are grown *in vivo*, the number of TAS1R3+ cells were significantly increased compared to *in vitro* culturing. We hypothesized that it could be driven by stimuli from the microenvironment. The importance of the tumor microenvironment (TME) in promoting cancer development has been increasingly recognized over the past decade (Sainz *et al.*, 2016). The TME has been related to the maintenance of cancer stemness and also to the direct promotion of different processes such as, angiogenesis, invasion, and metastasis (Bertolini *et al.*, 2015; Sainz *et al.*, 2016; Denton, Roberts and Fearon, 2018). Key cellular players include cancer-associated fibroblasts, mesenchymal stem cells, immune cells and endothelial cells (Raggi *et al.*, 2015). To verify whether physiologically relevant tumor microenvironment stimuli could be influencing TAS1R3 expression, A549 and H460 cells were cocultured with conditioned medium (CM) from murine macrophages, endothelial cells, and fibroblast, or in direct coculture with stroma cells in a ratio 1:3 (tumor:stroma cells). Our results showed a slight modulation of TAS1R3 mainly driven by macrophages and it was more evident in the direct coculture experiment rather than with the

conditioned medium for both cell lines. Macrophages in the TME, called tumor-associated macrophages (TAMs), are one of the most abundant types of cells, and exhibit different phenotypes and functions in response to various microenvironmental signals generated from tumor and stromal cells (Wei *et al.*, 2019). Interestingly, there is now growing evidence that macrophages enhance tumor progression by directly communicating with CSC to promote their stemness (Raggi *et al.*, 2015; Sainz *et al.*, 2016). Liu *et al.* have recently reported that the direct interaction of TAMs with breast cancer cells promotes cancer stemness *in vivo* (D. Liu *et al.*, 2019). This may point again to the link of TAS1R3 with stemness, however, further experiments should be carried out to deeper understand the mechanisms and implications of that interaction.

In addition, we were able to successfully overexpress TAS1R3 in the NSCLC cell line A549 to study the phenotypic changes that cells experience when TAS1R3 is upregulated. An empty vector was used as negative control. Proliferation, migration, and invasion capacity were evaluated. TAS1R3+ cells showed no differences in the proliferation capacity *in vitro*, by measuring the incorporation of EdU (5-ethynyl-2'-deoxyuridine) into newly synthesized DNA. Next, a significant reduction in the migration capacity was observed by a wound healing assay. The wound healing assay implies that cells move in two dimensions while they maintain their intercellular junctions in a confluent plate of cells, this kind of movement is known as collective cell migration or sheet migration (Jonkman *et al.*, 2014; Schaeffer *et al.*, 2014). Importantly, the slower migration of T1R3+ cells was not due to a decrease in proliferation. Lastly, TAS1R3+ cells showed increased invasiveness assessed by an *in vitro* transwell invasion assay using Matrigel under chemotactic conditions (growth factor-free medium in the upper chamber and growth factor-containing medium in the lower chamber). This assay can be used to analyze the ability of single cells to directionally respond to different chemo-attractants whether they are chemokines, growth factors, lipids, or nucleotides, through a physical barrier (e.g. Matrigel) (Justus *et al.*, 2014). Migration and invasion are normally reported as positively correlated during different processes such as EMT and

metastatic dissemination (Ahn *et al.*, 2017; Fan *et al.*, 2017). However, Schaeffer *et al.* have demonstrated that migration and invasion can be uncoupled during EMT using TWIST1 overexpressing cells (promotes EMT) compared to control cells (Schaeffer *et al.*, 2014). T1R3⁻ cells may maintain stronger cell-cell adhesions that enhance the movement of confluent monolayers for a collective migration (Friedl and Gilmour, 2009). Future experiments would allow us to elucidate this controversy in the role of TAS1R3 in migration, for example, performing a cell-cell adhesion assay or a transwell migration assay that measure the ability of single cells to migrate (Pijuan *et al.*, 2019).

Considering that *in vitro* cell-based assays related to migration or even invasion not always reliably predict the *in vivo* metastatic process, *in vivo* experiments were set in order to test if TAS1R3 cells are able to metastasize *in vivo*, where the full impact of the microenvironment can influence the process. T1R3^{+/-} cells were injected in nude mice and the metastatic potential of both was evaluated. Firstly, T1R3⁺ group showed a significantly reduced tumorigenicity compared to T1R3⁻ group. Interestingly, when we analyzed the tumors, some different molecular traits were observed: T1R3⁺ tumors were significantly enriched in the stem markers CD133 and SOX2, and moderately increased in OCT4 and NANOG, while there were not statistically significant differences in TAS1R3 expression at the end of the experiment. Furthermore, T1R3⁺ tumors presented a slight decrease in E-CAD and increase in SNAI2, that could be explained by the progressive loss of epithelial features towards an intermediate phenotype. Accumulating evidence in the literature demonstrates that dissemination of CTCs can occur at early stages of cancer progression (Hüsemann *et al.*, 2008; Kang and Pantel, 2013), and as was mentioned before, partial EMT has been shown to mediate dissemination and possible acquisition of stem-cell-like traits thus attaining their metastatic initiating potential (Hen and Barkan, 2020). This may be a possibility to explain why the TAS1R3 expression in the tumors of the T1R3⁺ group is no superior to the control group at the end of the experiment, TAS1R3⁺ cells may be the first ones to disseminate from the primary tumor.

Next, the blood of mice was taken from the heart and analyzed for CTC count and characterization. Importantly, we could only detect CTCs in the T1R3+ group but not in the T1R3- group (5 CTCs/mL vs. 0 CTCs/mL, respectively), and the 100% of CTCs found in the T1R3+ group were TAS1R3 and eGFP positive, indicating that they come from the transfected cells injected in the flanks of the mice (T1R3+ GFP+). In the past decade, numerous clinical trials have demonstrated the clinical/biological value of CTCs enumeration. There is growing evidence of the diagnostic and prognostic value of CTC count in peripheral blood in metastatic breast (Bidard *et al.*, 2014), colorectal (Cohen *et al.*, 2008), lung (Krebs *et al.*, 2011), pancreas (Court *et al.*, 2018), and prostate (De Bono *et al.*, 2008) cancers. CTC count has been correlated with the number of organs bearing metastases (Hamilton and Rath, 2017), and Court *et al.* have demonstrated the potential of CTC enumeration for identifying patients at high risk of occult metastatic disease (Court *et al.*, 2018). This data may suggest that the use of TAS1R3 in combination with other CTC markers may be useful for identifying a distinct CTC subpopulation, with an intermediate EMT phenotype, stem features and potentially different biological role.

Lastly, the lungs were analyzed, and a significantly higher number of disseminated tumor cells was observed in the T1R3+ group. It is important to remark that the primary tumors of the T1R3+ group were significantly smaller at the end of the experiment; however, more metastatic cells were found in the lungs. Furthermore, DTCs were significantly enriched in TAS1R3 and CD133 when compared to the primary tumors. This was observed for the T1R3+ group, but also in the T1R3- group. Strikingly, T1R3- cells with no detectable levels of TAS1R3 at the beginning of the experiment, were able to endogenously upregulate TAS1R3 to succeed in dissemination and colonization of the lungs. Metastasis is a highly inefficient process, it is estimated that less than 0.02% of CTCs actually become DTCs (Massagué and Obenauf, 2016; Hen and Barkan, 2020). Evidence in the literature highlights the striking similarities between the biology of DTCs and the biology of CSCs or CSC-like cells (Chaffer *et al.*, 2011, 2013; Shiozawa *et al.*, 2013; Hen and Barkan,

2020). These similarities are related to intrinsic mechanisms for survival, quiescence, and their cross-talk with mediators produced in surrounding niches that may either support their dormancy or outgrowth (Hen and Barkan, 2020). This result strongly supports that TAS1R3 endows cells with enhanced capabilities to disseminate, survive in circulation and metastasize and point again to a CSC link.

In an independent *in vivo* experiment, we performed an experimental metastasis assay. This *in vivo* assay does not recapitulate the first steps of the metastatic cascade, but rather reflect homing of tumor cells circulating in the bloodstream to a particular secondary organ (Gomez-Cuadrado *et al.*, 2017). Tail vein injections often leads to the formation of lung metastases (Khanna and Hunter, 2005). Intravenous experimental metastasis has been widely used in the elucidation of tumor-host interactions required for the initial arrest and colonization at metastatic sites (Hiratsuka *et al.*, 2006; Gil-Bernabé *et al.*, 2012; Gomez-Cuadrado *et al.*, 2017; Caron *et al.*, 2018). We wanted to evaluate the capacity of T1R3+ cells to colonize the lungs, therefore, T1R3+/- cells were injected directly in the tail vein of nude mice and allowed to spontaneously form metastasis in the lungs without the steps of detaching from the primary tumor and intravasation into the circulation. On the contrary of the previous *in vivo* experiment, the same number of T1R3+/T1R3- tumor cells were in circulation, however, a significant increase in the number of disseminated cells in the lungs was observed in the T1R3+ group. Consistently, cells found in the lungs were overexpressing TAS1R3 and CD133 compared to their T1R3- counterparts. These results further confirm that TAS1R3 endow cells with superior ability to seed and initiate metastasis at distant organs.

During the metastatic cascade, cancer cells interact with immune cells and they influence each other in different steps of the process (Blomberg, Spagnuolo and De Visser, 2018). These interactions may produce both protumor and antitumor activities (Saini, Szczerba and Aceto, 2019). Beyond the interactions of the immune system and cancer cells at the primary tumor site, this crosstalk is maintained during cancer progression, i.e. in circulation and in sites of distal metastasis (Saini, Szczerba and Aceto, 2019). Tumor-infiltrating

immune cells, particularly myeloid cells, also actively participate in metastatic processes (Kitamura, Qian and Pollard, 2015). In this *in vivo* experiment we wanted to evaluate the ability of T1R3+ cells to recruit immune infiltrating cells and to escape their cancer immune control in the metastatic site, however, not significant differences were observed between the T1R3+ and T1R3- group, except from neutrophils that were reduced in the T1R3+ group. Undoubtedly, further experiments should be carried out in order to fully understand the role of TAS1R3+ cells in the establishment of an immune-suppressive environment that inhibits the development or the efficacy of anti-tumor immune responses.

To conclude, these results position TAS1R3 as a potential target for the development of therapeutics aimed to interrupt metastasis progression in NSCLC. Although more in-depth studies are still needed, these results demonstrate that TAS1R3 endows cells with certain advantages to disseminate and initiate metastasis. Further understanding of the biology of this receptor may allow us to more accurately design novel therapeutic strategies to impair metastasis.

FUTURE PERSPECTIVES

The identification of druggable targets in metastasis is a promising strategy to improve the outcome of NSCLC patients. Evidence in this work has pointed out TAS1R3 as a novel biomarker that plays a role in metastasis of NSCLC and has potential in other cancer types. TAS1R3 positive cells are able to disseminate more and successfully colonize distant organs, however, the mechanisms by which TAS1R3 is driving this superior ability in cells still remain unclear. Further understanding of its biology would help us to elucidate it. As it was mentioned before, metastatic cells need to acquire some modifications in order to succeed, including a change from epithelial to a more mesenchymal phenotype, the acquisition of stem-cell properties and phenotypic plasticity, and a change in their metabolism in a way that promotes survival and metastatic outgrowth (Tinhofer *et al.*, 2014; Mason *et al.*, 2017; De Francesco, Sotgia and Lisanti, 2018; Santamaría, Moreno-Bueno and Cano, 2019). Although we cannot definitely state that TAS1R3 is a CSC biomarker, our data support a

correlation between TAS1R3 and other CSC biomarkers and features. More in-depth studies are still needed to determine the exact role of TAS1R3 in CSC biology. Interestingly, TAS1R3 has been reported to be involved in the control of glucose metabolism and regulation of adipogenesis (Masubuchi *et al.*, 2017). Hence, it is possible that TAS1R3 provides metabolic advantages under uncertain conditions, such as the circulation in the bloodstream or in a completely new environment in a distant organ. This hypothesis could be further investigated.

As novel biomarkers are disclosed, novel drug discovery programs and/or biological development programs can be envisioned. GPCRs are the most commonly exploited targets in modern medicine. To date, 30 to 50 percent of marketed drugs are estimated to target GPCRs. Compelling evidence suggests that GPCRs play major roles in cancer including growth, migration, metastasis, invasion, and survival (Gad and Balenga, 2020). However, they have historically not been targeted in oncology, and therefore, only a handful of the marketed drugs for GPCRs are for oncology, a detailed description of these drugs can be found in ref. (V. Wu *et al.*, 2019).

Since TAS1R3 belongs to the GPCR family, the most druggable family of proteins, the use of a small molecule could be an interesting therapeutic option to explore. Small molecules are usually ≤ 500 Da size, with a well-defined chemical structure, and are often administered orally (Imai and Takaoka, 2006). Many small molecules focus on inactivating kinases and interrupting the signalling pathways which are dysregulated during carcinogenesis. Some of the main advantages of small molecules are that they can easily translocate through plasma membranes due to their small size, they are simple, stable, easily distributed, and non-immunogenic (Lee, Tan and Oon, 2018). Some successful small molecules in cancer therapy (crizotinib, afatinib, erlotinib, etc.) have been reviewed in the *Introduction* of this thesis. The approaches in the GPCR targeted drug discovery are targeting the signaling of the receptors using agonists or antagonists or targeting the specific interaction between GPCRs and their ligands (Usman *et al.*, 2020). Preliminary results in our laboratory using a described antagonist of TAS1R3, lactisole, an artificial sweetener,

showed a significant reduction in proliferation, migration, colony forming capacity, and induction of senescence of metastatic cancer cells, however, really high concentrations (1 mg/mL) of lactisole were needed to see those effects. Despite lactisole may not be a potent antagonist, these results nicely evidence the potential of TAS1R3 as a druggable target. In order to develop a potent small molecule against TAS1R3, a better understanding of the biology of TAS1R3 in oncology will be needed. There are still many open questions regarding the pathways in which TAS1R3 is involved, and what are the proteins downstream of TAS1R3 and the specific ligands in cancer. *In vitro* experiments with the transfected cell lines could help us to elucidate these questions. Different cancer cell lines could be transfected to have a wider picture of TAS1R3 in NSCLC. Proteomic analysis will allow the identification of the proteins that are upregulated when TAS1R3 is overexpressed in the cancer cell lines.

Some of the limitations of small molecules refer to their unspecificity, increasing the risk of toxicity, and that they have a short life span, thus requiring daily dosing (Lavanya *et al.*, 2014). One alternative to small drugs are the biologicals (e.g. monoclonal antibodies, proteins, cytokines, growth factors, enzymes, etc.). Monoclonal antibodies (mAb) against TAS1R3 could also be an interesting approach to explore. In 1985, the FDA approved the first mAb, against CD3, for the treatment of kidney transplant rejection (Norman *et al.*, 1988). From then, 76 mAb have received marketing approval, with near 30 mAb indicated for oncological treatment. The mAb field is relatively young but is growing fast, with more than 30 candidates in late-stage clinical trials for cancer therapy. MAb have exquisite target selectivity and hence, less toxicity than small molecules. They are of approx. 150 KDa, therefore they cannot enter cancer cells, so their targets must be extracellular (Shepard *et al.*, 2017). The clinical value of mAbs have been proven for a multitude of diseases including oncologic, inflammatory, autoimmune, cardiovascular, respiratory, neurologic, allergic, benign hematologic, infections, orthopedic, coagulopathy, metabolic and to decrease morbidity of disease (diminution of pain), modify disease progression, and potentially anatomic development (Pelletier and Mukhtar, 2020).

To date, two mAb targeting GPCRs have been approved by the FDA, mogamulizumab indicated for T cell lymphoma, acts on CC-chemokine receptor 4 (CCR4), and erenumab for the treatment of migraine, targeting the CGRP receptor (Dolgin, 2018; Mullard, 2018; Garces *et al.*, 2020). Some of the main challenges in targeting GPCRs refer to high conformational variability, and the small exposed area of extracellular epitopes (Jo and Jung, 2016). As an example, the above mentioned CCR4 GPCR only have 39 amino acids in the extracellular domain, however, TAS1R3, presents a large extracellular domain of 550 amino acids, suggesting that the development of a monoclonal antibody targeting TAS1R3 could be feasible. Preliminary experiments in our laboratory using a polyclonal antibody against TAS1R3 (the only available type of antibodies for TAS1R3 in the market), showed a dramatic mortality after one-hour incubation with TAS1R3+ lung cancer cells that was not observed in TAS1R3- cells. This result nicely suggests that TAS1R3 is a promising target for the development of therapeutic monoclonal antibodies.

Antibodies also provide further applications than small molecules, such as for cancer imaging and early detection, as well as to deliver cytotoxic agents (antibody-drug conjugates) and/or radiosensitizers, and also for patient stratification prior the selection of the targeted therapy, which make the development of a monoclonal antibody more attractive (V. Wu *et al.*, 2019). Targeting TAS1R3 as single agents or as part of new combination modalities may provide unprecedented opportunities for the development of novel strategies for metastatic NSCLC.

Lastly, nanotechnology offers the incorporation of different imaging modalities, therapeutic cargo, and targeting molecules into a single multifunctional nanosystem, that is called nanotheranostics (Vázquez-Ríos *et al.*, 2018). These exceptional nanosystems would ideally allow the concurrent diagnosis, patient stratification, therapy guidance, tracking drug release and penetration within tumors, and monitoring response (Wong *et al.* 2020). This field of research is rapidly growing, and many studies are ongoing. To date, no nanotheranostics have been approved by the FDA yet, but many of them are currently in various phases of clinical trials and are

producing good results. As an example, AGuIX[®] (Activation and Guidance of Irradiation by X-ray), a gadolinium-based nanoparticle of around 5 nm diameter for the treatment of multiple brain metastases is now in phase II clinical trials (NCT03818386). In this thesis, a multifunctional nanoplatform based on exosomes has been developed with great potential for the delivery of therapeutic molecules to selective targets. EMNs have demonstrated to be able to accommodate drugs of different nature (e.g., RNAs, DNAs, or hydrophobic compounds), and can be functionalized with biologicals (e.g. protein integrin $\alpha 6\beta 4$). EMNs could overcome some limitation of the small molecules related to specificity and short life span, given that the drug could be protected from premature degradation, and a targeted delivery would prevent the small molecule from binding to unspecific molecular targets including cell surface receptors. A specific targeting to TAS1R3 could be achieved by the functionalization of EMNs with ligands of TAS1R3, or with an antibody to directly deliver the cargo to metastatic cancer cells. EMNs are excellent candidates for the combination of different modalities for the development of a theranostic nanosystem for metastatic NSCLC.

Once we have the lead compound against TAS1R3, we will be able to proceed with the killer experiment to validate TAS1R3 as therapeutic target, a solid *in vivo* proof-of-concept showing that when TAS1R3 is blocked/neutralized, metastases are significantly reduced.

Altogether, this thesis proposes different strategies that can be pursued for the development of novel targeted therapies for a breakthrough in the management of metastatic NSCLC, and possibly, other cancer types.





CONCLUSIONS



11 CONCLUSIONS

In this thesis, **by closely looking at the tumor biology, new strategies for the development of innovative targeted therapeutics for advanced NSCLC have been described.** The experimental work enclosed in this manuscript allowed the setting of the following conclusions (C):

- C1.** Exosomes are natural transporters of RNAs and other biomolecules and have tumor-homing properties. Inspired by them, a nanoplatform that resembles their main characteristics (i.e., size, charge, morphology, lipid composition, drug loading capacity, low toxicity, and interaction with tumor cells), EMNs, has been successfully developed following a fast, simple, mild, safe, cost-efficient, and reproducible methodology.
- C2.** EMNs can be conveniently tailored to incorporate different lipid species, surface proteins, and molecules of interest for a broad range of applications.
- C3.** EMNs can be efficiently functionalized with active proteins with organotropic properties that provide them with enhanced abilities to interact with lung cancer cells. EMNs can also be efficiently loaded with therapeutic RNAs and have the capacity to transport them to the targeted cancer cells and deliver them intracellularly.
- C4.** EMNs show a similar behavior in delivering therapeutic biomolecules than tumor-derived exosomes according to *in vitro* and *in vivo* data, with the advantage that they are safer, and can be produced in shorter times following highly controlled procedures.

- C5.** CTCs are a source of interest for the identification of novel biomarkers linked to metastasis. Inspired by this, a new biomarker, TAS1R3, has been identified through liquid biopsy by the isolation and characterization of CTCs from advanced NSCLC patients.
- C6.** TAS1R3 does not show prognostic value under the studied conditions, a fact that can be related to their isolation based on EpCAM positive expression. For a more accurate evaluation of the prognostic value of TAS1R3, CTCs should be isolated avoiding the bias introduced by marker selection, such as based on physical properties or negative CTC enrichment.
- C7.** Analysis of PDX allowed concluding that TAS1R3 expression is related to advanced stages of the disease, with poorly-differentiated cells, metastasis, and is expressed in different tumor types such as pancreatic, colorectal, head and neck, and lung cancer.
- C8.** *In vitro* and *in vivo* studies indicate that TAS1R3 is associated to a cancer stem cell phenotype, provides cells with additional advantages to metastasize, and promotes colonization of distant organs.
- C9.** The results of this work indicate that TAS1R3 has potential for the development of new targeted therapeutics specifically design to halt metastasis.



REFERENCES



12 REFERENCES

- Adams, D. et al. (2018) 'Patisiran, an RNAi Therapeutic, for Hereditary Transthyretin Amyloidosis', *New England Journal of Medicine*, 379(1), 11–21. doi: 10.1056/NEJMoa1716153.
- Adams, M. N. et al. (2017) 'Expression of CDCA3 Is a Prognostic Biomarker and Potential Therapeutic Target in Non-Small Cell Lung Cancer', *Journal of Thoracic Oncology*, 12, 1071–1084. doi: 10.1016/j.jtho.2017.04.018.
- Adem, B., Vieira, P. F. and Melo, S. A. (2020) 'Decoding the Biology of Exosomes in Metastasis', *Trends in Cancer*, 6(1), 20–30. doi: 10.1016/j.trecan.2019.11.007.
- Ahmed, S. I. et al. (2018) 'CD133 Expression in Glioblastoma Multiforme: A Literature Review', *Cureus*, 10(10), 1–5. doi: 10.7759/cureus.3439.
- Ahn, J. H. et al. (2017) 'Mutant p53 stimulates cell invasion through an interaction with Rad21 in human ovarian cancer cells', *Scientific Reports*, 7(9076), 1–11. doi: 10.1038/s41598-017-08880-4.
- Akaza, H. (2020) 'TNM classification', *Japanese Journal of Urology*, 85(2), 229–241. doi: 10.5980/jpnjurol1989.85.229.
- Akinc, A. et al. (2019) 'The Onpattro story and the clinical translation of nanomedicines containing nucleic acid-based drugs', *Nature Nanotechnology*, 14(12), 1084–1087. doi: 10.1038/s41565-019-0591-y.
- Al-Ahmady, Z. and Kostarelos, K. (2016) 'Chemical Components for the Design of Temperature-Responsive Vesicles as Cancer Therapeutics', *Chemical Reviews*, 116(6), 3883–3918. doi: 10.1021/acs.chemrev.5b00578.
- Alcalá, S. et al. (2019) 'The Anthrax Toxin Receptor 1 (ANTXR1) Is Enriched in Pancreatic Cancer Stem Cells Derived from Primary Tumor Cultures', *Stem Cells International*, 2019, 1–13. doi: 10.1155/2019/1378639.

- Alix-Panabières, C., Mader, S. and Pantel, K. (2017) ‘Epithelial-mesenchymal plasticity in circulating tumor cells’, *Journal of Molecular Medicine*, 95(2), 133–142. doi: 10.1007/s00109-016-1500-6.
- Alonso-Nocelo, M et al. (2016) ‘Development and characterization of a three-dimensional co-culture model of tumor T cell infiltration’, *Biofabrication*, 8(2), 025002. doi: 10.1088/1758-5090/8/2/025002.
- Alonso-Nocelo, Marta et al. (2016) ‘Selective interaction of PEGylated polyglutamic acid nanocapsules with cancer cells in a 3D model of a metastatic lymph node’, *Journal of Nanobiotechnology*, 14(1), 1–9. doi: 10.1186/s12951-016-0207-8.
- Alvarez-Erviti, L. et al. (2011) ‘Delivery of siRNA to the mouse brain by systemic injection of targeted exosomes.’, *Nature biotechnology*, 29(4), 341–345. doi: 10.1038/nbt.1807.
- Amantini, C. et al. (2019) ‘Expression Profiling of Circulating Tumor Cells in Pancreatic Ductal Adenocarcinoma Patients: Biomarkers Predicting Overall Survival’, *Frontiers in Oncology*, 9(874), 1–13. doi: 10.3389/fonc.2019.00874.
- Amiri-Kordestani, L. et al. (2014) ‘FDA approval: Ado-trastuzumab emtansine for the treatment of patients with HER2-positive metastatic breast cancer’, *Clinical Cancer Research*, 20(17), 4436–4441. doi: 10.1158/1078-0432.CCR-14-0012.
- Andriani, F. et al. (2016) ‘Conversion to stem-cell state in response to microenvironmental cues is regulated by balance between epithelial and mesenchymal features in lung cancer cells’, *Molecular Oncology*, 10(2), 253–271. doi: 10.1016/j.molonc.2015.10.002.
- Anselmo, A. C. and Mitragotri, S. (2019) ‘Nanoparticles in the clinic: An update’, *Bioengineering & Translational Medicine*, 4(3), 1–16. doi: 10.1002/btm2.10143.
- Armstrong, A. J. et al. (2011) ‘Circulating tumor cells from patients with advanced prostate and breast cancer display both epithelial and mesenchymal markers’, *Molecular Cancer Research*, 9(8), 997–1007. doi: 10.1158/1541-7786.MCR-10-0490.
- Ashworth, T. R. (1869) ‘A case of cancer in which cells similar to those in the tumours were seen in the blood after death’, *Aust Med J.*, 14, 146–147.

- Assadi-Porter, F. M. et al. (2008) 'Direct NMR detection of the binding of functional ligands to the human sweet receptor, a heterodimeric family 3 GPCR', *Journal of the American Chemical Society*, 130(23), 7212–7213. doi: 10.1021/ja8016939.
- Assadi-Porter, F. M., Tonelli, M., et al. (2010) 'Interactions between the human sweet-sensing T1R2-T1R3 receptor and sweeteners detected by saturation transfer difference NMR spectroscopy', *Biochimica et Biophysica Acta - Biomembranes*, 1798(2), 82–86. doi: 10.1016/j.bbamem.2009.07.021.
- Assadi-Porter, F. M., Maillet, E. L., et al. (2010) 'Key Amino Acid Residues Involved in Multi-Point Binding Interactions between Brazzein, a Sweet Protein, and the T1R2-T1R3 Human Sweet Receptor', *Journal of Molecular Biology*, 398(4), 584–599. doi: 10.1016/j.jmb.2010.03.017.
- Awad, M. M. et al. (2016) 'MET exon 14 mutations in Non-small-cell lung cancer are associated with advanced age and stage-dependent MET genomic amplification and c-Met overexpression', *Journal of Clinical Oncology*, 34(7), 721–730. doi: 10.1200/JCO.2015.63.4600.
- Barbazán, J., Vieito, M., et al. (2012) 'A logistic model for the detection of circulating tumor cells in human metastatic colorectal cancer.', *Journal of Cellular and Molecular Medicine*, 16(10), 2342–2349. doi: 10.1111/j.1582-4934.2012.01544.x.
- Barbazán, J., Alonso-Alconada, L., et al. (2012) 'Molecular Characterization of Circulating Tumor Cells in Human Metastatic Colorectal Cancer', *PLoS ONE*. Edited by X. W. Wang, 7(7), e40476. doi: 10.1371/journal.pone.0040476.
- Barenholz, Y. (2012) 'Doxil®-the first FDA-approved nano-drug: lessons learned.', *Journal of controlled release*, 160(2), 117–34. doi: 10.1016/j.jconrel.2012.03.020.
- Baumgart, M. and Pandya, K. (2016) 'The use of biomarkers in the treatment of non-small cell lung cancer', *Expert Review of Precision Medicine and Drug Development*, 1(1), 25–36. doi: 10.1080/23808993.2016.1136558.
- Ben-Akiva, E. et al. (2020) 'Biomimetic anisotropic polymeric nanoparticles coated with red blood cell membranes for enhanced circulation and toxin removal', *Science Advances*, 6(16), 1–9. doi: 10.1126/sciadv.aay9035.

- Bertino, E. M. et al. (2016) ‘A Phase I Trial to Evaluate Antibody-Dependent Cellular Cytotoxicity of Cetuximab and Lenalidomide in Advanced Colorectal and Head and Neck Cancer’, *Molecular Cancer Therapeutics*, 15(9), 2244–2250. doi: 10.1158/1535-7163.MCT-15-0879.
- Bertolini, G. et al. (2009) ‘Highly tumorigenic lung cancer CD133+ cells display stem-like features and are spared by cisplatin treatment’, *Proceedings of the National Academy of Sciences*, 106(38), 16281–16286. doi: 10.1073/pnas.0905653106.
- Bertolini, G. et al. (2015) ‘Microenvironment-modulated metastatic CD133+ /CXCR4+ /EpCAM- lung cancer-initiating cells sustain tumor dissemination and correlate with poor prognosis’, *Cancer Research*, 75(17), 3636–3649. doi: 10.1158/0008-5472.CAN-14-3781.
- Bertotti, A. et al. (2011) ‘A molecularly annotated platform of patient-derived xenografts (“xenopatients”) identifies HER2 as an effective therapeutic target in cetuximab-resistant colorectal cancer’, *Cancer Discovery*, 1(6), 508–523. doi: 10.1158/2159-8290.CD-11-0109.
- Bidard, F. C. et al. (2014) ‘Clinical validity of circulating tumour cells in patients with metastatic breast cancer: A pooled analysis of individual patient data’, *The Lancet Oncology*, 15(4), 406–414. doi: 10.1016/S1470-2045(14)70069-5.
- Blomberg, O. S., Spagnuolo, L. and De Visser, K. E. (2018) ‘Immune regulation of metastasis: Mechanistic insights and therapeutic opportunities’, *DMM Disease Models and Mechanisms*, 11(10), 1–12. doi: 10.1242/dmm.036236.
- Blumenschein, G. R. et al. (2015) ‘A randomized phase II study of the MEK1/MEK2 inhibitor trametinib (GSK1120212) compared with docetaxel in KRAS-mutant advanced non-small-cell lung cancer (NSCLC)’, *Annals of Oncology*, 26(5), 894–901. doi: 10.1093/annonc/mdv072.
- Bobo, D. et al. (2016) ‘Nanoparticle-Based Medicines: A Review of FDA-Approved Materials and Clinical Trials to Date’, *Pharmaceutical Research*, 33(10), 2373–2387. doi: 10.1007/s11095-016-1958-5.
- De Bono, J. S. et al. (2008) ‘Circulating tumor cells predict survival benefit from treatment in metastatic castration-resistant prostate cancer’, *Clinical Cancer Research*, 14(19), 6302–6309. doi: 10.1158/1078-

0432.CCR-08-0872.

- Bono, N. et al. (2020) 'Non-viral in vitro gene delivery: It is now time to set the bar!', *Pharmaceutics*, 12(2). doi: 10.3390/pharmaceutics12020183.
- Bonzon-Kulichenko, E. et al. (2011) 'A Robust Method for Quantitative High-throughput Analysis of Proteomes by 18 O Labeling', *Molecular & Cellular Proteomics*, 10(1), M110.003335. doi: 10.1074/mcp.M110.003335.
- Borghaei, H. et al. (2015) 'Nivolumab versus Docetaxel in Advanced Nonsquamous Non-Small-Cell Lung Cancer.', *The New England journal of medicine*, 373(17), 1627–39. doi: 10.1056/NEJMoa1507643.
- Bottai, G. et al. (2017) 'Progress in nonviral gene therapy for breast cancer and what comes next?', *Expert Opinion on Biological Therapy*, 17(5), 595–611. doi: 10.1080/14712598.2017.1305351.
- Brahmer, J. et al. (2015) 'Nivolumab versus Docetaxel in Advanced Squamous-Cell Non-Small-Cell Lung Cancer', *N Engl J Med*, 373, 123–135. doi: 10.1056/NEJMoa1504627.
- Brahmer, J. R. et al. (2018) 'The Society for Immunotherapy of Cancer consensus statement on immunotherapy for the treatment of non-small cell lung cancer (NSCLC)', *Journal for Immunotherapy of Cancer*, 6(75), 1–15. doi: 10.1186/s40425-018-0382-2.
- Bray, F. et al. (2018) 'Global cancer statistics 2018: GLOBOCAN estimates of incidence and mortality worldwide for 36 cancers in 185 countries', *CA: A Cancer Journal for Clinicians*, 68(6), 394–424. doi: 10.3322/caac.21492.
- Bregoli, L. et al. (2016) 'Nanomedicine applied to translational oncology: A future perspective on cancer treatment', *Nanomedicine: Nanotechnology, Biology, and Medicine*, 12(1), 81–103. doi: 10.1016/j.nano.2015.08.006.
- Bronte, G. et al. (2019) 'Targeting RET-rearranged non-small-cell lung cancer: Future prospects', *Lung Cancer: Targets and Therapy*, 27–36. doi: 10.2147/LCTT.S192830.
- Brugnoli, F. et al. (2017) 'Up-modulation of PLC-β2 reduces the number and malignancy of triple-negative breast tumor cells with a CD133+/EpCAM+ phenotype: A promising target for preventing progression of TNBC', *BMC Cancer*, 17(617), 1–11. doi:

10.1186/s12885-017-3592-y.

- Bulbake, U. et al. (2017) ‘Liposomal formulations in clinical use: An updated review’, *Pharmaceutics*, 9(2), 1–33. doi: 10.3390/pharmaceutics9020012.
- Bylicki, O. et al. (2020) ‘Targeting the MET-Signaling Pathway in Non-Small-Cell Lung Cancer: Evidence to Date’, *OncoTargets and Therapy*, 13, 5691–5706. doi: 10.2147/ott.s219959.
- Calabuig-Fariñas, S. et al. (2016) ‘Circulating tumor cells versus circulating tumor DNA in lung cancer-which one will win?’, *Translational Lung Cancer Research*, 466–482. doi: 10.21037/tlcr.2016.10.02.
- Cancer System Performance (2020) Stage distribution | Cancer System Performance. Available at: <https://www.systemperformance.ca/disease-sites/lung/stage-distribution/> (Accessed: 17 July 2020).
- Cao, Z. Q., Wang, Z. and Leng, P. (2019) ‘Aberrant N-cadherin expression in cancer’, *Biomedicine and Pharmacotherapy*, 109320. doi: 10.1016/j.biopha.2019.109320.
- Caron, J. M. et al. (2018) ‘The HU177 Collagen Epitope Controls Melanoma Cell Migration and Experimental Metastasis by a CDK5/YAP-Dependent Mechanism’, *American Journal of Pathology*, 188(10), 2356–2368. doi: 10.1016/j.ajpath.2018.06.017.
- Catelain, C. et al. (2017) ‘Detection of gene rearrangements in circulating tumor cells: Examples of ALK-, ROS1-, RET-rearrangements in non-small-cell lung cancer and ERG-rearrangements in prostate cancer’, in *Advances in Experimental Medicine and Biology*, 169–179. doi: 10.1007/978-3-319-55947-6_9.
- Chaffer, C. L. et al. (2011) ‘Normal and neoplastic nonstem cells can spontaneously convert to a stem-like state’, *Proceedings of the National Academy of Sciences of the United States of America*, 108(19), 7950–7955. doi: 10.1073/pnas.1102454108.
- Chaffer, C. L. et al. (2013) ‘Poised chromatin at the ZEB1 promoter enables breast cancer cell plasticity and enhances tumorigenicity’, *Cell*, 154(1), 61–74. doi: 10.1016/j.cell.2013.06.005.
- Chen, Z. et al. (2018) ‘Characterization and validation of potential therapeutic targets based on the molecular signature of patient-derived xenografts in gastric cancer’, *Journal of Hematology and Oncology*,

- 11(20), 1–12. doi: 10.1186/s13045-018-0563-y.
- Chitty, J. L. et al. (2018) ‘Recent advances in understanding the complexities of metastasis’, *F1000Research*, 7, 1–18. doi: 10.12688/f1000research.15064.2.
- Cho, H. Y. et al. (2018) ‘Selective isolation and noninvasive analysis of circulating cancer stem cells through Raman imaging’, *Biosensors and Bioelectronics*, 102, 372–382. doi: 10.1016/j.bios.2017.11.049.
- Cirstoiu-Hapca, A. et al. (2010) ‘Benefit of anti-HER2-coated paclitaxel-loaded immuno-nanoparticles in the treatment of disseminated ovarian cancer: Therapeutic efficacy and biodistribution in mice.’, *Journal of controlled release: official journal of the Controlled Release Society*, 144(3), 324–31. doi: 10.1016/j.jconrel.2010.02.026.
- Cohen, S. J. et al. (2008) ‘Relationship of circulating tumor cells to tumor response, progression-free survival, and overall survival in patients with metastatic colorectal cancer’, *Journal of Clinical Oncology*, 26(19), 3213–3221. doi: 10.1200/JCO.2007.15.8923.
- Conlon, G. A. and Murray, G. I. (2019) ‘Recent advances in understanding the roles of matrix metalloproteinases in tumour invasion and metastasis’, *The Journal of Pathology*, 247(5), 629–640. doi: 10.1002/path.5225.
- Court, C. M. et al. (2018) ‘Circulating Tumor Cells Predict Occult Metastatic Disease and Prognosis in Pancreatic Cancer’, *Annals of Surgical Oncology*, 25(4), 1000–1008. doi: 10.1245/s10434-017-6290-8.
- Cox, A. et al. (2019) ‘Protein-functionalized nanoparticles derived from end-functional polymers and polymer prodrugs for crossing the blood-brain barrier’, *European Journal of Pharmaceutics and Biopharmaceutics*, 142, 70–82. doi: 10.1016/j.ejpb.2019.06.004.
- Cristofanilli, M. et al. (2004) ‘Circulating tumor cells, disease progression, and survival in metastatic breast cancer’, *New England Journal of Medicine*, 351(8), 781–791. doi: 10.1056/NEJMoa040766.
- Cui, M. et al. (2006) ‘The heterodimeric sweet taste receptor has multiple potential ligand binding sites’, *Current Pharmaceutical Design*, 12(35), 4591–4600. doi: 10.2174/138161206779010350.
- Curley, M. D. et al. (2009) ‘CD133 expression defines a tumor initiating cell

- population in primary human ovarian cancer’, *Stem Cells*, 27(12), 2875–2883. doi: 10.1002/stem.236.
- Dalesio, N. M. et al. (2018) ‘Olfactory, Taste, and Photo Sensory Receptors in Non-sensory Organs: It Just Makes Sense’, *Frontiers in Physiology*, 9(1673), 1–19. doi: 10.3389/fphys.2018.01673.
- Das, C. K. et al. (2019) ‘Exosome as a Novel Shuttle for Delivery of Therapeutics across Biological Barriers’, *Molecular Pharmaceutics*, 16(1), 24–40. doi: 10.1021/acs.molpharmaceut.8b00901.
- Dasgupta, A. et al. (2020) ‘Imaging-assisted anticancer nanotherapy’, *Theranostics*, 956–967. doi: 10.7150/thno.38288.
- Dasgupta, A., Lim, A. R. and Ghajar, C. M. (2017) ‘Circulating and disseminated tumor cells: harbingers or initiators of metastasis?’, *Molecular oncology*, 11(1), 40–61. doi: 10.1002/1878-0261.12022.
- Decarvalho, S., Rand, H. J. and Lewis, A. (1964) ‘Coupling of cyclic chemotherapeutic compounds to immune gamma-globulins’, *Nature*, 202(4929), 255–258. doi: 10.1038/202255a0.
- Deeks, E. D. (2019) ‘Polatuzumab Vedotin: First Global Approval’, *Drugs*, 79(13), 1467–1475. doi: 10.1007/s40265-019-01175-0.
- Denton, A. E., Roberts, E. W. and Fearon, D. T. (2018) ‘Stromal Cells in the Tumor Microenvironment.’, *Advances in experimental medicine and biology*, 1060, 99–114. doi: 10.1007/978-3-319-78127-3_6.
- Van Deun, J. et al. (2020) ‘Feasibility of Mechanical Extrusion to Coat Nanoparticles with Extracellular Vesicle Membranes’, *Cells*, 9, 1797. doi: 10.3390/cells9081797.
- Diaz, G. et al. (2018) ‘Protein Digestion, Ultrafiltration, and Size Exclusion Chromatography to Optimize the Isolation of Exosomes from Human Blood Plasma and Serum’, *Journal of Visualized Experiments*, (134), 57467. doi: 10.3791/57467.
- Dillekås, H., Rogers, M. S. and Straume, O. (2019) ‘Are 90% of deaths from cancer caused by metastases?’, *Cancer Medicine*, 8(12), 5574–5576. doi: 10.1002/cam4.2474.
- Dimitrov-Markov, S. et al. (2020) ‘Discovery of New Targets to Control Metastasis in Pancreatic Cancer by Single-cell Transcriptomics Analysis of Circulating Tumor Cells’, *Molecular cancer therapeutics*, 19(8), 1751–1760. doi: 10.1158/1535-7163.MCT-19-1166.

- Dolgin, E. (2018) 'First GPCR-directed antibody passes approval milestone', *Nature Reviews Drug Discovery*, 17(7), 457–459. doi: 10.1038/nrd.2018.103.
- Dotson, C. D. et al. (2008) 'Bitter taste receptors influence glucose homeostasis', *PLoS ONE*, 3(12). doi: 10.1371/journal.pone.0003974.
- Dowdy, S. F. (2017) 'Overcoming cellular barriers for RNA therapeutics', *Nature Biotechnology*, 35(3), 222–229. doi: 10.1038/nbt.3802.
- Dubochet, J. et al. (1988) 'Cryo-electron microscopy of vitrified specimens.', *Quarterly reviews of biophysics*, 21(2), 129–228.
- Dunbar, C. E. et al. (2018) 'Gene therapy comes of age', *Science*. doi: 10.1126/science.aan4672.
- El-Andaloussi, S. et al. (2012) 'Exosome-mediated delivery of siRNA in vitro and in vivo.', *Nature protocols*, 7(12), 2112–26. doi: 10.1038/nprot.2012.131.
- Endris, V. et al. (2019) 'Measurement of tumor mutational burden (TMB) in routine molecular diagnostics: in silico and real-life analysis of three larger gene panels', *International Journal of Cancer*, 144(9), 2303–2312. doi: 10.1002/ijc.32002.
- Engelman, J. A. et al. (2007) 'MET amplification leads to gefitinib resistance in lung cancer by activating ERBB3 signaling', *Science*, 316(5827), 1039–1043. doi: 10.1126/science.1141478.
- Eramo, A. et al. (2008) 'Identification and expansion of the tumorigenic lung cancer stem cell population', *Cell Death and Differentiation*, 15(3), 504–514. doi: 10.1038/sj.cdd.4402283.
- Fan, C. C. et al. (2017) 'EFHD2 promotes epithelial-to-mesenchymal transition and correlates with postsurgical recurrence of stage I lung adenocarcinoma', *Scientific Reports*, 7(14617), 1–11. doi: 10.1038/s41598-017-15186-y.
- Fares, J. et al. (2020) 'Molecular principles of metastasis: a hallmark of cancer revisited', *Signal Transduction and Targeted Therapy*, 5(28), 1–17. doi: 10.1038/s41392-020-0134-x.
- Farjadian, F. et al. (2019) 'Nanopharmaceuticals and nanomedicines currently on the market: Challenges and opportunities', *Nanomedicine*, 14(1), 93–126. doi: 10.2217/nmm-2018-0120.

- Feng, S. H. and Yang, S. T. (2019) 'The new 8th tmn staging system of lung cancer and its potential imaging interpretation pitfalls and limitations with ct image demonstrations', *Diagnostic and Interventional Radiology*, 270–279. doi: 10.5152/dir.2019.18458.
- Ferrer, I. et al. (2018) 'KRAS-Mutant non-small cell lung cancer: From biology to therapy', *Lung Cancer*, 53–64. doi: 10.1016/j.lungcan.2018.07.013.
- Finotti, A. et al. (2018) 'Liquid biopsy and PCR-free ultrasensitive detection systems in oncology (Review)', *International Journal of Oncology*, 1395–1434. doi: 10.3892/ijo.2018.4516.
- Fleischmann, K. K. et al. (2014) 'RNAi-mediated silencing of MLL-AF9 reveals leukemia-associated downstream targets and processes', *Molecular Cancer*, 13(27), 1–14. doi: 10.1186/1476-4598-13-27.
- De Francesco, E. M., Sotgia, F. and Lisanti, M. P. (2018) 'Cancer stem cells (CSCs): Metabolic strategies for their identification and eradication', *Biochemical Journal*, 475, 1611–1634. doi: 10.1042/BCJ20170164.
- Franses, J. W. et al. (2020) 'Pancreatic circulating tumor cell profiling identifies LIN28B as a metastasis driver and drug target', *Nature Communications*, 11(3303), 1–12. doi: 10.1038/s41467-020-17150-3.
- Friedl, P. and Gilmour, D. (2009) 'Collective cell migration in morphogenesis, regeneration and cancer', *Nature Reviews Molecular Cell Biology*, 10(7), 445–457. doi: 10.1038/nrm2720.
- Gad, A. A. and Balenga, N. (2020) 'The Emerging Role of Adhesion GPCRs in Cancer', *ACS Pharmacology and Translational Science*, 3(1), 29–42. doi: 10.1021/acspsci.9b00093.
- Gaj, T. et al. (2016) 'Genome-editing technologies: Principles and applications', *Cold Spring Harbor Perspectives in Biology*, 8(12). doi: 10.1101/cshperspect.a023754.
- Garces, F. et al. (2020) 'Molecular Insight into Recognition of the CGRPR Complex by Migraine Prevention Therapy Aimovig (Erenumab)', *Cell Reports*, 30(6), 1714–1723. doi: 10.1016/j.celrep.2020.01.029.
- Gay, L. J. and Felding-Habermann, B. (2011) 'Contribution of platelets to tumour metastasis.', *Nature reviews. Cancer*, 11(2), 123–34. doi: 10.1038/nrc3004.
- Gil-Bernabé, A. M. et al. (2012) 'Recruitment of monocytes/macrophages

- by tissue factor-mediated coagulation is essential for metastatic cell survival and premetastatic niche establishment in mice', *Blood*, 119(13), 3164–3175. doi: 10.1182/blood-2011-08-376426.
- Gkountela, S. and Aceto, N. (2016) 'Stem-like features of cancer cells on their way to metastasis', *Biology Direct*, 11(33), 1–14. doi: 10.1186/s13062-016-0135-4.
- Glendinning, J. I. et al. (2012) 'The role of T1r3 and Trpm5 in carbohydrate-induced obesity in mice', *Physiology and Behavior*, 107(1), 50–58. doi: 10.1016/j.physbeh.2012.05.023.
- Glumac, P. M. and LeBeau, A. M. (2018) 'The role of CD133 in cancer: a concise review', *Clinical and Translational Medicine*, 7(18), 1–14. doi: 10.1186/s40169-018-0198-1.
- Goh, W. J. et al. (2017) 'Bioinspired Cell-Derived Nanovesicles versus Exosomes as Drug Delivery Systems: a Cost-Effective Alternative', *Scientific Reports*, 7(1), 14322. doi: 10.1038/s41598-017-14725-x.
- Golding, B. et al. (2018) 'The function and therapeutic targeting of anaplastic lymphoma kinase (ALK) in non-small cell lung cancer (NSCLC)', *Molecular Cancer*, 17(52), 1–15. doi: 10.1186/s12943-018-0810-4.
- Gomez-Cuadrado, L. et al. (2017) 'Mouse models of metastasis: Progress and prospects', *DMM Disease Models and Mechanisms*, 10(9), 1061–1074. doi: 10.1242/dmm.030403.
- Green, M. R. et al. (2006) 'Abraxane®, a novel Cremophor®-free, albumin-bound particle form of paclitaxel for the treatment of advanced non-small-cell lung cancer', *Annals of Oncology*, 17(8), 1263–1268. doi: 10.1093/annonc/mdl104.
- Gribko, A. et al. (2019) 'Is small smarter? Nanomaterial-based detection and elimination of circulating tumor cells: Current knowledge and perspectives', *International Journal of Nanomedicine*, 14, 4187–4209. doi: 10.2147/IJN.S198319.
- Guo, Y. et al. (2019) 'Effects of exosomes on pre-metastatic niche formation in tumors', *Molecular Cancer*, 18(39), 1–11. doi: 10.1186/s12943-019-0995-1.
- Gupta, G. P. and Massagué, J. (2006) 'Cancer metastasis: building a framework.', *Cell*, 127(4), 679–95. doi: 10.1016/j.cell.2006.11.001.

- Habli, Z. et al. (2020) ‘Circulating tumor cell detection technologies and clinical utility: Challenges and opportunities’, *Cancers*, 12(7), 1–30. doi: 10.3390/cancers12071930.
- Hall, J. et al. (2016) ‘Delivery of therapeutic proteins via extracellular vesicles: Review and potential treatments for Parkinson’s disease, glioma and schwannoma’, *Cell Mol Neurobiol.*, 36(3), 417–427. doi: 10.1007/s10571-015-0309-0.Delivery.
- Hamilton, G. and Rath, B. (2017) ‘Circulating tumor cell interactions with macrophages: Implications for biology and treatment’, *Translational Lung Cancer Research*, 6(4), 418–430. doi: 10.21037/tlcr.2017.07.04.
- Hanahan, D. and Weinberg, R. A. (2011) ‘Hallmarks of Cancer: The Next Generation’, *Cell*, 144(5), 646–674. doi: 10.1016/j.cell.2011.02.013.
- Hardee, C. L. et al. (2017) ‘Advances in Non-Viral DNA Vectors for Gene Therapy’. doi: 10.3390/genes8020065.
- Harding, C. and Stahl, P. (1983) ‘Transferrin recycling in reticulocytes: pH and iron are important determinants of ligand binding and processing’, *Biochemical and Biophysical Research Communications*, 113(2), 650–658. doi: 10.1016/0006-291X(83)91776-X.
- Harding, C. V, Heuser, J. E. and Stahl, P. D. (2013) ‘Exosomes: looking back three decades and into the future.’, *The Journal of cell biology*, 200(4), 367–71. doi: 10.1083/jcb.201212113.
- Heeke, S. et al. (2019) ‘Never Travel Alone: The Crosstalk of Circulating Tumor Cells and the Blood Microenvironment’, *Cells*, 8(714), 1–12. doi: 10.3390/cells8070714.
- Hein, R., Uzundal, C. B. and Hennig, A. (2016) ‘Simple and rapid quantification of phospholipids for supramolecular membrane transport assays’, *Organic and Biomolecular Chemistry*, 14(7), 2182–2185. doi: 10.1039/c5ob02480c.
- Heist, R. S. et al. (2017) ‘Therapy of advanced Non-Small-cell lung cancer with an SN-38-Anti-Trop-2 drug conjugate, sacituzumab govitecan’, *Journal of Clinical Oncology*, 35(24), 2790–2797. doi: 10.1200/JCO.2016.72.1894.
- Hellmann, M. D. et al. (2018) ‘Nivolumab plus ipilimumab in lung cancer with a high tumor mutational burden’, *New England Journal of Medicine*, 378(22), 2093–2104. doi: 10.1056/NEJMoa1801946.

- Hen, O. and Barkan, D. (2020) 'Dormant disseminated tumor cells and cancer stem/progenitor-like cells: Similarities and opportunities', *Seminars in Cancer Biology*, 60, 157–165. doi: 10.1016/j.semcancer.2019.09.002.
- Hergueta-Redondo, M. et al. (2014) 'Gasdermin-B promotes invasion and metastasis in breast cancer cells.', *PloS one*. Edited by H. Wanjin, 9(3), 1–15. doi: 10.1371/journal.pone.0090099.
- Hermann, P. C. et al. (2007) 'Distinct Populations of Cancer Stem Cells Determine Tumor Growth and Metastatic Activity in Human Pancreatic Cancer', *Cell Stem Cell*, 1(3), 313–323. doi: 10.1016/j.stem.2007.06.002.
- Herreros-Pomares, A. et al. (2019) 'Lung tumorspheres reveal cancer stem cell-like properties and a score with prognostic impact in resected non-small-cell lung cancer', *Cell Death and Disease*, 10(660), 1–14. doi: 10.1038/s41419-019-1898-1.
- Hiratsuka, S. et al. (2006) 'Tumour-mediated upregulation of chemoattractants and recruitment of myeloid cells predetermines lung metastasis', *Nature Cell Biology*, 8(12), 1369–1375. doi: 10.1038/ncb1507.
- Hodi, F. S. et al. (2010) 'Improved Survival with Ipilimumab in Patients with Metastatic Melanoma', *New England Journal of Medicine*, 363(8), 711–723. doi: 10.1056/NEJMoa1003466.
- Hoshino, A. et al. (2015) 'Tumour exosome integrins determine organotropic metastasis.', *Nature*, 527(7578), 329–35. doi: 10.1038/nature15756.
- Howitt, M. R. et al. (2020) 'The Taste Receptor TAS1R3 Regulates Small Intestinal Tuft Cell Homeostasis', *ImmunoHorizons*, 4(1), 23–32. doi: 10.4049/immunohorizons.1900099.
- Howlader, N. et al. (2020) SEER Cancer Statistics Review, 1975-2017 - NCI. Available at: https://seer.cancer.gov/csr/1975_2016/ (Accessed: 10 September 2019).
- Hoy, S. M. (2018) 'Patisiran: First Global Approval', *Drugs*, 78(15), 1625–1631. doi: 10.1007/s40265-018-0983-6.
- Hoy, S. M. (2019) 'Onasemnogene Apeparvovec: First Global Approval', *Drugs*, 79(11), 1255–1262. doi: 10.1007/s40265-019-01162-5.

- Huang, K. L. et al. (2017) 'Proteogenomic integration reveals therapeutic targets in breast cancer xenografts', *Nature Communications*, 8(14864), 1–17. doi: 10.1038/ncomms14864.
- Hüsemann, Y. et al. (2008) 'Systemic Spread Is an Early Step in Breast Cancer', *Cancer Cell*, 13(1), 58–68. doi: 10.1016/j.ccr.2007.12.003.
- Imai, K. and Takaoka, A. (2006) 'Comparing antibody and small-molecule therapies for cancer', *Nature Reviews Cancer*, 6(9), 714–727. doi: 10.1038/nrc1913.
- Inoue, A. et al. (2019) 'Current and future horizons of patient-derived xenograft models in colorectal cancer translational research', *Cancers*, 11(1321), 1–24. doi: 10.3390/cancers11091321.
- Izumchenko, E. et al. (2017) 'Patient-derived xenografts effectively capture responses to oncology therapy in a heterogeneous cohort of patients with solid tumors', *Annals of Oncology*, 28(10), 2595–2605. doi: 10.1093/annonc/mdx416.
- Jan, A. et al. (2019) 'Biology, Pathophysiological Role, and Clinical Implications of Exosomes: A Critical Appraisal', *Cells*, 8(2), 99. doi: 10.3390/cells8020099.
- Jang, S. C. et al. (2013) 'Bioinspired exosome-mimetic nanovesicles for targeted delivery of chemotherapeutics to malignant tumors.', *ACS nano*, 7(9), 7698–7710. doi: 10.1021/nn402232g.
- Jebbink, M. et al. (2020) 'The force of HER2 – A druggable target in NSCLC?', *Cancer Treatment Reviews*, 86, 101996. doi: 10.1016/j.ctrv.2020.101996.
- Jen, E. Y. et al. (2018) 'Fda approval: Gemtuzumab ozogamicin for the treatment of adults with newly diagnosed cd33-positive acute myeloid leukemia', *Clinical Cancer Research*, 24(14), 3242–3246. doi: 10.1158/1078-0432.CCR-17-3179.
- Jiang, P. et al. (2004) 'The cysteine-rich region of T1R3 determines responses to intensely sweet proteins', *Journal of Biological Chemistry*, 279(43), 45068–45075. doi: 10.1074/jbc.M406779200.
- Jo, M. and Jung, S. T. (2016) 'Engineering therapeutic antibodies targeting G-protein-coupled receptors', *Experimental & molecular medicine*, 1–9. doi: 10.1038/emm.2015.105.
- Johnsen, K. B. et al. (2018) 'On the use of liposome controls in studies

- investigating the clinical potential of extracellular vesicle-based drug delivery systems – A commentary’, *Journal of Controlled Release*, 269, 10–14. doi: 10.1016/j.jconrel.2017.11.002.
- Jolly, M. K. et al. (2019) ‘Hybrid epithelial/mesenchymal phenotypes promote metastasis and therapy resistance across carcinomas’, *Pharmacology and Therapeutics*, 194, 161–184. doi: 10.1016/j.pharmthera.2018.09.007.
- Jonkman, J. E. N. et al. (2014) ‘Cell Adhesion & Migration An introduction to the wound healing assay using livecell microscopy An introduction to the wound healing assay using livecell microscopy’, *Cell adhesion and migration*, 8(5), 440–451. doi: 10.4161/cam.36224.
- Joyce, J. A. and Pollard, J. W. (2009) ‘Microenvironmental regulation of metastasis.’, *Nature reviews. Cancer*, 9(4), 239–52. doi: 10.1038/nrc2618.
- Justus, C. R. et al. (2014) ‘In vitro cell migration and invasion assays’, *Journal of Visualized Experiments*, 88(e51046), 1–8. doi: 10.3791/51046.
- Kang, Y. and Pantel, K. (2013) ‘Tumor Cell Dissemination: Emerging Biological Insights from Animal Models and Cancer Patients’, *Cancer Cell*, 23(5), 573–581. doi: 10.1016/j.ccr.2013.04.017.
- Katz, J., Janik, J. E. and Younes, A. (2011) ‘Brentuximab vedotin (SGN-35)’, *Clinical Cancer Research*, 17(20), 6428–6436. doi: 10.1158/1078-0432.CCR-11-0488.
- Kazama, S. et al. (2018) ‘Expression of the stem cell marker CD133 is related to tumor development in colorectal carcinogenesis’, *Asian Journal of Surgery*, 41(3), 274–278. doi: 10.1016/j.asjsur.2016.12.002.
- Khanna, C. and Hunter, K. (2005) ‘Modeling metastasis in vivo’, *Carcinogenesis*, 26(3), 513–523. doi: 10.1093/carcin/bgh261.
- Khoury, S. et al. (2018) ‘Quantification of lipids: Model, reality, and compromise’, *Biomolecules*, 1–16. doi: 10.3390/biom8040174.
- Khunger, A., Khunger, M. and Velcheti, V. (2018) ‘Dabrafenib in combination with trametinib in the treatment of patients with BRAF V600-positive advanced or metastatic non-small cell lung cancer: clinical evidence and experience’, *Therapeutic Advances in Respiratory Disease*, 12, 1–9. doi: 10.1177/1753466618767611.

- Kidess-Sigal, E. et al. (2016) 'Enumeration and targeted analysis of KRAS, BRAF and PIK3CA mutations in CTCs captured by a label-free platform: Comparison to ctDNA and tissue in metastatic colorectal cancer', *Oncotarget*, 7(51), 85349–85364. doi: 10.18632/oncotarget.13350.
- Kim, W. T. and Ryu, C. J. (2017) 'Cancer stem cell surface markers on normal stem cells', *BMB Reports*, 285–298. doi: 10.5483/BMBRep.2017.50.6.039.
- Kitamura, T., Qian, B. Z. and Pollard, J. W. (2015) 'Immune cell promotion of metastasis', *Nature Reviews Immunology*, 15(2), 73–86. doi: 10.1038/nri3789.
- Klebanov, L. and Yakovlev, A. (2007) 'How high is the level of technical noise in microarray data?', *Biology Direct*, 9. doi: 10.1186/1745-6150-2-9.
- Kojima, I. et al. (2014) 'Sweet Taste-Sensing Receptors Expressed in Pancreatic β -Cells: Sweet Molecules Act as Biased Agonists', *Endocrinology and metabolism*, 29(1), 12–19. doi: 10.3803/ENM.2014.29.1.12.
- Kojima, I. and Nakagawa, Y. (2011) 'The role of the sweet taste receptor in enteroendocrine cells and pancreatic β -cells', *Diabetes and Metabolism Journal*, 451–457. doi: 10.4093/dmj.2011.35.5.451.
- Kooijmans, S. a a et al. (2013) 'Electroporation-induced siRNA precipitation obscures the efficiency of siRNA loading into extracellular vesicles', *Journal of Controlled Release*, 172(1), 229–238. doi: 10.1016/j.jconrel.2013.08.014.
- Kosaka, T. et al. (2017) 'Response heterogeneity of EGFR and HER2 exon 20 insertions to covalent EGFR and HER2 inhibitors', *Cancer Research*, 77(10), 2712–2721. doi: 10.1158/0008-5472.CAN-16-3404.
- Krebs, M. G. et al. (2011) 'Evaluation and prognostic significance of circulating tumor cells in patients with non-small-cell lung cancer', *Journal of Clinical Oncology*, 29(12), 1556–1563. doi: 10.1200/JCO.2010.28.7045.
- Kyung-A Hyun et al. (2016) 'Epithelial-to-mesenchymal transition leads to loss of EpCAM and different physical properties in circulating tumor cells from metastatic breast cancer', *Oncotarget*, 7(17), 24677–24687. doi: 10.18632/oncotarget.8250.

- de la Fuente, M. et al. (2012) 'Exploring the efficiency of gallic acid-based dendrimers and their block copolymers with PEG as gene carriers.', *Nanomedicine* (London, England), 7(11), 1667–81. doi: 10.2217/nnm.12.51.
- de la Fuente, M., Seijo, B. and Alonso, M. J. (2008) 'Design of novel polysaccharidic nanostructures for gene delivery.', *Nanotechnology*, 19(7), 075105. doi: 10.1088/0957-4484/19/7/075105.
- Lai, W. V. et al. (2019) 'Afatinib in patients with metastatic or recurrent HER2-mutant lung cancers: a retrospective international multicentre study', *European Journal of Cancer*, 109, 28–35. doi: 10.1016/j.ejca.2018.11.030.
- Lallo, A. et al. (2017) 'Circulating tumor cells and CDX models as a tool for preclinical drug development', *Translational Lung Cancer Research*, 6(4), 397–408. doi: 10.21037/tlcr.2017.08.01.
- Lamb, Y. N. (2017) 'Inotuzumab Ozogamicin: First Global Approval', *Drugs*, 77(14), 1603–1610. doi: 10.1007/s40265-017-0802-5.
- Lamichhane, T. N., Raiker, R. S. and Jay, S. M. (2015) 'Exogenous DNA loading into extracellular vesicles via electroporation is size-dependent and enables limited gene delivery', *Molecular Pharmaceutics*, 12(10), 3650–3657. doi: 10.1021/acs.molpharmaceut.5b00364.
- Lavanya, V. et al. (2014) 'Small molecule inhibitors as emerging cancer therapeutics', *Integr Cancer Sci Ther.*, 1(3), 39–46. doi: 10.15761/ICST.1000109.
- Lazzari, C. et al. (2017) 'Historical evolution of second-line therapy in non-small cell lung cancer', *Frontiers in Medicine*, 4(4), 1–8. doi: 10.3389/fmed.2017.00004.
- Leach, J., Morton, J. P. and Sansom, O. J. (2019) 'Neutrophils: Homing in on the myeloid mechanisms of metastasis', *Molecular Immunology*, 110, 69–76. doi: 10.1016/j.molimm.2017.12.013.
- Lecharpentier, A. et al. (2011) 'Detection of circulating tumour cells with a hybrid (epithelial/ mesenchymal) phenotype in patients with metastatic non-small cell lung cancer', *British Journal of Cancer*, 105(9), 1338–1341. doi: 10.1038/bjc.2011.405.
- Ledford, H. (2016) 'Al-Ahmady', *Nature*, 533(7603), 304–305. doi: 10.1038/533304a.

- Lee, Y. T., Tan, Y. J. and Oon, C. E. (2018) 'Molecular targeted therapy: Treating cancer with specificity', *European Journal of Pharmacology*, 834, 188–196. doi: 10.1016/j.ejphar.2018.07.034.
- Li, G. et al. (2020) 'Epididymal protein 3A is upregulated and promotes cell proliferation in non-small cell lung cancer', *Oncology Letters*, 19(6), 4024–4030. doi: 10.3892/ol.2020.11517.
- Li, S. P. et al. (2018) 'Exosomal cargo-loading and synthetic exosome-mimics as potential therapeutic tools', *Acta Pharmacologica Sinica*, 39(4), 542–551. doi: 10.1038/aps.2017.178.
- Li, X. et al. (2002) 'Human receptors for sweet and umami taste', *Proceedings of the National Academy of Sciences*, 99(7), 4692–4696. doi: 10.1073/pnas.072090199.
- Li, X. et al. (2019) 'Challenges and opportunities in exosome research—Perspectives from biology, engineering, and cancer therapy', *APL Bioengineering*, 3(1), 011503. doi: 10.1063/1.5087122.
- Li, Y. F. et al. (2012) 'Cultivation and identification of colon cancer stem cell-derived spheres from the Colo205 cell line', *Brazilian Journal of Medical and Biological Research*, 45(3), 197–204. doi: 10.1590/S0100-879X2012007500015.
- Liang, H. and Wang, M. (2020) 'MET oncogene in non-small cell lung cancer: Mechanism of MET dysregulation and agents targeting the HGF/c-met axis', *OncoTargets and Therapy*, 2491–2510. doi: 10.2147/OTT.S231257.
- Lianidou, E. S. (2014) 'Molecular Characterization of Circulating Tumor Cells: Holy Grail for Personalized Cancer Treatment?', *Clinical Chemistry*, 60(10), 1249–1251. doi: 10.1373/clinchem.2014.230144.
- Lindeman, N. I. et al. (2018) 'Updated Molecular Testing Guideline for the Selection of Lung Cancer Patients for Treatment With Targeted Tyrosine Kinase Inhibitors: Guideline From the College of American Pathologists, the International Association for the Study of Lung Cancer, and the ', *Journal of Molecular Diagnostics*, 20(2), 129–159. doi: 10.1016/j.jmoldx.2017.11.004.
- Liou, G. Y. (2019) 'CD133 as a regulator of cancer metastasis through the cancer stem cells', *International Journal of Biochemistry and Cell Biology*, 106, 1–7. doi: 10.1016/j.biocel.2018.10.013.

- Liu, D. et al. (2019) 'LSEctin on tumor-associated macrophages enhances breast cancer stemness via interaction with its receptor BTN3A3', *Cell Research*, 29(5), 365–378. doi: 10.1038/s41422-019-0155-6.
- Liu, J. and Wang, X. (2019) 'Focus on exosomes—From pathogenic mechanisms to the potential clinical application value in lymphoma', *Journal of Cellular Biochemistry*, 120(12), 19220–19228. doi: 10.1002/jcb.29241.
- Liu, K. et al. (2018) 'miR-145 inhibits human non-small-cell lung cancer growth by dual-targeting R1OK2 and NOB1', *International Journal of Oncology*, 53(1), 257–265. doi: 10.3892/ijo.2018.4393.
- Liu, Q., Liao, Q. and Zhao, Y. (2016) 'Myeloid-derived suppressor cells (MDSC) facilitate distant metastasis of malignancies by shielding circulating tumor cells (CTC) from immune surveillance', *Medical Hypotheses*, 87, 34–39. doi: 10.1016/j.mehy.2015.12.007.
- Liu, W. T. et al. (2019) 'Expression of ALDH1A1 and CD133 is associated with the prognosis and effect of different chemotherapeutic regimens in gastric cancer', *Oncology Letters*, 18(5), 4573–4582. doi: 10.3892/ol.2019.10798.
- Liu, Z. et al. (2018) 'Isolation and characterization of human urine extracellular vesicles', *Cell Stress and Chaperones*, 23(5), 943–953. doi: 10.1007/s12192-018-0902-5.
- Llorente, A. et al. (2013) 'Molecular lipidomics of exosomes released by PC-3 prostate cancer cells', *Biochimica et Biophysica Acta - Molecular and Cell Biology of Lipids*, 1831(7), 1302–1309. doi: 10.1016/j.bbalip.2013.04.011.
- Lönn, P. et al. (2016) 'Enhancing Endosomal Escape for Intracellular Delivery of Macromolecular Biologic Therapeutics', *Scientific reports*, 6(32301), 1–9. doi: 10.1038/srep32301.
- López-Otín, C. and Matrisian, L. M. (2007) 'Emerging roles of proteases in tumour suppression', *Nature Reviews Cancer*, 7(10), 800–808. doi: 10.1038/nrc2228.
- Lu, C. et al. (2012) 'Phase I clinical trial of systemically administered TUSC2(FUS1)-nanoparticles mediating functional gene transfer in humans.', *PloS one*, 7(4). doi: 10.1371/journal.pone.0034833.
- Luca, A. C. et al. (2013) 'Impact of the 3D Microenvironment on

- Phenotype, Gene Expression, and EGFR Inhibition of Colorectal Cancer Cell Lines’, *PLoS ONE*, 8(3), 1–11. doi: 10.1371/journal.pone.0059689.
- Lunavat, T. R. et al. (2016) ‘RNAi delivery by exosome-mimetic nanovesicles – Implications for targeting c-Myc in cancer’, *Biomaterials*, 102, 231–238. doi: 10.1016/j.biomaterials.2016.06.024.
- Lv, H. et al. (2006) ‘Toxicity of cationic lipids and cationic polymers in gene delivery’, *Journal of Controlled Release*, 114(1), 100–109. doi: 10.1016/j.jconrel.2006.04.014.
- Lydic, T. A. et al. (2015) ‘Rapid and comprehensive “shotgun” lipidome profiling of colorectal cancer cell derived exosomes’, *Methods*, 87, 83–95. doi: 10.1016/j.ymeth.2015.04.014.
- Majem, M. et al. (2019) ‘SEOM clinical guidelines for the treatment of non-small cell lung cancer (2018)’, *Clinical and Translational Oncology*, 21(1), 3–17. doi: 10.1007/s12094-018-1978-1.
- Mariscal, J. et al. (2016) ‘Molecular Profiling of Circulating Tumour Cells Identifies Notch1 as a Principal Regulator in Advanced Non-Small Cell Lung Cancer’, *Scientific Reports*, 6(37820), 1–9. doi: 10.1038/srep37820.
- Mason, J. A. et al. (2017) ‘Metabolism during ECM Detachment: Achilles Heel of Cancer Cells?’, *Trends in Cancer*, 3(7), 475–481. doi: 10.1016/j.trecan.2017.04.009.
- Massagué, J. and Obenauf, A. C. (2016) ‘Metastatic colonization’, *Nature*, 529(7586), 298–306. doi: 10.1038/nature17038.
- Masubuchi, Y. et al. (2017) ‘T1R3 homomeric sweet taste receptor regulates adipogenesis through Gas-mediated microtubules disassembly and Rho activation in 3T3-L1 cells’, *PLoS ONE*, 12(7), 1–15. doi: 10.1371/journal.pone.0181293.
- Matsumura, Y. and Maeda, H. (1986) ‘A new concept for macromolecular therapeutics in cancer chemotherapy: mechanism of tumorotropic accumulation of proteins and the antitumor agent smancs.’, *Cancer research*, 46(12 Pt 1), 6387–92.
- McErlean, E. M., McCrudden, C. M. and McCarthy, H. O. (2016) ‘Delivery of nucleic acids for cancer gene therapy: overcoming extra- and intra-cellular barriers’, *Therapeutic Delivery*, 7(9), 619–637. doi:

- 10.1002/9781118903681.
- Meng, X. et al. (2009) 'Both CD133+ and CD133- subpopulations of A549 and H446 cells contain cancer-initiating cells', *Cancer Science*, 100(6), 1040–1046. doi: 10.1111/j.1349-7006.2009.01144.x.
- Miles, F. L. et al. (2008) 'Stepping out of the flow: capillary extravasation in cancer metastasis', *Clinical & Experimental Metastasis*, 25(4), 305–324. doi: 10.1007/s10585-007-9098-2.
- Miranda-Lorenzo, I. et al. (2014) 'Intracellular autofluorescence: A biomarker for epithelial cancer stem cells', *Nature Methods*, 11(11), 1161–1169. doi: 10.1038/nmeth.3112.
- Mo, D. et al. (2017) 'MiRNA-145 suppresses lung adenocarcinoma cell invasion and migration by targeting N-cadherin', *Biotechnology Letters*, 39(5), 701–710. doi: 10.1007/s10529-017-2290-9.
- Mohammadinejad, R. et al. (2020) 'In vivo gene delivery mediated by non-viral vectors for cancer therapy', *Journal of Controlled Release*, 325, 249–275. doi: 10.1016/j.jconrel.2020.06.038.
- Molinaro, R. et al. (2016) 'Biomimetic proteolipid vesicles for targeting inflamed tissues', *Nature Materials*, 15(9), 1037–46. doi: 10.1037/emo0000122.Do.
- Molinaro, R. et al. (2020) 'Leukocyte-mimicking nanovesicles for effective doxorubicin delivery to treat breast cancer and melanoma', *Biomaterials Science*, 8(1), 333–341. doi: 10.1039/c9bm01766f.
- Moro, M. et al. (2012) 'Patient-Derived Xenografts of Non Small Cell Lung Cancer: Resurgence of an Old Model for Investigation of Modern Concepts of Tailored Therapy and Cancer Stem Cells', *Journal of Biomedicine and Biotechnology*, 2012, 11. doi: 10.1155/2012/568567.
- Moro, M. et al. (2017) 'Establishment of patient derived xenografts as functional testing of lung cancer aggressiveness', *Scientific reports*, 7(6689), 1–12. doi: 10.1038/s41598-017-06912-7.
- Moro, M. et al. (2019) 'Coated cationic lipid-nanoparticles entrapping miR-660 inhibit tumor growth in patient-derived xenografts lung cancer models', *Journal of Controlled Release*, 308, 44–56. doi: 10.1016/j.jconrel.2019.07.006.
- Motzer, R. J. et al. (2015) 'Nivolumab versus Everolimus in Advanced Renal-Cell Carcinoma', *New England Journal of Medicine*, 373(19),

1803–1813. doi: 10.1056/NEJMoa1510665.

- Muinelo-Romay, L. et al. (2014) ‘Evaluation of circulating tumor cells and related events as prognostic factors and surrogate biomarkers in advanced NSCLC patients receiving first-line systemic treatment’, *Cancers*, 6(1), 153–165. doi: 10.3390/cancers6010153.
- Mullard, A. (2018) ‘FDA approves second GPCR-targeted antibody’, *Nature reviews. Drug discovery*, 17(9), 613. doi: 10.1038/nrd.2018.153.
- Mwesige, B., Yeo, S.-G. and Yoo, B. C. (2019) ‘Circulating Tumor Cells: Liquid Biopsy for Early Detection of Cancer’, *Soonchunhyang Medical Science*, 25(1), 1–9. doi: 10.15746/sms.19.001.
- Nakagawa, Y. et al. (2014) ‘Glucose promotes its own metabolism by acting on the cell-surface glucose-sensing receptor T1R3’, *Endocrine Journal*, 61(2), 119–131. doi: 10.1507/endocrj.EJ13-0431.
- Naseri, Z. et al. (2018) ‘Exosome-mediated delivery of functionally active miRNA-142-3p inhibitor reduces tumorigenicity of breast cancer in vitro and in vivo’, *International Journal of Nanomedicine*, 13, 7727–7747. doi: 10.2147/IJN.S182384.
- National Cancer Institute (2020) About Cancer - National Cancer Institute. Available at: <https://www.cancer.gov/about-cancer> (Accessed: 27 May 2020).
- Nejadmoghaddam, M.-R. et al. (2019) ‘Antibody-Drug Conjugates: Possibilities and Challenges.’, *Avicenna journal of medical biotechnology*, 11(1), 3–23.
- Nguyen, L. V. et al. (2012) ‘Cancer stem cells: An evolving concept’, *Nature Reviews Cancer*, 133–143. doi: 10.1038/nrc3184.
- Nie, H. et al. (2020) ‘Use of lung-specific exosomes for miRNA-126 delivery in non-small cell lung cancer’, *Nanoscale*, 12(2), 877–887. doi: 10.1039/c9nr09011h.
- Norman, D. J. et al. (1988) ‘Early Use of OKT3 Monoclonal Antibody in Renal Transplantation to Prevent Rejection’, *American Journal of Kidney Diseases*, 11(2), 107–110. doi: 10.1016/S0272-6386(88)80190-2.
- O’Brien, K. et al. (2020) ‘RNA delivery by extracellular vesicles in mammalian cells and its applications’, *Nature Reviews Molecular Cell Biology*, 1–22. doi: 10.1038/s41580-020-0251-y.

- Oczko-Wojciechowska, M. et al. (2020) 'Impact of the Tumor Microenvironment on the Gene Expression Profile in Papillary Thyroid Cancer', *Pathobiology*, 87(Suppl. 2), 143–154. doi: 10.1159/000507223.
- Ojha, T. et al. (2017) 'Pharmacological and physical vessel modulation strategies to improve EPR-mediated drug targeting to tumors', *Advanced Drug Delivery Reviews*, 119, 44–60. doi: 10.1016/j.addr.2017.07.007.
- de Oliveira Andrade, L. (2016) 'Understanding the role of cholesterol in cellular biomechanics and regulation of vesicular trafficking: The power of imaging', *Biomedical Spectroscopy and Imaging*, 5(s1), S101–S117. doi: 10.3233/bsi-160157.
- Oskarsson, T., Batlle, E. and Massagué, J. (2014) 'Metastatic stem cells: Sources, niches, and vital pathways', *Cell Stem Cell*, 14(3), 306–321. doi: 10.1016/j.stem.2014.02.002.
- Ozpolat, B., Sood, A. K. and Lopez-Berestein, G. (2014) 'Liposomal siRNA nanocarriers for cancer therapy.', *Advanced drug delivery reviews*, 66, 110–6. doi: 10.1016/j.addr.2013.12.008.
- Pahle, J. and Walther, W. (2015) 'Vectors and strategies for nonviral cancer gene therapy', *Expert Opinion on Biological Therapy*, 16(4), 443–461. doi: 10.1517/14712598.2016.1134480.
- Paik, P. K. et al. (2015) 'Response to MET inhibitors in patients with stage IV lung adenocarcinomas harboring met mutations causing exon 14 skipping', *Cancer Discovery*, 5(8), 842–850. doi: 10.1158/2159-8290.CD-14-1467.
- Pakkala, S. and Ramalingam, S. S. (2018) 'Personalized therapy for lung cancer: striking a moving target', *JCI insight*, 3(15), 1–14. doi: 10.1172/jci.insight.120858.
- Di Paolo, D. et al. (2011) 'Selective therapeutic targeting of the anaplastic lymphoma kinase with liposomal siRNA induces apoptosis and inhibits angiogenesis in neuroblastoma', *Molecular Therapy*, 19(12), 2201–2212. doi: 10.1038/mt.2011.142.
- Parodi, A. et al. (2017) 'Bio-inspired engineering of cell- and virus-like nanoparticles for drug delivery', *Biomaterials*, 147, 155–168. doi: 10.1016/j.biomaterials.2017.09.020.

- Pascual, G. et al. (2017) 'Targeting metastasis-initiating cells through the fatty acid receptor CD36', *Nature*, 541(7635), 41–45. doi: 10.1038/nature20791.
- Pastushenko, I. et al. (2018) 'Identification of the tumour transition states occurring during EMT', *Nature*, 556(7702), 463–468. doi: 10.1038/s41586-018-0040-3.
- Pathan, M. et al. (2015) 'FunRich: An open access standalone functional enrichment and interaction network analysis tool', *Proteomics*, 15(15), 2597–2601. doi: 10.1002/pmic.201400515.
- Pathan, M. et al. (2017) 'A novel community driven software for functional enrichment analysis of extracellular vesicles data.', *Journal of extracellular vesicles*, 6(1), 1321455. doi: 10.1080/20013078.2017.1321455.
- Patil, S. M., Sawant, S. S. and Kunda, N. K. (2020) 'Exosomes as drug delivery systems: A brief overview and progress update', *European Journal of Pharmaceutics and Biopharmaceutics*, 154, 259–269. doi: 10.1016/j.ejpb.2020.07.026.
- Patil, T. et al. (2019) 'Targeted therapies for ROS1-rearranged non-small cell lung cancer', *Drugs of Today*, 55(10), 641–652. doi: 10.1358/dot.2019.55.10.3030646.
- Peer, D. et al. (2007) 'Nanocarriers as an emerging platform for cancer therapy.', *Nature nanotechnology*, 2(12), 751–760. doi: 10.1038/nnano.2007.387.
- Peinado, H. et al. (2017) 'Pre-metastatic niches: organ-specific homes for metastases', *Nature Reviews Cancer*, 17(5), 302–317. doi: 10.1038/nrc.2017.6.
- Pelletier, J. P. R. and Mukhtar, F. (2020) 'Passive Monoclonal and Polyclonal Antibody Therapies', in *Immunologic Concepts in Transfusion Medicine*, 251–348. doi: 10.1016/b978-0-323-67509-3.00016-0.
- Pelt, J. et al. (2018) 'Chloroquine and nanoparticle drug delivery: A promising combination', *Pharmacology & Therapeutics*, 191, 43–49. doi: 10.1016/j.pharmthera.2018.06.007.
- Peng, H. et al. (2020) 'Exosome: a significant nano-scale drug delivery carrier', *Journal of Materials Chemistry B*. doi: 10.1039/d0tb01499k.

- Perez-Hernandez, D. et al. (2013) 'The intracellular interactome of tetraspanin-enriched microdomains reveals their function as sorting machineries toward exosomes.', *The Journal of biological chemistry*, 288(17), 11649–61. doi: 10.1074/jbc.M112.445304.
- Pfaffl, M. W. (2001) 'A new mathematical model for relative quantification in real-time RT-PCR.', *Nucleic acids research*, 29(9), e45. doi: 10.1093/nar/29.9.e45.
- Pijuan, J. et al. (2019) 'In vitro cell migration, invasion, and adhesion assays: From cell imaging to data analysis', *Frontiers in Cell and Developmental Biology*, 7, 1–16. doi: 10.3389/fcell.2019.00107.
- Di Pizio, A., Behrens, M. and Krautwurst, D. (2019) 'Beyond the flavour: The potential druggability of chemosensory G protein-coupled receptors', *International Journal of Molecular Sciences*, 20(6), 7–9. doi: 10.3390/ijms20061402.
- Planchard, D. et al. (2016) 'Dabrafenib plus trametinib in patients with previously treated BRAFV600E-mutant metastatic non-small cell lung cancer: an open-label, multicentre phase 2 trial', *The Lancet Oncology*, 17(7), 984–993. doi: 10.1016/S1470-2045(16)30146-2.
- Planchard, D. et al. (2018) 'Metastatic non-small cell lung cancer: ESMO Clinical Practice Guidelines for diagnosis, treatment and follow-up', *Annals of Oncology*, 29(Supplement 4), iv192–iv237. doi: 10.1093/annonc/mdy275.
- Pucci, C., Martinelli, C. and Ciofani, G. (2019) 'Innovative approaches for cancer treatment: Current perspectives and new challenges', *ecancermedicalscience*, 13(961), 1–26. doi: 10.3332/ecancer.2019.961.
- Qin, A. et al. (2016) 'Mechanisms of immune evasion and current status of checkpoint inhibitors in non-small cell lung cancer', *Cancer Medicine*, 2567–2578. doi: 10.1002/cam4.819.
- Qiu, X. et al. (2012) 'Characterization of sphere-forming cells with stem-like properties from the small cell lung cancer cell line H446', *Cancer Letters*, 323(2), 161–170. doi: 10.1016/j.canlet.2012.04.004.
- Rafei, H., Mehta, R. S. and Rezvani, K. (2019) 'Editorial: Cellular Therapies in Cancer', *Frontiers in Immunology*, 10, 1–3. doi: 10.3389/fimmu.2019.02788.
- Raggi, C. et al. (2015) 'Cancer stem cells and tumor-associated

- macrophages: A roadmap for multitargeting strategies’, *Oncogene*, 35(6), 671–682. doi: 10.1038/onc.2015.132.
- Ramamoorth, M. and Narvekar, A. (2015) ‘Non viral vectors in gene therapy - An overview’, *Journal of Clinical and Diagnostic Research*, 9(1), GE01–GE06. doi: 10.7860/JCDR/2015/10443.5394.
- Reck, M. et al. (2019) ‘Updated analysis of KEYNOTE-024: Pembrolizumab versus platinum-based chemotherapy for advanced non–small-cell lung cancer with PD-L1 tumor proportion score of 50% or greater’, *Journal of Clinical Oncology*, 37(7), 537–546. doi: 10.1200/JCO.18.00149.
- Record, M. et al. (2014) ‘Exosomes as new vesicular lipid transporters involved in cell-cell communication and various pathophysiologies’, *Biochimica et Biophysica Acta - Molecular and Cell Biology of Lipids*, 1841(1), 108–120. doi: 10.1016/j.bbalip.2013.10.004.
- Reungwetwattana, T. et al. (2017) ‘The race to target MET exon 14 skipping alterations in non-small cell lung cancer: The Why, the How, the Who, the Unknown, and the Inevitable’, *Lung Cancer*, 27–37. doi: 10.1016/j.lungcan.2016.11.011.
- Ri, L. et al. (2006) ‘ANNEX I SUMMARY OF PRODUCT CHARACTERISTICS - Glivec’, 809–822.
- Robert, C. et al. (2014) ‘Nivolumab in Previously Untreated Melanoma without BRAF Mutation’, *New England Journal of Medicine*, 372(4), 320–330. doi: 10.1056/NEJMoa1412082.
- Robichaux, J. P. et al. (2018) ‘Mechanisms and clinical activity of an EGFR and HER2 exon 20-selective kinase inhibitor in non-small cell lung cancer’, *Nature Medicine*, 24(5), 638–646. doi: 10.1038/s41591-018-0007-9.
- Robino, A. et al. (2019) ‘A Brief Review of Genetic Approaches to the Study of Food Preferences: Current Knowledge and Future Directions’, *Nutrients*, 11(8), 1735. doi: 10.3390/nu11081735.
- Rodrigues, G. A. et al. (2019) ‘Pharmaceutical Development of AAV-Based Gene Therapy Products for the Eye’, *Pharmaceutical Research*. doi: 10.1007/s11095-018-2554-7.
- Roma-Rodrigues, C. et al. (2020) ‘Gene Therapy in Cancer Treatment: Why Go Nano?’, *Pharmaceutics*, 12(233), 1–34. doi:

- 10.3390/pharmaceutics12030233.
- Russo, A. et al. (2020) 'NTRK and NRG1 gene fusions in advanced non-small cell lung cancer (NSCLC)', *Precision Cancer Medicine*, 3(0), 14–14. doi: 10.21037/pcm.2020.03.02.
- Rybinski, B. and Yun, K. (2016) 'Addressing intra-tumoral heterogeneity and therapy resistance', *Oncotarget*, 7(44), 72322–72342. doi: 10.18632/oncotarget.11875.
- Saeed, A. I. et al. (2003) 'TM4: A Free, Open-Source System for Microarray Data Management and Analysis', *BioTechniques*, 34(2), 374–378. doi: 10.2144/03342mt01.
- Saeed, A. I. et al. (2006) 'TM4 microarray software suite.', *Methods in enzymology*, 411, 134–93. doi: 10.1016/S0076-6879(06)11009-5.
- Saini, M., Szczerba, B. M. and Aceto, N. (2019) 'Circulating tumor cell-neutrophil tango along the metastatic process', *Cancer Research*, 6067–6073. doi: 10.1158/0008-5472.CAN-19-1972.
- Sainz, B. et al. (2016) 'Cancer Stem Cells and Macrophages: Implications in Tumor Biology and Therapeutic Strategies', *Mediators of Inflammation*, 2016, 1–15. doi: 10.1155/2016/9012369.
- San Juan, B. P. et al. (2019) 'The complexities of metastasis', *Cancers*. doi: 10.3390/cancers11101575.
- Sandler, A. et al. (2006) 'Paclitaxel-carboplatin alone or with bevacizumab for non-small-cell lung cancer', *New England Journal of Medicine*, 355(24), 2542–2550. doi: 10.1056/NEJMoa061884.
- Sanna, V., Pala, N. and Sechi, M. (2014) 'Targeted therapy using nanotechnology: focus on cancer.', *International journal of nanomedicine*, 9, 467–83. doi: 10.2147/IJN.S36654.
- Santamaría, P. G., Moreno-Bueno, G. and Cano, A. (2019) 'Contribution of Epithelial Plasticity to Therapy Resistance.', *Journal of clinical medicine*, 8(675), 1–23. doi: 10.3390/jcm8050676.
- Santander-Ortega, M. J. et al. (2012) 'Hydration forces as a tool for the optimization of core-shell nanoparticle vectors for cancer gene therapy', *Soft Matter*, 8(48), 12080. doi: 10.1039/c2sm26389k.
- Santander-Ortega, M. J. et al. (2014) 'Optimisation of synthetic vector systems for cancer gene therapy - the role of the excess of cationic

- dendrimer under physiological conditions.’, *Current topics in medicinal chemistry*, 14(9), 1172–81.
- Sathyanarayanan, V. and Neelapu, S. S. (2015) ‘Cancer immunotherapy: Strategies for personalization and combinatorial approaches’, *Molecular Oncology*, 2043–2053. doi: 10.1016/j.molonc.2015.10.009.
- Sato, Y. T. et al. (2016) ‘Engineering hybrid exosomes by membrane fusion with liposomes’, *Scientific reports*, 6, 21933. doi: 10.1038/srep21933.
- Saxena, K., Subbalakshmi, A. R. and Jolly, M. K. (2019) ‘Phenotypic heterogeneity in circulating tumor cells and its prognostic value in metastasis and overall survival’, *EBioMedicine*, 46, 4–5. doi: 10.1016/j.ebiom.2019.07.074.
- Scagliotti, G. et al. (2015) ‘Phase III Multinational, Randomized, Double-Blind, Placebo-Controlled Study of Tivantinib (ARQ 197) Plus Erlotinib Versus Erlotinib Alone in Previously Treated Patients With Locally Advanced or Metastatic Nonsquamous Non-Small-Cell Lung Cancer.’, *Journal of clinical oncology : official journal of the American Society of Clinical Oncology*, 33(24), 2667–74. doi: 10.1200/JCO.2014.60.7317.
- Scagliotti, G. V. et al. (2008) ‘Phase III study comparing cisplatin plus gemcitabine with cisplatin plus pemetrexed in chemotherapy-naive patients with advanced-stage non-small-cell lung cancer’, *Journal of Clinical Oncology*, 26(21), 3543–3551. doi: 10.1200/JCO.2007.15.0375.
- Schaeffer, D. et al. (2014) ‘Cellular Migration and Invasion Uncoupled: Increased Migration Is Not an Inexorable Consequence of Epithelial-to-Mesenchymal Transition’, *Molecular and Cellular Biology*, 34(18), 3486–3499. doi: 10.1128/mcb.00694-14.
- Schier, L. A. et al. (2019) ‘T1R2+T1R3-independent Chemosensory Inputs Contributing to Behavioral Discrimination of Sugars in Mice’, *Am J physiol Regul Integr Comp Physiol.*, 316(5), R448–R462.
- Schiller, J. H. et al. (2002) ‘Comparison of four chemotherapy regimens for advanced non-small-cell lung cancer’, *New England Journal of Medicine*, 346(2), 92–98. doi: 10.1056/NEJMoa011954.
- Sehgal, K. et al. (2018) ‘Targeting ROS1 rearrangements in non-small cell lung cancer with crizotinib and other kinase inhibitors’, *Translational Cancer Research*, 7(Suppl 7), S779–S786. doi:

- 10.21037/tcr.2018.08.11.
- Sercombe, L. et al. (2015) 'Advances and challenges of liposome assisted drug delivery', *Frontiers in Pharmacology*, 6(286), 1–13. doi: 10.3389/fphar.2015.00286.
- Serdons, K., Verbruggen, A. and Bormans, G. (2008) 'The presence of ethanol in radiopharmaceutical injections.', *Journal of nuclear medicine*, 49(12), 2071. doi: 10.2967/jnumed.108.057026.
- Shanker, M. et al. (2011) 'Tumor suppressor gene-based nanotherapy: from test tube to the clinic.', *Journal of drug delivery*, 2011, 465845. doi: 10.1155/2011/465845.
- Shepard, H. M. et al. (2017) 'Developments in therapy with monoclonal antibodies and related proteins', *Clinical Medicine, Journal of the Royal College of Physicians of London*, 17(3), 220–232. doi: 10.7861/clinmedicine.17-3-220.
- Shevchenko, A. et al. (1996) 'Mass spectrometric sequencing of proteins silver-stained polyacrylamide gels.', *Analytical chemistry*, 68(5), 850–8.
- Shilov, I. V et al. (2007) 'The Paragon Algorithm, a next generation search engine that uses sequence temperature values and feature probabilities to identify peptides from tandem mass spectra.', *Molecular & cellular proteomics: MCP*, 6(9), 1638–55. doi: 10.1074/mcp.T600050-MCP200.
- Shiozawa, Y. et al. (2013) 'Cancer stem cells and their role in metastasis', *Pharmacology and Therapeutics*, 138(2), 285–293. doi: 10.1016/j.pharmthera.2013.01.014.
- Shrivastava, S. et al. (2015) 'Identification of molecular signature of head and neck cancer stem-like cells', *Scientific Reports*, 5, 1–8. doi: 10.1038/srep07819.
- Shtam, T. a et al. (2013) 'Exosomes are natural carriers of exogenous siRNA to human cells in vitro.', *Cell communication and signaling*, 11(88), 1–10. doi: 10.1186/1478-811X-11-88.
- Siegel, R., Miller, K. and Jemal, A. (2017) 'Cancer statistics , 2017.', *CA Cancer J Clin*, 67(1), 7–30. doi: 10.3322/caac.21254.
- Skotland, T. et al. (2020) 'An emerging focus on lipids in extracellular vesicles', *Advanced Drug Delivery Reviews*, In Press. doi:

10.1016/j.addr.2020.03.002.

Skotland, T., Sandvig, K. and Llorente, A. (2017) 'Lipids in exosomes: Current knowledge and the way forward', *Progress in Lipid Research*, 66, 30–41. doi: 10.1016/j.plipres.2017.03.001.

Sohn, H. M. et al. (2019) 'Effect of CD133 overexpression on bone metastasis in prostate cancer cell line LNCaP', *Oncology Letters*, 18(2), 1189–1198. doi: 10.3892/ol.2019.10443.

Sprouse, M. L. et al. (2019) 'PMN-MDSCs enhance CTC metastatic properties through reciprocal interactions via ROS/notch/nodal signaling', *International Journal of Molecular Sciences*, 20(8), 1–20. doi: 10.3390/ijms20081916.

Steinbichler, T. B. et al. (2017) 'The role of exosomes in cancer metastasis', *Seminars in Cancer Biology*, 44, 170–181. doi: 10.1016/j.semcancer.2017.02.006.

Stremersch, S. et al. (2016) 'Comparing exosome-like vesicles with liposomes for the functional cellular delivery of small RNAs', *Journal of Controlled Release*, 232, 51–61. doi: 10.1016/j.jconrel.2016.04.005.

Sun, M. and Duan, X. (2020) 'Recent advances in micro/nanoscale intracellular delivery', *Nanotechnology and Precision Engineering*, 3(1), 18–31. doi: 10.1016/j.npe.2019.12.003.

Tan, C. L. et al. (2016) 'Concordance of anaplastic lymphoma kinase (ALK) gene rearrangements between circulating tumor cells and tumor in non-small cell lung cancer', *Oncotarget*, 7(17), 23251–23262. doi: 10.18632/oncotarget.8136.

Tayoun, T. et al. (2019) 'CTC-Derived Models: A Window into the Seeding Capacity of Circulating Tumor Cells (CTCs)', *Cells*, 1–17. doi: 10.3390/cells8101145.

Tellez-Gabriel, M. et al. (2019) 'Circulating tumor cell-derived pre-clinical models for personalized medicine', *Cancers*, 11(19), 1–16. doi: 10.3390/cancers11010019.

Testa, U., Castelli, G. and Pelosi, E. (2018) 'Lung cancers: Molecular characterization, clonal heterogeneity and evolution, and cancer stem cells', *Cancers*, 10(248), 1–81. doi: 10.3390/cancers10080248.

Théry, C. et al. (2006) 'Isolation and characterization of exosomes from cell culture supernatants and biological fluids.', in *Current protocols in cell*

- biology. doi: 10.1002/0471143030.cb0322s30.
- Tian, T. et al. (2010) 'Visualizing of the cellular uptake and intracellular trafficking of exosomes by live-cell microscopy', *Journal of Cellular Biochemistry*, 111(2), 488–496. doi: 10.1002/jcb.22733.
- Tian, Y. et al. (2014) 'A doxorubicin delivery platform using engineered natural membrane vesicle exosomes for targeted tumor therapy', *Biomaterials*, 35(7), 2383–2390. doi: 10.1016/j.biomaterials.2013.11.083.
- Tickner, J. A. et al. (2014) 'Functions and Therapeutic Roles of Exosomes in Cancer', *Frontiers in Oncology*, 4(127), 1–8. doi: 10.3389/fonc.2014.00127.
- Tinhofer, I. et al. (2014) 'Cancer stem cell characteristics of circulating tumor cells', *International Journal of Radiation Biology*, 90(8), 622–627. doi: 10.3109/09553002.2014.886798.
- Torrvalvo, J. et al. (2019) 'The activity of immune checkpoint inhibition in kras mutated non-small cell lung cancer: A single centre experience', *Cancer Genomics and Proteomics*, 16(6), 577–582. doi: 10.21873/cgp.20160.
- Toyono, T. et al. (2007) 'CCAAT/Enhancer-binding protein β regulates expression of human T1R3 taste receptor gene in the bile duct carcinoma cell line, HuCCT1', *Biochimica et Biophysica Acta - Gene Structure and Expression*, 1769(11–12), 641–648. doi: 10.1016/j.bbaexp.2007.08.003.
- Treesukosol, Y., Smith, K. R. and Spector, A. C. (2011) 'The Functional Role of the T1R Family of Receptors in Sweet Taste and Feeding', *Physiology behaviour*, 105(1), 14–26. doi: 10.1016/j.physbeh.2011.02.030.
- Usman, S. et al. (2020) 'The current status of anti GPCR drugs against different cancers', *Journal of Pharmaceutical Analysis*, In Press. doi: 10.1016/j.jpha.2020.01.001.
- Valastyan, S. and Weinberg, R. A. (2011) 'Tumor metastasis: molecular insights and evolving paradigms', *Cell*, 147(2), 275–292. doi: 10.1016/j.cell.2011.09.024.
- Varillas, J. I. et al. (2019) 'Microfluidic isolation of circulating tumor cells and cancer stem-like cells from patients with pancreatic ductal

- adenocarcinoma', *Theranostics*, 9(5), 1417–1425. doi: 10.7150/thno.28745.
- Vázquez-Ríos, A. J. et al. (2018) 'Nanotheranostics and their potential in the management of metastatic cancer', in *Handbook of Nanomaterials for Cancer Theranostics*, 199–244. doi: 10.1016/B978-0-12-813339-2.00008-6.
- Villalobos, P. and Wistuba, I. I. (2017) 'Lung Cancer Biomarkers', *Hematology/Oncology Clinics of North America*, 31(1), 13–29. doi: 10.1016/j.hoc.2016.08.006.
- Wagner, J. and Kroetz, D. (2016) 'Transforming Translation: Impact of Clinical and Translational Science', *Clinical and Translational Science*, 9(1), 3–5. doi: 10.1111/cts.12380.
- Wang, H. et al. (2015) 'Recent progress in microRNA delivery for cancer therapy by non-viral synthetic vectors', *Advanced Drug Delivery Reviews*, 81, 142–160. doi: 10.1016/j.addr.2014.10.031.
- Wang, L., Park, P. and Lin, C. Y. (2009) 'Characterization of stem cell attributes in human osteosarcoma cell lines', *Cancer Biology and Therapy*, 8(6), 543–552. doi: 10.4161/cbt.8.6.7695.
- Wang, R. et al. (2014) 'Comparison of mammosphere formation from breast cancer cell lines and primary breast tumors', *Journal of Thoracic Disease*, 6(6), 829–837. doi: 10.3978/j.issn.2072-1439.2014.03.38.
- Wang, X. (2012) 'A new vision of definition, commentary, and understanding in clinical and translational medicine', *Clinical and Translational Medicine*, 1(5), 1–3. doi: 10.1186/2001-1326-1-5.
- Wang, X. (2017) 'Isolation of Extracellular Vesicles from Breast Milk', in *Methods in molecular biology*, 351–353. doi: 10.1007/978-1-4939-7253-1_28.
- Wauson, E. M. et al. (2015) 'Differential Regulation of ERK1/2 and mTORC1 Through T1R1/T1R3 in MIN6 Cells.', *Molecular endocrinology*, 29(8), 1114–1122. doi: 10.1210/ME.2014-1181.
- Wauson, E. M., Zaganjor, E. and Cobb, M. H. (2013) 'Amino acid regulation of autophagy through the GPCR TAS1R1-TAS1R3', *Autophagy*, 9(3), 418–419. doi: 10.4161/auto.22911.
- Wee, P. and Wang, Z. (2017) 'Epidermal growth factor receptor cell proliferation signaling pathways', *Cancers*, 9(5), 1–45. doi:

- 10.3390/cancers9050052.
- Wei, C. et al. (2019) ‘Crosstalk between cancer cells and tumor associated macrophages is required for mesenchymal circulating tumor cell-mediated colorectal cancer metastasis’, *Molecular Cancer*, 18(64), 1–23. doi: 10.1186/s12943-019-0976-4.
- Wilhelm, S. et al. (2016) ‘Analysis of nanoparticle delivery to tumours’, *Nature Reviews Materials*, 1(16014), 1–12. doi: 10.1038/natrevmats.2016.14.
- Wolf, J. et al. (2019) ‘Capmatinib (INC280) in METΔex14 -mutated advanced non-small cell lung cancer (NSCLC): Efficacy data from the phase II GEOMETRY mono-1 study. ’, *Journal of Clinical Oncology*, 37(15_suppl), 9004–9004. doi: 10.1200/jco.2019.37.15_suppl.9004.
- Wood, K. et al. (2016) ‘Prognostic and predictive value in KRAS in non-small-cell lung cancer’, *JAMA Oncology*, 2(6), 805–812. doi: 10.1001/jamaoncol.2016.0405.
- Workman, P. et al. (2010) ‘Guidelines for the welfare and use of animals in cancer research’, *British Journal of Cancer*, 1555–1577. doi: 10.1038/sj.bjc.6605642.
- Wu, V. et al. (2019) ‘Illuminating the Onco-GPCRome: Novel G protein-coupled receptor-driven oncocrine networks and targets for cancer immunotherapy’, *Journal of Biological Chemistry*, 294(29), 11062–11086. doi: 10.1074/jbc.REV119.005601.
- Wu, Z. et al. (2019) ‘Update on liquid biopsy in clinical management of non-small cell lung cancer’, *OncoTargets and Therapy*, 12, 5097–5109. doi: 10.2147/OTT.S203070.
- Xia, P. et al. (2015) ‘Prognostic value of circulating CD133+ cells in patients with gastric cancer’, *Cell Proliferation*, 48(3), 311–317. doi: 10.1111/cpr.12175.
- Xu, H., Li, Z. and Si, J. (2014) ‘Nanocarriers in gene therapy: A review’, *Journal of Biomedical Nanotechnology*, 10(12), 3483–3507. doi: 10.1166/jbn.2014.2044.
- Xu, M. J., Johnson, D. E. and Grandis, J. R. (2017) ‘EGFR-targeted therapies in the post-genomic era’, *Cancer and Metastasis Reviews*, 36(3), 463–473. doi: 10.1007/s10555-017-9687-8.
- Yanagita, M. et al. (2016) ‘A prospective evaluation of circulating tumor

- cells and cell-free DNA in EGFR-mutant non-small cell lung cancer patients treated with erlotinib on a phase II trial', *Clinical Cancer Research*, 22(24), 6010–6020. doi: 10.1158/1078-0432.CCR-16-0909.
- Yang, H. et al. (2019) 'Matrix Metalloproteinase 11 Is a Potential Therapeutic Target in Lung Adenocarcinoma', *Molecular Therapy - Oncolytics*, 14, 82–93. doi: 10.1016/j.omto.2019.03.012.
- Yang, S. T. et al. (2016) 'The role of cholesterol in membrane fusion', *Chemistry and Physics of Lipids*, 199, 136–143. doi: 10.1016/j.chemphyslip.2016.05.003.
- Yasukawa, M. et al. (2018) 'Histological grade: Analysis of prognosis of non-small cell lung cancer after complete resection', *In Vivo*, 32(6), 1505–1512. doi: 10.21873/invivo.11407.
- Ye, L. et al. (2017) 'Circulating Tumor Cells Were Associated with the Number of T Lymphocyte Subsets and NK Cells in Peripheral Blood in Advanced Non-Small-Cell Lung Cancer', *Disease Markers*, 2017, 1–6. doi: 10.1155/2017/5727815.
- Yuan, M. et al. (2019) 'The emerging treatment landscape of targeted therapy in non-small-cell lung cancer', *Signal Transduction and Targeted Therapy*, 4(61), 1–14. doi: 10.1038/s41392-019-0099-9.
- Zahurak, M. et al. (2007) 'Pre-processing Agilent microarray data', *BMC Bioinformatics*, 8. doi: 10.1186/1471-2105-8-142.
- Zamorano, J. L. et al. (2016) '2016 ESC Position Paper on cancer treatments and cardiovascular toxicity developed under the auspices of the ESC Committee for Practice Guidelines', *European Heart Journal*, 37(36), 2768–2801. doi: 10.1093/eurheartj/ehw211.
- Zappa, C. and Mousa, S. A. (2016) 'Non-small cell lung cancer: Current treatment and future advances', *Translational Lung Cancer Research*, 5(3), 288–300. doi: 10.21037/tlcr.2016.06.07.
- Zavridou, M. et al. (2020) 'Direct comparison of size-dependent versus EpCAM-dependent CTC enrichment at the gene expression and DNA methylation level in head and neck squamous cell carcinoma', *Scientific Reports*, 10(6551), 1–9. doi: 10.1038/s41598-020-63055-y.
- Zavyalova, M. V. et al. (2019) 'Intravasation as a Key Step in Cancer Metastasis', *Biochemistry*, 84(7), 762–772. doi: 10.1134/S0006297919070071.

- Zhang, R. X. et al. (2018) 'Importance of integrating nanotechnology with pharmacology and physiology for innovative drug delivery and therapy - An illustration with firsthand examples', *Acta Pharmacologica Sinica*, 825–844. doi: 10.1038/aps.2018.33.
- Zhao, C., Setrerrahmane, S. and Xu, H. (2015) 'Enrichment and characterization of cancer stem cells from a human non-small cell lung cancer cell line', *Oncology Reports*, 34(4), 2126–2132. doi: 10.3892/or.2015.4163.
- Zhao, P. et al. (2020) 'Recent advances of antibody drug conjugates for clinical applications', *Acta Pharmaceutica Sinica B*, In Press. doi: 10.1016/j.apsb.2020.04.012.
- Zhao, Y. et al. (2018) 'Liquid Biopsy of Vitreous Reveals an Abundant Vesicle Population Consistent With the Size and Morphology of Exosomes.', *Translational vision science & technology*, 7(3), 1–20. doi: 10.1167/tvst.7.3.6.
- Zhou, J. et al. (2017) 'Clinical significance of circulating tumor cells in gastric cancer patients', *Oncotarget*, 8(15), 25713–25720. doi: 10.18632/oncotarget.14879.
- Zhou, Y. et al. (2018) 'Methionine and valine activate the mammalian target of rapamycin complex 1 pathway through heterodimeric amino acid taste receptor (TAS1R1/TAS1R3) and intracellular Ca²⁺ in bovine mammary epithelial cells', *Journal of Dairy Science*, 101(12), 11354–11363. doi: 10.3168/jds.2018-14461.
- Zhou, Z. et al. (2017) 'Nonviral Cancer Gene Therapy: Delivery Cascade and Vector Nanoproperty Integration', *Advanced Drug Delivery Reviews*, 115, 115–154. doi: 10.1016/j.addr.2017.07.021.



ABBREVIATIONS AND ACRONYMS





13 ABBREVIATIONS AND ACRONYMS

2D	Two dimensional
3D	Three dimensional
7-AAD	7-aminoactinomycin D
ACTB	Actin, cytoplasmic 1
ADC	Antibody Drug Conjugates
ADC	Adenocarcinoma
AE	Association efficiency
AJCC	American Joint Committee on Cancer
AKT	Protein kinase B
ALDH1A	Aldehyde dehydrogenase 1A1
ALK	Anaplastic lymphoma kinase
ALL	Acute Lymphoblastic Leukemia
ANOVA	Analysis of variance
APC	Antigen-presenting cells
AQP1	Aquaporin-1
ASO	Antisense Oligonucleotide
ATCC	American Type Culture Collection
ATS	American Thoracic Society
B2M	Beta-2-microglobulin
BBB	Brain Blood Barrier
bFGF	Basic Fibroblast Growth Factor
BLI	bioluminescence intensity
bp	base pairs

BRAF	v-raf murine sarcoma viral oncogene homolog B1
BSA	Bovine Serum Albumin
BSC	Best Supportive Care
CAF	Cancer-Associated Fibroblasts
CAGR	Compound Annual Growth Rate
CAR	chimeric antigen receptor
Cas9	CRISPR-associated protein 9
CD133	Prominin-1
CD19	B-lymphocyte antigen CD19
CD33	Myeloid cell surface antigen CD33
CD34	Hematopoietic progenitor cell antigen CD34
CD36	Platelet glycoprotein 4
CD45	Receptor-type tyrosine-protein phosphatase C
CDCA3	Cycle associated 3 protein
CDKN1B	Cyclin-dependent kinase inhibitor 1B
cDNA	Complementary DNA
CDX	CTC-derived Xenograft
Cer	Ceramide
CFA	Colony Forming Assay
CH	Cholesterol
CI	Confidence interval
CM	Conditioned Medium
CMV	Cytomegalovirus
CRC	Colorectal Cancer
CRD	Cysteine-Rich Domain
CRISPR	Clustered Regularly Interspaced Short Palindromic Repeats
CRO	Contract Research Organization
CryoTEM	Cryogenic transmission electron microscopy
CSC	Cancer Stem Cells

CSLM	Confocal Laser-Scanning Microscope
CT	Chemotherapy
CT	Computed Tomography
C_t	Cycle threshold
CTAB	Cetyltrimethylammonium bromide
CTC	Circulating Tumor Cell
CTLA-4	Cytotoxic T- lymphocyte-associated antigen-4
CV	Coefficient Variation
CX3CL1	Fractalkine
Cy3	Cyanine 3
Cy5	Cyanine 5
DAB	3,3'-diaminobenzidine
DAB1	Disabled homolog 1
DAPI	4',6-diamidino-2-phenylindole
DC	Dendritic cells
DC	Detergent Compatible
DC-CH	3beta-(N(N',N'-dimethylaminoethane)-carbamoyl) cholesterol
DDX	DTC-derived Xenograft
DiD	Tetramethylindotricarbocyanine perchlorate
DiR	Tetramethylindotricarbocyanine iodide
DLS	Dynamic Light Scattering
DMEM	Dulbecco's Modified Eagle Medium
DNA	Deoxyribonucleic acid
DOTAP	1,2-dioleoyl-3-trimethylammonium-propane
dsDNA	double stranded DNA
DTCs	Disseminated Tumor Cells
E/M	Epithelial/Mesenchymal
EBF2	Transcription factor COE2
ECAD	E-cadherin

ECL	Enhanced chemiluminescence
ECM	Extracellular matrix
EDDM3A	Epididymal protein 3A
EDTA	Ethylenediaminetetraacetic acid
EdU	5-Ethynyl-2'-deoxyuridine
EE	Encapsulation efficiency
EGF	Epidermal Growth Factor
eGFP	Enhanced Green Fluorescent Protein
EGFR	Epidermal growth factor receptor
EMA	European Medicines Agency
EMN	Exosome-mimetic nanoplatfrom
EMT	Epithelial to Mesenchymal Transition
EpCAM	Epithelial cell adhesion molecule
EPR	Enhanced Permeability and Retention
ErbB2/HER2	Erb-b2 receptor tyrosine kinase 2
ERK	Extracellular regulated kinase
ERS	European Respiratory Society
F-EMNs	Functionalized EMNs
FACS	Flow cytometry
FBS	Fetal Bovine Serum
FcR	Fragment crystallizable Receptors
FDA	Food and Drug Administration
FDR	False Discovery Rate
GAPDH	Glyceraldehyde-3-phosphate dehydrogenase
GBM	Glioblastoma
GDF15	Growth/differentiation factor 15
GEO	Gene Expression Omnibus
GFL	Glial Cell Line-Derived Neurotrophic Factor Family of Ligands
GFP	Green Fluorescent Protein

GPCR	G-Protein coupled receptor
GPI	Glycosyl-phosphatidylinositol
GUSB	Beta-glucuronidase
H+L	Heavy and Light chains
hATTR	Hereditary Transthyretin Amyloidosis
HER2	Human Epidermal growth factor Receptor 2
HGF	Hepatocyte Growth Factor
HIV	Human Immunodeficiency Virus
HLA	Human Leukocyte Antigen
HPRT	Hypoxanthine-guanine phosphoribosyltransferase
HR	Hazard Ratio
HRP	Horseradish peroxidase
IASCL	International Association for the Study of Lung Cancer
ICIs	Immune checkpoint inhibitors
ICOS	Inducible T-cell costimulator
IgG	Immunoglobulin G
IHC	Immunohistochemistry
IND	Investigational New Drugs
IPA	Ingenuity Pathway Software
IRES	Internal Ribosome Entry Site
ITGα6β4	integrin alpha 6 beta 4
ITS	Insulin-Transferrin-Selenium
IV	Intravenous
JAK	Janus tyrosine kinase
KLK6	Kallikrein-6
KRAS	Kirsten rat sarcoma viral oncogene homolog
LC-MS/MS	Liquid chromatography-tandem mass spectrometry
LCC	Large-Cell Carcinoma
LDA	Laser Doppler Anemometry

LYS	Lysozyme
mAb	Monoclonal Antibody
MAPK	Mitogen-Activated Protein Kinase
MDSCs	Myeloid-derived suppressor cells
MEK	Mitogen-activated protein kinase kinase
MET	Hepatocyte growth factor receptor
MET	Mesenchymal to Epithelial Transition
METex14	<i>MET</i> exon 14 skipping mutations
microBCA	Micro Bicinchoninic Acid
miRNA	microRNA
miRscr	miRNA scramble
MMAE	Brentuximab-Monomethyl auristatin E
MMP	Matrix metalloproteinases
mRNA	messenger RNA
mTNBC	Metastatic Triple-Negative Breast Cancer
mTOR	Mammalian target of Rapamycin
MTT	3-(4,5-dimethylthiazol-2-yl)-2,5-diphenyltetrazolium bromide
NANOG	Homeobox protein NANOG
NBD	Nitrobenzofuran
NCCN	National Comprehensive Cancer Network
ncRNA	non-coding RNA
NCT	National Clinical Trial
NK	Natural killer
NMR	Nuclear magnetic resonance
NOTCH1	Neurogenic locus notch homolog protein 1
NSCLC	Non-Small Cell Lung Cancer
NTA	Nanoparticle Tracking Analysis
NTC	Non-Target Control
NTRK	Neurotrophin Tyrosine Receptor Kinase

OCT4	Octamer-binding transcription factor 4
ORF	Open Reading Frame
ORR	Overall response rate
OS	Overall Survival
PBS	Phosphate Buffered Saline
PC	Phosphatidylcholine
PCR	Polymerase Chain Reaction
PD-1	Programmed cell death-1
PD-L1	Programmed cell death ligand-1
PdI	Polidispersity Index
pDNA	plasmid DNA
PDXs	Patient-Derived Xenograft
PE	Phycoerythrin
PE	phosphatidylethanolamine
PEG	Poly(ethylene glycol)
PEI	Polyethylenimine
PerCP	Peridinin-Chlorophyll-protein
PET	Polyester
PFA	Paraformaldehyde
PFS	Progression Free Survival
PI3K	Phosphatidylinositol 3-kinase
PKC	Protein kinase C
PLC	Phospholipase C
PS	Performance Status
PTPRS	Receptor-type tyrosine-protein phosphatase S
PVDF	Polyvinylidene fluoride
R&D	Research and Development
RAF	Rapidly Accelerated Fibrosarcoma
RET	Proto-oncogene tyrosine-protein kinase receptor Ret

RIPA	Radioimmunoprecipitation assay buffer
RNA	Ribonucleic acid
RNAi	RNA interference
ROS	Reactive Oxygen Species
ROS1	ROS proto-oncogene 1
RoW	Rest of the world
RPKM	Reads Per Kilobase Million
RPMI	Roswell Park Memorial Institute
RT	Room temperature
RT-qPCR	Real Time-quantitative PCR
SAM	Significance Analysis for Microarrays
sc	subcutaneously
SCC	Squamous cell carcinoma
SCID	Severe combined immunodeficiency
SCLC	Small Cell Lung Cancer
SD	Standard deviation
SDS	Sodium Dodecyl Sulfate
SDS-PAGE	SDS–polyacrylamide gel electrophoresis
SEM	Standard error of the mean
SEMA3F	Semaphorin-3F
SERGAS	Servicio Galego de Saúde
SHP-1	Src homology phosphatase-1
SHP-2	Src homology phosphatase-2
shRNA	short-hairpin RNA
siRNA	Small interfering RNA
SM	Sphingomyelin
SMA	Spinal Muscular Atrophy
SMN	Survival Motor Neuron
SNAI2	Snail Family Transcriptional Repressor 2

SNCG	Gamma-synuclein
SOX2	(Sex determining region Y)-box 2
SRC	Proto-oncogene tyrosine-protein kinase
SSC	Side Light Scatter
ST	Stearylamine
STAT	Signal Transducer and Activator of Transcription
STR	Short Tandem Repeat
T1R3-	TAS1R3 negative cells
T1R3+	TAS1R3 positive cells
TALENs	Transcription Activator-Like Effector Nucleases
TAMs	Tumor-associated macrophages
TAS1R1 (T1R1)	Taste Receptor Type 1 Member 1
TAS1R2 (T1R2)	Taste Receptor Type 1 Member 2
TAS1R3 (T1R3)	Taste Receptor Type 1 Member 3
TEM	Transmission Electron Microscopy
TGF-α	Transforming growth factor-alpha
TGFA	Protransforming growth factor alpha
TGFβ	Transforming growth factor beta
TKIs	Tyrosine kinase inhibitors
TMB	Tumor Mutational Burden
TMD	Transmembrane Domain
TNM	Tumor Nodes Metastasis
TNR	Tenascin-R
TRK	Tropomyosin Receptor Kinase
TTBS	Tween 20-Tris-buffered saline
TUSC2	Tumor suppressor candidate 2
ULA	Ultra-low attachment
v/v	volume/volume

VCAMs	Vascular Cells Adhesion Molecules
VEGF	Vascular Endothelial Growth Factor
VFTM	Venus FlyTrap Module
w/w	Weight/weight
ZFNs	Zinc-Finger Nucleases
ZP	Zeta Potential



A large, light blue watermark of the USC logo is centered on the page. The logo consists of the letters 'USC' in a large, bold, sans-serif font, with the text 'UNIVERSITY OF SANTA BARBARA' and 'DEPARTMENT OF COMPOSITION' in a smaller font below it, all contained within a square border.

ETHICAL CONSIDERATIONS



14 ETHICAL CONSIDERATIONS

Images use:

In the case of images used in this work with copyright restrictions, permission has been asked to publishers and the source has been indicated at the bottom of the correspondent figures.

Human cell culture:

All cancer cell lines used in this work were acquired from commercially available resources (American Tissue Culture Collection, ATCC) and cultured in the conditions recommended by the manufacturers and only used for the research purposes specifically described in this thesis.

Animal studies:

The animal handling and the experimental procedures were approved by the internal ethical research and animal welfare committee (IIB, UAM), and by the Local Authorities (Comunidad de Madrid, PROEX424/15) which complied with the European Union (Directive 2010/63/UE) and Spanish Government guidelines (Real Decreto 53/20133). PDX models (1104/2015-PR) and animal studies (356/2016-PR) developed in the *Fondazione IRCCS, Istituto Nazionale dei Tumori* (Milan, Italy) were approved by the Italian Ministry of Health.

Patient's samples:

Blood and tissue samples were collected in accordance to the guidelines and protocols approved by the Institutional Ethical Committees, *Galician Clinical Research Ethics Committee*, SERGAS; code approval: 2008/277 and 2015/304, and the *Consorcio Hospital General Universitario de Valencia*, CEIC-CHGUV (2012 and 2014) (see annexes 8 and 9).

Conflict of interest:

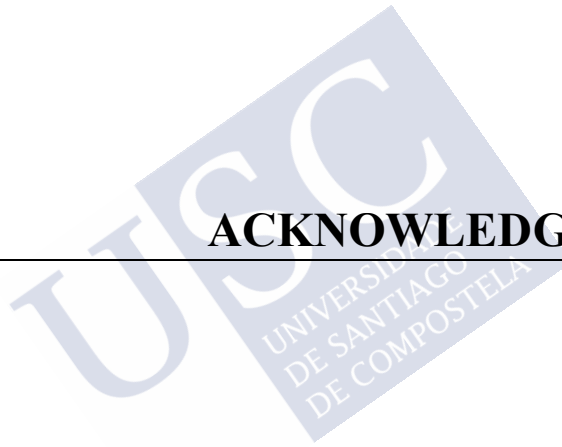
I declare the ownership of two patents filed during the doctoral thesis:

- M. de la Fuente Freire, R. López López, M. Alonso Nocelo, A.J. Vázquez Ríos. *Use of the TAS1R3 protein as a marker for therapeutic, diagnostic, and/or prognostic purposes for tumors that express said protein.* 15 January 2018.

- M. de la Fuente Freire, R. López López, A.J. Vázquez Ríos, B. López Bouzo, M. Alonso Nocelo. *Nanosystems as selective vehicles.* 15 January 2018.



ACKNOWLEDGEMENTS





15 ACKNOWLEDGEMENTS

No podría empezar este apartado mas que dándole las gracias a mis directores de tesis, **María de la Fuente** y **Rafael López**, por haberme dado la oportunidad de realizar esta tesis bajo su supervisión, por haberme permitido formar parte de su grupo de investigación y por las contribuciones científicas que han aportado. Gracias por haberme apoyado siempre para que pudiera presentar mi trabajo en numerosas jornadas y congresos, por los viajes, por los cursos de formación, realmente me siento muy privilegiada por toda la formación que he recibido.

Me gustaría agradecerle especialmente a **María** por haber confiado siempre en mí, incluso más que yo misma, por haberme impulsado a nuevos desafíos y retos más allá de las competencias básicas de un doctorado, por haber apoyado mis ideas siempre y darme la libertad de aprender por mí misma, por haberme enseñado, inspirado y despertado a una visión traslacional, intentando tener siempre claro por qué hacemos lo que hacemos. Algo que he podido aprender de tu ejemplo (que vale más que las palabras), es que en la vida hay luchas que vale la pena pelear, aunque tú no vayas a disfrutar directamente de la victoria. ¡Gracias por haber peleado por nosotras, las que vamos detrás!

Gracias al Instituto de Investigación Sanitaria de Santiago de Compostela (**IDIS**) y la **Fundación IDIS**, por proporcionarme las instalaciones y el soporte técnico para poder desarrollar mi tesis. A las entidades que han financiado esta investigación y mi estancia en el extranjero, la Xunta de Galicia (IN606A-201//001), el Programa de Formación de Profesorado Universitario del Gobierno de España (FPU15/06595, EST18/00845) y CIBERONC.

Gracias a todos los que han formado parte del laboratorio de **NanoOncología**, a mis compañeras Sandra Díez, Sainza, Marce, María, Cris, Olaia y Sofía, por todos los buenos ratos que hemos

pasado, por haber podido compartir con vosotras penas y alegrías y por hacer que las horas en el laboratorio sean mucho más placenteras. También agradecer a todas las personas que ya no están en el grupo, pero que su paso ha dejado una huella: Marta Alonso, Carmen Abuín, Surasa, Mariajo, Farimah, Andrea, Carmen, Alba, Raneem, Román, Miguel, Rebeca y Aurora. Gracias Marta por haber iniciado el trabajo y descubrimiento de TAS y haberme dejado un legado tan emocionante.

Especialmente me gustaría destacar a **Belén L. Bouzo**, por haberme iniciado en el mundo de la nanotecnología, por transmitirme tu pasión, tu buen hacer, por la paciencia y el cariño con que haces todo, porque no hay nadie mejor que tú para enseñar y yo tuve la suerte de aprender muchas cosas de ti.

También se merece una mención especial **Sandra Alijas**, por haber sido un gran apoyo para mí, por tu esfuerzo, tu trabajo duro, por todo lo que me has ayudado en esta tesis, por ser esas dos (o cuatro) manos extra, por tener siempre el laboratorio a punto, por las gestiones, las compras, por ser una todoterreno multivalente.

Gracias a todo el grupo **ONCOMET**, siempre dispuestos a ayudar en todo lo que he podido necesitar, es siempre un regalo poder formar parte de un grupo tan multidisciplinar. Gracias especialmente a Patri, porque Italia no hubiese sido igual sin ti, gracias por ser mi compañera de viajes y aventuras, por las risas y por las largas conversaciones.

Gracias al **Servicio de Oncología**, por todo lo que he podido aprender de clínica gracias a vosotros; gracias a las maravillosas enfermeras; y especialmente gracias al oncólogo Juan Ruiz, porque eres una de esas personas que siempre suman, con buenas ideas, con alegría, con entusiasmo, ha sido un placer coincidir contigo en esta etapa.

Gracias a toda la gente del **IDIS** con la que he tenido la suerte de coincidir estos años. Gracias a Susana Bravo, por todo lo que me has enseñado de proteómica, a Marta Picado por tu asistencia con la microscopía, a Manuel, por tu ayuda para entender e interpretar el RMN, a Laura Muínelo, por tu ayuda con las CTCs, a Anxo Vidal por tu ayuda con el FACS, vuestras contribuciones han sido esenciales

para este trabajo. Especialmente quiero agradecer al **grupo de Manuel Collado**, siempre recordaré con mucho cariño el tiempo que compartimos el laboratorio 13 en mis comienzos. A Jessica, Alba y Sabela, por estar siempre dispuestas a ayudar, habéis sido unas compañeras increíbles, tanto dentro como fuera del laboratorio y he aprendido tanto de vosotras...

Gracias a la gente del **CIMUS**, especialmente a María José Alonso y su laboratorio, por permitirme usar los equipos del laboratorio, por enseñarme y por ser siempre tan agradables conmigo, vuestra ayuda ha sido fundamental para la parte nano de esta tesis. A Sonia, Jose, Mati, Tamara, Carla y Ana de manera especial.

Gracias a todos los **colaboradores** que han aportado a este trabajo, Gema y Ángela por el trabajo con ratones y los exosomas, Silvia y Eloísa por el trabajo con los esferoides y las muestras de pacientes, y Antonio G. Tato por el análisis bioinformático.

Quiero extender mi agradecimiento a mi segunda casa del doctorado, el **Laboratorio de Genomica Tumorale** del Istituto Nazionale dei Tumori de Milán. To Luca for giving me the opportunity to do an internship in your lab for nine months and making me feel at home. Thank you for your mentoring and for stimulating me to think from new perspectives. Thanks Giulia for your amazing help and constant support, your passion is contagious, and it was incredible to learn from you, you are such a bright scientist. This thesis wouldn't have been possible without your support. To Monica, for your support in the animal house, your kindness is immensely appreciated. To all the lab members, thank you for you warm welcome, for all the moments we spent together (a pranzo and in the lab), and all the lessons I could learn from each one of you, you made me have such an amazing italian experience. *Especialmente, grazie a Ornella, Nina, Fede, Mavis, Miriam, Paty and Max, siete veramente meravigliosi!* I hope to see you again, in Spain?

Quiero agradecer también a todos aquellos que me ha apoyado de fuera del mundo científico, a mis **grandes amigos** (David, Poly, Nate, Ely, Noah, Julián, Allie), a mi **familia de la Unida** (especialmente, David, Eli, Emma, Adrián, Andrea, Jorge, María José y Habraham), porque me habéis acompañado en este camino y sé que lo seguiréis

haciendo con lo que venga, por interesaros por mis avances, por siempre preocuparos por mí, por alegraros conmigo, por animarme siempre. Vuestra vida es un regalo.

Gracias **Carla**, por ser esa amiga que todos necesitarían tener. Por las veces que hemos reído hasta llorar y llorado hasta reír. Por estar a mi lado en esta y cada una de las decisiones de mi vida. A **Sandra**, por ser de esas amigas que perduran en el tiempo y por siempre contagiarme con tu alegría.

Gracias a mi **familia**, gracias mamá y papá por siempre estar ahí apoyándome en todos los sentidos que pueda haber, por quererme tanto y tan bien, por animarme siempre a ir a por más, a no conformarme, a seguir soñando. Gracias por enseñarme lo que es la responsabilidad, el compromiso, el pensamiento crítico, la excelencia, gracias por enseñármelo con vuestro ejemplo. Gracias por hacer el esfuerzo de intentar entender lo que hago (“algo con unas cosas que se llaman exosomas” jajaja). Gracias a mis **hermanos y cuñados**, Esteban y Yomara, Jael y Marcos, Sara y Benja, y Laura, aunque quisiera, no me puedo imaginar a nadie mejor como familia. Gracias a mis **sobrinos** que son los mejores, Gemma, Isaac y Moi, aunque aún no os podéis enterar muy bien de lo que ha hecho la tía, algún día os enseñaré estas líneas, para que veáis cuánto os quiero. A mis **suegros**, Miguel y Pura, por su apoyo incesable, por ser casa, por ser familia.

Gracias a mi **abuela**, por acogerme en tu casa, por tratarme como a una princesa, porque nunca olvidaré cómo disfrutamos las dos de vivir juntas mientras hacía el máster, los paseos a por helados, las tardes de cine, las noches de calceta, por ponerte tan feliz siempre que me veías, por ser la mayor luchadora que he conocido, porque sé que estarías muy orgullosa de mí.

Gracias a mi **marido**, principalmente por elegir vivir esta vida conmigo, por tu apoyo incondicional, por ser mi bombona de oxígeno, por dejar un lado tus necesidades para suplir las mías, por entenderme, por ser el único capaz de explicar lo que hago y hacer que parezca que voy a salvar al mundo (jajaja), gracias por ser mi ayuda idónea. Love you!

Gracias a todos por formar parte de este apasionante viaje del doctorado.

Por último, pero más importante, quiero dar las gracias a **Dios**, por darme la fuerza, la capacidad, la pasión, porque si algo tengo, algo valgo, algo soy, a ti te lo debo. A ti sea la gloria.

“Aquel que es poderoso para hacer todas las cosas mucho más abundantemente de lo que pedimos o entendemos, por el poder que actúa en nosotros, a Él sea la gloria.”

Efesios 3:20







ANNEXES



16 ANNEXES

1. Book chapter: Vázquez-Ríos, A. J. *et al.* (2018) 'Nanotheranostics and their potential in the management of metastatic cancer', in *Handbook of Nanomaterials for Cancer Theranostics*, 199–244. doi: 10.1016/B978-0-12-813339-2.00008-6.
2. Permission to reproduce the full chapter in annex 1 by Elsevier and Copyright Clearance Center.
3. Journal Article: Vázquez-Ríos, A. J. *et al.* (2019) 'Exosome-mimetic nanoplatforms for targeted cancer drug delivery', *Journal of nanobiotechnology*, 17(1), 1–15. doi:10.1186/s12951-019-0517-8.
4. Review: Gutiérrez-Lovera, C. *et al.* (2017) 'The potential of zebrafish as a model organism for improving the translation of genetic anticancer nanomedicines', *Genes*. doi: 10.3390/genes8120349.
5. Journal Article: Nagachinta, S. *et al.* (2020) 'Sphingomyelin-based nanosystems (SNs) for the development of anticancer miRNA therapeutics', *Pharmaceutics*, 12(2). doi: 10.3390/pharmaceutics12020189.
6. Patent: Use of the TAS1R3 protein as a marker for therapeutic, diagnostic, and/or prognostic purposes for tumors that express said protein. Inventors: de la Fuente M., López-López R., Alonso-Nocelo M., Vázquez-Ríos A.J. WO2019/138140 A1.
7. Patent: Nanosystems as selective vehicles. Inventors; de la Fuente M., López-López R., López-Bouzo B., Vázquez-Ríos A.J., Alonso-Nocelo M. WO2019/138139 A1.
8. Informe favorable estudios que implican muestras de seres humanos (*Galician Clinical Research Ethics Committee, SERGAS*)
9. Informe favorable estudios que implican muestras de seres humanos (*Consortio Hospital General Universitario de Valencia, CEIC-CHGUV*).
10. Certificado de capacitación del doctorando para experimentación animal, funciones A+B+C.



Nanotheranostics and Their Potential in the Management of Metastatic Cancer

Abi Judit Vázquez-Ríos*, **Marta Alonso-Nocelo^{†,‡,§}**, **Belén López Bouzo***, **Juan Ruiz-Bañobre***, **María de la Fuente***

**Health Research Institute of Santiago de Compostela (IDIS), SERGAS, CIBERONC, Santiago de Compostela, Spain †Autonomous University of Madrid (UAM), Madrid, Spain ‡"Alberto Sols" Biomedical Research Institute, CSIC-UAM, Madrid, Spain §Ramón y Cajal Health Research Institute (IRYCIS), Madrid, Spain*

1 The Management of Metastatic Cancer, an Unmet Clinical Need

Cancer is a major public health problem worldwide and the second leading cause of death in the United States and Europe. The most common causes of cancer death are lung, colorectal, and prostate cancers in men, and lung, breast, and colorectal cancers in women. In the United States, these four cancers account for 46% of all cancer deaths, with more than one-quarter (26%) attributed to lung cancer (Siegel, Miller, & Jemal, 2017; WHO, 2017).

Metastases are the cause of 90% of human cancer deaths (Taketo, 2011). As an example, the 5-year survival rate for localized-stage colorectal cancer (CRC) is around 90%, declining to 71% and 14% for patients diagnosed with regional and distant stages respectively (American Cancer Society, 2017). In the case of pancreatic cancer, the 5-year survival for localized disease is around 29%, and falls to 3% in the locally advanced or metastatic setting (Ilic & Ilic, 2016). Metastasis is an exceedingly complex process that occurs through a series of sequential steps, as reviewed by Mehlen and Puisieux (2006). Despite the fact that tumors at an early stage can often be surgically removed, there is growing evidence that dissemination could indeed happen at a very early stage in the carcinogenesis process (Martínez-Cardús, Moran, Musulen, et al., 2016) a fact that could explain why, in some tumor types, the 5-year survival even for localized disease is so poor.

With the aim of increasing patients' survival, different drugs and some biologicals are given as single sequential therapies or in combination in different clinical scenarios, palliative, adjuvant, and neoadjuvant settings. The main problems are related to toxicity and secondary side effects and can worsen the quality of life in short and long term (Hall, Cameron, Waters, et al., 2014). Additionally, the clonal evolution of tumors under antineoplastic treatments pressure can lead to therapeutic failure and progress of the disease (Aparicio & Caldas, 2013).

The development of targeted therapies has resulted in substantial benefits in terms of survival and quality of life for cancer patients. In the last 20 years, different drugs have been approved by the Food and Drug Administration (FDA) and the European Medicines Agency (EMA) for several tumor types, as for example, trastuzumab (breast cancer and [gastric/gastroesophageal junction adenocarcinoma](#)) ([Amadori, Milandri, Comella, Saracchini, et al., 2011](#)), imatinib (gastrointestinal stromal tumors and dermatofibrosarcoma protuberans) ([Sugiura, Fujiwara, Ando, Kawai, et al., 2010](#)), or cetuximab (colorectal cancer and head and neck cancer) ([Bertino, McMichael, Mo, Trikha, et al., 2016](#)), among others. In the case of nonsmall cell lung cancer (NSCLC), the treatment breakthrough was the introduction of targeted therapies against EGFR mutations, rearrangements involving the ALK or ROS1 genes, and recently, B-RAF mutations ([Novello, Barlesi, Califano, et al., 2016](#); [Planchard, Besse, Groen, et al., 2016](#)). Another milestone is the development of immune-checkpoint inhibitors, a group of antibodies designed to block specific targets present on tumor cells or lymphocyte surface [as for example ipilimumab ([Hodi, O'Day, McDermott, et al., 2010](#)), the first approved anti-CTLA4 antibody, and nivolumab ([Borghaei, Paz-Ares, Horn, et al., 2015](#); [Brahmer, Reckamp, Baas, et al., 2015](#); [Motzer, Escudier, McDermott, et al., 2015](#); [Robert, Long, Brady, et al., 2014](#)), the first approved anti-PD-1 antibody], and consequently boosting the immune system against cancer. Nanomedicines have also been introduced into the clinic, as detailed in [Section 3](#), showing a well-tolerated toxicity profile and good results in terms of efficacy ([Thakor & Gambhir, 2013](#)). Due to these novel approaches, the median overall survival (OS) for patients with metastatic cancer has considerably improved. For example, for NSCLC and metastatic colorectal cancer, OS is ~12 and 30 months, respectively, more than double what it was 20 years ago ([Reck, Rodríguez-Abreu, Robinson, et al., 2016](#); [Rolfo, Passiglia, Ostrowski, et al., 2015](#); [Van Cutsem, Cervantes, Adam, et al., 2016](#)). Despite this, success is still limited, making it mandatory to focus our efforts on developing novel alternatives specifically tailored to make a breakthrough in the management of disseminated cancer.

2 The Metastatic Cascade

The process of metastasis is defined by a cascade of complex events in which malignant cells detach from the primary tumor, invade the basement membrane, and then migrate into the circulation, either via the blood or lymphatic vessels, to finally spread to distant sites to form metastases ([Chambers, Groom, & MacDonald, 2002](#); [Pantel & Brakenhoff, 2004](#)). The metastatic cascade can be divided into three main phases, (i) premetastatic initiation, (ii) dissemination, and (iii) colonization.

Premetastatic initiation starts with local invasiveness, that is, the entry of well-restrained cancer cells into the surrounding tumor-associated stroma. To accomplish this, tumor cells reduce their adhesion to neighbor cells, increasing their motility and degrading the basement membrane ([Kedrin, van Rheenen, Hernandez, Condeelis, & Segall, 2007](#); [Weber, 2008](#)). In the next step, tumor cells intravasate into the lymphatics and/or blood vessels, disseminating by hematogenous or lymphatic routes ([Pantel & Brakenhoff, 2004](#);

Sleeman, Cady, & Pantel, 2012). Next, tumor cells extravasate into distant organs and eventually colonize them to generate metastasis (Irmisch & Huelsken, 2013).

The metastatic process is complex and inefficient, with many cancer cells initially achieving access to circulation, but only a few finally succeeding in proliferating as distant metastases (Wong, Lee, Shientag, et al., 2001). Despite of this limited efficiency, stopping the spread of cancer cells from the primary tumor to distant sites continues to be one of the greatest challenges nowadays. Hence, the development of new approaches that target one or more steps in the metastatic cascade is needed, to ultimately improve the outcome of patients with metastatic cancer. Fig. 1 summarizes the metastatic cascade and compiles the key events susceptible of therapeutic intervention.

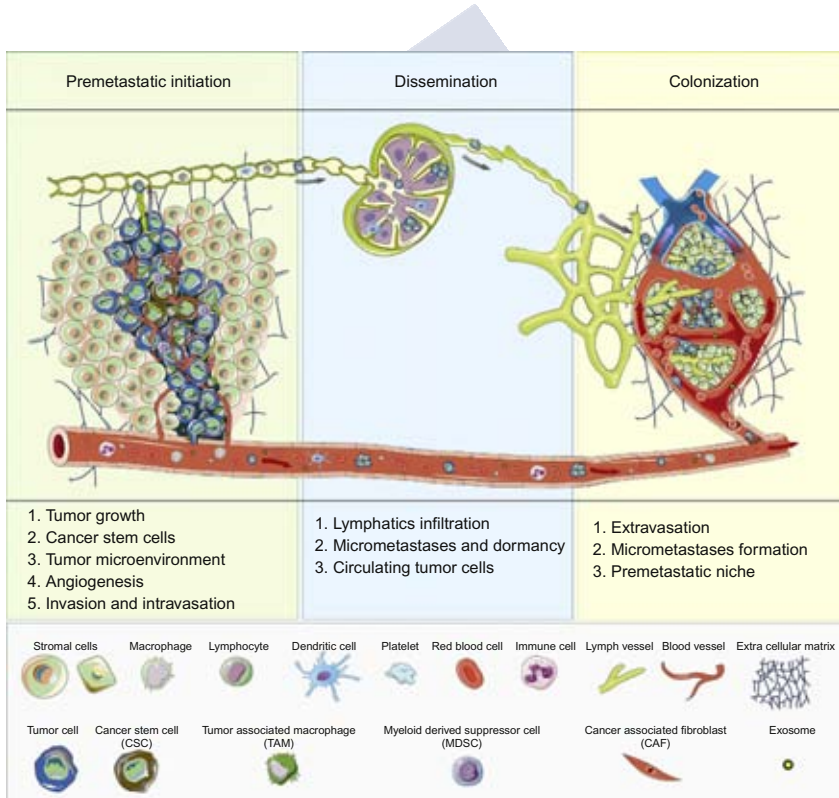


Fig. 1

Schematic representation of the process of metastasis.

3 The Impact of Nanomedicine in Cancer Therapy

Nanotechnology can be defined as the science of manipulating and controlling materials and systems on a molecular scale. The merging of nanotechnology and medicine, nanomedicine, has allowed the development of several nanoparticle delivery vehicles, specifically designed for carrying and delivering their cargo to disease sites for treatment, prevention, and/or diagnosis (Ledet & Mandal, 2012; Wang, Langer, & Farokhzad, 2012).

Nanomedicine has been widely explored in the last decades. Different nanosystems composed of a variety of materials have been proposed for the management of several diseases, as liposomes and other lipid-based nanosystems, polymer-based nanoparticles, micelles, polyplexes, dendrimers, polymersomes, and drug/protein conjugates (Beloqui, Memvanga, Coco, et al., 2016; Cordeiro, Alonso, & de la Fuente, 2015; de la Fuente, Csaba, Garcia-Fuentes, & Alonso, 2008; de la Fuente, Jones, Santander-Ortega, et al., 2015; de la Fuente, Raviña, Sousa-Herves, et al., 2012; de la Fuente, Seijo, & Alonso, 2008; Mazza, Alonso-Sande, Jones, & de la Fuente, 2013; Reimondez-Troitiño, Csaba, Alonso, & de la Fuente, 2015; Swain, Sahu, Beg, & Babu, 2016). Nanotechnology offers many advantages in drug delivery, including (i) protection of drugs from premature degradation, (ii) increased solubility and stability in biological media, (iii) prevention of premature interactions of drugs with the biological environment, (iv) controlled pharmacokinetics and biodistribution, (v) improved delivery of therapeutics across biological barriers, and (vi) targeting of drugs to the diseased area (Peer et al., 2007). Due to these properties and their ability to accommodate various types of drugs and biomolecules, with different physicochemical properties and activities, nanocarriers have emerged as attractive candidates for the development of personalized medicine (Sanna, Pala, & Sechi, 2014).

The application of nanotechnology in cancer therapy is already a reality that enables incremental, localized delivery of chemotherapeutics to the tumor, leading to improved pharmacological activities and significantly minimizing secondary side effects. In 1995, the FDA approved the first nanoparticle for cancer treatment, Doxil, a PEGylated liposome loaded with the chemotherapeutic drug doxorubicin (Barenholz, 2012). From then, some other nanotherapeutics have reached the market for different cancer treatments, being predominantly drug-loaded PEGylated liposomes, and as the main application, the treatment of unresectable locally advanced or metastatic cancer. Current FDA and EMA approved nanotherapeutics are summarized in Table 1. Most cases are examples of passively targeted first-generation PEGylated nanomedicines that mainly rely on modifying the pharmacokinetics and biodistribution of a drug by improving its accumulation in tumors, due to the phenomenon called Enhanced Permeability and Retention (EPR) effect, first described in 1986 by Matsumura and Maeda (1986). The attachment of the polymer polyethylene glycol (PEG) is widely used in nanomedicine to increase circulation lifetimes and reduce doses. The covalent attachment of PEG to proteins (i.e., enzymes, cytokines, antibodies, growth factors) has, for example, brought more than ten polymer-protein drugs into the market for different

Table 1: Clinically approved nanoparticles for cancer therapy

Commercial Name	Type of Nanoparticle	Drug/Therapy	Indication	Approval ^a (Year)
Doxil/Caelyx	Liposomal	Doxorubicin	HIV-related Kaposi sarcoma Breast cancer Ovarian cancer	FDA (1995) FDA (2005) FDA (2008)
DaunoXome	Liposomal	Daunorubicin	Advanced Kaposi's sarcoma Acute myeloid leukemia	FDA (1996) EMA (2008)
DepoCyt	Liposomal	Cytarabine	Lymphomatous meningitis	FDA (1996)
Myocet	Liposomal	Doxorubicin	Breast cancer	EMA (2000)
Mepact	Liposomal	Mifamurtide	Osteosarcoma	EMA (2009)
Marqibo	Liposomal	Vincristine	Acute lymphoblastic leukemia	FDA (2012)
Onivyde	Liposomal	Irinotecan	Pancreatic cancer	FDA (2015)
Opaxio	Polimeric nanoparticle	Paclitaxel	Glioblastoma	FDA (2012)
Oncaspar	Polimeric nanoparticle	PEGylated L-Asparaginase	Acute lymphoblastic leukemia	FDA (2006)
Eligard	Polimeric micelles	Leuprolide acetate	Prostate cancer	FDA (2002)
Eloxatin	Micelles	Oxaliplatin	Colon cancer	FDA (2004)
Neulasta	Polymer-protein conjugate	Filgrastim	Chemotherapy induced neutropenia	FDA (2002)
Abraxane	Protein-drug conjugate	Albumin-paclitaxel	Breast cancer Nonsmall-cell lung carcinoma	FDA (2005) FDA (2012)
Ontak	Protein-drug conjugate	Interleukina-2-diphtheria toxin	Pancreatic cancer Cutaneous T-cell lymphoma	FDA (2013) FDA (1999)
Adcetris	Antibody-drug conjugate	Brentuximab-monomethyl auristatin E (MMAE)	Hodgkin lymphoma Lymphoma (ALCL)	FDA (2011) FDA (2011)
Kadcyla	Antibody-drug conjugate	Trastuzumab-Emtansine	Breast cancer	FDA (2013)

Sources: <https://www.accessdata.fda.gov/scripts/cder/daf/>; <http://www.ema.europa.eu/ema/> (accessed 10 August 2017).

^a All the information found in: (1) FDA approved drug products. Drugs@FDA. www.accessdata.fda.gov/scripts/cder/drugsatfda/. Accessed August 10, 2017. (2) European Medicines Agency: <http://www.ema.europa.eu/ema/>. Accessed August 10, 2017.

diseases (e.g., PEGASYS or PEG-INTRON for chronic hepatitis C, Cimzia for Crohn's disease, or Oncaspar for acute lymphoblastic leukemia) (Alconcel, Baas, & Maynard, 2011). The other mechanism described by which nanoparticles can be accumulated in cancerous tissues is active targeting, which can be achieved through functionalization of nanoparticles' surfaces with bioactive molecules able to recognize cancer-specific targets overexpressed in malignant cells, such as transferrin, engineered antibodies or fragments, peptides, enzymes, and folic acid, among others (Bregoli et al., 2016). Although active targeted nanomedicines are advanced at the preclinical stage, to date, only antibody- and protein-based nanomedicines (Abraxane, Adcetris, Kadcyla, and Ontak) have been FDA approved. Ongoing clinical trials with nanotherapeutics are compiled in Table 2, suggesting that we are prone to see a growth

Table 2: Nanotherapeutics under clinical evaluation (active trials recruiting patients, active not yet recruiting and completed without published results) for the treatment of solid tumors

Investigational Drug Name	Drug/Therapy	Type of Nanoparticle		Disease	Clinical Trial Phase		NCT Number
		Drug/Therapy	Nanoparticle		Trial Phase	Trial Status	
ALN-VSP02	Anti-KSP and VEGFA siRNAs	Lipid nanoparticle		Solid tumors	1	Completed	NCT01158079
dHER2+AS15	Recombinant HER2 (dHER2) antigen and AS15 adjuvant	Liposome		Solid tumors Metastatic breast cancer	1 1/2	Completed Completed	NCT00882180 NCT00952692
ABI-009	Rapamycin	Albumin nanoparticle		Breast cancer Metastatic breast cancer Refractory central nervous System Cancer	1 1	Completed Active, not recruiting	NCT00058526 NCT00140738 NCT02975882
				Advanced genitourinary, gynecological or head and neck cancers	2	Active, not recruiting	NCT02646319
				Solid tumors PEComa	1 2	Completed Recruiting	NCT00635284 NCT02494570
				Non-muscle invasive bladder cancer	1/2	Recruiting	NCT02009332
anti-EGFR-IL-DOX	Doxorubicin	EGFR-targeting liposome		Advanced sarcoma	1/2	Recruiting	NCT03190174
Atu027	Antiprotein kinase N3 siRNAs	Liposome		Solid tumors Breast cancer	1 2	Completed Recruiting	NCT01702129 NCT02833766
Aurolase	Photothermal therapy	Silica core with a gold nano shell PSMA-targeting polymeric nanoparticle		Advanced pancreatic cancer Advanced solid tumors Prostate cancer	1/2 1 Device study	Completed Completed Recruiting	NCT01808638 NCT00938574 NCT02680535
BIND-014	Docetaxel			Metastatic castration-resistant prostate cancer	2	Completed	NCT01812746
				Advanced solid tumors	1	Completed	NCT01300533
				Non-small cell lung cancer	2	Completed	NCT01792479
				Advanced non-small cell lung cancer	2	Completed	NCT02283320
CPX-1	Irinotecan and floxuridine (1:1)	Liposome		Advanced colorectal cancer	2	Completed	NCT00361842

Nanotheranostics and Their Potential in the Management of Metastatic Cancer 205

CRLX101	Camptothecin	Cyclodextran conjugated	Ovarian cancer	1/2	Active, not recruiting	NCT02389985
			Solid tumors	1	Active, not recruiting	NCT02648711
			Recurrent ovarian, fallopian tube or primary peritoneal cancers	2	Active, not recruiting	NCT01652079
			Rectal cancer	1/2	Active, not recruiting	NCT02010567
			Advanced solid tumors	1/2	Active, not recruiting	NCT02380677
			Recurrent/persistent ovarian, fallopian tube and primary peritoneal cancers	1/2	Active, not recruiting	NCT02389985
			Solid tumors	1	Active, not recruiting	NCT02648711
			Rectal cancer	1/2	Active, not recruiting	NCT02010567
			Advanced stomach, gastroesophageal or esophageal cancers	Pilot study	Completed	NCT01612546
			Advanced solid tumors	1/2	Completed	NCT00333502
			Metastatic renal cell carcinoma	2	Completed	NCT02187302
			Solid tumors	1/2	Completed	NCT00333502
			Metastatic renal cell carcinoma	2	Completed	NCT02187302
			Refractory/recurrent small cell lung cancer	1/2	Recruiting	NCT02769962
CRLX301	Docetaxel	Polymer conjugated	Advanced solid tumors	1/2	Active, not recruiting	NCT02380677
CYT-6091	rhTNF	Colloidal gold nanoparticle	Advanced solid tumors	1	Completed	NCT00356980
DC-Chol-EGFR	EGFR antisense DNA	Liposome	Solid tumors	1	Completed	NCT00436410
DCR-MYC	Anti-MYC Dicer-substrate siRNA	Lipid nanoparticle	Head and neck cancer	1	Completed	NCT00009841
DOTAP: cholesterol-Fus1	Fus1 gene (insertion)	Liposome	Malignant mesothelioma	2	Active, not recruiting	NCT02293005
DPX-0907	Multi-tumor associated antigens	Liposome	Lung cancer	1	Completed	NCT00059605
			Lung cancer	1/2	Recruiting	NCT01455389
			Advanced breast, ovarian or prostate cancers	1	Completed	NCT01095848

Table 2: Nanotherapeutics under clinical evaluation (active trials recruiting patients, active not yet recruiting and completed without published results) for the treatment of solid tumors—cont'd

Investigational Drug Name	Drug/Therapy	Type of Nanoparticle	Disease	Clinical Trial Phase	Trial Status	NCT Number
EndoTAG-1	Paclitaxel	Liposome	Breast cancer Breast cancer Advanced pancreatic cancer Liver metastatic cancer Advanced pancreatic cancer	2 2 2 2 3	Completed Completed Completed Completed Not yet recruiting	NCT01537536 NCT00448305 NCT00377936 NCT00542048 NCT03126435
Genexol-PM	Paclitaxel	Polymeric micelle	Metastatic breast cancer Advanced urothelial cancers Advanced nonsmall cell lung cancer	3 2 2	Recruiting Completed Completed	NCT03002103 NCT01426126 NCT01770795
LERaFON	c-Raf antisense oligodeoxynucleotides	Liposome	Recurrent/metastatic breast cancer Advanced ovarian cancer Advanced pancreatic cancer Hepatocellular carcinoma	3 1 2 2	Completed Completed Recruiting Recruiting	NCT00876486 NCT00877253 NCT02739633 NCT03008512
Lipoplatin	Cisplatin	Pegylated liposome	Metastatic breast cancer	2	Recruiting	NCT01784120
Lipovaxin-MM	Melanoma antigens	Liposome	Gynecologic cancers	1	Recruiting	NCT02739529
MBP-426	Oxaliplatin	Transferrin receptor-targeting liposome	Advanced solid tumors Advanced solid tumors	1 1	Completed Completed	NCT00024661 NCT00024648
MM-302	Doxorubicin	HER2-targeting liposome	Advanced solid tumors	1	Completed	NCT00100672
Nal-IRI	Irinotecan	Liposome	Pleural malignancies Melanoma Solid tumors	1 1 1	Recruiting Completed Completed	NCT02702700 NCT01052142 NCT00355888
			Advanced breast cancer	1	Active, not recruiting	NCT01304977
			Metastatic pancreatic cancer	2	Active, not recruiting	NCT02697058
			Advanced cholangiocarcinoma	2	Not yet recruiting	NCT03043547
			Advanced biliary-tract cancers	2	Not yet recruiting	NCT03044587
			Pancreatic cancer	2	Recruiting	NCT02551991
			Diffuse intrinsic pontine glioma	1	Recruiting	NCT03086616

Nanotheranostics and Their Potential in the Management of Metastatic Cancer 207

Nanoplatin	Cisplatin	Polymeric micelle	Advanced pancreatic cancer	1/2	Completed	NCT00910741
NBTR3	Radiotherapy	Hafnium oxide NP	Head and neck cancer	1	Recruiting	NCT02817113
			Soft tissue sarcoma	1	Completed	NCT01433068
			Liver cancers	1/2	Recruiting	NCT02721056
			Prostate cancer	1/2	Recruiting	NCT02805894
			Head and neck cancer	1	Recruiting	NCT01946867
			Soft tissue sarcoma	2/3	Recruiting	NCT02379845
			Head and neck cancer	1/2	Recruiting	NCT02901483
			Rectal cancer	1/2	Recruiting	NCT02465593
NC-4016	Oxaliplatin	Polymeric micelle	Advanced solid tumors	1	Active, not recruiting	NCT03168035
NK012	SN-38 (irinotecan metabolite)	Polymeric micelle	Small cell lung cancer	2	Completed	NCT00951613
			Advanced breast cancer	2	Completed	NCT00951054
			Refractory solid tumors	1	Completed	NCT00542958
			Metastatic breast cancer	1	Completed	NCT01238952
			Solid tumors	1	Completed	NCT01238939
NK105	Paclitaxel	Polymeric micelle	Advanced breast cancer	3	Completed	NCT01644890
CT-2103 (Xyotax)	Paclitaxel	Polymer-drug conjugates (polyglumex)	Advanced fallopian tube, ovarian or primary peritoneal cancers	3	Active, not recruiting	NCT00108745
			Metastatic breast cancer	1	Completed	NCT00270907
			Recurrent/persistent ovarian or primary peritoneal cancers	2	Completed	NCT00045682
			Metastatic breast cancer	2	Completed	NCT00265733
			Prostate cancer	2	Completed	NCT00446836
			Ovarian, fallopian tube or primary peritoneal cancers	1	Completed	NCT00060359
			Advanced colorectal cancer	1	Completed	NCT00598247
			Metastatic breast cancer	2	Completed	NCT00148707
			Recurrent ovarian, fallopian tube or primary peritoneal cancers	1/2	Completed	NCT00017017
pbi-shRNA	Antistathmin 1 siRNA	Lipid nanoparticle	Ovarian cancer	2	Completed	NCT00069901
STMN1 LP	DNA oligonucleotide against BCL-2	Liposome	Advanced solid tumors	1	Completed	NCT01505153
PNT2258	Mitomycin-C	Liposome	Advanced solid tumors	1	Completed	NCT01191775
Promitil		Liposome	Solid tumors	1	Recruiting	NCT01705002

Continued

Table 2: Nanotherapeutics under clinical evaluation (active trials recruiting patients, active not yet recruiting and completed without published results) for the treatment of solid tumors—cont'd

Investigational Drug Name	Type of Nanoparticle		Clinical		NCT Number	
	Drug/Therapy	Nanoparticle	Disease	Trial Phase		Trial Status
SGT-53	Plasmid encoding normal human WT p53 DNA	Transferrin receptor-targeting liposome	Solid tumors	1	Completed	NCT00470613
			Recurrent glioblastoma	2	Recruiting	NCT02340156
siRNA-EphA2-DOPC	Anti-EphA5 siRNA	Liposome	Refractory/recurrent solid tumors	1	Recruiting	NCT02354547
			Metastatic pancreatic cancer	2	Recruiting	NCT02340117
Tecemotide	MUC1 antigen	Liposome	Advanced cancers	1	Recruiting	NCT01591356
			Colorectal carcinoma	2	Active, not recruiting	NCT01462513
ThermoDox	Doxorubicin	Liposome	Prostate cancer	2	Completed	NCT01496131
			Recurrent breast cancer	1/2	Completed	NCT00826085
TKM-080301	Anti-PLK1 siRNA	Lipid nanoparticle	Liver metastatic or primary cancers	1	Completed	NCT00441376
			Liver cancers	1	Completed	NCT02181075
			Hepatocellular carcinoma	3	Recruiting	NCT02112656
			Refractory solid tumors	1	Recruiting	NCT02536183
			Neuroendocrine or adrenocortical tumors	1/2	Completed	NCT01262235
			Advanced hepatocellular carcinoma	1/2	Completed	NCT02191878
			Liver metastatic or primary cancers	1	Completed	NCT01437007

Sources: Thakor, A. S., Gambhir, S. S. (2013). Nanoncology: the future of cancer diagnosis and therapy. *CA: A Cancer Journal for Clinicians*, 63(6), 395–418. doi:10.3322/caac.21199; Shi, J., Kantoff, P. W., Wooster, R., Farokhzad, O. C. (2016). Cancer nanomedicine: progress, challenges and opportunities. *Nature Publishing Group*, 17(1), 20–37. doi:10.1038/nrn.2016.108; Caster, J. M., Patel, A. N., Zhang, T., Wang, A. (2017). Investigational nanomedicines in 2016: a review of nanotherapeutics currently undergoing clinical trials. *Wiley Interdisciplinary Reviews. Nanomedicine and Nanobiotechnology*, 9(1). doi:10.1002/wnan.1416; <https://clinicaltrials.gov> (accessed 24 October 2017).

in the number of FDA-approved therapeutic nanoparticles over the foreseeable future, which will also integrate new molecular entities and novel classes of therapeutic agents (e.g., mRNA, siRNA, plasmids, DNA) (Caster, Patel, Zhang, & Wang, 2017; Shi, Kantoff, Wooster, & Farokhzad, 2016; Thakor & Gambhir, 2013).

Recently, the failure in phase II clinical trials of a promising targeted polymeric nanocarrier containing the chemotherapeutic drug docetaxel, BIND-014 (Bobo, Robinson, Islam, Thurecht, & Corrie, 2016; Ledford, 2016) has raised several questions regarding interindividual factors that could determine the efficacy of nanotherapies. According to a recent work, the average tumor uptake of nanoparticles is only about 0.7% of the injected dose (Wilhelm, Tavares, Dai, et al., 2016). This fact supports the idea that models fail to predict accumulation of systemic delivered nanoparticles into the tumor, as they are oversimplified and overlook multiple biological steps in the process. In order to overcome this hurdle, efforts are being made to classify patients by high EPR effect to determine if they are suitable candidates for nanotherapies. Understanding individual predisposition to nanoparticle accumulation in tumor sites is essential for selecting the correct nanotherapy. Some relevant studies related to this are disclosed in Section 5.1.1. Taking this scenario into consideration, we believe that our position should be to exploit the benefits of nanotechnology but recognize its limitations, and even more than before, work together with other modalities such as diagnosis to carefully select the patients most likely to benefit from a given nanotherapy. Nanotheranostics, we believe, would and should play an important role in this new situation.

4 Nanotheranostics

A great deal of effort has been made over the last three decades to develop a plethora of nanocarriers for cancer therapeutic purposes. However, the current low response rates and limited increase of overall patient survival evidenced that the chemotherapeutic revolution nanomedicines promised is still far from reality. It is essential now to move forward in the future toward personalized cancer medicine to produce real clinical impact and translation. Integrating imaging modalities and therapeutic molecules into a single multifunctional nanoparticle, a nanotheranostic, could help in the clinical practice by concurrently diagnosing disease, stratifying patients, guiding focal therapy, tracking drug release and penetration within tumors, monitoring response, and if required, switching treatments (Cui & Wang, 2016). These exceptional applications are particularly important in the era of precision medicine. Different theranostic modalities include photodynamic therapy, photothermal, magnetothermal and electrothermal therapies, photo- and ultrasound-triggered chemotherapeutic release, X-ray and radiofrequency, computed tomography (CT), magnetic resonance imaging (MRI), positron emission tomography (PET), and single-photon emission computed tomography (SPECT) (Park, Aalipour, Vermesh, Yu, & Gambhir, 2017; Sneider, VanDyke, Paliwal, & Rai, 2017; Thakor & Gambhir, 2013).

Considering nanoparticles that have been developed for cancer imaging, there are several examples in clinical practice or under clinical development, as extensively reviewed by Thakor et al. (Thakor & Gambhir, 2013) including superparamagnetic iron oxide nanoparticles and ultrasmall superparamagnetic iron oxide nanoparticles for MRI, heavy metal nanoparticles (i.e., gold, lanthanide and tantalum) for CT, ^{99m}Tc sulphur colloid nanoparticles for SPECT, I-labelled cRGDY silica nanoparticles for PET, surface-enhanced Raman scattering nanoparticles for optical imaging and single-walled carbon nanotubes for photoacoustic imaging. With respect to nanotheranostics, several nanoscaled materials have been explored during the last years, including liposomes (Dai & Yue, 2017), micelles (Pellosi et al., 2017), dendrimers (Zhu, Fu, Xiong, Shen, & Shi, 2015), solid lipid nanoparticles (Bae, Lee, Lee, Park, & Nam, 2013), polymeric nanoparticles (Alberti, Protti, Franck, et al., 2017), albumin-based nanoparticles (Huang, Yang, Liu, et al., 2017), quantum dots (QDs) (Guo, Qiu, Guo, et al., 2017), metallic nanoparticles (Rajkumar & Prabakaran, 2016; Shi, Ye, He, et al., 2014; Zhu, Zhou, Mao, & Yang, 2017), carbon nanotubes (Wang, Zhang, Yang, et al., 2016), nanobubbles (Duan et al., 2017), and iodinated nanoparticles (Lee, Chung, Cho, & Kim, 2016). However, despite the fact the field of nanotheranostics is drastically emerging, and many experiments show promising results, no formulation has reached the market yet. As far as we know, there is only one formulation undergoing clinical trials (phase I), AGuIX (Activation and Guidance of Irradiation by X-ray), a gadolinium-based nanoparticle of around 5 nm diameter for the treatment of multiple brain metastases (NCT02820454) with a double role, radiosensitizer and imaging agent. At first developed for imaging applications due to its magnetic resonance contrast properties, it was observed that, when combined with X-ray radiation, led to a threefold enhancement in the efficiency of the radiotherapy in mice (Detappe, Kunjachan, Rottmann, et al., 2015; Kotb, Detappe, Lux, et al., 2016).

The big challenge for the translation of all this technology into daily clinical practice is the need for a detailed understanding of the interactions between cancer nanotheranostics and the human body, the tumor, and the microenvironment. Moreover, a long-term assessment of toxicity, and the establishment of regulatory protocols for cancer nanotheranostics, will also be required (Chen, Zhang, Zhu, Xie, & Chen, 2017). As metastatic cancer is a systemic disease, this means that most commonly, patients are diagnosed and monitored by computed tomography (CT), magnetic resonance (MRI), and positron emission tomography (PET) (or PET/CT if available). Therefore, we believe that nanotheranostics designed for these modalities will initially have greater chances at translation.

5 Specific Interventions in the Metastatic Cascade Making Use of Nanotheranostics

As mentioned before, the metastatic process is very complex, with a series of consecutive events susceptible to therapeutic interventions. The biological mechanisms that specifically

drive each step of metastasis might be addressable using nanoparticles, and could also benefit from the development of more sophisticated nanotheranostics.

5.1 Premetastatic Initiation

5.1.1 Tumor growth

Targeting the primary tumor to interfere with tumor growth has been the main objective of most of the research work carried out in the nanomedicine field. In most cases, results refer to nanocarriers that encapsulate conventional anticancer drugs (e.g., doxorubicin, paclitaxel, docetaxel) (Chow & Ho, 2013), and are passively accumulated in the tumor, achieving prolonged circulation times, higher areas under the plasma concentration-time curve (AUC), lower clearance rates, decreased toxicities, higher accumulation in tumors (xenograft or orthotopic mice models), and improved therapeutic efficiencies, compared to the free drugs (Gabizon, Shmeeda, & Barenholz, 2003). However, as we mentioned before, there is generally little translation to clinic. One of the main problems is that, in reality, only a tiny dose of the administered drug actually accumulates into the tumor (Wilhelm et al., 2016). Molecular imaging can provide a solution to understand tumor heterogeneity and determine if nanoparticles can indeed accumulate into the tumors, for example by co-administering nanoparticles that can be tracked, in combination with the therapeutic nanoparticles. In this regard, magnetic nanoparticles (ferumoxytol) were administered together with paclitaxel PLGA-PEG nanoparticles to mice bearing subcutaneous human fibrosarcoma, with the purpose of tracking particle distribution within tumors and the microvasculature, and predicting the effectiveness of the therapeutic nanoparticles (Miller, Gadde, Pfirschke, et al., 2015). PET-radiolabeled nanoparticles (Zirconium-89 nanoreporter) were also co-injected with docetaxel-loaded liposomes (Doxil) for quantifying biodistribution, and predicting the therapeutic efficacy of the liposomes in a xenograft breast cancer mouse model (Pérez-Medina, Abdel-Atti, Tang, et al., 2016). Injection of iodine-labelled liposomes in rats bearing breast tumor xenografts has similarly been of utility for assessing tumor uptake by mammography and to classify animals into good and bad prognosis subgroups, previous treatment with liposomal doxorubicin. Interestingly, tumor progression correlated well with the subgroups of good and bad prognosis, confirming the high variability and relevance of the EPR effect status (Karathanasis, Suryanarayanan, Balusu, et al., 2009). This novel approach could, therefore, permit classification of patients that are prone to benefit from nanotherapeutics. Even if the works reported here actually refer to the combination of two individual nanostructures, multimodal all-in-one nanotheranostics could also have a real application for patient stratification, minimizing the delay between diagnosis and treatment, and allowing evaluation in real-time. Along with this, there are several other applications of potential interest for nanotheranostics, such as tracking drug release and penetration within tumors, imaging-guided local therapy, or monitoring therapeutic responses (Chen, Zhang, et al., 2017).

Improving the targeting of nanotheranostics to tumors beyond EPR-mediated effect can be achieved by tumor-specific delivery, upon decoration with molecules such as peptides, aptamers, and antibodies (Diou, Tsapis, & Fattal, 2012). In this regard, Zolata, Abbasi Davani, and Afarideh (2015) proposed the development of a complex multimodal nanoparticle based on minosilane-PEG coated magnetic nanoparticles, loaded with (Quail & Joyce, 2013). In radiolabeled doxorubicin, for bimodal tumor imaging (MRI/SPECT). These nanoparticles were functionalized with trastuzumab for specific targeting to HER2 receptor. Results in mice bearing HER2 positive breast tumors show the potential of this approach for accurate tumor imaging with improved sensitivity, allowing the simultaneous treatment with radio- and chemopharmaceuticals. A different active targeting with theranostic nanoparticles was proposed by Kim, Jeong, and Jon (2010) referring to the functionalization of doxorubicin-loaded gold nanoparticles with a prostate-specific membrane antigen (PSMA) RNA aptamer for CT imaging and targeted chemotherapy, but this formulation has not been tested in vivo yet.

The development of the so-called “smart” nanosystems, that is, nanoparticles that are able to deliver their drug or induce a cytotoxic effect in cancer cells just in response to an externally controlled exogenous stimulus (e.g., light, ultrasound, magnetism, temperature and electric field) is gaining increased attention for the development of nanotheranostics. Remotely triggered nanosystems present promising clinical benefits, as they have the ability to turn “on” or “off” the delivery of therapeutics depending on multiple variables, such as whether the nanoparticle reached the tumor or not, hence reducing the toxicity in “normal” tissue in a noninvasive fashion (Sneider et al., 2017). Exogenous stimuli can be provided by photodynamic therapy, photothermal therapy, and phototriggered chemotherapeutic release. Currently, only photodynamic therapy is clinically approved for cancer treatment, while photothermal and phototriggered modalities are still undergoing clinical trials. An example of a remotely triggered nanotherapy is NanoTherm, a thermoresponsive nanoformulation that effectively converts energy into heat that can also be tracked by CT for imaging purposes. Inorganic materials (i.e., gold, silica, silver) are being widely explored for photothermal therapy (PTT), however, the fact that they are not biodegradable has hampered their clinical translation. To overcome this limitation, a recent study reports the development of biocompatible and bioeliminable magnetoplasmonic nanoassemblies (MPNAs), formed by Fe_3O_4 nanoclusters and gelatin-coated with gold, which are efficient for computed tomography (CT), photoacoustic tomography (PAT), and magnetic resonance (MRI), and also allow photothermal cancer therapy. MPNAs showed extraordinary results, with complete tumor recession in liver-cancer-bearing mice after exposure to near infrared (NIR) light for 3 min (Li, Fu, Chen, et al., 2016; Fig. 2). Stimuli-responsive nanotheranostics are also being developed for gene delivery (Shim & Kwon, 2012). In a recent paper, Gao, Gao, Xu, et al. (2017) reported the development of nanodroplets for targeted ultrasound diagnosis and gene delivery in HER2-overexpressing breast cancer cells.

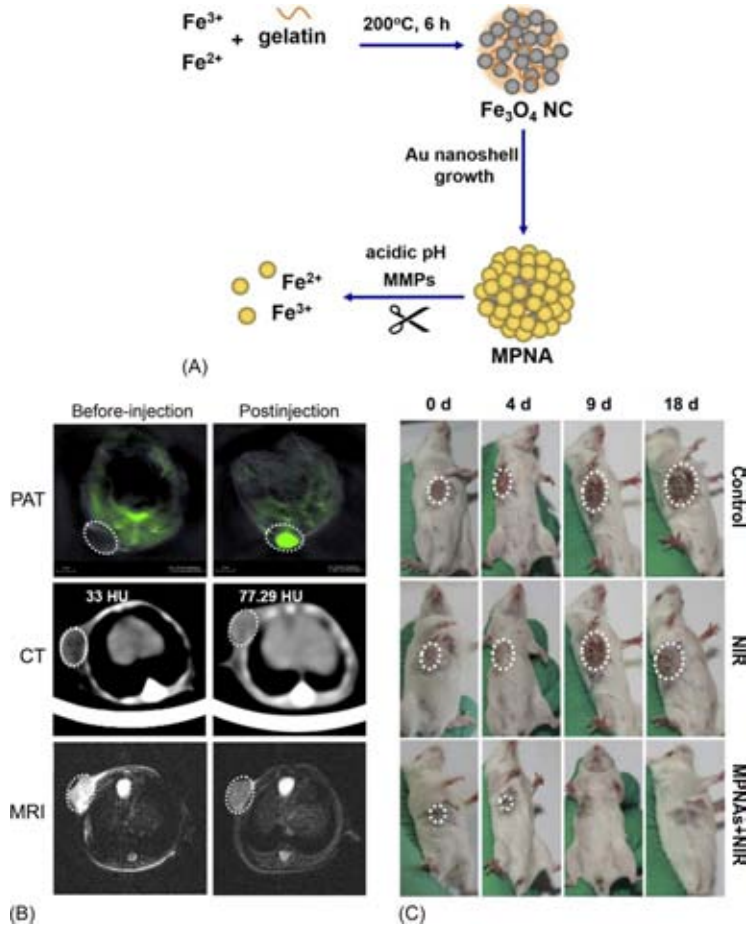


Fig. 2

(A) Schematic illustration of the biodegradable process of magnetoplasmonic nanoassemblies (MPNAs). (B) In vivo trimodal imaging of subcutaneous liver tumor bearing mice before and after 2 h of the intravenous injection of MPNAs as a contrast agent for photoacoustic tomography (PAT), computed tomography (CT) and magnetic resonance imaging (MRI). (C) In vivo photothermal therapy of MPNAs under a near infrared (NIR) light at different time intervals of therapy, compared with the control and NIR light alone. Data from Li, L., Fu, S., Chen, C., et al. (2016). Microenvironment-driven bioelimination of magnetoplasmonic nanoassemblies and their multimodal imaging-guided tumor photothermal therapy. *ACS Nano*, 10(7), 7094–7105. doi:10.1021/acsnano.6b03238, with the permission of American Chemical Society, Copyright (2017).

In general, it can be concluded that the field of nanotheranostics applied to cancer has drastically emerged over the last years. Despite this, further research still needs to be done in order to improve translation and have a clear impact in patient survival. More experiments should also focus on targeting other determinant phases of cancer disease, apart from the primary tumor, providing novel and complementary approaches for the management of metastatic cancer.

5.1.2 Cancer stem cells

Intratumor heterogeneity is a key factor contributing to the devastating outcome of cancer, therapeutic failure, and drug resistance, and should be taken into account for the development of efficient therapeutic strategies (Greaves, 2015; Huang, Shen, Ding, & Geng, 2014; Mcgranahan & Swanton, 2017). Tumors contain genetically and phenotypically distinct subpopulations of cancer cells with unique capacities for growth, differentiation, and invasion (Carey, Starchenko, McGregor, & Reinhart-King, 2013). This variability is present at multiple levels, that is, genetically, histologically, and physiologically (De Palma & Hanahan, 2012). Indeed, only a minority of all cancers are caused by germline mutations, whereas the enormous majority (90%) are associated dynamic processes related to somatic mutations and environmental factors (Grivennikov, Greten, & Karin, 2010). Changes in the subclonal composition can occur, for example, in the context of disease progression, that is, metastasis, or during drug treatment (Campbell, Yachida, Mudie, et al., 2010; Ding, Ley, Larson, et al., 2012). Thus, selective clones with specific phenotypic advantages will survive or predominate in the tumor. Cancer stem cells (CSCs), also known as tumor-initiating cells (TICs), constitute a biologically unique subset of stem-like cells within the bulk tumor cell population with exclusive characteristics, unlimited self-renewal, and pluripotency (Sainz Jr, Carron, Vallespinós, & Machado, 2016) and are related to the generation of resistances, tumor relapse, and formation of micrometastases (Mina & Sledge, 2011).

In the past few decades, different cell signaling pathways (Wnt/ β -catenin, Notch, PI3K/AKT, transforming growth factor- β , and hedgehog signaling) and specific markers (aldehyde dehydrogenases, CD44, CD90, and CD133), involved in CSC function and maintenance, have been disclosed (Hong, Jang, Lee, & Nam, 2015; Singh, Minz, & Sahoo, 2017). The fact that CSCs express different biomarkers at the cell surface makes them targetable by surface-decorated nanoparticles for drug delivery purposes (Livney & Assaraf, 2013). This has led to the development of different therapeutic strategies based on organic and inorganic magnetic nanoparticles, directed for example to inhibit ABC transporters overexpressed on the CSCs surface and associated with multidrug resistance, cell signaling pathways, quiescent CSCs, CSCs dedifferentiation, etc. (Gener, Rafael, Fernández, et al., 2016; Hong et al., 2015; Li, Li, Mo, & Dai, 2017; Li, Li, Wu, et al., 2017; Livney & Assaraf, 2013; Shen, Xia, & Wang, 2016; Singh et al., 2017; Steg, Katre, Goodman, et al., 2012; Takeishi et al., 2013). Besides all these encouraging advances, promising future perspectives imply the combination of these

innovative therapeutic strategies with different imaging modalities for precise identification of this cell subpopulation. Within this premise, [Barth, Altinoglu, Shanmugavelandy, et al. \(2011\)](#) reported the preparation of calcium phosphosilicate nanoparticles, decorated with a surface biomarker of leukemia stem cells (anti-CD117 antibody) to selectively deliver a photosensitizer (indocyanine green) for diagnostic purposes and photodynamic therapy. This strategy led to a 29% disease-free survival in a myeloid leukemia mouse model, with some mice exhibiting leukemia-free survival, revealing a successful CSCs eradication. In another recent paper, [Tang, Zhou, Liu, et al. \(2017\)](#) reported the design of a multifunctional magnetic nanosystem based on a magnetic Fe₃O₄ core for imaging and hyperthermia treatment, a polypyrrole shell to allow high drug loading capacity (DAPT), and hyaluronic acid for targeting CD44. This multimodal nanosystem allowed monitoring of the drug distribution within the tumor by MRI and photoacoustic imaging, and the combination of chemotherapy and magnetohyperthermia therapy to significantly inhibit tumor growth and blood vessels density, altogether revealing an effective elimination of CSC without causing side effects in 4T1 breast tumor-bearing mice. A novel theranostic strategy, was also developed by [Mohanty, Chen, Li, et al. \(2017\)](#) in this case for glioblastoma multiforme (GBM). Glioblastoma-initiating cells (GIC) are resistant to the limited number of current therapies leading to poor prognosis and 90% of recurrence in GBM patients. Cross-linked iron oxide nanoparticles (CLIO) were loaded with a VDA-prodrug (azademethylcolchicine) and conjugated to a highly potent vascular disrupting agent (ICT) linked to a matrix-metalloproteinase (MMP-14) cleavable peptide. These nanoparticles were followed by MRI and efficiently disrupted the tumor vasculature of MMP-14 expressing GBM, induced GIC apoptosis, and almost led to a complete reduction of orthotopic glioblastoma tumors, with a significant impact on survival.

Despite the encouraging results, much work still needs to be done in order to move nanotheranostics forward to clinical practice for this particular approach. However, we believe that this is a promising strategy to determine the efficiency of the therapy in this particular cell subpopulation, which is more resistant to current treatments and responsible for tumor-relapse and recurrence.

5.1.3 Tumor microenvironment

It is known now that malignant features of tumor cells cannot be revealed without an important interplay between them and their local environment ([Alonso-Nocelo, Abuíñ, López-López, & de la Fuente, 2016](#); [Sounni & Noel, 2013](#)). Communication between cells and their associated stroma is crucial for normal tissue homeostasis and tumor growth, influencing disease initiation, progression, and patient prognosis ([Quail & Joyce, 2013](#)). Specifically, tumor cells are surrounded by a complex and diverse stroma composed by different nontransformed cells, such as fibroblasts, endothelial cells and immune cells, constituting the so-called Tumor Microenvironment (TME) ([Balkwill & Mantovani, 2001](#); [Hanahan & Coussens, 2012](#); [Junttila & de Sauvage, 2013](#); [Mueller & Fusenig, 2004](#);

Quail & Joyce, 2013). Infiltrating immune cells produce chemokines, growth factors, and matrix degrading enzymes that can create a permissive environment of chronic inflammation, ideal for tumor growth and progression. Several studies have shown that tumor-associated macrophages (TAMs) facilitate tumor cell dissemination, guiding tumor cells towards the circulation (Bonde, Tischler, Kumar, Soltermann, & Schwendener, 2012; Pollard, 2004; Solinas, Schiarea, Liguori, et al., 2010). Cancer-associated fibroblasts (CAFs) are also present in high numbers and elicit pro-tumorigenic functions, producing pro-inflammatory cytokines and vascular endothelial growth factors (VEGF), which induce vascular permeability and angiogenesis and enhance the metastatic process (Xing, Saidou, & Watabe, 2010). Elucidating the nature of interactions and the mechanisms of co-evolution of tumor cells and their microenvironment is crucial for understanding what drives tumor initiation and progression, and for the development of better cancer preventive and therapeutic interventions.

Stimulated by advances made in the field of material sciences and drug delivery, nanosystem able to deliver their cargo in a spatial-temporal fashion and dosage-controlled manner, taking advantage of the singularities presented in the TME, such as pH variations (Aires, Ocampo, Simões, et al., 2016; Kim, Lee, Oh, Gao, & Bae, 2008; Ling, Xia, Park, et al., 2014; Mo, Jiang, DiSanto, Tai, & Gu, 2014; Mok, Veiseh, Fang, et al., 2010; Mura, Nicolas, & Couvreur, 2013; Sawant, Hurley, Salmaso, et al., 2006; Shen, Huang, Han, et al., 2012; Zou, Yu, Wang, et al., 2010), metabolic state (Tennant, Durán, & Gottlieb, 2010; Vaupel, Kallinowski, & Okunieff, 1989), hypoxic state (Garcia-Mazas, Csaba, & Garcia-Fuentes, 2017; Kanapathipillai, Brock, & Ingber, 2014), and redox state (Cavallaro, Campisi, Licciardi, Ogris, & Giammona, 2006; Kirpotin, Hong, Mullah, Papahadjopoulos, & Zalipsky, 1996; Saito, Swanson, & Lee, 2003; West & Otto, 2005) have been developed. An example with nanotheranostics refers to the development of pH-sensitive modified-dextran/polyvinyl alcohol (PVA) nanoparticles, loaded with near infrared (NIR) emissive probes and doxorubicin. Apart from tracking the nanoparticle distribution, the imaging probe was of use to reveal the release of the drug during the degradation of the nanoparticles in the acidic environment (Yu, Chen, Zhang, et al., 2014). pH-sensitive nanotheranostics, composed of a nanogel functionalized with folic acid for active targeting, labeled with rhodamine B, and loaded with the drug triptolide, have also been proposed for the treatment of hepatocellular carcinoma (HCC). In this case, in vivo results showed a good accumulation in the tumor cells and the release of the drug during endosome maturation (Ling et al., 2014). Triggered delivery can also be achieved by endogenous intracellular concentrations of certain metabolites. In this regards, Qian, Chen, Zhu, et al. (2016) have developed an ATP-responsive and near-infrared (NIR)-emissive conjugated polymer-based nanocarrier for the controlled release of anticancer drugs and real-time monitoring. At the significantly higher intracellular ATP concentrations, the drug doxorubicin was efficiently disassociated, leading to a good pharmacological response in terms of tumor growth. Real-time NIR fluorescent imaging was efficient for monitoring nanoparticle biodistribution. In a different work, Chen, Jia,

Tham, et al. (2017) describe the use of glutathione (GSH)-responsive nanosized vesicles for the synergetic delivery of a drug (camptothecin), siRNA (siP1K1), and a fluorescence turn-on mechanism that allows monitoring of the cellular uptake of the nanovesicles in real-time. Lastly, Feng, Cheng, Dong, et al. (2017) have described the use of a theranostic liposome for encapsulation of a hydrophilic hypoxia-activated prodrug (AQ4N) plus a hydrophobic photosensitizer (hexadecylamine conjugated chlorin e6 (*hCe6*)), which only demonstrate toxicity when reaching hypoxic conditions in the TME. Moreover, association of $^{64}\text{Cu}^{2+}$ allowed tracking of the liposomes by PET, and verification of the successful accumulation of the nanotheranostics into the tumor after intravenous administration to mice bearing breast cancer tumors.

It has been suggested that active targeting of specific tumor microenvironment-infiltrated immune cells and cells from the stroma could be a promising strategy for the development of novel therapeutic approaches that can benefit from nanotechnology (Allavena, Sica, Solinas, Porta, & Mantovani, 2008; Cirri & Chiarugi, 2011; Franco, Shaw, Strand, & Hayward, 2010; Junttila & de Sauvage, 2013; Patel & Janjic, 2015; Serafini, Borrello, & Bronte, 2006). To date, very few reports refer to the specific use of nanotheranostics for targeting immune cells into the tumor microenvironment (de la Fuente, Langer, & Alonso, 2014). An interesting example refers to the use of gold nanoparticles loaded with Alexa Fluor 488-labelled siRNA anti-VEGF and decorated with the M2pep peptide for selective targeting to TAMs. After intratracheal administration to mice bearing orthotopic lung tumors, results showed an efficient accumulation in TAMs, accompanied by a decrease in VEGF TAM-derived protein expression of 80%, thus, reducing their recruitment to the inflammatory tumor environment and leading to a complete tumor regression after 36 days of therapy (Conde, Bao, Tan, et al., 2015). Another recent study refers to the development of PEGylated carboxymethylcellulose nanoparticles loaded with docetaxel and DiI as fluorescent marker. In vivo studies in human pancreatic xenografts demonstrated a 90% reduction of CAFs after three cycles of treatment, which translates in significant tumor regression (Ernsting, Hoang, Lohse, et al., 2015). As a last example, lipid nanocapsules loaded with both C12 carbon chain modified gemcitabine and DiD were developed for specific target of the monocytic-myeloid derived suppressor cells (M-MDSC) (Sasso, Lollo, Pitorre, et al., 2016). After subcutaneous administration to melanoma-bearing mice, results demonstrated the effective targeting capacity of the formulation to M-MDSCs, and an improved effect in terms of tumor growth.

Considering this information, it is possible to conclude that there is a lot of potential for the application of nanotheranostics to improve the understanding of tumor-stroma interactions in cancer progression and to determine the relevance of eliminating specific subpopulations of immune-infiltrated cells from the tumor equation to block tumor progression and dissemination.

5.1.4 Angiogenesis

Angiogenesis is a crucial process and key step during tumor progression and dissemination, decisive for getting a good supply of nutrients and oxygen (Quail & Joyce, 2013; Weis & Cheresh, 2011). Tumors reaching a size of 2 mm suffer a process of increased interstitial pressure that inhibits the uptake of nutrients and metabolites. At that moment, the establishment of hypoxic areas prompt the sprouting of new blood vessels from the preexisting ones (Danhier, Feron, & Pr eat, 2010). Activation of oncogenes as *RAS* and *MYC* initiates the induction of a transcriptional program that enhances tumor microenvironment remodeling and an angiogenic switch (Grivennikov et al., 2010). Angiogenesis process also involves cell-to-cell (i.e., vascular endothelial cells, fibroblasts, myeloid cells, monocytes, and pericytes) and cell to ECM interactions (Ruoslahti & Pierschbacher, 1987; Weis & Cheresh, 2011). However, the new tumor vasculature is imperfect and deeply contributes to cells access and intravasation into the circulatory or lymphatic systems (Morikawa et al., 2002).

Selective delivery of drugs to tumor vasculature is a promising strategy that has been widely explored in cancer therapeutics (Byrne, Betancourt, & Brannon-Peppas, 2008; Chen & Cai, 2014; Chung, Lee, & Ferrara, 2010; Desgrosellier & Cheresh, 2010). Moreover, imaging of the tumor vasculature is of high interest for patient stratification and diagnosis purposes (Baetke, Lammers, & Kiessling, 2015; Cai & Chen, 2008; Liu, Miyoshi, & Nakamura, 2007). Over the last years, and paralleled to the relevant advances in the nanotechnology and chemical engineering field, different formulations have emerged as targeted systems to specific biomarkers expressed in the tumor vasculature, including integrins ($\alpha_v\beta_3$, $\alpha_v\beta_5$, $\alpha_5\beta_1$, and $\alpha_3\beta_1$), vascular endothelial growth factor receptors (VEGFRs), and endoglin (CD105), among others (Kunjachan, Pola, Gremse, et al., 2014; Seon, Haba, Matsuno, et al., 2011; Weis & Cheresh, 2011). Several types of nanosystems have been developed for antiangiogenesis targeting purposes comprising polymer conjugates (Fonsatti, Nicolay, Altomonte, Covre, & Maio, 2010; Mitra et al., 2005; Oliveira & Faintuch, 2015; Park, Lee, Jung, et al., 2008; Yin, Hui, Yao, et al., 2015), liposomes (Ren, Chen, Li, et al., 2016; Sonali, Singh, Sharma, et al., 2016; V lkel, H lig, Merdan, M ller, & Kontermann, 2004; Zhang, Feng, Henning, et al., 2009), inorganic nanoparticles (Chen, Ayala-Orozco, Biswal, et al., 2014; Chen, Hong, Zhang, et al., 2013; Gao, Xie, Chen, et al., 2014; Liu, Chen, Li, & Xu, 2016; Schleich, Po, Jacobs, et al., 2014; Yang, Hong, Grailer, et al., 2011; Zhang et al., 2014), and organic nanoparticles (Dahmani et al., 2016; Danhier, Danhier, Schleich, et al., 2016; Du, Zhang, Jing, et al., 2015; Murphy, Majeti, Barnes, et al., 2008; Schleich et al., 2014).

Several peptide-derived sequences have been described to target the integrin family, and could, therefore, be exploited for the functionalization of nanotheranostics. Arginine-glycine-aspartate amino acid sequence, named RGD motif, was the first endothelial binding peptide described in 1987 (Ruoslahti & Pierschbacher, 1987). A recent work published by Dahmani et al. (2016) describes auto-assembled nanoparticles, formed by the conjugation of heparin

(LMWH) with a cyclic RGD-derived peptide c(RGDyK), of use for the encapsulation of the hydrophobic antiangiogenic drug, gambogic acid, and labelled with Cy7 for optical imaging. In vivo studies show the successful delivery of this targeted nanotheranostics to both cancer cells and endothelial cells, and an efficient inhibition of tumor growth in U87MG xenografts (Dahmani et al., 2016). PEGylated liposomes decorated with c(RGDyK) have also been proposed for lung cancer theranostics, upon encapsulation of hydrophobic and hydrophilic anticancer drugs (paclitaxel and carboplatin) and gadodiamide for MRI imaging. In vivo results show a tumor signal 36-fold higher than the commercial contrast agent Omniscan, after 5-h administration, and a synergistic effect due to the combination of both drugs into a single nanostructure (Ren et al., 2016). Another interesting example describes RGD-TPGS decorated liposomes containing docetaxel (DCX) and quantum dots (QDs) for brain cancer, to improve tumor imaging and drug accumulation in the tumor (Sonali et al., 2016). PLA nanoparticles functionalized with a novel peptide, GX1 (CGNSNPKSC) (Hui, Han, Liang, et al., 2008), were developed for encapsulation of a recombinant antiangiogenic endostatin (GPENs) and labeled with IRDye 800CW for optical imaging (Du et al., 2015). Results demonstrate that this nanotheranostic formulation successfully delivered the drug to the tumor vasculature and exhibited an enhanced antitumor efficacy in colorectal tumor-bearing xenografts. Last example refers to the use of mesoporous silica nanoparticles (MSN), decorated with TRC105 (Fab), for targeting endoglin. Dual-labeling with ⁶⁴Cu and IRDye 800CW allowed successful in vivo PET/NIRF imaging and determining the biodistribution of the nanostructures in 4T1 breast tumor-bearing mice, showing an improved accumulation in the actively-proliferating tumor vasculature (Chen et al., 2013).

We are convinced that many other interesting multicomponent nanotheranostic approaches will be described in the upcoming years, both to interfere with and monitor the angiogenic switch, as well as to stratify patients according to their tumor microvasculature, in an attempt to predict the accumulation and prognosis of therapeutic nanoparticles.

5.1.5 Invasion and intravasation

To initiate invasion, cancer cells must redefine their communication with surrounding cells and the extracellular matrix (ECM). For that purpose, tumor cells overexpress dynamic cell adhesion molecules (CAMs) on their surface, such as integrins (mediating cell-ECM adhesions) and cadherins (involved in cell-cell interactions) (Van Zijl, Krupitza, & Mikulits, 2011). They also secrete cytokines such as vascular endothelial growth factor (VEGF), inducing the formation of leaky blood vessel or causing endothelial cell death by releasing reactive oxygen species (Lin et al., 2011). As a result, tumor cells experiment with changes in their transcriptional program, for example, expression molecules responsible for motility control and migration, to enhance the epithelial-to-mesenchymal transition process (EMT) (Kedrin et al., 2007). The ECM has the ability to influence tumor initiation and progression towards malignancy as well. Different mechanisms have been proposed to mediate cancer cell

entry into the circulation such as collagen crosslinking, stiffening of the extracellular matrix (ECM), and increased focal adhesions (Levental, Yu, Kass, et al., 2009). Indeed, primary tumors of different metastatic potential vary in stiffness and composition of both tumor- and stroma-derived ECM components (Branco da Cunha, Klumpers, Li, et al., 2014; Chaudhuri, Koshy, Branco da Cunha, et al., 2014). Immune cells of the TME can also facilitate tumor cell dissemination through a plethora of cytokines and the production of proteases that pave the way degrading the ECM, clearing a path for migration, and guiding tumor cells towards the bloodstream (Bonde et al., 2012; Pollard, 2004; Solinas et al., 2010).

Several therapeutic strategies making use of nanotechnology have been reported during the last few years with the purpose of interfering with these processes, for example, addressing cell adhesion proteins (e.g., cadherins, integrins), proteinases (e.g., metalloproteinases (MMPs), the cofilin family of proteins), ion/water channels (e.g., aquaporins, chloride and calcium channels), transcription factors, and signal transducers (e.g., SNAIL, STAT3, Twist, chemokine receptors), as well as to interfere with the formation of invadopodia (Eckert, Lwin, Chang, et al., 2011; Gallo, Kamaly, Lavdas, et al., 2014; Hatakeyama, Akita, Ishida, et al., 2007; Olmeda, Jordá, Peinado, Fabra, & Cano, 2007; Veiseh, Kievit, Ellenbogen, & Zhang, 2011; Zhu, Kate, & Torchilin, 2012; Zou, He, He, et al., 2015). With respect to the specific use of nanotheranostics in this field, there are only a limited number of works. An example refers to the use of gold nanocages, functionalized with a peptide for selective targeting of prostate cancer cells and subsequent NIR irradiation for both imaging and photothermal therapy (Avvakumova, Galbiati, Sironi, et al., 2016). In vitro results in PC3 cells confirmed a highly selective interaction and, interestingly, a complete loss of surface microvilli and different morphology of treated cells compared to control cells. This loss of microvilli on tumor cells is highly interesting for preventing the disease development and progression, because microvilli play a key role in cell migration, cell attachment, and invasion. In another recent paper, Ali, Hsu, Hsieh, et al. (2016) designed ultra-small superparamagnetic iron oxide nanoparticles conjugated to erlotinib for targeted therapy and noninvasive real-time monitoring of tumors. In vitro results showed a suppression of the expression of MMP-9 and XIAP, and subsequently inhibition of the migration and invasion capabilities of cancer cells. These results were also confirmed in vivo in xenograft bearing mice, additionally revealing the imaging (MRI) capabilities of their nanoparticles. Targeting strategies to MMPs can also include the use of a unique targeting agent, scorpion venom chlorotoxin (El-Ghlban, Kasai, Shigehiro, et al., 2014; Mok et al., 2010; Soroceanu, Gillespie, Khazaeli, & Sontheimer, 1998; Sun, Fang, Stephen, et al., 2008; Veiseh, Gunn, Kievit, et al., 2009). The conjugation of superparamagnetic iron oxide nanoparticles (SPIONs) with the 36-residue peptide of chlorotoxin resulted in the inhibition of cell invasion by deactivation of the membrane-bound matrix metalloproteinase 2 (MMP-2), and highlights the potential of this strategy for noninvasive diagnosis (Veiseh et al., 2009). Another interesting strategy is the incorporation of gene therapies into the formulations, considering that some microRNAs have been reported to mediate the process of tumor cell migration and tissue invasion (e.g., miRNA 218, miRNA

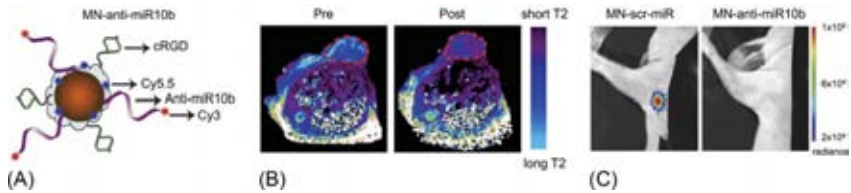


Fig. 3

(A) Schematic representation of magnetic nanoparticles conjugated to Cy5.5, a tumor targeting peptide (cRGD), and the therapeutic knockdown oligonucleotide miRNA-10b with a 3'-Cy3 modification. (B) MRI images of orthotopic breast cancer tumors before (left) and 24 h after the injection of the nanotheranostics (right) showing effective accumulation in the tumor. (C) Bioluminescence images of tumor-bearing mice, showing effective metastasis prevention capacity in lymph nodes for mice treated with the nanodrug MN-anti-miR10b, compared to the inactive control nanoparticles MN-scr-miR. Data from Yigit, M. V., Ghosh, S. K., Kumar, M., et al. (2013). Context-dependent differences in miR-10b breast oncogenesis can be targeted for the prevention and arrest of lymph node metastasis, *Oncogene* 32 (12), 1530–1538, doi:10.1038/onc.2012.173, with the permission of Nature Publishing Group, copyright (2017).

320a, miRNA 520a, miRNA 10b) (Cui et al., 2017; Lv, Wu, Wang, et al., 2016; Tu, Gao, Li, et al., 2013). As an example, Yigit, Ghosh, Kumar, et al. (2013) have developed a theranostic nanosystem for the inhibition of the pro-metastatic microRNA-10b based on ultrasmall magnetic nanoparticles (imaging capability) functionalized with the RGD peptide (targeting to integrins) and decorated with therapeutic nucleic acid oligonucleotides. This nanosystem allowed a noninvasive imaging of the whole body by near infrared fluorescence optical imaging, and a close up of the target tumor by MRI. In vivo results after intravenous injection to breast cancer orthotopic mouse models showed the inhibition of the invasion and migration of cancer cells and, therefore, the complete prevention of metastatic dissemination from the primary tumor to lymph nodes (Fig. 3).

Overall, cancer cell invasion is a highly complex process that involves several molecular pathways leading to the fatal progression of cancer metastasis. Nanotheranostics, multifunctional nanosystems that can simultaneously target several molecular pathways and incorporate imaging agents for noninvasive diagnosis are well suited to improve understanding and tackling of this phenomenon.

5.2 Dissemination

5.2.1 Tumor-infiltrated local and distal lymph nodes

Tumor cells can disseminate by lymphatic or haematogenous routes (Pantel & Brakenhoff, 2004; Sleeman et al., 2012). Because of its particular architecture, characterized by thin-wall large vessels and slow fluid flow, the lymphatic route is mainly accessible for invasive

tumor cells in comparison to blood vessels (Abellán-Pose, Csaba, & Alonso, 2016; Sleeman & Thiele, 2009). Additionally, chemokines and other factors (i.e., CCL21, VEGF) produced by tumor or stromal cells play a key role in promoting the entry of tumor cells into the lymphatics (Hirakawa et al., 2006; Tomei, Siegert, Britschgi, Luther, & Swartz, 2009). Tumor-associated lymphatic vessels act as channels by which disseminating tumor cells access regional lymph nodes. Once there, cells can stay in a dormant state before traveling to other organs to form secondary metastases (Li & Li, 2015). Indeed, monitoring and detection of metastases within the first draining lymph node, the sentinel lymph node (SLN), has major prognostic value for patient survival in different types of cancer such as breast and lung, and frequently determines the type of treatment (Nathanson & Mahan, 2011). One of the limitations for detection of infiltrated tumor cells in the lymph nodes is the fact that they can exist in a quiescent state, or as micro-metastases in which proliferation is balanced by cell death through apoptosis. Consequently, detection of micrometastases is a great challenge in oncology, because it can be a promising strategy to stop metastatic growth (Ryan, Kaminskas, & Porter, 2014; Trevaskis, Kaminskas, & Porter, 2015). Mimicking this condition through the development of sophisticated 3D in vitro models has been proposed for the development of tailored nanotherapeutics (Alonso-Nocelo, Abellan-Pose, Vidal, et al., 2016).

Various nanoprobes, mainly based on MRI, PET, NIR, and SPECT/CT imaging techniques, have been developed to date for noninvasive SLN imaging, for example, mesoporous silica-based nanoprobes for trimodal imaging (NIR/MRI/PET), and lipid-calcium phosphate nanoparticles for SPECT/CT imaging (Huang, Zhang, Lee, et al., 2012; Tseng, Xu, Guley, Yuan, & Huang, 2014). On the other side, nanotherapeutic strategies designed to target metastatic cells placed into the lymphatic circulation and/or organs have similarly been proposed (Hirano, Hunt, Strubbe, & MacGregor, 1985; Ryan et al., 2014). An example of eradication of metastatic cells retained into SLN is methotrexate (MTX)-conjugated dendrimers, which efficiently accumulate in draining lymph nodes after subcutaneous injection to rats (Kaminskas, McLeod, Ascher, et al., 2014).

The application of nanotheranostics for targeting disseminated cancer cells and infiltrated lymph nodes seems therefore coherent. Simultaneous detection and eradication could have a big impact on interfering with lymphatic dissemination of the tumor cells and allowing monitoring of the efficacy of the proposed therapies. Some examples of nanotheranostics in this field include nanosystems designed for photothermal therapy. This is the case of phase-transition nanodroplets developed for optical, photoacoustic, and ultrasound imaging modalities, which showed improved efficiencies for detection and elimination of breast cancer cells located in SLN of rabbits (Yang, Cheng, Chen, et al., 2017), nitrogen-doped carbon nanodots, which combine photothermal therapy with photoacoustic imaging and led to complete tumor ablation without recurrence in SLN of rat and mouse models (Lee, Kwon, Beack, et al., 2016), graphene oxides modified with iron oxide nanoparticles for photothermal therapy and MRI and NIR imaging, efficient for imaging and treatment of

regional lymph nodes in pancreatic cancer (Wang et al., 2016), and $W_{18}O_{49}$ nanoparticles designed for CT imaging-guided photothermal ablation of HER-2 positive breast malignancy in metastatic lymph nodes (Huo, He, Li, et al., 2014). Some other nanotheranostics suited for different types of therapy are iron oxide nanoparticles, which were co-encapsulated with the chemotherapeutic drug doxorubicin into PLGA microbubbles for dual imaging (US/MRI) and chemotherapy of lymph node metastasis in rabbits (Niu, Wang, Lu, et al., 2013), nanoparticles loaded with indocyanine green for fluorescence imaging and photodynamic therapy of lymph node metastasis of gastric cancer (Tsujiyama, Morimoto, Takahata, et al., 2015), and iron oxide nanoparticles, combined with the immunostimulatory activity of polyinosinic-polycytidylic acid (poly I:C) and labeled with the radionucleotide fac-[$^{99m}Tc(OH)_2_3(CO)_3$], for dual MRI/SPECT imaging and targeted and programmable immunotherapy of metastatic lymph nodes (Cobaleda-Siles, Henriksen-Lacey, De Angulo, et al., 2014).

These examples evidence the potential benefits of using nanotheranostics for disseminated and metastatic cancer cells located in the lymph nodes in future clinical practices, allowing noninvasive imaging techniques, and more specific and local therapies without causing damage to the neighboring tissues.

5.2.2 *Circulating tumor cells*

During circulation, circulating tumor cells (CTCs) travel the bloodstream and overcome a range of events (e.g., anchorage-free survival, shear stress) in order to reach distant organs, representing the metastatic intermediates between the primary tumor and sites of dissemination. Still, it remains controversial whether CTCs have the ability to actively target certain organs, or if they are passively arrested within capillary beds, such as those in lung and liver, due to the architecture of the vasculature (Miles, Pruitt, van Golen, & Cooper, 2008). CTCs can also form clusters, known as circulating tumor microemboli (CTM), and large aggregates with platelets in order to both protect themselves from shear forces and evade immune detection (Gay & Felding-Habermann, 2011). It has also been suggested that CTCs might fuse with macrophages, providing metastatic cells with myeloid characteristics, advantageous for their survival in circulation (Pawelek & Chakraborty, 2008). Although it is thought that only 0.01% of CTCs are able to survive in circulation and produce metastasis, they are responsible for more than 90% cancer-related deaths (Fidler, 1970). Therefore, effective strategies in order to detect and eradicate CTCs to block metastasis are urgently required. Recent technological advances have facilitated the identification of biomolecules characteristic of CTCs for detection within the bloodstream of carcinoma patients, and some therapeutic drugs (e.g., docetaxel, gemcitabine, doxorubicin) are also being investigated for eradicating CTCs (Aires et al., 2016; Barbazán, Vieito, Abalo, et al., 2012; Chen, Gowda, Newswanger, et al., 2016; Deng, Wu, Zhao, et al., 2015; Muínelo-Romay, Vieito, Abalo, et al., 2014; Yang, Jiang, Zhang, et al., 2015).

In the past decade, most efforts have been focused on *ex vivo* CTCs detection and isolation from blood samples for diagnosis and monitoring of the disease progression, because the number of CTCs detected in a blood sample has been reported to directly correlate with disease severity (Danila, Pantel, Fleisher, & Scher, 2011). These novel technologies rely on characteristic properties of CTCs, for example, large size, characteristic surface molecules, deformability, and density (Alix-Panabières & Pantel, 2014). For instance, some CTC detection methods in advanced stage of clinical translation are CellSearch, ISET, and CTC-chip. CellSearch, the only currently FDA-approved system for automated CTC detection, relies on immunomagnetic separation by antibodies against EpCAM; ISET is based on size separation by 8 μm pore filters because of the larger size of CTCs compared to hematological cells, and CTC-chip, is an immunoaffinity-based microfluidic device functionalized with anti-EpCAM antibody-coated microposts. However, due to the rarity of CTCs (around one CTC for every billion or so of normal blood cells) and the small processing capacity of these technologies *ex vivo* (1–10 mL of blood), the number of detected and isolated CTCs is quite limited and cannot fulfill the requirements for in-depth clinical studies.

Many of the emerging CTC detection techniques use inorganic and organic nanoparticles functionalized with targeting ligands to coat surfaces for *ex vivo* enrichment of CTCs and further analysis (Huang, O'Connor, & Kwizera, 2017; Liu, Xu, He, Deng, & Zhu, 2013; Myung, Roengvoraphoj, Tam, et al., 2015; Sun, Wang, Ji, et al., 2015; Yoon, Kozminsky, & Nagrath, 2014). These nanoparticles provide devices with an increased sensitivity and imaging properties (photoacoustic, fluorescence, SERS, and high-resolution X-ray imaging) in order to intercept and quantify CTCs. Nanoparticles are also being explored for *in vivo* enrichment and detection of CTCs. For instance, Galanzha, Shashkov, et al. (2009) have reported the use of surface-decorated magnetic nanoparticles for binding to CTCs after intravenous injection to xenograft mouse models. Once internalized by CTCs, nanoparticles could be concentrated and trapped by an external magnet attached to the skin, above a peripheral blood vessel, for *in situ* detection by photoacoustics, or for microsurgical extraction of CTCs for *ex vivo* analysis.

The possibility of *in vivo* monitoring the number of CTCs without the need for blood sample extraction and preparation would allow the screening of larger volumes of blood (~5 L) compared to the small blood samples taken for *ex vivo* analysis (1–10 mL) and, therefore, significantly improve sensitivity. In addition, novel *in vivo* strategies capable of simultaneously detecting, monitoring, and killing CTCs in the entire blood circulation may dramatically enhance the outcome of the disease by blocking the metastatic cascade and inhibit disease progression, making a breakthrough in cancer research. In this sense, functionalized theranostic nanosystems hold great promise for (1) screening the whole blood for intercepting and detecting CTCs *in vivo*, (2) enrichment of CTCs for biological function assays *in vivo* or minimally invasive extraction of CTCs for *ex vivo* analysis (molecular and genetic assessments), (3) monitoring the treatment response *in vivo*, *in situ*, and in real-time,

(4) targeting delivery of therapeutics to destroy CTCs and interrupt the metastatic cascade, taking advantage, for example, of the development of remotely triggered nanotheranostic (Kim, Galanzha, Zaharoff, Griffin, & Zharov, 2014; Sneider et al., 2017; Xie, Gao, Zhao, et al., 2015).

The current status of nanotheranostics in CTC detection and therapy is almost unexplored. However, some pioneering experiments show encouraging results. In 2009, Galanzha, Kim, and Zharov (2009) demonstrated, for the first time, in vivo real-time imaging and therapy of CTCs by combining magnetic nanoparticles for capturing circulating tumor cells under a magnet with a second contrast agent, golden carbon nanotubes as super contrast photoacoustic and photothermal agents for improving sensitivity. In vivo results show efficient photoacoustic detection and photothermal ablation of CTCs on a xenograft mouse model of human breast cancer.

Despite all the potential benefits, many challenges still need to be overcome before nanotheranostics can reach their full clinical potential for this application, such as understanding the heterogeneity of the CTC population (there are several CTC phenotypes between epithelial-mesenchymal that can simultaneously coexist in circulation), the formation of clusters of CTCs (different drug resistance among CTCs), and the shielding of CTCs with platelets and other cell types (physical barrier to nanoparticles penetrate in CTCs) (Li, Sharkey, Huang, & King, 2015). If these challenges are overcome, the multimodal nanoplatforams for theranostic purposes to detect and eliminate CTCs may catalyze a paradigm shift in cancer research.

5.3 Colonization

5.3.1 Extravasation and formation of micrometastases

Extravasation of CTCs is one of the critical events in metastasis. This process includes several steps, such as cells getting arrested into the microvasculature, entering into the parenchyma of distant tissues, adapting to survive in foreign microenvironments, and eventually colonizing to generate metastasis (Tsai & Yang, 2013). CTCs can initially show a leukocyte-like rolling behavior on the vascular walls. They create transient interactions with the endothelium, followed by stronger adhesions mediated by selectins and vascular cell adhesion molecules (VCAMs), respectively. Neutrophils and platelets can secrete cytokines to induce the expression of these adhesion proteins on endothelial cells, to allow the establishment of temporary interactions with tumor cells (Kim, Borsig, Han, Varki, & Varki, 1999; Labelle & Hynes, 2012; Laubli, Spanaus, & Borsig, 2009). Their adherence to vascular fibronectin deposits has also been described (Barbazán et al., 2017). CTCs can also be trapped into isolated small vessels into the microcirculation, becoming activated and therefore transmigrating (Chambers et al., 2002; Van Zijl et al., 2011). Moreover, accumulating evidence supports tumor cell plasticity and reprogramming during metastatic

colonization, controlling epithelial and mesenchymal traits of tumor cells. So, the EMT genetic program triggered during invasion and tumor dissemination might be suppressed upon arrival at the site of metastasis, and the reciprocal program MET (mesenchymal-to-epithelial transition) would be consequently induced to help cells form extensive macro-metastasis at distant organs (Luo, Brooks, & Wicha, 2015; Tsai & Yang, 2013). After seeding, growth of metastatic tumors requires adaptation to a new microenvironment, but also remodeling it into a supportive niche (Aguirre-Ghiso, 2007). The mechanisms by which tumor cells alter this scenario (ECM remodeling as well as other stromal cellular components) still remains unclear. Recent evidence suggests that the metastatic sites can be transformed prior to tumor cell arrival, creating the so-called “premetastatic niche” (Sceney, Smyth, & Möller, 2013) that will be discussed in the next section. The local environment might provide suitable factors that support tumor cell growth as well as for the establishment of new vasculature through the production of angiogenic factors and recruitment of vascular cells (Rafii, Lyden, Benezra, Hattori, & Heissig, 2002). This niche would also drive the creation of dormant cells, trapped in a quiescent state, until activated by certain factors or signaling pathways that make the scenario suitable for metastases development.

Once these disseminated tumor cells reach the distant organ and survive in the new environment, they are typically resistant to current therapies, unable to control their speedy proliferation and growth (He, Guoc, Qiana, & Chen, 2015). Therefore, it is of utmost importance to battle metastasis before reaching this point. Early metastasis intervention procedures, such as detection and treatment of micrometastasis or interfering the metastatic niche remodeling, may offer new therapeutic opportunities. Detection of micrometastases, that is, deposits of single tumor cells or very small clusters of cancer cells in a distal organ or lymph nodes, is currently limited by the sensitivity of clinical detection of a tumor mass, and only highly invasive molecular methods that suffer from low efficiency are applicable (McGowan, Kirstein, & Chambers, 2009; Pantel, Alix-Panabières, & Riethdorf, 2009). The development of a rapid, noninvasive detection tool that can give accurate whole-body readouts of occult micrometastases and eliminate them might, therefore, have substantial clinical impact in the management of disseminated disease before the burden of metastases.

Nanotheranostics, we believe, have the potential to increase the sensibility of current diagnosis techniques and deliver new therapeutic entities more selective for treating disseminated cells avoiding unspecific effects in the surrounding tissue (Wan, Pantel, & Kang, 2013). Preclinical studies with a multifunctional nanosystem based on poly(methacrylic acid)-polysorbate 80-grafted-starch for the delivery of anticancer drugs (doxorubicin) and imaging agents (Gadolinium and Hoechst) to the brain highlight the potential of this approach for brain metastasis (Li, Cai, Shalviri, et al., 2014). Upconversion luminescent lanthanide nanoparticles were also proposed for this application due to their unique optical properties and chemo-/photo-stability, which is ideal for photodynamic therapy, and they efficiently inhibited tumor growth and metastasis formation in pulmonary and hepatic mouse models of

micrometastases (Li, Tang, Pan, et al., 2016). Zhou, Zhao, Tian, et al. (2015) also designed a theranostic nanoplatform for combinational therapy (radiotherapy and photothermal therapy) based on copper-64-labeled copper sulfide PEG-nanoparticles ($[^{64}\text{Cu}]\text{CuS}$ NPs) that could efficiently suppress lung metastasis in orthotopic 4T1 breast tumor models through eradication of initiating cells (Fig. 4). This system was tracked by PET/CT imaging showing that more than 90% of the radioactivity remained in the tumor 24 h after intratumor injection, much more higher than the 25% of the aqueous solution of $^{64}\text{CuCl}_2$. The combined therapy of

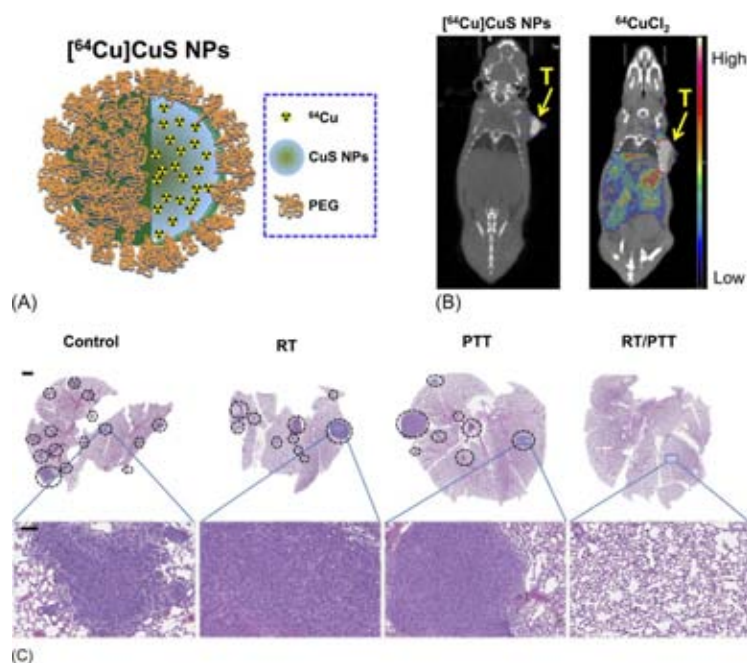


Fig. 4

(A) Schematic representation of the theranostic nanoplatform based on copper-64-labeled copper sulfide PEG-nanoparticles ($[^{64}\text{Cu}]\text{CuS}$ NPs). (B) PET/CT images of subcutaneous breast tumor-bearing mice 24 h after intratumoral injection of $[^{64}\text{Cu}]\text{CuS}$ NPs and the aqueous solution of $^{64}\text{CuCl}_2$ as control. (C) Histology analysis of 4T1 breast tumor mice showing the number of metastatic nodules after radiotherapy (RT), photothermal therapy (PTT) or RT/PTT therapy compared to the control group. Data from Zhou, M., Zhao, J., Tian, M., et al. (2015). Radio-photothermal therapy mediated by a single compartment nanoplatform depletes tumor initiating cells and reduces lung metastasis in the orthotopic 4T1 breast tumor model. *Nanoscale*, 7(46), 19438–19447. doi: 10.1039/C5NR04587H, with the permission of Royal Society of Chemistry, copyright (2017).

RT/PTT in 4T1 breast tumor mice significantly reduced the number of metastatic nodules in lung compared to the control group and the monotherapies (RT, PTT). In vivo results showed a significantly prolonged survival of breast tumor mice after RT/PTT therapy.

Detection and eradication of micrometastases is still a challenging task, with a high potential for prevention of the onset of metastasis. Nanotheranostics will have a lot to offer, but progress must necessarily be accompanied by the development of more sensitive and sophisticated imaging detection systems as well as improved imaging processing tools.

5.3.2 Premetastatic niche

Evidence suggests that distant organs are not just casual targets of the metastatic process, and that the primary tumor itself is indeed able to modify the environment of secondary organs, facilitating the formation of future supportive microenvironments called “premetastatic niches” (Peinado, Zhang, Matei, et al., 2017; Sceneay et al., 2013). Early on, signals released by the primary tumor such as cytokines, enzymes, and exosomes, are revealed as able to regulate tumor cell homing and assist CTC extravasation during the metastatic cascade (Kaplan, Riba, Zacharoulis, et al., 2005; Massagué & Obenauf, 2016; Peinado, Lavotshkin, & Lyden, 2011). Immune cells, especially myeloid cells, have also been described as key components of the premetastatic niche formation. They can be recruited through chemoattractant inflammatory proteins, such as S100A8 and S100A9, and angiogenic cytokines such as VEGF, forming localized accumulations within the niche (Kaplan et al., 2005). Once there, these cells collaborate with other stromal cells, either recruited or residing in the tissue parenchyma (i.e., fibroblast, immune cells). ECM composition and structure, together with matrix metalloproteinases secretion, are also essential for local tissue remodeling (Høye & Erler, 2016). Several reports have recently highlighted the importance of matrix proteins in the establishment of premetastatic and metastatic niches of various cancer types (Oskarsson, Acharyya, Zhang, et al., 2011; Wong, Gilkes, Zhang, et al., 2011).

The role of primary tumor-derived exosomes preparing the premetastatic niche at distant organs for colonization by disseminated cancer cells has been reported in several recent works (Costa-Silva, Aiello, Ocean, et al., 2015; Hoshino, Costa-Silva, Shen, et al., 2015; Steinbichler, Dudás, Riechelmann, & Skvortsova, 2017; Weidle, Birzele, Kollmorgen, & Rüger, 2017). These lipidic extracellular vesicles containing biofunctional molecules (i.e., proteins, lipids, DNA, and RNA), are secreted by most cellular types in healthy and pathological conditions, and can be efficiently transferred to recipient cells at distant sites (Kharaziha, Ceder, Li, & Panaretakis, 2012). Specific integrins expressed on tumor-derived exosomes are related to tissue organotropism of future metastasis, and blocking this exosome communication at some point has been proposed as a promising strategy to stop the premetastatic niche remodeling. One of the proposed strategies includes the use of gold nanoparticles to tackle the biogenesis of exosomes, their circulation pathway, or their uptake by recipient cells (Roma-Rodrigues et al., 2017).

Regarding premetastatic niche formation, much still remains to be understood, but it is undoubtedly a window for new therapeutic strategies against metastasis. For example, Yamamoto, Kikuchi, Ohta, et al. (2008) have reported that blocking the chemoquine CXCR2 and interleukine IL-12 secreted from TK-4 cancer cells with neutralizing antibodies significantly inhibited liver metastasis in orthotopic colon cancer mouse models. In another paper, Belle, Ali, Lonic, et al. (2015) found that PTPN14 (also known as Pez, PTPD2, PTP36) acts as a suppressor of metastasis, particularly to the metastatic niche in the bone, by reducing intracellular protein trafficking through the secretory pathway in xenograft breast cancer models. With respect to the specific use of nanotechnology, Kang, Zhu, Wei, et al. (2017) have recently developed a novel nanoparticle inspired by neutrophils ((poly(lactic-co-glycolic acid) nanoparticles coated with neutrophils membranes) due to the ability of neutrophils for targeting both CTCs and the premetastatic niche by intrinsic cell adhesion molecules on their surface membrane. When these nanoparticles were loaded with the drug carfilzomib, CTCs were selectively depleted, and the formation of the metastatic niche inhibited, providing an advanced strategy for metastasis prevention and treatment. Imaging techniques can also help to elucidate the premetastatic niche formation process. Shokeen, Zheleznyak, Wilson, et al. (2012) have recently demonstrated throw a high-affinity PET probe ^{64}Cu -labeled 11-bis(carboxymethyl)-1,4,8,11-tetraazabicyclo[6.6.2] hexadecane (CB-TE2A)-LLP2A that bone marrow-derived (BMD) cells that express vascular endothelial growth factor receptor-1 and very late antigen-4 (VLA-4) arrive first at sites of metastasis to form a receptive environment for tumor cells. Metastatic mouse models were used to perform these experiments by PET/CT.

As we mentioned before, the process of premetastatic niche formation still remains unclear; however, theranostic nanoplatfroms combining imaging techniques, targeting capabilities, and therapeutic applications could provide insight into this phenomenon and relevant clues for inhibiting the formation of metastasis.

6 Conclusive Remarks

Cancer nanotechnology is an interdisciplinary research that involves biology, chemistry, engineering, and medicine with the clear objective of leading to major advances in cancer detection, diagnosis, and treatment. In recent decades, an increasing knowledge of functional molecular and biological basis combined to create advances in the materials field, has led to new and modern improvements in the development of innovative nanotechnologies for cancer detection and targeted treatments. Nevertheless, a small number of works have been specifically addressed to improve the management and outcome of metastatic cancer. As highlighted in this chapter, the generation of metastases is a very complex process with a lot of unknowns. A deeper understanding of the tumor biology and the process of metastases will necessarily accompany advances in cancer nanotechnology. Reciprocally, nanotheranostics

will certainly play a key role in allowing a more rational development of nanotechnologies that can cover unmet clinical needs and quickly reach translation.

To achieve a breakthrough in the field, it is mandatory to better understand the metastatic process, develop better experimental models for metastasis disease, identify genotypic and phenotypic differences (e.g., targetable receptors) between primary and metastasized tumors, define biomolecules and signatures of CTCs and disseminated cancer cells, and explore novel antimetastatic strategies. In our understanding, strategies for targeting metastatic cancer should tackle one or more processes simultaneously, among the following: (1) targeting the primary tumor to block the metastatic capacity of tumor cells (i.e., antimigration, antiangiogenesis, antiinvasion), (2) targeting the tumor microenvironment, (3) targeting specifically tumor cells subpopulations, related to cancer resistance, metastases, and tumor escape (cancer stem cells), (4) targeting cancer circulating cells before they reach distal tissues, (5) targeting dormant cells in order to move them out of the dormant state so they might be sensitive to conventional chemotherapy or alternatively, maintaining the dormant state to prevent the emergence of metastasis, and (6) targeting established colonization process and the formation of metastatic tumors (oligometastasis or polymetastasis). We believe that within this approach, important advances in the management of metastatic cancer will be achieved in the near future, and this will surely involve the development of tailored nanotheranostics.

Acknowledgments

The authors acknowledge the support of the Carlos III Health Institute/FEDER (PI15/00828), and the Spanish Ministry of Education, Culture, and Sport (FPU15/06595).

References

- Abellán-Pose, R., Csaba, N., & Alonso, M. J. (2016). Lymphatic targeting of nanosystems for anticancer drug therapy. *Current Pharmaceutical Design*, 22(9), 1194–1209. <https://doi.org/10.2174/1381612822666151216150809>.
- Aguirre-Ghiso, J. A. (2007). Models, mechanisms and clinical evidence for cancer dormancy. *Nature Reviews Cancer*, 7(11), 834–846. <https://doi.org/10.1038/nrc2256>.
- Aires, A., Ocampo, S. M., Simões, B. M., et al. (2016). Multifunctionalized iron oxide nanoparticles for selective drug delivery to CD44-positive cancer cells. *Nanotechnology*, 27(6), 65103. <https://doi.org/10.1088/0957-4484/27/6/065103>.
- Alberti, D., Protti, N., Franck, M., et al. (2017). Theranostic nanoparticles loaded with imaging probes and rubrocurcumin for combined cancer therapy by folate receptor targeting. *ChemMedChem*, 12(7), 502–509. <https://doi.org/10.1002/cmdc.201700039>.
- Alconcel, S. N. S., Baas, A. S., & Maynard, H. D. (2011). FDA-approved poly(ethylene glycol)-protein conjugate drugs. *Polymer Chemistry*, 2(7), 1442. <https://doi.org/10.1039/c1py00034a>.
- Ali, A. A. A., Hsu, F., Hsieh, C., et al. (2016). Erlotinib-conjugated iron oxide nanoparticles as a smart cancer-targeted theranostic probe for MRI. *Nature Publishing Group*, 6(1), 1–16. <https://doi.org/10.1038/srep36650>.
- Alix-Panabières, C., & Pantel, K. (2014). Technologies for detection of circulating tumor cells: facts and vision. *Lab on a Chip*, 14(1), 57–62. <https://doi.org/10.1039/c3lc50644d>.

- Allavena, P., Sica, A., Solinas, G., Porta, C., & Mantovani, A. (2008). The inflammatory micro-environment in tumor progression: the role of tumor-associated macrophages. *Critical Reviews in Oncology/Hematology*, 66(1), 1–9. <https://doi.org/10.1016/j.critrevonc.2007.07.004>.
- Alonso-Nocelo, M., Abellan-Pose, R., Vidal, A., et al. (2016). Selective interaction of PEGylated polyglutamic acid nanocapsules with cancer cells in a 3D model of a metastatic lymph node. *Journal of Nanobiotechnology*, 14(1), 51. <https://doi.org/10.1186/s12951-016-0207-8>.
- Alonso-Nocelo, M., Abuín, C., López-López, R., & de la Fuente, M. (2016). Development and characterization of a three-dimensional co-culture model of tumor T cell infiltration. *Biofabrication*, 8(2), 25002. <https://doi.org/10.1088/1758-5090/8/2/025002>.
- Amadori, D., Milandri, C., Comella, G., Saracchini, S., et al. (2011). A phase I/II trial of non-pegylated liposomal doxorubicin, docetaxel and trastuzumab as first-line treatment in HER-2-positive locally advanced or metastatic breast cancer. *European Journal of Cancer*, 47(14), 2091–2098. <https://doi.org/10.1016/j.ejca.2011.05.005>.
- American Cancer Society. (2017). *Colorectal cancer facts&figures 2017-2019*. Atlanta: American Cancer Society. [https://doi.org/10.1016/S0140-6736\(13\)61649-9](https://doi.org/10.1016/S0140-6736(13)61649-9).
- Aparicio, S., & Caldas, C. (2013). The implications of clonal genome evolution for cancer medicine. *The New England Journal of Medicine*, 368(9), 842–851. <https://doi.org/10.1056/NEJMra1204892>.
- Avvakumova, S., Galbiati, E., Sironi, L., et al. (2016). Theranostic nanocages for imaging and photothermal therapy of prostate cancer cells by active targeting of neuropeptide-Y receptor. *Bioconjugate Chemistry*, 27(12), 2911–2922. <https://doi.org/10.1021/acs.bioconjchem.6b00568>.
- Bae, K. H., Lee, J. Y., Lee, S. H., Park, T. G., & Nam, Y. S. (2013). Optically traceable solid lipid nanoparticles loaded with siRNA and paclitaxel for synergistic chemotherapy with in situ imaging. *Advanced Healthcare Materials*, 2(4), 576–584. <https://doi.org/10.1002/adhm.201200338>.
- Baetke, S. C., Lammers, T., & Kiessling, F. (2015). Applications of nanoparticles for diagnosis and therapy of cancer. *The British Journal of Radiology*, 88(1054), 1–12. <https://doi.org/10.1259/bjr.20150207>.
- Balkwill, F., & Mantovani, A. (2001). Inflammation and cancer: back to Virchow? *Lancet*, 357(9255), 539–545. [https://doi.org/10.1016/S0140-6736\(00\)04046-0](https://doi.org/10.1016/S0140-6736(00)04046-0).
- Barbazán, J., Alonso-Alconada, L., Elkhatib, N., Geraldo, S., Gurchenkov, V., Glentis, A., et al. (2017). Liver metastasis is facilitated by the adherence of circulating tumor cells to vascular fibronectin deposits. *Cancer Research*, 77(13), 3431–3441. <https://doi.org/10.1158/0008-5472.CAN-16-1917>.
- Barbazán, J., Veito, M., Abalo, A., et al. (2012). A logistic model for the detection of circulating tumor cells in human metastatic colorectal cancer. *Journal of Cellular and Molecular Medicine*, 16(10), 2342–2349. <https://doi.org/10.1111/j.1582-4934.2012.01544.x>.
- Barenholz, Y. (2012). Doxil®—the first FDA-approved nano-drug: lessons learned. *Journal of Controlled Release*, 160(2), 117–134. <https://doi.org/10.1016/j.jconrel.2012.03.020>.
- Barth, B. M., Altinoglu, E. I., Shanmugavelandy, S. S., et al. (2011). Targeted indocyanine-green-loaded calcium phosphosilicate nanoparticles for in vivo photodynamic therapy of leukemia. *5(7)*, 5325–5337. <https://doi.org/10.1021/nn2005766>.
- Belle, L., Ali, N., Lonic, A., et al. (2015). The tyrosine phosphatase PTPN14 (Pez) inhibits metastasis by altering protein trafficking. *Science Signaling*, 8(364), 1–13. <https://doi.org/10.1126/scisignal.2005547>.
- Beloqui, A., Memvanga, P. B., Coco, R., et al. (2016). A comparative study of curcumin-loaded lipid-based nanocarriers in the treatment of inflammatory bowel disease. *Colloids and Surfaces B, Biointerfaces*, 1(143), 327–335. <https://doi.org/10.1016/j.colsurfb.2016.03.038>.
- Bertino, E., McMichael, E., Mo, X., Trikha, P., et al. (2016). A phase I trial to evaluate antibody-dependent cellular cytotoxicity of cetuximab and lenalidomide in advanced colorectal and head and neck cancer. *Molecular Cancer Therapeutics*, 15(9), 2244–2250. <https://doi.org/10.1158/1535-7163.MCT-15-0879>.
- Bobo, D., Robinson, K. J., Islam, J., Thurecht, K. J., & Corrie, S. R. (2016). Nanoparticle-based medicines: a review of FDA-approved materials and clinical trials to date. *Pharmaceutical Research*, 33(10), 2373–2387. <https://doi.org/10.1007/s11095-016-1958-5>.
- Bonde, A.-K., Tischler, V., Kumar, S., Soltermann, A., & Schwendener, R. A. (2012). Intratumoral macrophages contribute to epithelial-mesenchymal transition in solid tumors. *BMC Cancer*, 12, 35. <https://doi.org/10.1186/1471-2407-12-35>.

- Borghaei, H., Paz-Ares, L., Horn, L., et al. (2015). Nivolumab versus docetaxel in advanced nonsquamous non-small-cell lung cancer. *The New England Journal of Medicine*, 373(17), 1627–1639. <https://doi.org/10.1056/NEJMoa1507643>.
- Brahmer, J., Reckamp, K. L., Baas, P., et al. (2015). Nivolumab versus docetaxel in advanced squamous-cell non-small-cell lung cancer. *The New England Journal of Medicine*, 2015, 373123–373135.
- Branco da Cunha, C., Klumpers, D. D., Li, W. A., et al. (2014). Influence of the stiffness of three-dimensional alginate/collagen-I interpenetrating networks on fibroblast biology. *Biomaterials*, 35(32), 8927–8936. <https://doi.org/10.1016/j.biomaterials.2014.06.047>.
- Bregoli, L., Movia, D., Gavigan-Imedio, J. D., Lysaght, J., Reynolds, J., & Prina-Mello, A. (2016). Nanomedicine applied to translational oncology: a future perspective on cancer treatment. *Nanomedicine: Nanotechnology, Biology and Medicine*, 12(1), 81–103. <https://doi.org/10.1016/j.nano.2015.08.006>.
- Byrne, J. D., Betancourt, T., & Brannon-Peppas, L. (2008). Active targeting schemes for nanoparticle systems in cancer therapeutics. *Advanced Drug Delivery Reviews*, 60(15), 1615–1626. <https://doi.org/10.1016/j.addr.2008.08.005>.
- Cai, W., & Chen, X. (2008). Multimodality molecular imaging of tumor angiogenesis. *Journal of Nuclear Medicine*, 49(Suppl_2), 113S–128S. <https://doi.org/10.2967/jnumed.107.045922>.
- Campbell, P. J., Yachida, S., Mudie, L. J., et al. (2010). The patterns and dynamics of genomic instability in metastatic pancreatic cancer. *Nature*, 467(7319), 1109–1113. <https://doi.org/10.1038/nature09460>.
- Carey, S. P., Starchenko, A., McGregor, A. L., & Reinhart-King, C. A. (2013). Leading malignant cells initiate collective epithelial cell invasion in a three-dimensional heterotypic tumor spheroid model. *Clinical & Experimental Metastasis*, 30(5), 615–630. <https://doi.org/10.1007/s10585-013-9565-x>.
- Caster, J. M., Patel, A. N., Zhang, T., & Wang, A. (2017). Investigational nanomedicines in 2016: a review of nanotherapeutics currently undergoing clinical trials. *Wiley Interdisciplinary Reviews Nanomedicine and Nanobiotechnology*, 9(1), e1416. <https://doi.org/10.1002/wnan.1416>.
- Cavallaro, G., Campisi, M., Licciardi, M., Ogris, M., & Giammona, G. (2006). Reversibly stable thiopolyplexes for intracellular delivery of genes. *Journal of Controlled Release*, 115(3), 322–334. <https://doi.org/10.1016/j.jconrel.2006.07.027>.
- Chambers, A. F., Groom, A. C., & MacDonald, I. C. (2002). Dissemination and growth of cancer cells in metastatic sites. *Nature Reviews Cancer*, 2(8), 563–572. <https://doi.org/10.1038/nrc865>.
- Chaudhuri, O., Koshy, S. T., Branco da Cunha, C., et al. (2014). Extracellular matrix stiffness and composition jointly regulate the induction of malignant phenotypes in mammary epithelium. *Nature Materials*, 13(10), 970–978. <https://doi.org/10.1038/nmat4009>.
- Chen, W., Ayala-Orozco, C., Biswal, N. C., et al. (2014). Targeting pancreatic cancer with magneto-fluorescent theranostic gold nanoshells. *Nanomedicine (London, England)*, 9(8), 1209–1222. <https://doi.org/10.2217/nnm.13.84>.
- Chen, F., & Cai, W. (2014). Tumor vasculature targeting: a generally applicable approach for functionalized nanomaterials. *Small*, 10(10), 1887–1893. <https://doi.org/10.1002/sml.201303627>.
- Chen, Y.-C., Gowda, R., Newswanger, R. K., et al. (2016). Targeting cholesterol transport in circulating melanoma cells to inhibit metastasis. *International Journal of Laboratory Hematology*, 38(1), 42–49. <https://doi.org/10.1111/ijlh.12426>.
- Chen, F., Hong, H., Zhang, Y., et al. (2013). In vivo tumor targeting and image-guided drug delivery with antibody-conjugated, radio labeled mesoporous silica nanoparticles. *ACS Nano*, 7(10), 9027–9039. <https://doi.org/10.1021/nn403617j>.
- Chen, H., Jia, H., Tham, H. P., et al. (2017). Theranostic prodrug vesicles for imaging guided co-delivery of camptothecin and siRNA in synergetic cancer therapy. *ACS Applied Materials & Interfaces*, 9(28), 23536–23543. <https://doi.org/10.1021/acsami.7b06936>.
- Chen, H., Zhang, W., Zhu, G., Xie, J., & Chen, X. (2017). Rethinking cancer nanotheranostics. *Nature Reviews Materials*, 2(May), 17024. <https://doi.org/10.1038/natrevmats.2017.24>.
- Chow, E. K., & Ho, D. (2013). Cancer nanomedicine: from drug delivery to imaging. *Science Translational Medicine*, 5(216), 1–12. <https://doi.org/10.1126/scitranslmed.3005872>.

- Chung, A. S., Lee, J., & Ferrara, N. (2010). Targeting the tumour vasculature: insights from physiological angiogenesis. *Nature Reviews Cancer*, *10*(7), 505–514. <https://doi.org/10.1038/nrc2868>.
- Cirri, P., & Chiarugi, P. (2011). Cancer associated fibroblasts: the dark side of the coin. *American Journal of Cancer Research*, *1*(4), 482–497. <http://www.pubmedcentral.nih.gov/articlerender.fcgi?artid=3186047&tool=pmcentrez&rendertype=abstract>.
- Cobaleda-Siles, M., Henriksen-Lacey, M., De Angulo, A. R., et al. (2014). An iron oxide nanocarrier for dsRNA to target lymph nodes and strongly activate cells of the immune system. *Small*, *10*(24), 5054–5067. <https://doi.org/10.1002/sml.201401353>.
- Conde, J., Bao, C., Tan, Y., et al. (2015). Dual targeted immunotherapy via In vivo delivery of biohybrid RNAi-peptide nanoparticles to tumor-associated macrophages and cancer cells. *Advanced Functional Materials*, *25*, 4183–4194. <https://doi.org/10.1002/adfm.201501283>.
- Cordeiro, A. S., Alonso, M. J., & de la Fuente, M. (2015). Nanoengineering of vaccines using natural polysaccharides. *Biotechnology Advances*, *33*(6 Pt 3), 1279–1293. <https://doi.org/10.1016/j.biotechadv.2015.05.010>.
- Costa-Silva, B., Aiello, N. M., Ocean, A. J., et al. (2015). Pancreatic cancer exosomes initiate pre-metastatic niche formation in the liver. *Nature Cell Biology*, *17*(6), 816–826. <https://doi.org/10.1038/ncb3169>.
- Cui, S., Liu, L., Wan, T., Jiang, L., Shi, Y., & Luo, L. (2017). MiR-520b inhibits the development of glioma by directly targeting MBD2. *American Journal of Cancer Research*, *7*(7), 1528–1539.
- Cui, H., & Wang, J. (2016). Progress in the development of nanotheranostic systems. *Theranostics*, *6*(7), 915–917. <https://doi.org/10.7150/thno.16153>.
- Dahmani, F. Z., Xiao, Y., Zhang, J., Yu, Y., Zhou, J., & Yao, J. (2016). Multifunctional polymeric nanosystems for dual-targeted combinatorial chemo/angiogenesis therapy of tumors. *Advanced Healthcare Materials*, *5*(12), 1447–1461. <https://doi.org/10.1002/adhm.201600169>.
- Dai, Z., & Yue, X. (2017). Liposomal nanotechnology for cancer theranostics. *Current Medicinal Chemistry*, *24*(999), 1. <https://doi.org/10.2174/0929867324666170306105350>.
- Danhier, F., Danhier, P., Schleich, N., et al. (2016). Tumor targeting by RGD-grafted PLGA-based nanotheranostics loaded with paclitaxel and superparamagnetic iron oxides. In Y. J. Kang (Ed.), *Methods in pharmacology & toxicology* (pp. 1–29). Switzerland: Springer International Publishing AG. Humana Press. https://doi.org/10.1007/7653_2015_43.
- Danhier, F., Feron, O., & Préat, V. (2010). To exploit the tumor microenvironment: passive and active tumor targeting of nanocarriers for anti-cancer drug delivery. *Journal of Controlled Release*, *148*(2), 135–146. <https://doi.org/10.1016/j.jconrel.2010.08.027>.
- Danila, D. C., Pantel, K., Fleisher, M., & Scher, H. I. (2011). Circulating tumors cells as biomarkers: progress toward biomarker qualification. *Cancer Journal*, *17*(6), 438–450. <https://doi.org/10.1097/PPO.0b013e31823e69ac.Circulating>.
- de la Fuente, M., Csaba, N., Garcia-Fuentes, M., & Alonso, M. J. (2008). Nanoparticles as protein and gene carriers to mucosal surfaces. *Nanomedicine (London, England)*, *3*(6), 845–857. <https://doi.org/10.2217/17435889.3.6.845>.
- de la Fuente, M., Jones, M. C., Santander-Ortega, M. J., et al. (2015). A nano-enabled cancer-specific ITCH RNAi chemotherapy booster for pancreatic cancer. *Nanomedicine*, *11*(2), 369–377. <https://doi.org/10.1016/j.nano.2014.09.010>.
- Fuente, de la, Langer, M., & Alonso, M. J. (2014). Nanotechnology approaches for cancer immunotherapy and immunomodulation. In M. José Alonso & M. Garcia-Fuentes (Eds.), *Nano-oncologicals: New targeting and delivery approaches*. (pp. 215–242). Switzerland: Springer. https://doi.org/10.1007/978-3-319-08084-0_8.
- de la Fuente, M., Raviña, M., Sousa-Herves, A., et al. (2012). Exploring the efficiency of gallic acid-based dendrimers and their block copolymers with PEG as gene carriers. *Nanomedicine (London, England)*, *7*(11), 1667–1681. <https://doi.org/10.2217/nmm.12.51>.
- de la Fuente, M., Seijo, B., & Alonso, M. J. (2008). Design of novel polysaccharidic nanostructures for gene delivery. *Nanotechnology*, *19*(7), 075105. <https://doi.org/10.1088/0957-4484/19/7/075105>.

- De Palma, M., & Hanahan, D. (2012). The biology of personalized cancer medicine: facing individual complexities underlying hallmark capabilities. *Molecular Oncology*, 6, 111–127. <https://doi.org/10.1016/j.molonc.2012.01.011>.
- Deng, S., Wu, Q., Zhao, Y., et al. (2015). Biodegradable polymeric micelle-encapsulated doxorubicin suppresses tumor metastasis by killing circulating tumor cells. *Nanoscale*, 7(12), 5270–5280. <https://doi.org/10.1039/C4NR07641A>.
- Desgrosellier, J. S., & Cheresch, D. A. (2010). Integrins in cancer: biological implications and therapeutic opportunities. *Nature Reviews Cancer*, 10(1), 9–22. <https://doi.org/10.1038/nrc2748>.
- Detappe, A., Kunjachan, S., Rottmann, J., et al. (2015). AGLX nanoparticles as a promising platform for image-guided radiation therapy. *Cancer Nanotechnology*, 6(1), 4. <https://doi.org/10.1186/s12645-015-0012-3>.
- Ding, L., Ley, T. J., Larson, D. E., et al. (2012). Clonal evolution in relapsed acute myeloid leukaemia revealed by whole-genome sequencing. *Nature*, 481(7382), 506–510. <https://doi.org/10.1038/nature10738>.
- Diou, O., Tsapis, N., & Fattal, E. (2012). Targeted nanotheranostics for personalized cancer therapy. *Expert Opinion on Drug Delivery*, 9(12), 1475–1487. <https://doi.org/10.1517/17425247.2012.736486>.
- Du, Y., Zhang, Q., Jing, L., et al. (2015). GX1-conjugated poly(lactic acid) nanoparticles encapsulating endostar for improved in vivo anticancer treatment. *International Journal of Nanomedicine*, 10, 3791–3802. <https://doi.org/10.2147/IJN.S82029>.
- Duan, S., Guo, L., Shi, D., Shang, M., Meng, D., & Li, J. (2017). Development of a novel folate-modified nanobubbles with improved targeting ability to tumor cells. *Ultrasonics Sonochemistry*, 37, 235–243. <https://doi.org/10.1016/j.ulsonch.2017.01.013>.
- Eckert, M. A., Lwin, T. M., Chang, A. T., et al. (2011). Twist1-induced invadopodia formation promotes tumor metastasis. *Cancer Cell*, 19(3), 372–386. <https://doi.org/10.1016/j.ccr.2011.01.036>.
- El-Ghlban, S., Kasai, T., Shigehiro, T., et al. (2014). Chlorotoxin-Fe fusion inhibits release of MMP-2 from pancreatic cancer cells. *BioMed Research International*, 2014, 152659. <https://doi.org/10.1155/2014/152659>.
- Ernsting, M. J., Hoang, B., Lohse, I., et al. (2015). Targeting of metastasis-promoting tumor-associated fibroblasts and modulation of pancreatic tumor-associated stroma with a carboxymethylcellulose-docetaxel nanoparticle. *Journal of Controlled Release*, 206, 122–130. <https://doi.org/10.1016/j.jconrel.2015.03.023>.
- Feng, L., Cheng, L., Dong, Z., et al. (2017). Theranostic liposomes with hypoxia-activated prodrug to effectively destruct hypoxic tumors post-photodynamic therapy. *ACS Nano*, 11(1), 927–937. <https://doi.org/10.1021/acsnano.6b07525>.
- Fidler, I. J. (1970). Metastasis: quantitative analysis of distribution and fate of tumour emboli labeled with 125I-5-iodo-2[prime]-deoxyuridine. *Journal of the National Cancer Institute*, 45, 773–782.
- Fonsatti, E., Nicolay, H. J. M., Altomonte, M., Covre, A., & Maio, M. (2010). Targeting cancer vasculature via endoglin/CD105: a novel antibody-based diagnostic and therapeutic strategy in solid tumours. *Cardiovascular Research*, 86(1), 12–19. <https://doi.org/10.1093/cvr/cvp332>.
- Franco, O. E., Shaw, A. K., Strand, D. W., & Hayward, S. W. (2010). Cancer associated fibroblasts in cancer pathogenesis. *Seminars in Cell & Developmental Biology*, 21(1), 33–39. <https://doi.org/10.1016/j.semcdb.2009.10.010>.
- Gabizon, A., Shmeeda, H., & Barenholz, Y. (2003). Pharmacokinetics of pegylated liposomal doxorubicin: review of animal and human studies. *Clinical Pharmacokinetics*, 42(5), 419–436. <https://doi.org/10.2165/00003088-200342050-00002>.
- Galanza, E. I., Kim, J. W., & Zharov, V. P. (2009). Nanotechnology-based molecular photoacoustic and photothermal flow cytometry platform for in-vivo detection and killing of circulating cancer stem cells. *Journal of Biophotonics*, 2(12), 725–735. <https://doi.org/10.1002/jbio.200910078>.
- Galanza, E. I., Shashkov, E. V., Kelly, T., Kim, J.-W., Yang, L., & Zharov, V. P. (2009). In vivo magnetic enrichment and multiplex photoacoustic detection of circulating tumour cells. *Nature Nanotechnology*, 4(12), 855–860. <https://doi.org/10.1038/nnano.2009.333>.
- Gallo, J., Kamaly, N., Lavdas, I., et al. (2014). CXCR4-targeted and MMP-responsive iron oxide nanoparticles for enhanced magnetic resonance imaging. *Angewandte Chemie, International Edition*, 53(36), 9550–9554. <https://doi.org/10.1002/anie.201405442>.

- Gao, D., Gao, J., Xu, M., et al. (2017). Targeted ultrasound-triggered phase transition nanodroplets for Her2-overexpressing breast cancer diagnosis and gene transfection. *Molecular Pharmaceutics*, 14(4), 984–998. <https://doi.org/10.1021/acs.molpharmaceut.6b00761>.
- Gao, Y., Xie, J., Chen, H., et al. (2014). Nanotechnology-based intelligent drug design for cancer metastasis treatment. *Biotechnology Advances*, 32(4), 761–777. <https://doi.org/10.1016/j.biotechadv.2013.10.013>.
- Garcia-Mazas, C., Csaba, N., & Garcia-Fuentes, M. (2017). Biomaterials to suppress cancer stem cells and disrupt their tumoral niche. *International Journal of Pharmaceutics*, 523(2), 490–505. <https://doi.org/10.1016/j.ijpharm.2016.12.013>.
- Gay, L. J., & Felding-Habermann, B. (2011). Contribution of platelets to tumour metastasis. *Nature Reviews Cancer*, 11(2), 123–134. <https://doi.org/10.1038/nrc3004>.
- Gener, P., Rafael, D. F., Fernández, Y., et al. (2016). Cancer stem cells and personalized cancer nanomedicine. *Nanomedicine*, 11(3), 307–320. <https://doi.org/10.2217/nmm.15.200>.
- Greaves, M. (2015). Evolutionary determinants of cancer. *Cancer Discovery*, 5(8), 806–820. <https://doi.org/10.1158/2159-8290.CD-15-0439>.
- Grivnickov, S. I., Greten, F. R., & Karin, M. (2010). Immunity, inflammation, and cancer. *Cell*, 140(6), 883–899. <https://doi.org/10.1016/j.cell.2010.01.025>.
- Guo, W., Qiu, Z., Guo, C., et al. (2017). Multifunctional theranostic agent of Cu₂(OH)PO₄ quantum dots for photoacoustic image-guided photothermal/photodynamic combination cancer therapy. *ACS Applied Materials & Interfaces*, 9(11), 9348–9358. <https://doi.org/10.1021/acsami.6b15703>.
- Hall, E., Cameron, D., Waters, R., et al. (2014). Comparison of patient reported quality of life and impact of treatment side effects experienced with a taxane-containing regimen and standard anthracycline based chemotherapy for early breast cancer: 6 year results from the UK TACT trial (CRUK/01/001). *European Journal of Cancer*, 50, 2375–2389. <https://doi.org/10.1016/j.ejca.2014.06.007>.
- Hanahan, D., & Coussens, L. M. (2012). Accessories to the crime: functions of cells recruited to the tumor microenvironment. *Cancer Cell*, 21(3), 309–322. <https://doi.org/10.1016/j.ccr.2012.02.022>.
- Hatakeyama, H., Akita, H., Ishida, E., et al. (2007). Tumor targeting of doxorubicin by anti-MT1-MMP antibody-modified PEG liposomes. *International Journal of Pharmaceutics*, 342(1–2), 194–200. <https://doi.org/10.1016/j.ijpharm.2007.04.037>.
- He, Q., Guoc, S., Qiana, Z., & Chen, X. (2015). Development of individualized anti-metastasis strategies by engineering nanomedicines. *Chemical Society Reviews*, 44(17), 6258–6286. <https://doi.org/10.1039/c4cs00511b>.
- Hirakawa, S., Brown, L. F., Kodama, S., Paavonen, K., Alitalo, K., & Detmar, M. (2006). VEGF-C-induced lymphangiogenesis in sentinel lymph nodes promotes tumor metastasis to distant sites. *Blood*, 109(3), 1010–1017. <https://doi.org/10.1182/blood-2006-05-021758>.
- Hirano, K., Hunt, C. A., Strubbe, A., & MacGregor, R. D. (1985). Lymphatic transport of liposome-encapsulated drugs following intraperitoneal administration—effect of lipid composition. *The American Association of Pharmaceutical Scientists Journal*, 2(6), 271–278. <https://doi.org/10.1023/A:1016337500364>.
- Hodi, F. S., O'Day, S. J., McDermott, D. F., et al. (2010). Improved survival with ipilimumab in patients with metastatic melanoma. *The New England Journal of Medicine*, 363(8), 711–723. <https://doi.org/10.1056/NEJMoa1003466>.
- Hong, I.-S., Jang, G.-B., Lee, H.-Y., & Nam, J.-S. (2015). Targeting cancer stem cells by using the nanoparticles. *International Journal of Nanomedicine*, 10(Special Issue), 251–260. <https://doi.org/10.2147/IJN.S88310>.
- Hoshino, A., Costa-Silva, B., Shen, T.-L., et al. (2015). Tumour exosome integrins determine organotropic metastasis. *Nature*, 527(7578), 329–335. <https://doi.org/10.1038/nature15756>.
- Høye, A. M., & Erler, J. T. (2016). Structural ECM components in the premetastatic and metastatic niche. *American Journal of Physiology Cell Physiology*, 310(11), C955–C967. <https://doi.org/10.1152/ajpcell.00326.2015>.
- Huang, X., O'Connor, R., & Kwizera, E. A. (2017). Gold nanoparticle based platforms for circulating cancer marker detection. *Nanotheranostics*, 1(1), 80–102. <https://doi.org/10.7150/ntno.18216>.
- Huang, M., Shen, A., Ding, J., & Geng, M. (2014). Molecularly targeted cancer therapy: some lessons from the past decade. *Trends in Pharmacological Sciences*, 35(1), 41–50. <https://doi.org/10.1016/j.tips.2013.11.004>.
- Huang, H., Yang, D.-P., Liu, M., et al. (2017). pH-sensitive Au–BSA–DOX–FA nanocomposites for combined CT imaging and targeted drug delivery. *International Journal of Nanomedicine*, 12, 2829–2843. <https://doi.org/10.2147/IJN.S128270>.

- Huang, X., Zhang, F., Lee, S., et al. (2012). Long-term multimodal imaging of tumor draining sentinel lymph nodes using mesoporous silica-based nanoprobes. *Biomaterials*, 33(17), 4370–4378. <https://doi.org/10.1016/j.biomaterials.2012.02.060>.
- Hui, X., Han, Y., Liang, S., et al. (2008). Specific targeting of the vasculature of gastric cancer by a new tumor-homing peptide CGNSNPKSC. *Journal of Controlled Release*, 131(2), 86–93. <https://doi.org/10.1016/j.jconrel.2008.07.024>.
- Huo, D., He, J., Li, H., et al. (2014). X-ray CT guided fault-free photothermal ablation of metastatic lymph nodes with ultrafine HER-2 targeting W18O49 nanoparticles. *Biomaterials*, 35(33), 9155–9166. <https://doi.org/10.1016/j.biomaterials.2014.07.034>.
- Ilic, M., & Ilic, I. (2016). Epidemiology of pancreatic cancer. *World Journal of Gastroenterology*, 22(44), 9694–9705. <https://doi.org/10.3748/wjg.v22.i44.9694>.
- Irmisch, A., & Huelsken, J. (2013). Metastasis: new insights into organ-specific extravasation and metastatic niches. *Experimental Cell Research*, 319, 1604–1610. <https://doi.org/10.1016/j.yexcr.2013.02.012>.
- Junttila, M. R., & de Sauvage, F. J. (2013). Influence of tumour micro-environment heterogeneity on therapeutic response. *Nature*, 501(7467), 346–354. <https://doi.org/10.1038/nature12626>.
- Kaminskas, L. M., McLeod, V. M., Ascher, D. B., et al. (2014). Methotrexate-conjugated PEGylated dendrimers show differential patterns of deposition and activity in tumor-burdened lymph nodes after intravenous and subcutaneous administration in rats. *Molecular Pharmaceutics*, 12(2), 432–443. <https://doi.org/10.1021/mp500531e>.
- Kanapathipillai, M., Brock, A., & Ingber, D. E. (2014). Nanoparticle targeting of anti-cancer drugs that alter intracellular signaling or influence the tumor microenvironment. *Advanced Drug Delivery Reviews*, 79, 107–118. <https://doi.org/10.1016/j.addr.2014.05.005>.
- Kang, T., Zhu, Q., Wei, D., et al. (2017). Nanoparticles coated with neutrophil membranes can effectively treat cancer metastasis. *ACS Nano*, 11(2), 1397–1411. <https://doi.org/10.1021/acsnano.6b06477>.
- Kaplan, R. N., Riba, R. D., Zacharoulis, S., et al. (2005). VEGFR1-positive haematopoietic bone marrow progenitors initiate the pre-metastatic niche. *Nature*, 438(7069), 820–827. <https://doi.org/10.1038/nature04186>.
- Karathanasis, E., Suryanarayanan, S., Balusu, S. R., et al. (2009). Imaging nanoprobe for prediction of outcome of nanoparticle chemotherapy by using mammography. *Radiology*, 250(2), 398–406. <https://doi.org/10.1148/radiol.2502080801>.
- Kedrin, D., van Rheenen, J., Hernandez, L., Condeelis, J., & Segall, J. E. (2007). Cell motility and cytoskeletal regulation in invasion and metastasis. *Journal of Mammary Gland Biology and Neoplasia*, 12(2–3), 143–152. <https://doi.org/10.1007/s10911-007-9046-4>.
- Kharaziha, P., Ceder, S., Li, Q., & Panaretakis, T. (2012). Tumor cell-derived exosomes: a message in a bottle. *Biochimica et Biophysica Acta, Reviews on Cancer*, 1826(1), 103–111. <https://doi.org/10.1016/j.bbcan.2012.03.006>.
- Kim, Y. J., Borsig, L., Han, H.-L., Varki, N. M., & Varki, A. (1999). Distinct selectin ligands on colon carcinoma mucins can mediate pathological interactions among platelets, leukocytes, and endothelium. *The American Journal of Pathology*, 155(2), 461–472. [https://doi.org/10.1016/S0002-9440\(10\)65142-5](https://doi.org/10.1016/S0002-9440(10)65142-5).
- Kim, J.-W., Galanzha, E. I., Zaharoff, D. A., Griffin, R. J., & Zharov, V. P. (2014). Nanotheranostics of circulating tumor cells, infections and other pathological features. *In Vivo*, 10(3), 813–830. <https://doi.org/10.1021/mp300577s>. Nanotheranostics.
- Kim, D., Jeong, Y. Y., & Jon, S. (2010). A drug loaded aptamer-gold nanoparticle bioconjugate for combined CT imaging and therapy of prostate cancer. *ACS Nano*, 4(7), 3689–3696. <https://doi.org/10.1021/nn901877h>.
- Kim, D., Lee, E. S., Oh, K. T., Gao, Z., & Bae, Y. H. (2008). Doxorubicin-loaded polymeric micelle overcomes multidrug resistance of cancer by double-targeting folate receptor and early endosomal pH. *Small*, 4(11), 2043–2050. <https://doi.org/10.1002/sml.200701275>.
- Kirpotin, D., Hong, K., Mullah, N., Papahadjopoulos, D., & Zalipsky, S. (1996). Liposomes with detachable polymer coating: destabilization and fusion of dioleoylphosphatidylethanolamine vesicles triggered by cleavage of surface-grafted poly(ethylene glycol). *FEBS Letters*, 388(2–3), 115–118. [https://doi.org/10.1016/0014-5793\(96\)00521-2](https://doi.org/10.1016/0014-5793(96)00521-2).

- Kotb, S., Detappe, A., Lux, F., et al. (2016). Gadolinium-based nanoparticles and radiation therapy for multiple brain melanoma metastases: proof of concept before phase I trial. *Theranostics*, 6(3), 418–427. <https://doi.org/10.7150/thno.14018>.
- Kunjachan, S., Pola, R., Gremse, F., et al. (2014). Passive versus active tumor targeting using RGD- and NGR-modified polymeric nanomedicines. *Nano Letters*, 14(2), 972–981. <https://doi.org/10.1021/nl404391r>.
- Labelle, M., & Hynes, R. O. (2012). The initial hours of metastasis: the importance of cooperative host-tumor cell interactions during hematogenous dissemination. *Cancer Discovery*, 2(12), 1091–1099. <https://doi.org/10.1158/2159-8290.CD-12-0329>.
- Laubli, H., Spanaus, K.-S., & Borsig, L. (2009). Selectin-mediated activation of endothelial cells induces expression of CCL5 and promotes metastasis through recruitment of monocytes. *Blood*, 114(20), 4583–4591. <https://doi.org/10.1182/blood-2008-10-186585>.
- Ledet, G., & Mandal, T. K. (2012). Nanomedicine: emerging therapeutics for the 21st century. *US Pharmacist*, 37(3), 7–11.
- Ledford, H. (2016). Bankruptcy filing worries developers of nanoparticle cancer drugs. *Nature*, 533(7603), 304–305. <https://doi.org/10.1038/533304a>.
- Lee, J.-Y., Chung, S.-J., Cho, H.-J., & Kim, D.-D. (2016). Iodinated hyaluronic acid oligomer-based nanoassemblies for tumor-targeted drug delivery and cancer imaging. *Biomaterials*, 85, 218–231. <https://doi.org/10.1016/j.biomaterials.2016.01.060>.
- Lee, C., Kwon, W., Beack, S., et al. (2016). Biodegradable nitrogen-doped carbon nanodots for non-invasive photoacoustic imaging and photothermal therapy. *Theranostics*, 6(12), 2196–2208. <https://doi.org/10.7150/thno.16923>.
- Levental, K. R., Yu, H., Kass, L., et al. (2009). Matrix crosslinking forces tumor progression by enhancing integrin signaling. *Cell*, 139(5), 891–906. <https://doi.org/10.1016/j.cell.2009.10.027>.
- Li, J., Cai, P., Shalviri, A., et al. (2014). A multifunctional polymeric nanotheranostic system delivers doxorubicin and imaging agents across the blood brain barrier targeting brain metastases of breast cancer. *ACS Nano*, 8(10), 9925–9940. <https://doi.org/10.1021/nn501069c>.
- Li, L., Fu, S., Chen, C., et al. (2016). Microenvironment-driven bioelimination of magnetoplasmonic nanoassemblies and their multimodal imaging-guided tumor photothermal therapy. *ACS Nano*, 10(7), 7094–7105. <https://doi.org/10.1021/acsnano.6b03238>.
- Li, S., & Li, Q. (2015). Cancer stem cells, lymphangiogenesis, and lymphatic metastasis. *Cancer Letters*, 357(2), 438–447. <https://doi.org/10.1016/j.canlet.2014.12.013>.
- Li, B., Li, Q., Mo, J., & Dai, H. (2017). Drug-loaded polymeric nanoparticles for cancer stem cell targeting. *Frontiers in Pharmacology*, 8(February), 1–12. <https://doi.org/10.3389/fphar.2017.00051>.
- Li, L., Li, X., Wu, Y., et al. (2017). Multifunctional nucleus-targeting nanoparticles with ultra-high gene transfection efficiency for *in vivo* gene therapy. *Theranostics*, 7(6), 1633–1649. <https://doi.org/10.7150/thno.17588>.
- Li, J., Sharkey, C. C., Huang, D., & King, M. R. (2015). Nanobiotechnology for the therapeutic targeting of cancer cells in blood. *Cellular and Molecular Bioengineering*, 8(1), 137–150. <https://doi.org/10.1007/s12195-015-0381-z>.
- Li, Y., Tang, J., Pan, D. X., et al. (2016). A versatile imaging and therapeutic platform based on dual-band luminescent lanthanide nanoparticles toward tumor metastasis inhibition. *ACS Nano*, 10(2), 2766–2773. <https://doi.org/10.1021/acsnano.5b07873>.
- Lin, R.-Z., Wang, T.-P., Hung, R.-J., Chuang, Y.-J., Chien, C.-C.M., & Chang, H.-Y. (2011). Tumor-induced endothelial cell apoptosis: roles of NAD(P)H oxidase-derived reactive oxygen species. *Journal of Cellular Physiology*, 226(7), 1750–1762. <https://doi.org/10.1002/jcp.22504>.
- Ling, D., Xia, H., Park, W., et al. (2014). pH-sensitive nanoformulated triptolide as a targeted therapeutic strategy for hepatocellular carcinoma. *ACS Nano*, 8(8), 8027–8039.
- Liu, Z., Chen, W., Li, Y., & Xu, Q. (2016). Integrin $\alpha_v\beta_3$ -targeted C-dot nanocomposites as multifunctional agents for cell targeting and photoacoustic imaging of superficial malignant tumors. *Analytical Chemistry*, 88(23), 11955–11962. <https://doi.org/10.1021/acs.analchem.6b03927>.

- Liu, Y., Miyoshi, H., & Nakamura, M. (2007). Nanomedicine for drug delivery and imaging: a promising avenue for cancer therapy and diagnosis using targeted functional nanoparticles. *International Journal of Cancer*, 120(12), 2527–2537. <https://doi.org/10.1002/ijc.22709>.
- Liu, H., Xu, S., He, Z., Deng, A., & Zhu, J. J. (2013). Supersandwich cytosensor for selective and ultrasensitive detection of cancer cells using aptamer-DNA concatamer-quantum dots probes. *Analytical Chemistry*, 85(6), 3385–3392. <https://doi.org/10.1021/ac303789x>.
- Livney, Y. D., & Assaraf, Y. G. (2013). Rationally designed nanovehicles to overcome cancer chemoresistance. *Advanced Drug Delivery Reviews*, 65(13–14), 1716–1730. <https://doi.org/10.1016/j.addr.2013.08.006>.
- Luo, M., Brooks, M., & Wicha, M. S. (2015). Epithelial-mesenchymal plasticity of breast cancer stem cells: implications for metastasis and therapeutic resistance. *Current Pharmaceutical Design*, 21(10), 1301–1310.
- Lv, G., Wu, M., Wang, M., et al. (2016). miR-320a regulates high mobility group box 1 expression and inhibits invasion and metastasis in hepatocellular carcinoma. *International Journal of Laboratory Hematology*, 38(1), 42–49. <https://doi.org/10.1111/ijlh.12426>.
- Martínez-Cardús, A., Moran, S., Musulen, E., et al. (2016). Epigenetic homogeneity within colorectal tumors predicts shorter relapse-free and overall survival times for patients with locoregional cancer. *Gastroenterology*, 151(5), 961–972. <https://doi.org/10.1053/j.gastro.2016.08.001>.
- Massagué, J., & Obenauf, A. C. (2016). Metastatic colonization by circulating tumour cells. *Nature*, 529(7586), 298–306. <https://doi.org/10.1038/nature17038>.
- Matsumura, Y., & Maeda, H. (1986). A new concept for macromolecular therapeutics in cancer chemotherapy: mechanism of tumorotropic accumulation of proteins and the antitumor agent smancs. *Cancer Research*, 46(12 Pt 1), 6387–6392.
- Mazza, M., Alonso-Sande, M., Jones, M. C., & de la Fuente, M. (2013). The potential of nanoemulsions in biomedicine. In I. F. Uchehgbu, A. G. Schätzlein, W. P. Cheng, & A. Lalatsa (Eds.), *Fundamentals of pharmaceutical nanoscience*. (pp. 117–155). Switzerland: Springer. <https://doi.org/10.1007/978-1-4614-9164-4>.
- McGowan, P. M., Kirstein, J. M., & Chambers, A. F. (2009). Micrometastatic disease and metastatic outgrowth: clinical issues and experimental approaches. *Future Oncology*, 5(7), 1083–1098. <https://doi.org/10.2217/fon.09.73>.
- Mcgranahan, N., & Swanton, C. (2017). Clonal heterogeneity and tumor evolution: past, present, and the future. *Cell*, 168(4), 613–628. <https://doi.org/10.1016/j.cell.2017.01.018>.
- Mehlen, P., & Puisieux, A. (2006). Metastasis: a question of life or death. *Nature Reviews Cancer*, 6(6), 449–458. <https://doi.org/10.1038/nrc1886>.
- Miles, F. L., Pruitt, F. L., van Golen, K. L., & Cooper, C. R. (2008). Stepping out of the flow: capillary extravasation in cancer metastasis. *Clinical & Experimental Metastasis*, 25(4), 305–324. <https://doi.org/10.1007/s10585-007-9098-2>.
- Miller, M. A., Gadde, S., Pfirschke, C., et al. (2015). Predicting therapeutic nanomedicine efficacy using a companion magnetic resonance imaging nanoparticle. *Science Translational Medicine*, 7(314), 314ra183. <https://doi.org/10.1126/scitranslmed.aac6522>.
- Mina, L. A., & Sledge, G. W. (2011). Rethinking the metastatic cascade as a therapeutic target. *Nature Reviews Clinical Oncology*, 8(6), 325–332. <https://doi.org/10.1038/nrclinonc.2011.59>.
- Mitra, A., Mulholland, J., Nan, A., McNeill, E., Ghandehari, H., & Line, B. R. (2005). Targeting tumor angiogenic vasculature using polymer-RGD conjugates. *Journal of Controlled Release*, 102(1), 191–201. <https://doi.org/10.1016/j.jconrel.2004.09.023>.
- Mo, R., Jiang, T., DiSanto, R., Tai, W., & Gu, Z. (2014). ATP-triggered anticancer drug delivery. *Nature Communications*, 5, 3364. <https://doi.org/10.1038/ncomms4364>.
- Mohanty, S., Chen, Z., Li, K., et al. (2017). A novel theranostic strategy for MMP-14 expressing glioblastomas impacts survival. *Molecular Cancer Therapeutics*, 16(9), 1909–1921. <https://doi.org/10.1158/1535-7163.MCT-17-0022>.
- Mok, H., Veisoh, O., Fang, C., et al. (2010). pH-sensitive siRNA nanovector for targeted gene silencing and cytotoxic effect in cancer cells. *Molecular Pharmaceutics*, 7(6), 1930–1939.

- Morikawa, S., Baluk, P., Kaidoh, T., Haskell, A., Jain, R. K., & McDonald, D. M. (2002). Abnormalities in pericytes on blood vessels and endothelial sprouts in tumors. *The American Journal of Pathology*, *160*(3), 985–1000. [https://doi.org/10.1016/S0002-9440\(10\)64920-6](https://doi.org/10.1016/S0002-9440(10)64920-6).
- Motzer, R. J., Escudier, B., McDermott, D. F., et al. (2015). Nivolumab versus everolimus in advanced renal-cell carcinoma. *The New England Journal of Medicine*, *373*(19), 1803–1813. <https://doi.org/10.1056/NEJMoa1510665>.
- Mueller, M. M., & Fusenig, N. E. (2004). Friends or foes—bipolar effects of the tumour stroma in cancer. *Nature Reviews Cancer*, *4*(11), 839–849. <https://doi.org/10.1038/nrc1477>.
- Muinelto-Romay, L., Vieito, M., Abalo, A., et al. (2014). Evaluation of circulating tumor cells and related events as prognostic factors and surrogate biomarkers in advanced NSCLC patients receiving first-line systemic treatment. *Cancers*, *6*(1), 153–165. <https://doi.org/10.3390/cancers6010153>.
- Mura, S., Nicolas, J., & Couvreur, P. (2013). Stimuli-responsive nanocarriers for drug delivery. *Nature Materials*, *12*(11), 991–1003. <https://doi.org/10.1038/nmat3776>.
- Murphy, E. A., Majeti, B. K., Barnes, L. A., et al. (2008). Nanoparticle-mediated drug delivery to tumor vasculature suppresses metastasis. *Proceedings of the National Academy of Sciences of the United States of America*, *105*(27), 9343–9348. <https://doi.org/10.1073/pnas.0803728105>.
- Myung, J. H., Roengvoraphoj, M., Tam, K. A., et al. (2015). Effective capture of circulating tumor cells from a transgenic mouse lung cancer model using Dendrimer surfaces immobilized with anti-EGFR. *Analytical Chemistry*, *87*(19), 10096–10102. <https://doi.org/10.1021/acs.analchem.5b02766>.
- Nathanson, S. D., & Mahan, M. (2011). Sentinel lymph node pressure in breast cancer. *Annals of Surgical Oncology*, *18*(13), 3791–3796. <https://doi.org/10.1245/s10434-011-1796-y>.
- Niu, C., Wang, Z., Lu, G., et al. (2013). Doxorubicin loaded superparamagnetic PLGA-iron oxide multifunctional microbubbles for dual-mode US/MR imaging and therapy of metastasis in lymph nodes. *Biomaterials*, *34*(9), 2307–2317. <https://doi.org/10.1016/j.biomaterials.2012.12.003>.
- Novello, S., Barlesi, F., Califano, R., et al. (2016). Metastatic non-small-cell lung cancer: ESMO clinical practice guidelines for diagnosis, treatment and follow-up. *Annals of Oncology*, *27*(Supplement 5), V1–V27. <https://doi.org/10.1093/annonc/mdw326>.
- Oliveira, E. A., & Faintuch, B. L. (2015). Radiolabeling and biological evaluation of the GX1 and RGD-GX1 peptide sequence for angiogenesis targeting. *Nuclear Medicine and Biology*, *42*(2), 123–130. <https://doi.org/10.1016/j.nucmedbio.2014.09.004>.
- Olmeda, D., Jordá, M., Peinado, H., Fabra, A., & Cano, A. (2007). Snail silencing effectively suppresses tumour growth and invasiveness. *Oncogene*, *26*(13), 1862–1874. <https://doi.org/10.1038/sj.onc.1209997>.
- Oskarsson, T., Acharyya, S., Zhang, X. H., et al. (2011). Breast cancer cells produce tenascin C as a metastatic niche component to colonize the lungs. *Nature Medicine*, *17*(7), 867–874. <https://doi.org/10.1038/nm.2379>.
- Pantel, K., Alix-Panabières, C., & Riethdorf, S. (2009). Cancer micrometastases. *Nature Reviews Clinical Oncology*, *6*(6), 339–351. <https://doi.org/10.1038/nrclinonc.2009.44>.
- Pantel, K., & Brakenhoff, R. H. (2004). Dissecting the metastatic cascade. *Nature Reviews Cancer*, *4*(6), 448–456. <https://doi.org/10.1038/nrc1370>. pii: nrc1370.
- Park, S., Aalipour, A., Vermesh, O., Yu, J. H., & Gambhir, S. S. (2017). Towards clinically translatable in vivo nanodiagnosics. *Nature Reviews Materials*, *2*, 1–20. 17014. <https://doi.org/10.1038/natrevmats.2017.14>.
- Park, J. A., Lee, J. J., Jung, J. C., et al. (2008). Gd-DOTA conjugate of RGD as a potential tumor-targeting MRI contrast agent. *ChemBioChem*, *9*(17), 2811–2813. <https://doi.org/10.1002/cbic.200800529>.
- Patel, S. K., & Janjic, J. M. (2015). Macrophage targeted theranostics as personalized nanomedicine strategies for inflammatory diseases. *Theranostics*, *5*(2), 150–172. <https://doi.org/10.7150/thno.9476>.
- Pawelek, J. M., & Chakraborty, A. K. (2008). Fusion of tumour cells with bone marrow-derived cells: a unifying explanation for metastasis. *Nature Reviews Cancer*, *8*(5), 377–386. <https://doi.org/10.1038/nrc2371>.
- Peer, D., Karp, J. M., Hong, S., Farokhzad, O. C., Margalit, R., & Langer, R. (2007). Nanocarriers as an emerging platform for cancer therapy. *Nature Nanotechnology*, *2*(12), 751–760.
- Peinado, H., Lavotshkin, S., & Lyden, D. (2011). The secreted factors responsible for pre-metastatic niche formation: old sayings and new thoughts. *Seminars in Cancer Biology*, *21*(2), 139–146. <https://doi.org/10.1016/j.semcancer.2011.01.002>.

- Peinado, H., Zhang, H., Matei, I. R., et al. (2017). Pre-metastatic niches: organ-specific homes for metastases. *Nature Reviews Cancer*, 17(5), 302–317. <https://doi.org/10.1038/nrc.2017.6>.
- Pellosi, D. S., Calori, I. R., de Paula, L. B., Hioka, N., Quaglia, F., & Tedesco, A. C. (2017). Multifunctional theranostic Pluronic mixed micelles improve targeted photoactivity of Verteporfin in cancer cells. *Materials Science and Engineering: C*, 71, 1–9. <https://doi.org/10.1016/j.msec.2016.09.064>.
- Pérez-Medina, C., Abdel-Atti, D., Tang, J., et al. (2016). Nanoreporter PET predicts the efficacy of anti-cancer nanotherapy. *Nature Communications*, 7(May), 11838. <https://doi.org/10.1038/ncomms11838>.
- Planchard, D., Besse, B., Groen, H. J. M., et al. (2016). Dabrafenib plus trametinib in patients with previously treated BRAFV600E-mutant metastatic non-small cell lung cancer: an open-label, multicentre phase 2 trial. *The Lancet Oncology*, 17(7), 984–993. [https://doi.org/10.1016/S1470-2045\(16\)30146-2](https://doi.org/10.1016/S1470-2045(16)30146-2).
- Pollard, J. W. (2004). Tumour-educated macrophages promote tumour progression and metastasis. *Nature Reviews Cancer*, 4(1), 71–78. <https://doi.org/10.1038/nrc1256>.
- Qian, C., Chen, Y., Zhu, S., et al. (2016). ATP-responsive and near-infrared-emissive nanocarriers for anticancer drug delivery and real-time imaging. *Theranostics*, 6(7), 1053–1064. <https://doi.org/10.7150/thno.14843>.
- Quail, D. F., & Joyce, J. A. (2013). Microenvironmental regulation of tumor progression and metastasis. *Nature Medicine*, 19(11), 1423–1437. <https://doi.org/10.1038/nm.3394>.
- Rafii, S., Lyden, D., Benezra, R., Hattori, K., & Heissig, B. (2002). Vascular and haematopoietic stem cells: novel targets for anti-angiogenesis therapy? *Nature Reviews Cancer*, 2(11), 826–835. <https://doi.org/10.1038/nrc925>.
- Rajkumar, S., & Prabakaran, M. (2016). Theranostics based on iron oxide and gold nanoparticles for imaging-guided photothermal and photodynamic therapy of cancer. *Current Topics in Medicinal Chemistry*, (November). <http://www.ncbi.nlm.nih.gov/pubmed/27875977>. Accessed May 31, 2017.
- Reck, M., Rodríguez-Abreu, D., Robinson, A. G., et al. (2016). Pembrolizumab versus chemotherapy for PD-L1-positive non-small-cell lung cancer. *The New England Journal of Medicine*, 375(19), 1823–1833. <https://doi.org/10.1056/NEJMoa1606774>.
- Reimondez-Troitiño, S., Csaba, N., Alonso, M. J., & de la Fuente, M. (2015). Nanotherapies for the treatment of ocular diseases. *European Journal of Pharmaceutics and Biopharmaceutics*, 95(Pt B), 279–293. <https://doi.org/10.1016/j.ejpb.2015.02.019>.
- Ren, L., Chen, S., Li, H., et al. (2016). MRI-guided liposomes for targeted tandem chemotherapy and therapeutic response prediction. *Acta Biomaterialia*, 35, 260–268. <https://doi.org/10.1016/j.actbio.2016.02.011>.
- Robert, C., Long, G. V., Brady, B., et al. (2014). Nivolumab in previously untreated melanoma without BRAF mutation. *The New England Journal of Medicine*, 372(4), 320–330. <https://doi.org/10.1056/NEJMoa1412082>.
- Rolfo, C., Passiglia, F., Ostrowski, M., et al. (2015). Improvement in lung cancer outcomes with targeted therapies: an update for family physicians. *Journal of American Board of Family Medicine*, 28(1), 124–133. <https://doi.org/10.3122/jabfm.2015.01.140072>.
- Roma-Rodrigues, C., Raposo, L. R., Cabral, R., Paradinha, F., Baptista, P. V., & Fernandes, A. R. (2017). Tumor microenvironment modulation via gold nanoparticles targeting malicious exosomes: implications for cancer diagnostics and therapy. *International Journal of Molecular Sciences*, 18(1), 162–188. <https://doi.org/10.3390/ijms18010162>.
- Ruoslahti, E., & Pierschbacher, M. (1987). New perspectives in cell adhesion: RGD and integrins. *Science*, 238(4826), 491–497. <https://doi.org/10.1126/science.2821619>.
- Ryan, G. M., Kaminskas, L. M., & Porter, C. J. H. (2014). Nano-chemotherapeutics: maximising lymphatic drug exposure to improve the treatment of lymph-metastatic cancers. *Journal of Controlled Release*, 193, 241–256. <https://doi.org/10.1016/j.jconrel.2014.04.051>.
- Sainz, B., Jr., Carron, E., Vallespinós, M., & Machado, H. L. (2016). Cancer stem cells and macrophages: implications in tumor biology and therapeutic strategies. *Mediators of Inflammation*, 2016, 1–15. <https://doi.org/10.1155/2016/9012369>.
- Saito, G., Swanson, J. A., & Lee, K. D. (2003). Drug delivery strategy utilizing conjugation via reversible disulfide linkages: role and site of cellular reducing activities. *Advanced Drug Delivery Reviews*, 55(2), 199–215. [https://doi.org/10.1016/S0169-409X\(02\)00179-5](https://doi.org/10.1016/S0169-409X(02)00179-5).
- Sanna, V., Pala, N., & Sechi, M. (2014). Targeted therapy using nanotechnology: focus on cancer. *International Journal of Nanomedicine*, 9, 467–483. <https://doi.org/10.2147/IJN.S36654>.

- Sasso, M. S., Lollo, G., Pitorre, M., et al. (2016). Low dose gemcitabine-loaded lipid nanocapsules target monocytic myeloid-derived suppressor cells and potentiate cancer immunotherapy. *Biomaterials*, 96, 47–62. <https://doi.org/10.1016/j.biomaterials.2016.04.010>.
- Sawant, R. M., Hurley, J. P., Salmaso, S., et al. (2006). “SMART” drug delivery systems: double-targeted pH-responsive pharmaceutical nanocarriers. *Bioconjugate Chemistry*, 17(4), 943–949. <https://doi.org/10.1021/bc060080h>.
- Sceneay, J., Smyth, M. J., & Möller, A. (2013). The pre-metastatic niche: finding common ground. *Cancer Metastasis Reviews*, 32(3–4), 449–464. <https://doi.org/10.1007/s10555-013-9420-1>.
- Schleich, N., Po, C., Jacobs, D., et al. (2014). Comparison of active, passive and magnetic targeting to tumors of multifunctional paclitaxel/SPIO-loaded nanoparticles for tumor imaging and therapy. *Journal of Controlled Release*, 194, 82–91. <https://doi.org/10.1016/j.jconrel.2014.07.059>.
- Seon, B. K., Haba, A., Matsuno, F., et al. (2011). Endoglin-targeted cancer therapy. *Current Drug Delivery*, 8(1), 135–143. <http://www.ingentaconnect.com/content/ben/cdd/2011/00000008/00000001/art00009>.
- Serafini, P., Borrello, I., & Bronte, V. (2006). Myeloid suppressor cells in cancer: recruitment, phenotype, properties, and mechanisms of immune suppression. *Seminars in Cancer Biology*, 16(1), 53–65. <https://doi.org/10.1016/j.semcancer.2005.07.005>.
- Shen, M., Huang, Y., Han, L., et al. (2012). Multifunctional drug delivery system for targeting tumor and its acidic microenvironment. *Journal of Controlled Release*, 161(3), 884–892. <https://doi.org/10.1016/j.jconrel.2012.05.013>.
- Shen, S., Xia, J.-X., & Wang, J. (2016). Nanomedicine-mediated cancer stem cell therapy. *Biomaterials*, 74, 1–18. <https://doi.org/10.1016/j.biomaterials.2015.09.037>.
- Shi, J., Kantoff, P. W., Wooster, R., & Farokhzad, O. C. (2016). Cancer nanomedicine: progress, challenges and opportunities. *Nature Publishing Group*, 17(1), 20–37. <https://doi.org/10.1038/nrc.2016.108>.
- Shi, H., Ye, X., He, X., et al. (2014). Au@Ag/Au nanoparticles assembled with activatable aptamer probes as smart “nano-doctors” for image-guided cancer radiotherapy. *Nanoscale*, 6(15), 8754–8761. <https://doi.org/10.1039/c4nr01927j>.
- Shim, M. S., & Kwon, Y. J. (2012). Stimuli-responsive polymers and nanomaterials for gene delivery and imaging applications. *Advanced Drug Delivery Reviews*, 64(11), 1046–1059. <https://doi.org/10.1016/j.addr.2012.01.018>.
- Shokeen, M., Zheleznyak, A., Wilson, J. M., et al. (2012). Molecular imaging of very late antigen-4 ($\alpha 4\beta 1$ Integrin) in the premetastatic niche. *Journal of Nuclear Medicine*, 53, 779–786. <https://doi.org/10.2967/jnumed.111.100073>.
- Siegel, R., Miller, K., & Jemal, A. (2017). Cancer statistics, 2017. *CA: a Cancer Journal for Clinicians*, 67(1), 7–30. <https://doi.org/10.3322/caac.21254>.
- Singh, D. Q., Minz, A. P., & Sahoo, S. K. (2017). Nanomedicine-mediated drug targeting of cancer stem cells. *Drug Discovery Today*, 22(6), 952–959. <https://doi.org/10.1016/j.drudis.2017.04.005>.
- Sleeman, J. P., Cady, B., & Pantel, K. (2012). The connectivity of lymphogenous and hematogenous tumor cell dissemination: biological insights and clinical implications. *Clinical & Experimental Metastasis*, 29(7), 737–746. <https://doi.org/10.1007/s10585-012-9489-x>.
- Sleeman, J. P., & Thiele, W. (2009). Tumor metastasis and the lymphatic vasculature. *International Journal of Cancer*, 125(12), 2747–2756. <https://doi.org/10.1002/ijc.24702>.
- Sneider, A., VanDyke, D., Paliwal, S., & Rai, P. (2017). Remotely triggered nano-theranostics for cancer applications. *Nanotheranostics*, 1(1), 1–22. <https://doi.org/10.1038/nbt.3121.ChIP-nexus>.
- Solinas, G., Schiarea, S., Liguori, M., et al. (2010). Tumor-conditioned macrophages secrete migration-stimulating factor: a new marker for M2-polarization, influencing tumor cell motility. *Journal of Immunology*, 185(1), 642–652. <https://doi.org/10.4049/jimmunol.1000413>.
- Sonali, Singh, R. P., Sharma, G., et al. (2016). RGD-TPGS decorated theranostic liposomes for brain targeted delivery. *Colloids and Surfaces B, Biointerfaces*, 147, 129–141. <https://doi.org/10.1016/j.colsurfb.2016.07.058>.
- Soroceanu, L., Gillespie, Y., Khazaeli, M. B., & Sontheimer, H. (1998). Use of chlorotoxin for targeting of primary brain tumors. *Cancer Research*, 58(21), 4871–4879. <http://cancerres.aacrjournals.org/content/58/21/4871.short>.

- Sounni, N. E., & Noel, A. (2013). Targeting the tumor microenvironment for cancer therapy. *Clinical Chemistry*, 59(1), 85–93. <https://doi.org/10.1373/clinchem.2012.185363>.
- Steg, A. D., Katre, A. A., Goodman, B., et al. (2012). Targeting the notch ligand Jagged1 in both tumor cells and stroma in ovarian cancer. *Clinical Cancer Research*, 17(17), 5674–5685. <https://doi.org/10.1158/1078-0432.CCR-11-0432.Targeting>.
- Steinbichler, T. B., Dudás, J., Riechelmann, H., & Skvortsova, I. I. (2017). The role of exosomes in cancer metastasis. *Seminars in Cancer Biology*, 44, 170–181. <https://doi.org/10.1016/j.semcancer.2017.02.006>.
- Sugiura, H., Fujiwara, Y., Ando, M., Kawai, A., et al. (2010). Multicenter phase II trial assessing effectiveness of imatinib mesylate on relapsed or refractory KIT-positive or PDGFR-positive sarcoma. *Journal of Orthopaedic Science*, 15(5), 654–660. <https://doi.org/10.1007/s00776-010-1506-9>.
- Sun, C., Fang, C., Stephen, Z., et al. (2008). Tumor-targeted drug delivery and MRI contrast enhancement by chlorotoxin-conjugated iron oxide nanoparticles. *Nanomedicine*, 3(4), 495–505. <https://doi.org/10.2217/17435889.3.4.495>.
- Sun, N., Wang, J., Ji, L., et al. (2015). A cellular compatible chitosan nanoparticle surface for isolation and in situ culture of rare number CTCs. *Small*, 11(40), 5444–5451. <https://doi.org/10.1002/sml.201501718>.
- Swain, S., Sahu, P. K., Beg, S., & Babu, S. M. (2016). Nanoparticles for cancer targeting: current and future directions. *Current Drug Delivery*, 13(8), 1290–1302.
- Takeishi, S., Matsumoto, A., Onoyama, I., Naka, K., Hirao, A., & Nakayama, K. I. (2013). Ablation of Fbxw7 eliminates leukemia-initiating cells by preventing quiescence. *Cancer Cell*, 23(3), 347–361. <https://doi.org/10.1016/j.ccr.2013.01.026>.
- Taketo, M. M. (2011). Reflections on the spread of metastasis to cancer prevention. *Cancer Prevention Research (Philadelphia, PA)*, 4(3), 324–328. <https://doi.org/10.1158/1940-6207.CAPR-11-0046>.
- Tang, J., Zhou, H., Liu, J., et al. (2017). Dual-mode imaging-guided synergistic chemo- and magnetohyperthermia therapy in a versatile nanoplatform to eliminate cancer stem cells. *ACS Applied Materials & Interfaces*, 9(28), 23497–23507. <https://doi.org/10.1021/acsami.7b06393>.
- Tennant, D. A., Durán, R. V., & Gottlieb, E. (2010). Targeting metabolic transformation for cancer therapy. *Nature Reviews Cancer*, 10(4), 267–277. <https://doi.org/10.1038/nrc2817>.
- Thakor, A. S., & Gambhir, S. S. (2013). Nanooncology: the future of cancer diagnosis and therapy. *CA: a Cancer Journal for Clinicians*, 63(6), 395–418. <https://doi.org/10.3322/caac.21199>.
- Tomei, A. A., Siegart, S., Britschgi, M. R., Luther, S. A., & Swartz, M. A. (2009). Fluid flow regulates stromal cell organization and CCL21 expression in a tissue-engineered lymph node microenvironment. *Journal of Immunology*, 183(7), 4273–4283. <https://doi.org/10.4049/jimmunol.0900835>.
- Trevaskis, N. L., Kaminskas, L. M., & Porter, C. J. H. (2015). From sewer to saviour—targeting the lymphatic system to promote drug exposure and activity. *Nature Reviews Drug Discovery*, 14(11), 781–803. <https://doi.org/10.1038/nrd4608>.
- Tsai, J. H., & Yang, J. (2013). Epithelial-mesenchymal plasticity in carcinoma metastasis. *Genes & Development*, 27(20), 2192–2206. <https://doi.org/10.1101/gad.225334.113>.
- Tseng, Y. C., Xu, Z., Guley, K., Yuan, H., & Huang, L. (2014). Lipid-calcium phosphate nanoparticles for delivery to the lymphatic system and SPECT/CT imaging of lymph node metastases. *Biomaterials*, 35(16), 4688–4698. <https://doi.org/10.1016/j.biomaterials.2014.02.030>.
- Tsujimoto, H., Morimoto, Y., Takahata, R., et al. (2015). Theranostic photosensitive nanoparticles for lymph node metastasis of gastric cancer. *Annals of Surgical Oncology*, 22(December), 923–928. <https://doi.org/10.1245/s10434-015-4594-0>.
- Tu, Y., Gao, X., Li, G., et al. (2013). MicroRNA-218 inhibits glioma invasion, migration, proliferation, and cancer stem-like cell self-renewal by targeting the polycomb group gene Bmi1. *Cancer Research*, 73(19), 6046–6055. <https://doi.org/10.1158/0008-5472.CAN-13-0358>.
- Van Cutsem, E., Cervantes, A., Adam, R., et al. (2016). ESMO consensus guidelines for the management of patients with metastatic colorectal cancer. *Annals of Oncology*, 27(8), 1386–1422.
- Van Zijl, F., Krupitza, G., & Mikulits, W. (2011). Initial steps of metastasis: cell invasion and endothelial transmigration. *Mutation Research, Reviews in Mutation Research*, 728(1–2), 23–34. <https://doi.org/10.1016/j.mrrev.2011.05.002>.
- Vaupel, P., Kallinowski, F., & Okunieff, P. (1989). Blood flow, oxygen and nutrient supply, and metabolic microenvironment human tumors: a review. *Cancer Research*, 49(23), 6449–6465.

- Veisoh, O., Gunn, J. W., Kievit, F. M., et al. (2009). Inhibition of tumor-cell invasion with chlorotoxin-bound superparamagnetic nanoparticles. *Small*, 5(2), 256–264. <https://doi.org/10.1002/sml.200800646>.
- Veisoh, O., Kievit, F. M., Ellenbogen, R. G., & Zhang, M. (2011). Cancer cell invasion: treatment and monitoring opportunities in nanomedicine. *Advanced Drug Delivery Reviews*, 63(8), 582–596. <https://doi.org/10.1016/j.addr.2011.01.010>.
- Völkel, T., Hölig, P., Merdan, T., Müller, R., & Kontermann, R. E. (2004). Targeting of immunoliposomes to endothelial cells using a single-chain Fv fragment directed against human endoglin (CD105). *Biochimica et Biophysica Acta, Biomembranes*, 1663(1–2), 158–166. <https://doi.org/10.1016/j.bbmem.2004.03.007>.
- Wan, L., Pantel, K., & Kang, Y. (2013). Tumor metastasis: moving new biological insights into the clinic. *Nature Medicine*, 19(11), 1450–1464. <https://doi.org/10.1038/nm.3391>.
- Wang, A. Z., Langer, R., & Farokhzad, O. C. (2012). Nanoparticle delivery of cancer drugs. *Annual Review of Medicine*, 63(1), 185–198. <https://doi.org/10.1146/annurev-med-040210-162544>.
- Wang, S., Zhang, Q., Yang, P., et al. (2016). Manganese oxide-coated carbon nanotubes as dual-modality lymph mapping agents for photothermal therapy of tumor metastasis. *ACS Applied Materials & Interfaces*, 8(6), 3736–3743. <https://doi.org/10.1021/acsami.5b08087>.
- Weber, G. F. (2008). Molecular mechanisms of metastasis. *Cancer Letters*, 270(2), 181–190. <https://doi.org/10.1016/j.canlet.2008.04.030>.
- Weidle, U. H., Birzele, F., Kollmorgen, G., & Rügger, R. (2017). The multiple roles of exosomes in metastasis. *Cancer Genomics & Proteomics*, 14(1), 1–16. <https://doi.org/10.21873/cgp.20015>.
- Weis, S. M., & Cheresch, D. A. (2011). Tumor angiogenesis: molecular pathways and therapeutic targets. *Nature Medicine*, 17(11), 1359–1370. <https://doi.org/10.1038/nm.2537>.
- West, K. R., & Otto, S. (2005). Reversible covalent chemistry in drug delivery. *Current Drug Discovery Technologies*, 2(3), 123–160. <https://doi.org/10.2174/1570163054866882>.
- WHO. (2017). *Cancer*. Geneva, Switzerland: WHO. <http://www.who.int/topics/cancer/en/>.
- Wilhelm, S., Tavares, A. J., Dai, Q., et al. (2016). Analysis of nanoparticle delivery to tumours. *Nature Reviews Materials*, 1, 1–12. <https://doi.org/10.1038/natrevmats.2016.14>.
- Wong, C.C.-L., Gilkes, D. M., Zhang, H., et al. (2011). Hypoxia-inducible factor 1 is a master regulator of breast cancer metastatic niche formation. *Proceedings of the National Academy of Sciences of the United States of America*, 108(39), 16369. <https://doi.org/10.1073/pnas.1113483108>.
- Wong, C. W., Lee, A., Shientag, L., et al. (2001). Apoptosis: an early event in metastatic inefficiency. *Cancer Research*, 61(1), 333–338.
- Xie, J., Gao, Y., Zhao, R., et al. (2015). Ex vivo and in vivo capture and deactivation of circulating tumor cells by dual-antibody-coated nanomaterials. *Journal of Controlled Release*, 209, 159–169. <https://doi.org/10.1016/j.jconrel.2015.04.036>.
- Xing, F., Saidou, J., & Watabe, K. (2010). Cancer associated fibroblasts (CAFs) in tumor microenvironment. *Frontiers in Bioscience*, 15, 166–179.
- Yamamoto, M., Kikuchi, H., Ohta, M., et al. (2008). TSU68 prevents liver metastasis of colon cancer xenografts by modulating the premetastatic niche. *Cancer Research*, 68(23), 9754–9762. <https://doi.org/10.1158/0008-5472.CAN-08-1748>.
- Yang, L., Cheng, J., Chen, Y., et al. (2017). Phase-transition nanodroplets for real-time photoacoustic/ultrasound dual-modality imaging and photothermal therapy of sentinel lymph node in breast cancer. *Scientific Reports*, 7(March), 45213. <https://doi.org/10.1038/srep45213>.
- Yang, X., Hong, H., Grailler, J. J., et al. (2011). CRGD-functionalized, DOX-conjugated, and 64Cu-labeled superparamagnetic iron oxide nanoparticles for targeted anticancer drug delivery and PET/MR imaging. *Biomaterials*, 32(17), 4151–4160. <https://doi.org/10.1016/j.biomaterials.2011.02.006>.
- Yang, N., Jiang, Y., Zhang, H., et al. (2015). Active targeting docetaxel-PLA nanoparticles eradicate circulating lung cancer stem-like cells and inhibit liver metastasis. *Molecular Pharmaceutics*, 12(1), 232–239. <https://doi.org/10.1021/mp500568z>.
- Yigit, M. V., Ghosh, S. K., Kumar, M., et al. (2013). Context-dependent differences in miR-10b breast oncogenesis can be targeted for the prevention and arrest of lymph node metastasis. *Oncogene*, 32, 1530–1538.
- Yin, J., Hui, X., Yao, L., et al. (2015). Evaluation of Tc-99 m labeled dimeric GX1 peptides for imaging of colorectal cancer vasculature. *Molecular Imaging and Biology*, 17(5), 661–670. <https://doi.org/10.1007/s11307-015-0838-4>.

- Yoon, H. J., Kozminsky, M., & Nagrath, S. (2014). Emerging role of nanomaterials in circulating tumor cell isolation and analysis. *American Chemical Society*, 8(3), 1995–2017. <https://doi.org/10.1021/nn5004277>.
- Yu, J., Chen, Y., Zhang, Y., et al. (2014). pH-responsive and near-infrared-emissive polymer nanoparticles for simultaneous delivery, release, and fluorescence tracking of doxorubicin in vivo. *Chemical Communications (Cambridge, England)*, 50(36), 4699–4702. <https://doi.org/10.1039/c3cc49870k>.
- Zhang, D., Feng, X. Y., Henning, T. D., et al. (2009). MR imaging of tumor angiogenesis using sterically stabilized Gd-DTPA liposomes targeted to CD105. *European Journal of Radiology*, 70(1), 180–189. <https://doi.org/10.1016/j.ejrad.2008.04.022>.
- Zhang, S., Gong, M., Zhang, D., Yang, H., Gao, F., & Zou, L. (2014). Thiol-PEG-carboxyl-stabilized Fe₂O₃/Au nanoparticles targeted to CD105: synthesis, characterization and application in MR imaging of tumor angiogenesis. *European Journal of Radiology*, 83(7), 1190–1198. <https://doi.org/10.1016/j.ejrad.2014.03.034>.
- Zhou, M., Zhao, J., Tian, M., et al. (2015). Radio-photothermal therapy mediated by a single compartment nanoplatform depletes tumor initiating cells and reduces lung metastasis in the orthotopic 4T1 breast tumor model. *Nanoscale*, 7(46), 19438–19447. <https://doi.org/10.1039/C5NR04587H>.
- Zhu, J., Fu, F., Xiong, Z., Shen, M., & Shi, X. (2015). Dendrimer-entrapped gold nanoparticles modified with RGD peptide and alpha-tocopheryl succinate enable targeted theranostics of cancer cells. *Colloids and Surfaces B, Biointerfaces*, 133, 36–42. <https://doi.org/10.1016/j.colsurfb.2015.05.040>.
- Zhu, L., Kate, P., & Torchilin, V. P. (2012). Matrix metalloprotease 2-responsive multifunctional liposomal nanocarrier for enhanced tumor targeting. *ACS Nano*, 6(4), 3491–3498. <https://doi.org/10.1021/nn300524f>.
- Zhu, L., Zhou, Z., Mao, H., & Yang, L. (2017). Magnetic nanoparticles for precision oncology: theranostic magnetic iron oxide nanoparticles for image-guided and targeted cancer therapy. *Nanomedicine*, 12(1), 73–87. <https://doi.org/10.2217/nnm-2016-0316>.
- Zolata, H., Abbasi Davani, F., & Afarideh, H. (2015). Synthesis, characterization and theranostic evaluation of indium-111 labeled multifunctional superparamagnetic iron oxide nanoparticles. *Nuclear Medicine and Biology*, 42(2), 164–170. <https://doi.org/10.1016/j.nucmedbio.2014.09.007>.
- Zou, Z., He, X., He, D., et al. (2015). Programmed packaging of mesoporous silica nanocarriers for matrix metalloprotease 2-triggered tumor targeting and release. *Biomaterials*, 58, 35–45. <https://doi.org/10.1016/j.biomaterials.2015.04.034>.
- Zou, P., Yu, Y., Wang, Y. A., et al. (2010). Superparamagnetic iron oxide nanotheranostics for targeted cancer cell imaging and pH-dependent intracellular drug release. *Molecular Pharmaceutics*, 7(6), 1974–1984.

Aug 25, 2020

This Agreement between Miss. Abi Judit Vázquez Ríos ("You") and Elsevier ("Elsevier") consists of your license details and the terms and conditions provided by Elsevier and Copyright Clearance Center.

License Number	4896190345487
License date	Aug 25, 2020
Licensed Content Publisher	Elsevier
Licensed Content Publication	Elsevier Books
Licensed Content Title	Handbook of Nanomaterials for Cancer Theranostics
Licensed Content Author	Abi Judit Vázquez-Ríos, Marta Alonso-Nocelo, Belén López Bouzo, Juan Ruiz-Bañobre, María de la Fuente
Licensed Content Date	Jan 1, 2018
Licensed Content Pages	46
Start Page	199
End Page	244
Type of Use	reuse in a thesis/dissertation

I am an academic or government institution with a full-

text subscription to this journal and the audience of the material consists of students and/or employees of this institute?	No
Portion	full chapter
Circulation	8
Format	both print and electronic
Are you the author of this Elsevier chapter?	Yes
Will you be translating?	No
Title	Development of a targeted therapeutic strategy for metastatic lung cancer
Institution name	USC
Expected presentation date	Sep 2020
Requestor Location	Miss. Abi Judit Vázquez Ríos Hospital Clínico Universitario Edificio C. Sótano -2. Lab 13
Publisher Tax ID	GB 494 6272 12
Billing Type	Invoice
Billing Address	Miss. Abi Judit Vázquez Ríos Hospital Clínico Universitario Edificio C. Sótano -2. Lab 13
	Santiago de Compostela, Spain 15706

Total 0.00 EUR

Terms and Conditions

INTRODUCTION

1. The publisher for this copyrighted material is Elsevier. By clicking "accept" in connection with completing this licensing transaction, you agree that the following terms and conditions apply to this transaction (along with the Billing and Payment terms and conditions established by Copyright Clearance Center, Inc. ("CCC"), at the time that you opened your Rightslink account and that are available at any time at <http://myaccount.copyright.com>).

GENERAL TERMS

2. Elsevier hereby grants you permission to reproduce the aforementioned material subject to the terms and conditions indicated.

3. Acknowledgement: If any part of the material to be used (for example, figures) has appeared in our publication with credit or acknowledgement to another source, permission must also be sought from that source. If such permission is not obtained then that material may not be included in your publication/copies. Suitable acknowledgement to the source must be made, either as a footnote or in a reference list at the end of your publication, as follows:

"Reprinted from Publication title, Vol /edition number, Author(s), Title of article / title of chapter, Pages No., Copyright (Year), with permission from Elsevier [OR APPLICABLE SOCIETY COPYRIGHT OWNER]." Also Lancet special credit - "Reprinted from The Lancet, Vol. number, Author(s), Title of article, Pages No., Copyright (Year), with permission from Elsevier."

4. Reproduction of this material is confined to the purpose and/or media for which permission is hereby given.

5. Altering/Modifying Material: Not Permitted. However figures and illustrations may be altered/adapted minimally to serve your work. Any other abbreviations, additions, deletions and/or any other alterations shall be made only with prior written authorization of Elsevier Ltd. (Please contact Elsevier's permissions helpdesk [here](#)). No modifications can be made to any Lancet figures/tables and they must be reproduced in full.

6. If the permission fee for the requested use of our material is waived in this instance, please be advised that your future requests for Elsevier materials may attract a fee.

7. Reservation of Rights: Publisher reserves all rights not specifically granted in the combination of (i) the license details provided by you and accepted in the course of this licensing transaction, (ii) these terms and conditions and (iii) CCC's Billing and Payment terms and conditions.

8. License Contingent Upon Payment: While you may exercise the rights licensed immediately upon issuance of the license at the end of the licensing process for the

transaction, provided that you have disclosed complete and accurate details of your proposed use, no license is finally effective unless and until full payment is received from you (either by publisher or by CCC) as provided in CCC's Billing and Payment terms and conditions. If full payment is not received on a timely basis, then any license preliminarily granted shall be deemed automatically revoked and shall be void as if never granted. Further, in the event that you breach any of these terms and conditions or any of CCC's Billing and Payment terms and conditions, the license is automatically revoked and shall be void as if never granted. Use of materials as described in a revoked license, as well as any use of the materials beyond the scope of an unrevoked license, may constitute copyright infringement and publisher reserves the right to take any and all action to protect its copyright in the materials.

9. Warranties: Publisher makes no representations or warranties with respect to the licensed material.

10. Indemnity: You hereby indemnify and agree to hold harmless publisher and CCC, and their respective officers, directors, employees and agents, from and against any and all claims arising out of your use of the licensed material other than as specifically authorized pursuant to this license.

11. No Transfer of License: This license is personal to you and may not be sublicensed, assigned, or transferred by you to any other person without publisher's written permission.

12. No Amendment Except in Writing: This license may not be amended except in a writing signed by both parties (or, in the case of publisher, by CCC on publisher's behalf).

13. Objection to Contrary Terms: Publisher hereby objects to any terms contained in any purchase order, acknowledgment, check endorsement or other writing prepared by you, which terms are inconsistent with these terms and conditions or CCC's Billing and Payment terms and conditions. These terms and conditions, together with CCC's Billing and Payment terms and conditions (which are incorporated herein), comprise the entire agreement between you and publisher (and CCC) concerning this licensing transaction. In the event of any conflict between your obligations established by these terms and conditions and those established by CCC's Billing and Payment terms and conditions, these terms and conditions shall control.

14. Revocation: Elsevier or Copyright Clearance Center may deny the permissions described in this License at their sole discretion, for any reason or no reason, with a full refund payable to you. Notice of such denial will be made using the contact information provided by you. Failure to receive such notice will not alter or invalidate the denial. In no event will Elsevier or Copyright Clearance Center be responsible or liable for any costs, expenses or damage incurred by you as a result of a denial of your permission request, other than a refund of the amount(s) paid by you to Elsevier and/or Copyright Clearance Center for denied permissions.

LIMITED LICENSE

The following terms and conditions apply only to specific license types:

15. **Translation:** This permission is granted for non-exclusive world **English** rights only unless your license was granted for translation rights. If you licensed translation rights you may only translate this content into the languages you requested. A professional translator must perform all translations and reproduce the content word for word preserving the integrity of the article.

16. Posting licensed content on any Website: The following terms and conditions apply as follows: Licensing material from an Elsevier journal: All content posted to the web site must maintain the copyright information line on the bottom of each image; A hyper-text must be included to the Homepage of the journal from which you are licensing at <http://www.sciencedirect.com/science/journal/xxxxx> or the Elsevier homepage for books at <http://www.elsevier.com>; Central Storage: This license does not include permission for a scanned version of the material to be stored in a central repository such as that provided by Heron/XanEdu.

Licensing material from an Elsevier book: A hyper-text link must be included to the Elsevier homepage at <http://www.elsevier.com> . All content posted to the web site must maintain the copyright information line on the bottom of each image.

Posting licensed content on Electronic reserve: In addition to the above the following clauses are applicable: The web site must be password-protected and made available only to bona fide students registered on a relevant course. This permission is granted for 1 year only. You may obtain a new license for future website posting.

17. For journal authors: the following clauses are applicable in addition to the above:

Preprints:

A preprint is an author's own write-up of research results and analysis, it has not been peer-reviewed, nor has it had any other value added to it by a publisher (such as formatting, copyright, technical enhancement etc.).

Authors can share their preprints anywhere at any time. Preprints should not be added to or enhanced in any way in order to appear more like, or to substitute for, the final versions of articles however authors can update their preprints on arXiv or RePEc with their Accepted Author Manuscript (see below).

If accepted for publication, we encourage authors to link from the preprint to their formal publication via its DOI. Millions of researchers have access to the formal publications on ScienceDirect, and so links will help users to find, access, cite and use the best available version. Please note that Cell Press, The Lancet and some society-owned have different preprint policies. Information on these policies is available on the journal homepage.

Accepted Author Manuscripts: An accepted author manuscript is the manuscript of an article that has been accepted for publication and which typically includes author-incorporated changes suggested during submission, peer review and editor-author communications.

Authors can share their accepted author manuscript:

- immediately
 - via their non-commercial person homepage or blog
 - by updating a preprint in arXiv or RePEc with the accepted manuscript
 - via their research institute or institutional repository for internal institutional uses or as part of an invitation-only research collaboration work-group
 - directly by providing copies to their students or to research collaborators for their personal use
 - for private scholarly sharing as part of an invitation-only work group on commercial sites with which Elsevier has an agreement
- After the embargo period

- via non-commercial hosting platforms such as their institutional repository
- via commercial sites with which Elsevier has an agreement

In all cases accepted manuscripts should:

- link to the formal publication via its DOI
- bear a CC-BY-NC-ND license - this is easy to do
- if aggregated with other manuscripts, for example in a repository or other site, be shared in alignment with our hosting policy not be added to or enhanced in any way to appear more like, or to substitute for, the published journal article.

Published journal article (JPA): A published journal article (PJA) is the definitive final record of published research that appears or will appear in the journal and embodies all value-adding publishing activities including peer review co-ordination, copy-editing, formatting, (if relevant) pagination and online enrichment.

Policies for sharing publishing journal articles differ for subscription and gold open access articles:

Subscription Articles: If you are an author, please share a link to your article rather than the full-text. Millions of researchers have access to the formal publications on ScienceDirect, and so links will help your users to find, access, cite, and use the best available version.

Theses and dissertations which contain embedded PJAs as part of the formal submission can be posted publicly by the awarding institution with DOI links back to the formal publications on ScienceDirect.

If you are affiliated with a library that subscribes to ScienceDirect you have additional private sharing rights for others' research accessed under that agreement. This includes use for classroom teaching and internal training at the institution (including use in course packs and courseware programs), and inclusion of the article for grant funding purposes.

Gold Open Access Articles: May be shared according to the author-selected end-user license and should contain a [CrossMark logo](#), the end user license, and a DOI link to the formal publication on ScienceDirect.

Please refer to Elsevier's [posting policy](#) for further information.

18. **For book authors** the following clauses are applicable in addition to the above: Authors are permitted to place a brief summary of their work online only. You are not allowed to download and post the published electronic version of your chapter, nor may you scan the printed edition to create an electronic version. **Posting to a repository:** Authors are permitted to post a summary of their chapter only in their institution's repository.

19. **Thesis/Dissertation:** If your license is for use in a thesis/dissertation your thesis may be submitted to your institution in either print or electronic form. Should your thesis be published commercially, please reapply for permission. These requirements include permission for the Library and Archives of Canada to supply single copies, on demand, of the complete thesis and include permission for Proquest/UMI to supply single copies, on demand, of the complete thesis. Should your thesis be published commercially, please reapply for permission. Theses and dissertations which contain embedded PJAs as part of the formal submission can be posted publicly by the awarding institution with DOI links back to the formal publications on ScienceDirect.

Elsevier Open Access Terms and Conditions

You can publish open access with Elsevier in hundreds of open access journals or in nearly 2000 established subscription journals that support open access publishing. Permitted third party re-use of these open access articles is defined by the author's choice of Creative Commons user license. See our [open access license policy](#) for more information.

Terms & Conditions applicable to all Open Access articles published with Elsevier:

Any reuse of the article must not represent the author as endorsing the adaptation of the article nor should the article be modified in such a way as to damage the author's honour or reputation. If any changes have been made, such changes must be clearly indicated.

The author(s) must be appropriately credited and we ask that you include the end user license and a DOI link to the formal publication on ScienceDirect.

If any part of the material to be used (for example, figures) has appeared in our publication with credit or acknowledgement to another source it is the responsibility of the user to ensure their reuse complies with the terms and conditions determined by the rights holder.

Additional Terms & Conditions applicable to each Creative Commons user license:

CC BY: The CC-BY license allows users to copy, to create extracts, abstracts and new works from the Article, to alter and revise the Article and to make commercial use of the Article (including reuse and/or resale of the Article by commercial entities), provided the user gives appropriate credit (with a link to the formal publication through the relevant DOI), provides a link to the license, indicates if changes were made and the licensor is not represented as endorsing the use made of the work. The full details of the license are available at <http://creativecommons.org/licenses/by/4.0>.

CC BY NC SA: The CC BY-NC-SA license allows users to copy, to create extracts, abstracts and new works from the Article, to alter and revise the Article, provided this is not done for commercial purposes, and that the user gives appropriate credit (with a link to the formal publication through the relevant DOI), provides a link to the license, indicates if changes were made and the licensor is not represented as endorsing the use made of the work. Further, any new works must be made available on the same conditions. The full details of the license are available at <http://creativecommons.org/licenses/by-nc-sa/4.0>.

CC BY NC ND: The CC BY-NC-ND license allows users to copy and distribute the Article, provided this is not done for commercial purposes and further does not permit distribution of the Article if it is changed or edited in any way, and provided the user gives appropriate credit (with a link to the formal publication through the relevant DOI), provides a link to the license, and that the licensor is not represented as endorsing the use made of the work. The full details of the license are available at <http://creativecommons.org/licenses/by-nc-nd/4.0>. Any commercial reuse of Open Access articles published with a CC BY NC SA or CC BY NC ND license requires permission from Elsevier and will be subject to a fee.

Commercial reuse includes:

- Associating advertising with the full text of the Article
- Charging fees for document delivery or access
- Article aggregation
- Systematic distribution via e-mail lists or share buttons

Posting or linking by commercial companies for use by customers of those companies.

20. Other Conditions:

v1.10

Questions? customer care@copyright.com or +1-855-239-3415 (toll free in the US) or +1-978-646-2777.



<https://jnanobiotechnology.biomedcentral.com/articles/10.1186/s12951-019-0517-8>





<https://pubmed.ncbi.nlm.nih.gov/29182542/>





<https://www.ncbi.nlm.nih.gov/pmc/articles/PMC7076701/>





(12) INTERNATIONAL APPLICATION PUBLISHED UNDER THE PATENT COOPERATION TREATY (PCT)

(19) World Intellectual Property
Organization
International Bureau(43) International Publication Date
18 July 2019 (18.07.2019)

WIPO | PCT

(10) International Publication Number
WO 2019/138140 A1

(51) International Patent Classification:

G01N 33/574 (2006.01) A61K 31/00 (2006.01)

(21) International Application Number:

PCT/EP2019/050981

(22) International Filing Date:

15 January 2019 (15.01.2019)

(25) Filing Language:

English

(26) Publication Language:

English

(30) Priority Data:

18382013.3 15 January 2018 (15.01.2018) EP

(71) Applicants: **FUNDACIÓN INSTITUTO DE INVESTIGACIÓN SANITARIA DE SANTIAGO DE COMPOSTELA (FIDIS)** [ES/ES]; TRAVESA DA CHOUPANA, S/N, 15706 Santiago de Compostela (ES). **SERVIZO GALEGO DE SAÚDE** [ES/ES]; Edificio Administrativo de San Lázaro, s/n, 15703 Santiago de Compostela (ES).

(72) Inventors: **DE LA FUENTE FREIRE, María**; SERVIZO GALEGO DE SAÚDE, TRAVESA DA CHOUPANA, S/N, 15706 Santiago de Compostela (ES). **LÓPEZ LÓPEZ, Rafael**; SERVIZO GALEGO DE SAÚDE, TRAVESA DA CHOUPANA, S/N, 15706 Santiago de Compostela (ES). **ALONSO NOCELO, Marta**; FUNDACIÓN PARA A INVESTIGACIÓN, DESENVOLVEMENTO E INNOVACIÓN RAMÓN DOMÍNGUEZ, TRAVESA DA CHOUPANA, S/N, 15706 Santiago de Compostela (ES). **VÁZQUEZ RÍOS, Abi Judit**; FUNDACIÓN PARA A INVESTIGACIÓN, DESENVOLVEMENTO E INNOVACIÓN RAMÓN DOMÍNGUEZ, TRAVESA DA CHOUPANA, S/N, 15706 SANTIAGO DE COMPOSTELA (ES).

(74) Agent: **HOFFMANN EITLE S.L.U.**; Paseo de la Castellana 140, Planta 3ª, Edificio Lima., 28046 Madrid (ES).

(81) Designated States (unless otherwise indicated, for every kind of national protection available): AE, AG, AL, AM, AO, AT, AU, AZ, BA, BB, BG, BH, BN, BR, BW, BY, BZ, CA, CH, CL, CN, CO, CR, CU, CZ, DE, DJ, DK, DM, DO,

DZ, EC, EE, EG, ES, FI, GB, GD, GE, GH, GM, GT, HN, HR, HU, ID, IL, IN, IR, IS, JO, JP, KE, KG, KH, KN, KP, KR, KW, KZ, LA, LC, LK, LR, LS, LU, LY, MA, MD, ME, MG, MK, MN, MW, MX, MY, MZ, NA, NG, NI, NO, NZ, OM, PA, PE, PG, PH, PL, PT, QA, RO, RS, RU, RW, SA, SC, SD, SE, SG, SK, SL, SM, ST, SV, SY, TH, TJ, TM, TN, TR, TT, TZ, UA, UG, US, UZ, VC, VN, ZA, ZM, ZW.

(84) Designated States (unless otherwise indicated, for every kind of regional protection available): ARIPO (BW, GH, GM, KE, LR, LS, MW, MZ, NA, RW, SD, SL, ST, SZ, TZ, UG, ZM, ZW), Eurasian (AM, AZ, BY, KG, KZ, RU, TJ, TM), European (AL, AT, BE, BG, CH, CY, CZ, DE, DK, EE, ES, FI, FR, GB, GR, HR, HU, IE, IS, IT, LT, LU, LV, MC, MK, MT, NL, NO, PL, PT, RO, RS, SE, SI, SK, SM, TR), OAPI (BF, BJ, CF, CG, CI, CM, GA, GN, GQ, GW, KM, ML, MR, NE, SN, TD, TG).

Published:

- with international search report (Art. 21(3))
- with sequence listing part of description (Rule 5.2(a))

(54) Title: USE OF THE TASIR3 PROTEIN AS A MARKER FOR THERAPEUTIC, DIAGNOSTIC, AND/OR PROGNOSTIC PURPOSES FOR TUMORS THAT EXPRESS SAID PROTEIN

(57) Abstract: In the present invention, the use of the TASIR3 receptor as a biomarker for application in cancer diagnosis, monitoring, and therapy is described for the first time. In this sense, the authors of the present invention have demonstrated that TASIR3 is a biomarker of interest in oncology, useful for the diagnosis of the disease, and capable of providing relevant information thereupon, to monitor the evolution, select the treatment, and selectively direct therapeutic molecules. It has been determined that it is possible to identify therapies against this receptor, and that it is also possible to direct conjugates and controlled release systems of drugs, such as nanoparticles, observing a very effective intracellular accumulation thereof in primary, disseminated and metastatic tumor cells. On the other hand, the presence of TASIR3 in circulating tumor cells (CTCs) has also been demonstrated. These are tumor cells released into the bloodstream by the primary tumor and are considered key factors in the creation of metastases, so that their detection in early stages will serve as an early detector of metastasis, and are also useful in monitoring the disease and evaluating of the response to drugs.



(12) INTERNATIONAL APPLICATION PUBLISHED UNDER THE PATENT COOPERATION TREATY (PCT)

(19) World Intellectual Property
Organization
International Bureau



(43) International Publication Date
18 July 2019 (18.07.2019)

WIPO | PCT

(10) International Publication Number
WO 2019/138139 A1

(51) International Patent Classification:

A61K 9/107 (2006.01) A61K 47/44 (2017.01)
A61K 47/10 (2017.01) A61K 49/00 (2006.01)
A61K 47/12 (2006.01) A61K 49/10 (2006.01)
A61K 47/14 (2017.01) A61K 49/18 (2006.01)

(21) International Application Number:

PCT/EP2019/050979

(22) International Filing Date:

15 January 2019 (15.01.2019)

(25) Filing Language:

English

(26) Publication Language:

English

(30) Priority Data:

18382012.5 15 January 2018 (15.01.2018) EP

(71) Applicants: **FUNDACIÓN INSTITUTO DE INVESTIGACIÓN SANITARIA DE SANTIAGO DE COMPOSTELA (FIDIS)** [ES/ES]; TRAVESA DA CHOUPANA, S/N, 15706 Santiago de Compostela (ES). **SERVIZO GALEGO DE SAÚDE** [ES/ES]; EDIFICIO ADMINISTRATIVO SAN LÁZARO, S/N, 15703 SANTIAGO DE COMPOSTELA (ES).

(72) Inventors: **DE LA FUENTE FREIRE, María**; SERVIZO GALEGO DE SAÚDE, EDIFICIO ADMINISTRATIVO SAN LÁZARO, S/N, 15703 Santiago de Compostela (ES). **LÓPEZ LÓPEZ, Rafael**; SERVIZO GALEGO DE SAÚDE, EDIFICIO ADMINISTRATIVO SAN LÁZARO, S/N, 15703 SANTIAGO DE COMPOSTELA (ES). **LÓPEZ BOUZO, Belén**; FUNDACIÓN PARA A INVESTIGACIÓN, DESENVOLVEMENTO E INNOVACIÓN RAMÓN DOMÍNGUEZ, TRAVESA DA CHOUPANA, S/N, 15706 Santiago de Compostela (ES). **VÁZQUEZ RÍOS, Abi Judit**; FUNDACIÓN PARA A INVESTIGACIÓN, DESENVOLVEMENTO E INNOVACIÓN RAMÓN DOMÍNGUEZ, TRAVESA DA CHOUPANA, S/N, 15706 Santiago de Compostela (ES). **ALONSO NOCELO, Marta**; FUNDACIÓN PARA A INVESTIGACIÓN, DESENVOLVEMENTO E INNOVACIÓN RAMÓN DOMÍNGUEZ, TRAVESA DA CHOUPANA, S/N, 15706 Santiago de Compostela (ES).

(74) Agent: **HOFFMANN EITLE S.L.U.**; Paseo de la Castellana 140, Planta 3ª, Edificio Lima, 28046 Madrid (ES).

(81) Designated States (*unless otherwise indicated, for every kind of national protection available*): AE, AG, AL, AM, AO, AT, AU, AZ, BA, BB, BG, BH, BN, BR, BW, BY, BZ, CA, CH, CL, CN, CO, CR, CU, CZ, DE, DJ, DK, DM, DO, DZ, EC, EE, EG, ES, FI, GB, GD, GE, GH, GM, GT, HN, HR, HU, ID, IL, IN, IR, IS, JO, JP, KE, KG, KH, KN, KP, KR, KW, KZ, LA, LC, LK, LR, LS, LU, LY, MA, MD, ME, MG, MK, MN, MW, MX, MY, MZ, NA, NG, NI, NO, NZ, OM, PA, PE, PG, PH, PL, PT, QA, RO, RS, RU, RW, SA, SC, SD, SE, SG, SK, SL, SM, ST, SV, SY, TH, TJ, TM, TN, TR, TT, TZ, UA, UG, US, UZ, VC, VN, ZA, ZM, ZW.

(84) Designated States (*unless otherwise indicated, for every kind of regional protection available*): ARIPO (BW, GH, GM, KE, LR, LS, MW, MZ, NA, RW, SD, SL, ST, SZ, TZ, UG, ZM, ZW), Eurasian (AM, AZ, BY, KG, KZ, RU, TJ, TM), European (AL, AT, BE, BG, CH, CY, CZ, DE, DK, EE, ES, FI, FR, GB, GR, HR, HU, IE, IS, IT, LT, LU, LV, MC, MK, MT, NL, NO, PL, PT, RO, RS, SE, SI, SK, SM, TR), OAPI (BF, BJ, CF, CG, CI, CM, GA, GN, GQ, GW, KM, ML, MR, NE, SN, TD, TG).

Published:

- with international search report (Art. 21(3))
- with sequence listing part of description (Rule 5.2(a))

(54) Title: NANOSYSTEMS AS SELECTIVE VEHICLES

(57) Abstract: In the present invention, the development of various oil-in-water (O/W) nanoemulsions containing an oil phase or oil core, preferably selected from vitamin E or oleic acid, stabilized by a sphingolipid of the sphingomyelin type, and optionally other lipids such as phospholipids, cholesterol, octadecylamine, DOTAP (N-[1-(2,3-Dioleoyloxy)propyl]-N,N,N-trimethylammonium methyl-sulfate), and PEGylated derivatives (derivatives with polyethylene glycol), for use as a nanotech vehicle, in particular for the management of cancer and metastatic disease, is herein described. Said nanoemulsions can be functionalized with ligands capable of interacting or binding to receptors expressed on the cell membrane of tumor cells, and in particular capable of interacting or binding to receptors expressed on the membrane of primary and/or disseminated or metastatic tumor cells. Also, antitumor drugs or therapeutic biomolecules can be encapsulated in said nanoemulsions and, finally, contrast agents can be incorporated for their use in the *in vivo* diagnosis in said nanoemulsions.



WO 2019/138139 A1





DICTAMEN DEL COMITÉ AUTONÓMICO DE ÉTICA DE LA INVESTIGACIÓN DE GALICIA

Paula M. López Vázquez, Secretaria del Comité Autonomo de Ética de la Investigación de Galicia

CERTIFICA:

Que este Comité evaluó en su reunión del día 28/05/15 :

Título: Descubrimiento y desarrollo biomarcadores innovadores para medicina personalizada y terapias para el tratamiento eficaz del cáncer de pulmón

Promotor: Amadix, Advanced Marker Discovery

Tipo de estudio: EPA-SP

Version: versión 6 de marzo de 2015 y HIP/CI versión 5 de marzo de 2015

Código del Promotor: AMD-PLA-2015-01

Código de Registro: 2015/304

Y, tomando en consideración las siguientes cuestiones:

- La pertinencia del estudio, teniendo en cuenta el conocimiento disponible, así como los requisitos legales aplicables, y en particular la Ley 14/2007, de investigación biomédica, el Real Decreto 1716/2011, de 18 de noviembre, por el que se establecen los requisitos básicos de autorización y funcionamiento de los biobancos con fines de investigación biomédica y del tratamiento de las muestras biológicas de origen humano, y se regula el funcionamiento y organización del Registro Nacional de Biobancos para investigación biomédica, la ORDEN SAS/3470/2009, de 16 de diciembre, por la que se publican las Directrices sobre estudios Posautorización de Tipo Observacional para medicamentos de uso humano, y la Circular nº 07 / 2004, investigaciones clínicas con productos sanitarios.
- La idoneidad del protocolo en relación con los objetivos del estudio, justificación de los riesgos y molestias previsibles para el sujeto, así como los beneficios esperados.
- Los principios éticos de la Declaración de Helsinki vigente.
- Los Procedimientos Normalizados de Trabajo del CEIC de Galicia

Emite un **INFORME FAVORABLE** para la realización del estudio por el/la investigador/a del centro:

Centros	Investigadores Principales
C.H. Universitario de Santiago	Rafael López López



Y HACE CONSTAR QUE:

- 1 El CAEIG cumple los requisitos legales vigentes (R.D 223/2004 por el que se regulan los ensayos clínicos con medicamentos, y la Ley 14/2007 de Investigación Biomédica).
- 2 El CAEIG tanto en su composición como en sus PNTs cumple las Normas de Buena Práctica Clínica (CPMP/ICH/135/95).
- 3 La composición actual del CAEIG es:

Manuel Portela Romero. (Presidente). Médico Especialista en Medicina Familiar y Comunitaria.

Irene Zarra Ferro. (Vicepresidenta). Farmacéutica de Atención Especializada.

Paula M^a López Vázquez, (Secretaria). Médico Especialista en Farmacología Clínica.

Juan Vázquez Lago (Secretario Suplente). Médico Especialista en Medicina Preventiva y Salud Pública.

Jesús Alberdi Sudupe. Médico especialista en Psiquiatría.

Rosendo Bugarín González. Médico Especialista en Medicina Familiar y Comunitaria.

Juan Casariego Rosón. Médico Especialista en Cardiología.

Xoán X. Casas Rodríguez. Médico Especialista en Medicina Familiar y Comunitaria.

Juana M^a Cruz del Río. Trabajadora Social.

Juan Fernando Cueva Bañuelos. Médico Especialista en Oncología Médica.

José Álvaro Fernández Rial. Médico Especialista en Medicina Interna.

José Luis Fernández Trisac. Médico Especialista en Pediatría.

M^a José Ferreira Díaz. Diplomada Universitaria de Enfermería

Pablo Nimo Ríos. Licenciado en Derecho. Miembro externo

Pilar Gayoso Diz. Médico Especialista en Medicina Familiar y Comunitaria.

Agustín Pía Morandeira. Farmacéutico de Atención Primaria

Salvador Pita Fernández. Médico Especialista en Medicina Familiar y Comunitaria.

Carmen Rodríguez-Tenreiro Sánchez. Licenciada en Farmacia.

Susana María Romero Yuste. Médico Especialista en Reumatología.

M^a Asunción Verdejo González. Médico Especialista en Farmacología Clínica.

En Santiago de Compostela, a 01 de junio de 2015

Firmado digitalmente por LOPEZ VAZQUEZ PAULA MARIA - DNI
46900339G

Nombre de reconocimiento (DN): c=ES, o=XUNTA DE GALICIA,
ou=certificado electrónico de empleado público,
serialNumber=46900339G, sn=LOPEZ VAZQUEZ,
givenName=PAULA MARIA, cn=LOPEZ VAZQUEZ PAULA MARIA -
DNI 46900339G
Fecha: 2015.06.01 12:54:46 +02'00'



DICTAMEN DEL COMITÉ AUTONÓMICO DE ÉTICA DE LA INVESTIGACIÓN DE GALICIA

Paula M. López Vázquez, Secretaria del Comité Autonómico de Ética de la Investigación de Galicia,

CERTIFICA:

Que este Comité evaluó en su reunión del día 30/06/2015, la enmienda del estudio:

Título: Descubrimiento y desarrollo biomarcadores innovadores para medicina personalizada y terapias para el tratamiento eficaz del cáncer de pulmón

Versión Enmienda: *ampliación al Hospital Universitario Lucus Augusti (Sergio Vázquez Estévez)*

Tipo de estudio: EPA-SP

Promotor: *Amadix, Advanced Marker Discovery*

Código del Promotor: AMD-PLA-2015-01

Código de Registro: 2015/304

Y que este Comité acepta de conformidad con sus procedimientos normalizados de trabajo y tomando en cuenta los requisitos éticos, metodológicos y legales exigibles a los estudios de investigación con seres humanos, sus muestras o registros, que dicha enmienda sea incorporada al estudio de investigación que se está realizando en los centros aprobados.

Centros	Investigadores principales
C.H. Universitario de Santiago; Hospital Universitario Lucus Augusti	Rafael López López; Sergio Vázquez Estévez



Y HACE CONSTAR QUE:

- 1 El CAEIG cumple los requisitos legales vigentes (R.D 223/2004 por el que se regulan los ensayos clínicos con medicamentos, y la Ley 14/2007 de Investigación Biomédica).
- 2 El CAEIG tanto en su composición como en sus PNTs cumple las Normas de Buena Práctica Clínica (CPMP/ICH/135/95).
- 3 La composición actual del CAEIG es:

Manuel Portela Romero. (Presidente). Médico Especialista en Medicina Familiar y Comunitaria.

Irene Zarra Ferro. (Vicepresidenta). Farmacéutica de Atención Especializada.

Paula M^a López Vázquez, (Secretaria). Médico Especialista en Farmacología Clínica.

Juan Vázquez Lago (Secretario Suplente). Médico Especialista en Medicina Preventiva y Salud Pública.

Jesús Alberdi Sudupe. Médico especialista en Psiquiatría.

Rosendo Bugarín González. Médico Especialista en Medicina Familiar y Comunitaria.

Juan Casariego Rosón. Médico Especialista en Cardiología.

Xoán X. Casas Rodríguez. Médico Especialista en Medicina Familiar y Comunitaria.

Juana M^a Cruz del Río. Trabajadora Social.

Juan Fernando Cueva Bañuelos. Médico Especialista en Oncología Médica.

José Álvaro Fernández Rial. Médico Especialista en Medicina Interna.

José Luis Fernández Trisac. Médico Especialista en Pediatría.

M^a José Ferreira Díaz. Diplomada Universitaria de Enfermería

Pablo Nimo Ríos. Licenciado en Derecho. Miembro externo

Pilar Gayoso Diz. Médico Especialista en Medicina Familiar y Comunitaria.

Agustín Pía Morandeira. Farmacéutico de Atención Primaria

Salvador Pita Fernández. Médico Especialista en Medicina Familiar y Comunitaria.

Carmen Rodríguez-Tenreiro Sánchez. Licenciada en Farmacia.

Susana María Romero Yuste. Médico Especialista en Reumatología.

M^a Asunción Verdejo González. Médico Especialista en Farmacología Clínica.

En Santiago de Compostela, a 02 de junio de 2015

Firmado digitalmente por LOPEZ VAZQUEZ PAULA MARIA - CN=4690339G
Número de reconocimiento: DNI_C=ES_o=XUNTA_DE_GALICIA_s=certificado
electrónico de empleado público, serialNumber=4690339G, sn=LOPEZ
VAZQUEZ, o=verName=PAULA MARIA, cn=LOPEZ VAZQUEZ PAULA MARIA -
CNI=4690339G
Fecha: 2015.07.02 13:20:14 +0200



DESTINATARIO:

**D^a MARTA HERREROS VILLANUEVA
AMADIX, ADVANCED MARKER DISCOVERY
ACERA RECOLETOS 2-1^oB
47004 - VALLADOLID**

Fecha: 21 de abril de 2015

REFERENCIA: ESTUDIO AMD-NSCLP

**ASUNTO: NOTIFICACIÓN DE PROPUESTA DE RESOLUCION DE
CLASIFICACIÓN DE ESTUDIO CLÍNICO O EPIDEMIOLÓGICO**

Adjunto se remite propuesta de resolución de clasificación sobre el estudio titulado "Descubrimiento y desarrollo biomarcadores innovadores para medicina personalizada y terapias para el tratamiento eficaz del cáncer de pulmón", con código AMD-PLA-2015-01





ASUNTO: PROPUESTA DE RESOLUCIÓN DEL PROCEDIMIENTO DE CLASIFICACIÓN DE ESTUDIO CLÍNICO O EPIDEMIOLÓGICO

DESTINATARIO: D^a MARTA HERREROS VILLANUEVA

Vista la solicitud formulada con fecha **17 de abril de 2015**, por **D^a MARTA HERREROS VILLANUEVA** para la clasificación del estudio titulado **“Descubrimiento y desarrollo biomarcadores innovadores para medicina personalizada y terapias para el tratamiento eficaz del cáncer de pulmón”**, con código **AMD-PLA-2015-01**, y cuyo promotor es **AMADIX, ADVANCED MARKER DISCOVERY**, se emite propuesta de resolución.

El Departamento de Medicamentos de Uso Humano de la Agencia Española de Medicamentos y Productos Sanitarios (AEMPS), de conformidad con los preceptos aplicables⁽¹⁾, propone clasificar el estudio citado anteriormente como **“Estudio Posautorización de seguimiento prospectivo** (abreviado como EPA-SP)

El promotor del estudio deberá remitir solicitud de autorización del mismo ⁽²⁾ a todas aquellas Comunidades Autónomas en las que se pretenda llevar a cabo, incluyendo la siguiente documentación (una copia en papel y otra en formato electrónico) y enviando una copia de la misma (papel y formato electrónico) a la AEMPS en el momento de la primera solicitud de autorización:

- Carta de presentación dirigida a los responsables de esta materia en la Comunidad Autónoma⁽³⁾ en la que se solicite la autorización del estudio e indique la dirección y contacto del solicitante y la relación de documentos que se incluyen⁽⁴⁾.
- Resolución de la AEMPS sobre la clasificación del estudio
- Protocolo completo, incluidos los anexos, y donde conste el número de pacientes que se pretenden incluir en España, desglosado por Comunidad Autónoma.
- Dictamen favorable del estudio por un CEIC acreditado en España.
- Listado de Centros Sanitarios donde se pretende realizar el estudio, desglosado por Comunidad Autónoma
- Listado de investigadores participantes en la Comunidad Autónoma.
- Si el estudio se pretende realizar en otros países, situación del mismo en éstos
- Documento acreditativo de haber satisfecho las tasas correspondientes, en aquellas CC.AA. donde se exijan.

El plazo máximo establecido para emitir resolución por parte de cada CC.AA. será de **90 días naturales**. Si transcurrido el mismo la CC.AA. no se hubiese pronunciado, se entenderá autorizado el estudio en esa CC.AA.



A todos los efectos, se le notifica la propuesta de resolución del procedimiento de clasificación de estudio clínico o epidemiológico, y se le comunica que dispone de un plazo de quince días para presentar alegaciones y cuantos documentos estime necesarios o los que a su derecho convenga.

Madrid, a 21 de abril de 2015

La Jefe de División de Farmacoepidemiología y Farmacovigilancia

María Dolores Montero Corominas

¹ Son de aplicación al presente procedimiento la Ley 30/1992, de 26 de noviembre, de Régimen Jurídico de las Administraciones Públicas y del Procedimiento Administrativo Común; la Ley 12/2000, de 29 de diciembre, de medidas fiscales, administrativas y de orden social; la Ley 29/2006, de 26 de julio, de Garantías y Uso Racional de los Medicamentos y Productos Sanitarios; el Real Decreto 223/2004, de 6 de febrero, por el que se regulan los ensayos clínicos con medicamentos; el Real Decreto 1275/2011, de 16 de septiembre, por el que se crea la Agencia estatal "Agencia Española de Medicamentos y Productos Sanitarios" y se aprueba su estatuto; el Real Decreto 577/2013, de 26 de julio, por el que se regula la farmacovigilancia de medicamentos de uso humano y la Orden SAS/3470/2009, de 16 de diciembre, por la que se publican las directrices sobre estudios posautorización de tipo observacional para medicamentos de uso humano.

² De acuerdo con la Orden SAS/3470/2009, de 16 de diciembre.

³ Directorio disponible en la página web de la AEMPS (<http://www.aemps.es/actividad/invClinica/estudiosPostautorizacion.htm>)

⁴ En el caso de que el promotor no sea quien presente la documentación, se deberá incluir en la misma un documento que indique las responsabilidades delegadas por el promotor a la persona o empresa que actúa en su nombre.




APROBACIÓN PROYECTO DE INVESTIGACIÓN

Valencia, 4 de Julio de 2012

Esta Comisión tras evaluar en su reunión de 3 de Julio de 2012 el Proyecto de Investigación:

Título:	"Análisis del valor pronóstico de biomarcadores asociados a células madre tumorales en cáncer de pulmón no microcítico en estadios reseccables".		
I.P.:	Dr. Carlos Camps Herrero	Servicio/Unidad	Oncología

Acuerda respecto a esta documentación:	
- Que cumple con los requisitos exigidos por esta Comisión para su realización, por tanto se decide su APROBACIÓN.	
Lo que comunico a efectos oportunos:	<p>Fdo. Dr. Ricardo Guillermo Jorge Presidente de la Comisión de Investigación:</p>  <p>INVESTIGACIÓN HOSPITAL GENERAL UNIVERSITARI VALENCIA</p>

APROBACIÓN PROYECTOS DE INVESTIGACIÓN

- ANEXO 11 -

Este CEIC tras evaluar en su reunión de 26 de Julio de 2012 el Proyecto de Investigación:

Título:	"Identificación de biomarcadores moleculares asociados a células madre tumorales en cáncer de pulmón no microcítico. Implicación en el desarrollo de nuevas estrategias terapéuticas."		
I.P.:	Dr. Carlos Camps	Servicio/Unidad	Oncología

Acuerda respecto a esta documentación:

- Que el Proyecto de Investigación y Hoja de Información al Paciente y Consentimiento Informado presentado reúnen las condiciones exigidas por este CEIC, por tanto se decide su APROBACIÓN.

Los miembros que evaluaron esta documentación:

		Presente
Presidente	Dr. Severiano Marín	
Vocales	D. Ernesto Bataller	
	D. Alejandro Moner	X
	D. Germán García	
	Dr. D. José Manuel Irazo	
	Dr. D. Miguel Armengot	
	Dr. D. Julio Cortijo	X
	Dra. Dña. Elena Rubio	X
	Dr. D. Gustavo Juan	X
	Dra. Pilar Blasco	
	Dña. M ^a Teresa Jareño	X
	Dra. M ^a José Safont	
	Dra. Ana Blasco	
	Dr. Antonio Martorell	X
	Dr. Aurelio Quesada	X
	Dra. Begoña Peris	X
Dr. Fco. Javier Cervera	X	
Dr. José Vte. Roig Vila		

Consorcio Hospital General Universitario de Valencia

Comité Ético de Investigación Clínica

	Dr. Rafael Poveda	
	Dra. Inmaculada Sáez	X
	Dr. Alberto Berenguer	X
	Dr. Javier Milara	X
	Dña. Encarna Domingo	X
Secretario	Dra. Ana Minguez	X

Lo que comunico a efectos oportunos:



APROBACIÓN PROYECTO DE INVESTIGACIÓN

Esta Comisión tras evaluar en su reunión de 30 de Septiembre de 2014 el Proyecto de Investigación:

Título:	Descubrimiento y desarrollo biomarcadores innovadores para medicina personalizada y terapias para el tratamiento eficaz del cáncer de pulmón		
I.P.:	Carlos Camps Herrero	Servicio/Unidad	Oncología

Acuerda respecto a esta documentación:

- Que cumple con los requisitos exigidos por esta Comisión para su realización, por tanto se decide su APROBACIÓN.

Los miembros que evaluaron esta documentación:

		Presente	Ausente	Disculpa
Presidente	Dr. Ricardo Guijarro Jorge	X		
	Dr. Julio Cortijo Gimeno	x		
	Dra. Goizane Marcaida Benito	x		
	Dr. Carlos Sánchez Juan	X		
	D. Federico Palomar Llatas		x	
	Dr. Emilio López Alcina	x		
Vocales	Dr. Alfonso Berrocal Jaime	x		
	Dr. Julio Álvarez Pitti	x		
	Dr. Miguel Armengot Carceller		x	
	Dña. Ángela Garrido Bartolomé	x		
	Dr. Miguel Sanfeliu Giner		x	
	Dr. Manuel Navarro Villena			x
Secretario	Dra. Amparo Esteban Reboll	x		
	D. Carlos Gil Santiago	x		

Lo que comunico a efectos oportunos a
miércoles, 08 de octubre de 2014:



FUNDACIÓ
INVESTIGACIÓ
HOSPITAL GENERAL
UNIVERSITARI
VALÈNCIA

Fdo. Dr. Ricardo Guijarro Jorge
Presidente de la Comisión de Investigación:



APROBACIÓN PROYECTOS DE INVESTIGACIÓN

- ANEXO 11 -

Este CEIC tras evaluar en su reunión de 30 de octubre de 2014 el Proyecto de Investigación:

Título:	"Descubrimiento y desarrollo biomarcadores innovadores para medicina personalizada y terapias para el tratamiento eficaz del cáncer de pulmón"		
I.P.:	Dr. Carlos Camps Herrero	Servicio/Unidad	Oncología/Laboratorio biología molecular

Acuerda respecto a esta documentación:

Que en la Hoja de Información al Paciente y Consentimiento Informado v2 del 03/06/2014 de la línea de investigación Oncología Molecular y aprobado el 31/07/2014 a la cual está adscrito este proyecto reúnen las condiciones exigidas por este CEIC, por tanto se decide su APROBACIÓN.

Los miembros que evaluaron esta documentación:

Presidente	Dr. Severiano Marin Bertolin
	D. Ernesto Bataller Alonso
	D. Alejandro Moner González
Miembros Lego	Dña. Mª Teresa Jareño Roglan
	Dña. Encarna Domingo Cebrían
	D. Jaime Alapont Pérez
	Dña. Carmen Sarmiento Cabañes
	D. Antonio Baltasar Olivas Nevado
Vocales	Dr. D. José Manuel Iranzo Miguélez
	Dr. D. Miguel Armengot Carceller
	Dr. D. Julio Cortijo Gimeno
	Dra. Dña. Elena Rubio Gomis
	Dr. D. Gustavo Juan Samper
	Dra. Pilar Blasco Segura
	Dra. Mª José Safont Aguilera
Dra. Ana Blasco Cordellat	

Presente	Ausente	Disculpa
x		
	x	
	x	
	x	
X		
X		
X		
		X
	X	
X		
		x
X		
X		
X		
x		
X		

363

Dr. Antonio Martorell Aragonés
 Dr. Aurelio Quesada Dorador
 Dr. Pedro Polo Martin
 Dra. Inmaculada Sáez Ferrer
 Dr. Alberto Berenguer Jofresa
 Dra. Goitzane Marcaida Benito
 Dr. Javier Milara Payá
 Secretario Dra. Ana Minguez Martí

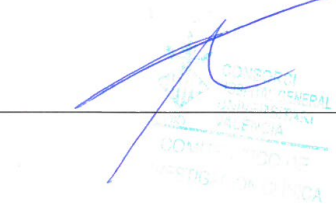
Presente	Ausente	Disculpa
X		
X		
x		
		X
		x
X		
X		
X		

En dicha reunión se cumplieron los requisitos establecidos en la legislación vigente- Real Decreto 223/2004- para que la decisión del citado CEIC sea válida. El CEIC en su composición, como en los PNT cumple con las normas de BPC (CPMP/ICH/135/95).

Lo que comunico a efectos oportunos:

Valencia a 10 de noviembre de 2014

Fdo. Dr Severiano Marin Bertolin
 (Presidente CEIC CHGV)



CERTIFICADO ACADÉMICO PERSONAL


La doctora, Dña. Mónica López Barahona,
Directora General Académica del Centro de Estudios Biosanitarios,

CERTIFICA QUE:

D^a. ABI JUDIT VÁZQUEZ RÍOS
con D.N.I./Pasaporte número: 53192107-F

Ha superado los estudios correspondientes al **Curso de Experimentación Animal de la Función A**, según Orden ECC/566/2015, con una duración de 20 horas (10 teóricas y 10 prácticas) el 17 de marzo de 2017.

Esta actividad docente de enseñanza está reconocida por la Comunidad de Madrid para todos los grupos de especies animales incluidas en el Anexo II de la Orden ECC/566/2015.



Fdo.: Mónica López Barahona
Directora General Académica
Centro de Estudios Biosanitarios

CERTIFICADO ACADÉMICO PERSONAL

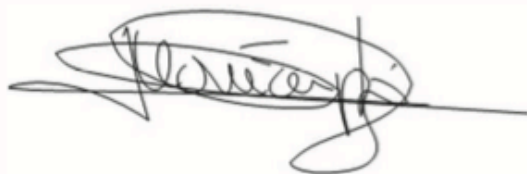
La doctora, Dña. Mónica López Barahona,
Directora General Académica del Centro de Estudios Biosanitarios,

CERTIFICA QUE:

D^a. ABI JUDIT VÁZQUEZ RÍOS
con D.N.I./Pasaporte número: 53192107-F

Ha superado los estudios correspondientes al **Curso de Experimentación Animal de la Función B**, según Orden ECC/566/2015, con una duración de 30 horas (15 teóricas y 15 prácticas) el 17 de marzo de 2017.

Esta actividad docente de enseñanza está reconocida por la Comunidad de Madrid para todos los grupos de especies animales incluidas en el Anexo II de la Orden ECC/566/2015.



Fdo.: Mónica López Barahona
Directora General Académica
Centro de Estudios Biosanitarios

CERTIFICADO ACADÉMICO PERSONAL

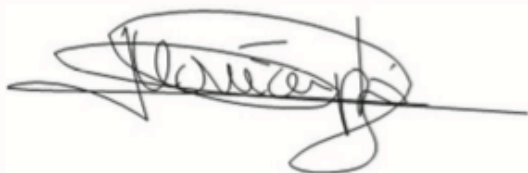
La doctora, Dña. Mónica López Barahona,
Directora General Académica del Centro de Estudios Biosanitarios,

CERTIFICA QUE:

D^a. ABI JUDIT VÁZQUEZ RÍOS
con D.N.I./Pasaporte número: 53192107-F

Ha superado los estudios correspondientes al **Curso de Experimentación Animal de la Función C**, según Orden ECC/566/2015, con una duración de 60 horas (30 teóricas y 30 prácticas) el 17 de marzo de 2017.

Esta actividad docente de enseñanza está reconocida por la Comunidad de Madrid para todos los grupos de especies animales incluidas en el Anexo II de la Orden ECC/566/2015.



CEB Centro de Estudios
Biosanitarios
C/ Porferrada, nº 54 - 28029 Madrid
C.I.F.: B-83154104

Fdo.: Mónica López Barahona
Directora General Académica
Centro de Estudios Biosanitarios



